Antibiotics from Aquatic-Derived Actinomycete Bacteria that Inhibit *M. tuberculosis*.

BY

MICHAEL W. MULLOWNEY
B.F.A., Arizona State University, 2002
Post-Baccalaureate, DePaul University, 2009-2012

DISSERTATION

Submitted as fulfillment of the requirements
for the degree of Doctor of Philosophy in Pharmacognosy
in the Graduate College of the
University of Illinois at Chicago, 2016

Chicago, Illinois

Defense Committee:

Brian T. Murphy, Medicinal Chemistry and Pharmacognosy, Chair and Advisor
Scott G. Franzblau, Medicinal Chemistry and Pharmacognosy and the Institute for Tuberculosis Research, Co-advisor
Alexander Mankin, Center for Biomolecular Sciences
Jimmy Orjala, Medicinal Chemistry and Pharmacognosy, Director of Graduate Studies
Duncan Wardrop, Chemistry

DEDICATION

This is dedicated to my kids. Always ask questions and push yourself to do difficult, intimidating things.

This is also dedicated to my amazing wife Annie, my parents, my grandparents, and the rest of my family. I was able to accomplish this because you have believed that I could accomplish anything. Thank you.

Lastly, this is dedicated to future generations that this work is intended to serve. May you be in good health and always recognize the rarity and irreplaceable value of our environment that justifies its preservation.

ACKNOWLEDGMENTS

Foremost, I would like to show appreciation to my advisor, Brian T. Murphy, for accepting me into his lab, setting me up for success, and providing for an incredibly exciting, educational, and overall the most enriching experience of my life. I would also like to thank the other members of my dissertation committee, Scott G. Franzblau, Alexander Mankin, Jimmy Orjala, and Duncan Wardrop, for their support and insight. Thanks to Russell L. Cuhel of the R/V Neeskay from the School of Freshwater Sciences at the University of Wisconsin–Milwaukee for collections in Lake Michigan that were the foundation for the discovery of diazaquinomycins H and J in Chaper 2. Thanks to Van Pham Cuong and the staff at VAST for assistance and collaboration in collecting samples from the East Sea of Vietnam that resulted in the identification of compounds in Appendix A1.2 and discovery of the diterpene in Chapter 4. I would also like to express gratitude to Sesselja Ómarsdóttir of Háskóli Íslands for the collaborative field collections that resulted in the experiments described in Appendix A1.3. Thanks also to Ben Ramirez and David Lankin for assistance in acquiring and analyzing NMR spectra and Gerd Prehna for support and assistance in acquiring circular dichroism spectra.

In the summers of 2014 and 2015, I was fortunate enough to venture out into remote areas of the Icelandic aquatic environment for field collections by SCUBA and aboard the Icelandic Coast Guard vessels Thor and Ægir. For the opportunity, I would like to thank my mentor Brian Murphy, Sesselja Ómarsdóttir, the Icelandic Coast Guard, and funding from the National Center for Complementary and Integrative Health (NCCIH) and the American Foundation for Pharmaceutical Education (AFPE). In addition, I would like to thank Eydís Einarsdóttir, Erlendur Bogasson, Sævör Dagný Erlendsdóttir, Gunnar Egill Sævarsson, Maria Sofia Costa, and Ana Margarida Costa for their companionship on those trips.

Others who were supportive during my graduate studies were within the Department of Medicinal Chemistry and Pharmacognosy in the College of Pharmacy at UIC, including Andrew Newsome, Dejan Nikolic, Caleb Neinow, and Monika Lysakowska of the van Breemen and RRC mass spectrometry labs; James Paul Marks, Kolya Aleksashin, Teresa Szal of the Mankin lab for collaborations and research guidance; Larry Klein and Michael Tufano in the ITR for diazaquinomycin A synthesis and medicinal chemistry guidance; Jeff Anderson and Sura Mulugeta in the ITR for mycobacterial molecular biology guidance and collaboration; Chang Hwa Hwang, Baojie Wan, Yuehong Wang, Edyta Grzelak, and Sang Hyun Cho in the ITR for TB bioassay screening; Eoghainín O hainmhire and Wei-Lun Chen of the Burdette lab for cytotoxicity screening; Laura Sanchez for guidance; the Center of Biomolecular Sciences, especially members of the Federle, Burdette, Sodhi, Lee, Orjala, Mankin, Eustaquio, and Johnson Labs for being good neighbors; and Murphy Lab members Urszula Tanouye, Skylar Carlson, Vanessa Nepomuceno, Chase Clark, Hiyoung Kim, Collin McCafferty, Brian Kim, Antonio Hernandez, Xiomei Wei, Jeong Ho Lee, Maryam Elfeki, Sofia Maria Costa, Jhewelle Fitz-Henley, Anam Shaikh, and Mark Sadek.

This work is supported by the Office of the Director, National Institutes of Health (OD) and National Center for Complementary and Integrative Health (NCCIH) (5T32AT007533) through a T32 pre-doctoral training fellowship, a pre-doctoral fellowship from the American Foundation for Pharmaceutical Education (AFPE), a PhD scholarship from the International Association for Great Lakes Research (IAGLR), and a W. E. van Doren scholarship from the Department of Medicinal Chemistry and Pharmacognosy in the College of Pharamcy at UIC.

MWM

CONTRIBUTIONS OF AUTHORS

Chapter 1 is an original work by Michael Mullowney with editing provided by Dr. Brian T. Murphy. Chapter 2, sections 2.1 through 2.2.6, 2.3.1 through 2.3.10 and 2.4 are from a manuscript published in ACS Infectious Diseases in 2015 with some minor additions. Thomas Speltz assisted with the large-scale fermentation of strain B026. Andrew Newsome of the van Breemen lab provided guidance and critical insight on the structure elucidation of the novel diazaquinomycin analogs. Xiaomei Wei initially identified the presence of what were eventually identified as novel diazaquinomycin analogs in marine and freshwater actinomycete strains in the Murphy lab. Chang Hwa Hwang, Baojie Wan, Edyta Grzelak, and Sang Hyun Cho performed anti-tuberculosis bioassays, including the thymidine supplementation assay at the Institute for Tuberculosis Research at UIC directed by Scott G. Franzblau with the consultation and manuscript proofing of both Scott G. Franzblau and Sang Hyun Cho. Nanthida Joy Barranis screened DAQA against the Bacillus strains in the lab of Hyunwoo Lee at the University of Illinois at Chicago, Skylar Carlson performed the bioassay of DAQA against *Streptococcus* strains in the Murphy lab, and Siyun Liao screened against the remaining microbial strains in the lab of Larry Danziger. Wei-Lun Chen and Eoghainín Ó hAinmhire performed the cancer cell line panel bioassays in the lab of Joanna Burdette. Kalyanaraman Krishnamoorthy and John White performed the thymidylate synthase enzyme inhibition assay in the lab of Pradipsinh K. Rathod at the University of Washington, Rachel Kokoczka screened DAQA against the *M. tuberculosis* OE mutants in the lab of Tanya Parish at the Infectious Disease Research Institute (IDRI). Principal investigator Brian T. Murphy advised throughout, edited drafts, and was the corresponding author on the publication. Sections added following publication include synthesis, biocatalysis, mechanism of action, and *in vivo* studies. Larry Klein and Mike Tufano performed total synthesis of diazaquinomycins and also provided guidance in diazaquinomycin analog generation. Christian Willrodt of the Andreas

Schmid lab at The Helmholtz-Centre for Environmental Research GmbH – UFZ in Leipzig, Germany provided plasmids and guidance for whole-cell biocatalysis while Kolya Aleksashin and Teresa Szal of the Aleksander Mankin lab assisted in generating the *E. coli* transformants for that experiment. Anthony Goering assisted in LCMS analysis of biocatalysis extracts in the Neil Kelleher lab at Northwestern University. Sang Hyun Cho performed the thymidine and thymine supplementation assays and additional *M. tuberculosis* mutant screenings. Edyta Grzelak performed screening against *M. tuberculosis* $mc^2$7000. Helena Boshoff in the Clifton Barry lab at the NIH performed *M. tuberculosis* mutant screenings, transcription profiling, and the ATP assay as well as provided invaluable insight into the analysis of mechanism of action data. Vinayak Singh of the Valerie Mizrahi lab at The University of Cape Town performed mutant screenings and the uracil supplementation and synergy assays. The analysis of spectral data, the characterization of novel diazaquinomycin analogs, semi-synthesis, whole-cell biocatalysis, screening of environmental actinomycetes, and mechanism of action data analysis was completed by Michael Mullowney. Chapter 3 is a manuscript published in Marine Drugs in 2014 with minor modifications. The bioassays and follow-up mechanism of action studies are the work of Eoghainín Ó hAinmhire in the laboratory of Dr. Joanna Burdette. Anam Shaikh provided technical assistance in the prep-scale chromatographic separation of the reported compounds, Xiaomei Wei initially identified the presence of novel diazaquinomycin analogs in strain F001, Urszula Tanouye provided technical assistance in the isolation of the active *Streptomyces* strain from the environmental sample. Dr. Bernard Santarsiero preformed X-ray experiments and analysis on the co-crystallized DAQF and DAQG. Brian Murphy advised throughout, edited drafts, and was the corresponding author on the publication. The analysis of spectral data and the characterization of novel diazaquinomycin analogs was completed by Michael Mullowney. Chapter 4 is a manuscript published in Marine Drugs in 2015. Van Coung Pham was the lead in the expedition that resulted

in the environmental sample from which strain G039 was isolated and he proofed the final version of the manuscript. The MABA and LORA assays were performed by Baojie Wan and Sang Hyun Cho at the Institute for Tuberculosis Research at UIC directed by Scott G. Franzblau while cytotoxicity bioassays are the work of Eoghainín Ó hAinmhire in the laboratory of Dr. Joanna Burdette. Urszula Tanouye provided technical assistance in the isolation of the producing *Micromonospora* strain from the environmental sample. Brian Murphy advised throughout, edited drafts, and was the corresponding author on the publication. Analysis of spectral data and characterization of the novel diterpene and the angucyclines was completed by Michael Mullowney. Chapter 5 is an original work by Michael Mullowney discussing the future direction of the natural products field. Appendix I is a summary of selected projects by Michael Mullowney involving dereplication of known compounds in the laboratory of Brian T. Murphy in collaboration with the Institute for Tuberculosis Research (ITR) and the lab of Joanna Burdette. All chromatography, NMR spectroscopy, mass spectrometry, and structure elucidation experiments were executed by Michael Mullowney.

TABLE OF CONTENTS

LIST OF TABLES

LIST OF FIGURES

FIGURE PAGE

LIST OF ABBREVIATIONS

5-FU	5-fluorouracil
ABC	ATP-binding cassette
ACN	acetonitrile
AcOH	acetic acid
ADC	albumin-dextrose-catalase
ADP	adenosine diphosphate
ALA	aminolevulinic acid hydrochloride
ATc	anhydrotetracycline
ATCC	American Type Culture Collection
ATP	adenosine triphosphate
AU	absorbance units
BCG	bacillus Calmette–Guérin vaccine
BDQ	bedaquiline
BPO	benzoyl peroxide
CACO-2	human colon epithelial cancer cell line
calcd.	calculated
CCCP	carbonyl cyanide chlorophenylhydrazone
CCDC	The Cambridge Crystallographic Data Centre
CD	circular dichroism
CFU	colony forming units
CIMminer	clustered image maps miner
CLF	clofazimine
COSY	homonuclear correlation spectroscopy
CS	cycloserine
Cy3/Cy5	cyanines
DAQ	diazaquinomycin
DAQA	diazaquinomycin A
DAQC	diazaquinomycin C
DAQE	diazaquinomycin E

DAQF	diazaquinomycin F
DAQG	diazaquinomycin G
DAQH	diazaquinomycin H
DAQJ	diazaquinomycin J
DAPI	4′,6-diamidino-2-phenylindole
DARTS	drug affinity responsive target stability
DCPK	dicyclopropyl ketone
DCM	dichloromethane (methylene chloride)
DEPTQ	distortionless enhancement by polarization transfer with quaternaries
DMF	N,N-dimethylformamide (N,N-dimethylmethanamide)
DMSO	dimethyl sulfoxide
DNA	deoxyribonucleic acid
DPPtdCho	dipalmitoylphosphatidylcholine
DOT	Directly Observed Therapy
DOTS	Directly Observed Treatment, Short-course
dTMP	deoxythymidine monophosphate
dUMP	deoxyuridine monophosphate
EDTA	ethylenediaminetetraacetic acid
EMA	European Medicine Agency
EtBr	ethidium bromide
ETC	electron transport chain
EtOH	ethanol
F_{420}	8-hydroxy-5-deazaflavin
FAD	flavin adenine dinucleotide
FBS	fetal bovine serum
GAS	glycerol-alanine-salts
G+	Gram-negative
G-	Gram-positive
HBSS	Hanks balanced salt solution
HEX	hexanes

HGSOC	high grade serous ovarian cancer
HMBC	heteronuclear multiple-bond correlation spectroscopy
HPLC	high performance liquid chromatography
HR-ESI-IT-TOF	high-resolution-electrospray-ionization-ion-trap-time-of-flight
Hsp60	heatshock protein 60
HSQC	heteronuclear single quantum coherence spectroscopy
HsThyA	human thymidylate synthase
HT-29	human colorectal adenocarcinoma cell line
IBC	Institutional Biosafety Committee
IC_{50}	half maximal inhibitory concentration
IDRI	Infectious Disease Research Institute
INH	isoniazid
IP	intraperitoneal injection
IPTG	isopropyl β-D-1-thiogalactopyranoside
ITR	Institute of Tuberculosis Research
IT-TOF	ion-trap-time-of-flight
K*i*	inhibitor equilibrium dissociation constant
KM	kanamycin
LC_{50}	half maximal lethal concentration
LCMS	liquid chromatography mass spectrometry
LOQ	limit of quantitation
LORA	low oxygen recovery assay
LuxABCDE	bioluminescence lux operon reporter
M9*	modified M9 nutrient media
MABA	microplate alamar blue assay
MBC	minimum bactericidal concentration
MDA-MB-231	human breast adenocarcinoma cell line
MDA-MB-435	human melanoma cell line
MDR TB	multidrug-resistant *Mycobacterium tuberculosis*
MeOH	methanol

MIC	minimum inhibitory concentration
MmpL	mycobacterial membrane protein, large
MOA	mechanism of action
MOE	murine oviductal epithelial
MOSE	murine ovarian surface epithelium
MRSA	methicillin-resistant *Staphylococcus aureus*
MSSA	methicillin-sensitive *Staphylococcus aureus*
MTS-PMS	3-(4,5-dimethylthiazol-2-yl)-5-(3-carboxymethoxyphenyl)-2-(4-sulfophenyl)-2H-tetrazolium - phenazine methosulfate
MtThy	*Mycobacterium tuberculosis* thymidylate synthase
m/z	mass to charge ratio
NAME	nonanoic acid methyl ester (methyl nonanoate)
NBS	N-bromosuccinimide
NCCIH	National Center for Complementary and Integrative Health
NCCLS	National Committee on Clinical Laboratory Standards
NCI	National Cancer Institute
NIH	National Institutes of Health
NMR	nuclear magnetic resonance spectroscopy
NOESY	nuclear Overhauser spectroscopy
NP-Si	normal phase silica gel
NTM	nontuberculosis mycobacteria
OACIB	Office of Animal Care and Institutional Biosafety
OADC	oleic acid-albumin-dextrose-catalase
OD	optical density
OE	overexpression
OPC67683	delamanid
OVCAR	ovarian carcinoma cell line
PA824	pretomanid
PARP	poly(adenosine diphosphate-ribose) polymerase
PAS	p-aminosalicylic acid

PBS	phosphate buffered saline
PEG	polyethylene glycol
PK	pharmacokinetic
PLC	preparative layer chromatography
PO	*per os* (oral gavage)
PONAR	sediment sampling device
ppm	parts per million
QQQ	triple-quadrupole
Q-TOF	quadrupole-time-of-flight
RCF	relative centrifugal force
RIF	rifampin
RLU	relative luminescence units
RNA	ribonucleic acid
ROS	reactive oxygen species
RP-C_{18}	reversed phase octadecyl carbon chain-bonded silica
SAR	structure-activity relationships
SDS-PAGE	sodium dodecyl sulfate polyacrylamide gel electrophoresis
SM	streptomycin
SPE	solid phase extraction
TAM	tirandamycin
TB	tuberculosis; *Mycobacterium tuberculosis*
TCEP	tris(2-carboxyethyl)phosphine
Tet	tetracycline
Thy	thymidylate synthase
TES	2-[tris(hydroxymethyl)-methylamino]-ethanesulfonic acid buffer
TFA	trifluoroacetic acid
TIC	total ion chromatogram
TMC207	bedaquiline
1D-TOCSY	one-dimensional total correlation spectroscopy
TraSH	transposon site hybridization

Tw	Tween™ 80
UIC	University of Illinois at Chicago
USFDA	United States Food and Drug Administration
UV	ultraviolet
vol	volume
VRE	vancomycin-resistant enterococci
WHO	World Health Organization
WT	wild type
wt	weight
XDR TB	extensively drug-resistant *Mycobacterium tuberculosis*

SUMMARY

Chapter 1 provides a history of the impact of *M. tuberculosis* on society and efforts towards treatment of infection with the pathogen. In addition, natural products are presented as a prolific source of anti-infective treatments and antibiotics from actinomycete bacteria, specifically those from aquatic environment, are proposed as a promising source for new drug-leads to combat *M. tuberculosis*. Both Chapter 2 and 3 detail the isolation, structure elucidation, derivatization, bioactivity profiling, and efforts toward understanding the mechanism of action and *in vivo* potential of the diazaquinomycin class of antibiotics. The former describes among the first actinomycete-derived antibiotics sourced from fresh water and investigates the anti-tuberculosis activity of the diazaquinomycins, while the latter presents the elucidation of novel diazaquinomycin analogs from a marine-derived actinomycete with characterization of cytotoxicity. Results presented in these chapters suggest the potential for this class of compound to reveal new modes of tuberculosis treatment. Chapter 4 explains the rare discovery of a diterpene from an actinomycete whose initially observed anti-tuberculosis activity was attributed to a set of co-isolated cytotoxic angucycline compounds. The appendix describes known natural products identified and deprioritized in the process of investigating TB-active actinomycete extract fractions and contains supplemental data and figures for the preceding chapters. Chapter 5 concludes with remarks on the current state and future outlook of the global tuberculosis crisis while covering current innovations in natural products drug discovery and proposing new directions for the field that might contribute to an eradication of the disease.

1. INTRODUCTION

1.1 The ongoing arms race to combat *Mycobacterium tuberculosis* infection.

1.1.1 History of the deadliest bacterial human pathogen.

M. tuberculosis (TB) is an ancient pathogen.[1] Coalescent whole genome analyses have revealed that the disease-causing microbe emerged about 70,000 years ago, migrating, expanding, and evolving with the human population as it spread from Africa and grew in density during the dawn of agriculture in the Neolithic period.[2] Written records from 1600 to 1800 describing the effect of TB on whole populations indicate that it killed twenty percent of adults in the Western world during those years.[3] For centuries, this disease once termed phthisis (Greek for "wasting away"), consumption, scrofula, Pott's disease, and the White Plague, has been recognized as a completely hopeless, incurable burden.[4]

1.1.2 Early treatments for *M. tuberculosis* infection.

Tuberculosis treatment preceding the advent of modern antimicrobial agents mostly treated symptoms and consisted of herbal remedies, misguided and often harmful use of stimulant and sedative chemicals, risky practices such as bloodletting and purging, fresh air (aerotherapy), sunshine (heliotherapy), and dietary interventions.[4] Addressing the failures of such approaches, renowned British doctor James Clark wrote "…we must admit the humiliating truth, that there is no reason to believe the physicians of the present day are more successful than their predecessors were ten, nay twenty centuries ago."[5] In 1921, an attenuated form of the bovine pathogen *Mycobacterium bovis* known as "bacille Calmette Guérin" (BCG) was developed for use as a vaccine. Though still in use today, for unknown reasons it has not been shown to reliably protect against adult pulmonary TB infection.[6]

1.1.3 First and second line anti-tuberculosis drugs and leads currently in clinical trials.

Fortunately, the birth of the golden era of antibiotics in the in mid-twentieth century resulted in the discovery of the aminoglycoside antibiotic streptomycin, which was shown to effectively reduce TB-caused mortality by inhibiting protein synthesis in *M. tuberculosis*.[7-9] This discovery caused the rapid abandonment of previous, ineffective treatments. However, streptomycin monotherapy became associated with relapses, and resistance to the drug arose just five years after it was made widely available.[10] Following a series of important clinical studies, it was established in 1964 that streptomycin resistance was circumvented and treatment was more effective when the drug was used in combination with p-aminosalicylic acid (PAS) and isoniazid (INH) for a 24-month period of therapy.[8, 11-16] Combination therapy was established as critical to successful tuberculosis treatment – taking any mono-therapy resulted in resistance to that drug.[17] Therapy duration was repeatedly reduced into the late 1970s with successive introductions of new drugs. The previous three-drug regimen was eventually made obsolete with the introduction of rifampin (RIF),[18] the replacement of PAS with the better tolerated ethambutol,[19] and the addition of pyrazinamide.[20] Thus, the "first line" drugs streptomycin, isoniazid, ethambutol, rifampin, and pyrazinamide were established as the foundation for effective combination tuberculosis chemotherapy – a two month "intensive" treatment phase with a subsequent four month "continuation" phase – that is still in use today (Figure 1).[21, 22] Currently, various strategies using these and "second line" drugs - those of lesser efficacy or with additional side-effects - are employed when pathogen populations exhibit resistance or are not eradicated in the "intensive" and "continuation" phases.[23] The most extreme cases make use of "third line" drugs, or those which are not as efficient, have even less established efficacy, or have limited availability in developing countries.[24]

Figure 1. Current first and second line anti-TB drugs.

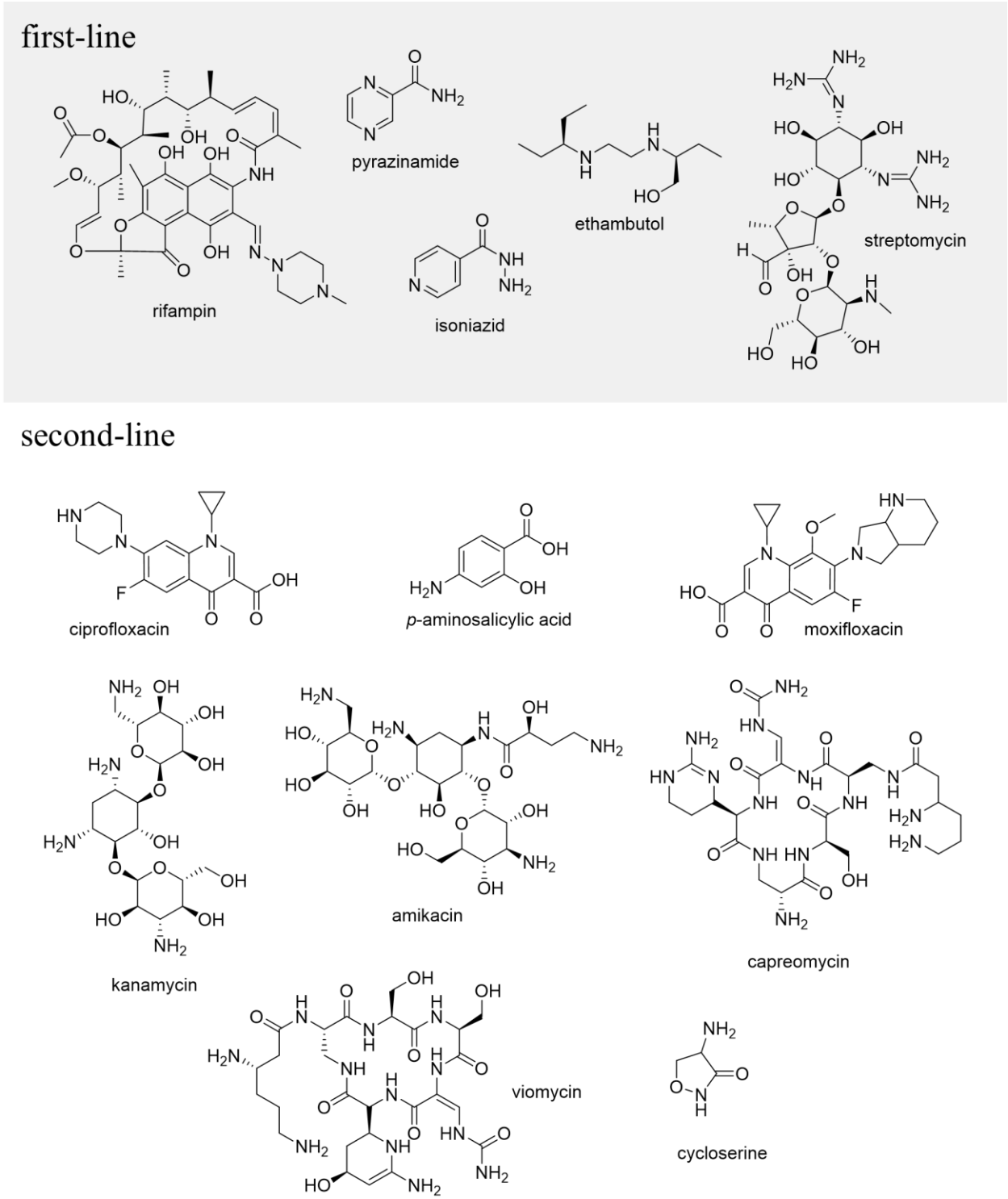

In the early 1970s, the search for novel TB treatments was all but suspended after the discovery and addition of RIF to this regimen of drugs.[18] The first line drug therapies were able to mitigate the threat of TB for a time and are still in use today with few modifications despite increasing incidence of resistant strains. A major contributing factor to the development of resistance had been a lack of patient compliance to the lengthy regimen and frequent abandonment of treatment altogether.[25] This prompted the establishment of 'Directly Observed Therapy' (DOT) and 'Directly Observed Treatment, Short-course' (DOTS) in the 1980s and 90s in lieu of unsuccessful self-administration.[25, 26] The program was first promoted and propagated globally by the WHO in the early 2000s but its impact has been debated.[27-29] Unfortunately, during this same time a lack of economic interest in developing new anti-TB drug-leads due to the scarcity of the disease in more advanced countries caused a gap in discovery. Despite this and other setbacks, recent decades have seen an increased interest in anti-TB drug discovery and development with initiatives managed by non-profits like the TB Alliance and collaborative efforts like The Stop TB Partnership.[30, 31]

Drugs with clinical trials currently listed as active or recruiting on clinicaltrials.gov were well reviewed in 2015 by Schito, et al. and are shown in Table 1.[32] Of these, bedaquiline (TMC207) and delamanid (OPC67683) have been selected for conditional or accelerated approval by the United States Food and Drug Administration (USFDA) and the European Medicine Agency (EMA) based on their inhibition of resistant strains.[33, 34] Though these drugs represent a major step in alleviating the current burden of drug resistance, they do not simplify the first line drug regimen or reduce treatment duration, both of which are desperately needed for the eradication of TB.

Table 1. The most recent TB drugs in clinical trials.[a]

Drug name	Class	Licensor/Sponsor	Mechanism of action	Phase
Delamanid (OPC67683)	nitroimidazole	Otsuka	*M. tuberculosis*-activated prodrug – mycolic acid synthesis inhibitor	III
Moxifloxacin	fluoroquinolone	Bayer/Global TB Alliance	DNA topoisomerase II inhibitor	III
Gatifloxacin	fluoroquinolone	EU/TDR	DNA topoisomerase II inhibitor	III
Pretomanid (PA824)	nitroimidazole	Global TB Alliance	*M. tuberculosis*-activated prodrug – lipid and protein synthesis inhibitor	II
Bedaquiline (TMC207)	diarylquinoline	Tibotec/Johnson & Johnson	ATP synthase subunit C inhibitor	II
SQ109	ethylene diamine	Sequella	inhibition of efflux, cellular respiration, and menaquinone and ATP synthesis[35]	II
Sutezolid (PNU100480)	oxazolidinone	Sequella	inhibition of protein synthesis by binding 23S RNA and 50S ribosomal subunits	II
Sudoterb (LL3858)	pyrrole	Lupin	N/A	I

[a] adapted from Beena, Rawat, updated with data from ClinicalTrials.gov[24, 36]

1.1.4 Modes of action for *M. tuberculosis* inhibition.

Of the 4,000 total genes that comprise the *M. tuberculosis* $H_{37}Rv$ genome, between 200 and 800 have been deemed essential using various mutagenesis techniques.[37, 38] These genes code for biomolecules which hypothetically may be exploited as targets for bactericidal inhibition. Of the hundreds of potential targets, only approximately twenty known gene products are exploited by drugs on the market. The aminoglycosides streptomycin and kanamycin inhibit protein synthesis; isoniazid, ethambutol, ethionamide, cycloserine, pyrazinamide, and delamanid target the cell wall or membrane; the quinolones target DNA gyrase; bedaquiline targets ATP synthase; while targets of others are less understood (PAS, clofazimine, etc.).[39] *M. tuberculosis* has a profound intrinsic tolerance to antibiotics, accumulating resistance plasmids or transposons for multidrug efflux pumps establishing the current need for combination therapy.[40]

1.1.5 The current global burden of *M. tuberculosis*.

In 1993, with the increasing incidence of drug-resistant TB and coinfections with HIV, the WHO declared TB a global health emergency.[41] In its most recent report, the WHO estimated that

1.5 million deaths were attributed to TB infection in 2014 with 9.6 million new cases of the disease reported. In addition, one-third of the world's population was infected with the latent form of tuberculosis.[42] The most significant immediate threat is multidrug- and extensively drug-resistant strains of *M. tuberculosis* (MDR- and XDR-TB), which are resistant to first and second line drug regimens and resulted in 190,000 fatalities in 2014 (of the 480,000 total estimated MDR- and XDR-TB infections).[42-44] Additionally, reports of patients with TB infections that are resistant to all available drug treatments (totally drug-resistant tuberculosis; TDR-TB) have begun surfacing in the past decade.[45] In extreme cases, partial surgical lung resection coupled with an MDR-TB drug regimen is the only promising intervention remaining.[22] A major deficiency of current TB treatment is its long duration, which is necessary to eliminate a persistent subpopulation of slow-growing or non-replicating cells (NRP-TB). This extended treatment time results in high cost and frequent patient noncompliance. To make matters more complex, one third of the world's population is infected with latent TB, showing no symptoms but serving as a reservoir for active infections that could prohibit eradication of the disease for decades.[42] Importantly, the predominance of tuberculosis in underprivileged populations in the developing world, together with its frequent acquisition of drug-resistance and its ease of transmission between humans has solidified it as a pathogen of global concern.[46] These deterrents serve to support a continual evolution of MDR- and XDR-TB that has been forging ahead faster than the development of new antibiotic scaffolds, thus, there is a crucial need for new sources of potent, faster-acting drugs that inhibit *M. tuberculosis* infection.

1.1.6 Future outlook.

In 2014 the WHO established the "End TB Strategy," which aims to reduce the global incidence of tuberculosis infection from >1,000 per million people in 2015 to <100 per million people by 2035.[47] If this goal is to be achieved, it will be through efforts on various fronts,

including drug discovery. Current clinical studies focus primarily on repurposing old drugs or finding new, more efficacious combination therapies, but the search for new drugs is also critical.[36] Along with new drugs, identification of new targets that might facilitate monotherapeutic inhibition of *M. tuberculosis* would be revolutionary. TB is the deadliest infectious agent humanity has ever known, and though the best treatment regimen available is inefficient and lengthy, it is indeed a cure. Unfortunately, populations most burdened by TB also lack the resources to fully treat and cure, or even detect and report the disease.[42] This creates an environment that fosters a drug resistance reservoir. Poorly treated *M. tuberculosis* infection could gain and spread pan-resistance to other pathogens, contributing greatly to a return to a pre-antibiotic era, when pathogens gain resistance to the last lines of defense.[48] This becomes a critical global health emergency. It is in the interest of all of society to put forth the funds and human capital toward research efforts aimed at TB eradication.

1.2 Natural products as drug therapies.

1.2.1 The origins of natural products drug discovery.

Fossil records indicate the use of well-known medicinal plants by early humans since at least as early as 60,000 years ago in the Middle Paleolithic age.[49, 50] Specific use of natural products by ancient civilizations for their antibiotic properties began with use of herbs, honey, and even animal feces, with records of topical application of moldy bread being evidenced in ancient societies in China, Egypt, and Rome.[51] Amazingly, traces of tetracyclines have been detected in the bones of Nubians from almost 2,000 year ago, the evidence strongly suggesting that the source was a regularly ingested fermented beer intentionally inoculated with a tetracycline-producing actinomycete strain.[51, 52] Since the 1940s, natural products have proven essential as components of drug discovery; they serve as both a direct source of small molecule therapies and as an inspiration for biologically active synthetic derivatives.[53] These compounds account for greater than 50% of

marketed small molecule therapies (Figure 2).[53, 54] Additionally, nearly half of the first and second line tuberculosis drugs are natural products or their derivatives and all of these are of microbial origin.[22, 23] Extracts, fractions, and compounds that inhibit TB both *in vitro* and *in vivo* have been discovered and reported from plants, animals, and microbes from all environments.[55]

Figure 2. Origins of all approved drugs by percent from 1981−2014.[a]

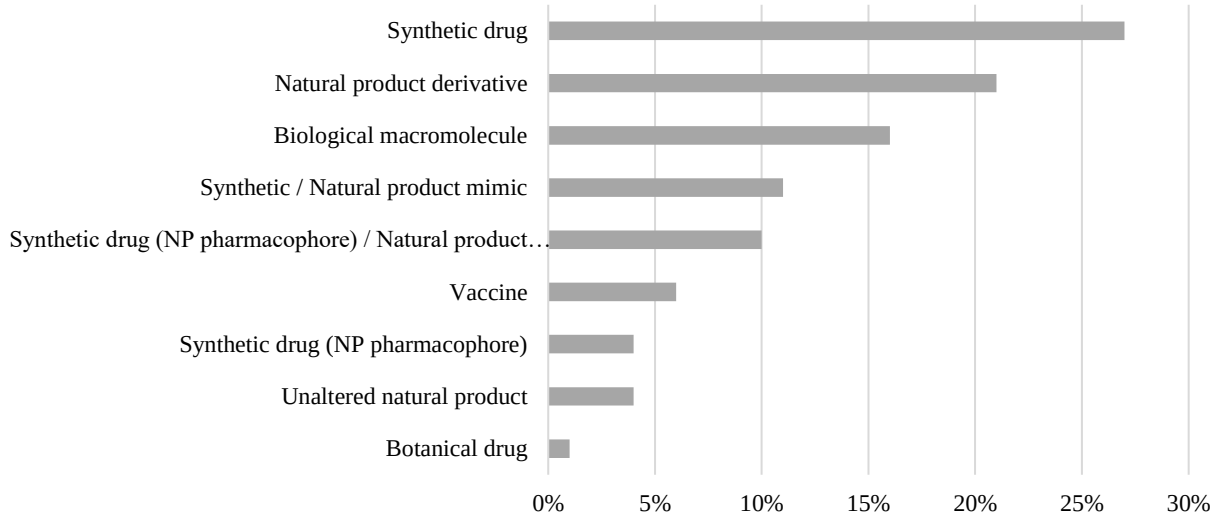

[a] n = 1562; adapted from Newman, Cragg, 2016.[53]

In the 1990s, a wave of new technologies including combinatorial chemistry, high-throughput screening, and computer-assisted design of small-molecules emerged that was widely considered to be an improvement over traditional drug discovery.[54] Though these methods have advanced a handful of TB inhibitors into clinical trials, it has been claimed that they often lack a rationality suitable for the continued efficient development of TB treatments.[40, 54] Conversely, natural products are privileged structures, having been honed for the targeting of biological targets over millennia of evolution.[56] This advantage is made clear by the fact that the first four rules of Lipinski's "Rule of Five" do not apply to natural products when considering "druggable chemical entities."[53, 57] Recognition of this inherent potential and a realization that biological diversity had

not been sufficiently explored led to a reemergence of efforts focused on natural products drug discovery in the past two decades.[54]

1.2.2 Terrestrial actinomycete bacteria as prolific providers of drug leads.

Actinomycete bacteria in particular have been an abundant source of bioactive secondary metabolites for more than 50 years, providing greater than half of current antibiotics used clinically.[53, 54] Following the discovery of penicillin in the 1930s and the anti-TB antibiotic streptomycin in the 1940's, and propelled by the steady emergence of bacterial resistance, a research focus on terrestrial actinomycete bacteria yielded more than 120 drugs for the treatment of various human diseases.[53, 58-60] Unfortunately, the earliest antibiotic screenings exhausted the repertoire of taxonomically unique terrestrial actinomycetes and the novel bioactive small molecules that could be accessed using the technology of the time, resulting in the continuous re-isolation of known antibiotic scaffolds.

1.2.3 Drug-lead discovery from the marine environment.

As a result, researchers shifted their focus, prospecting new sources for drug lead discovery such as the ocean. Libraries of macroorganisms, microorganisms, and their resulting secondary metabolites were created that had not been incorporated in the biological screening efforts of previous decades.[54, 59 61-63] For many years, this immense resource had been overlooked due to the prohibitive expense of additional technology and skill sets needed for ocean sampling. As a result, the majority of marine microbiota remain unexplored. The recent development of more sophisticated sampling technologies and moderate investments in marine exploration and microbiology have allowed considerable progress, affording the development of several drugs from marine sources (Prialt, Yondelis, Halaven).[61, 62, 64] Interestingly, environmental pressures and nutrient composition completely distinct from the terrestrial environment have been shown to

support microorganisms with structurally unique secondary metabolite capabilities. Importantly, molecules isolated from microbes hold promise for TB inhibition.[40, 65]

1.2.4 Freshwater-derived actinomycetes as a source of novel drug leads.

Despite easily adaptable technology and expertise from exploration of the marine environment, freshwater environments remain virtually unexplored for bioactive secondary metabolites from actinomycete bacteria. Currently, only a handful of drug discovery research groups have begun research using fresh waters as a source of microbes, none of them exploring actinomycetes.[66, 67] The Murphy and the Institute for Tuberculosis Research (ITR) labs are uniquely positioned in the Great Lakes region to study freshwater systems, which are a virtually unexplored source for pharmacologically active secondary metabolites. A primary focus of our program is the exploration of the capacity of freshwater-derived actinomycete bacteria to produce bioactive secondary metabolites. The occurrence of actinomycete bacteria in freshwater systems has been known for over fifty years. Cross and Goodfellow summarize the earliest cultivation studies of *Micromonospora*, *Rhodococcus*, *Actinoplanes*, *Streptomyces* and strains of several other genera collected from a diversity of fresh water lake and stream sediments.[68, 69] Early cultivation-based studies described that representatives of common terrestrial genera, *Streptomyces* and *Thermoactinomyces*, were isolated from shallow water sites, but that *Micromonospora* spp. were found to be more prevalent in sediment at greater depths, likely due to their ability to survive in microaerophilic environments and efficiently degrade benthic nutrients such as chitin and cellulose.[70-73] The abundance of *Micromonospora* in deeper sediment led some to postulate that they were indigenous inhabitants of these freshwater systems. More recent molecular-based screening techniques support these findings, revealing freshwater-derived actinomycetes that were taxonomically distinct from those of terrestrial and marine origin, likely due to distinct environmental selection pressures and growth conditions.[74] Further support for claims of

freshwater endemic actinomycetes are found in reports of clades from bacterioplankton communities around the world that are exclusive to freshwater environments.[75-80] Culture independent studies of freshwater bacterial communities around the world have indicated the presence of actinomycete clades that are exclusive to freshwater environments, the most abundant of which appear to fall within the acI lineage.[75-80] Few cultured representatives of these clades exist.[76, 77] Importantly, the majority of these studies focused on bacterioplankton rather than sediment actinomycetes. These promising new freshwater sources can easily be exploited using the techniques that have allowed for the discovery of bioactive secondary metabolites from marine sediment-derived actinomycete bacteria. The search for novel actinomycete taxa in freshwater environments is significant as it applies a similar paradigm that afforded marine researchers a wealth of chemical diversity and successes in drug-lead discovery.[64, 81-84] Extraordinarily little is known about the diversity of secondary metabolites produced by actinomycete bacteria derived from freshwater systems. The next logical step is to expand the marine paradigm to freshwater environments, which harbor distinct environmental selection pressures and growth conditions, and to date are virtually unexplored for their capacity to afford unique actinomycete bacteria. Furthermore, despite several cultivation independent studies aimed at characterizing lake actinomycete populations,[74] to the best of our knowledge few efforts (including one study from our lab) have identified secondary metabolites from freshwater-derived actinomycetes. Included in this gap is a notable absence of studies aimed specifically at generating anti-TB drug-leads.[40, 85, 86]

1.3 Hypothesis.

We hypothesize that actinomycetes isolated from aquatic (both marine and freshwater) environments serve as important and underexplored resources for antibiotics that inhibit *M. tuberculosis*. This hypothesis is founded on the knowledge that a) the aquatic environment is

largely unexplored for its chemical diversity and b) observations of the cohabitation of pathogenic mycobacteria with actinomycetes in the aquatic environment[87] may act as a selection pressure, eliciting the generation of actinomycete secondary metabolic pathways tailored to the production of antimycobacterial antibiotics.[87, 88] We propose that interactions between the genera have established long standing selection pressures, causing the generation of actinomycete secondary metabolic pathways tailored to the production of antimycobacterial antibiotics. Culture-independent analyses of sediment samples collected from Massachusetts, Vietnam, and Lake Michigan have confirmed the phenomenon of mycobacterial diversity co-habiting with actinomycetes (data not shown). Furthermore, these environmental mycobacteria are found useful as infection models for TB due to their morphological and genetic similarities, thus a conjecture that anti-mycobacterial antibiotics from actinomycetes in the environment might have activity against TB is valid.

2. DIAZA-ANTHRACENE ANTIBIOTICS FROM A FRESHWATER-DERIVED ACTINOMYCETE WITH SELECTIVE ANTIBACTERIAL ACTIVITY TOWARD *M. TUBERCULOSIS*.[†]

2.1 Introduction.

Included in the scarcity of freshwater-derived microbe research is a notable absence of studies aimed specifically at generating drug-leads.[40, 85, 86] Thus, a major focus of our antibiotic discovery program is to study Actinobacteria derived from the Great Lakes and other freshwater bodies. We have created an extensive library of these bacteria and their resulting secondary metabolite fractions (Figure A16). A preliminary *in vitro* growth inhibition screening of this fraction library against *M. tuberculosis* H_{37}Rv led to the identification of a *Micromonospora* sp. isolated from Lake Michigan sediment, whose fraction exhibited submicromolar inhibitory activity. From this strain we isolated and characterized two novel secondary metabolites, diazaquinomycins H and J (DAQH and DAQJ), which to our knowledge are among the only freshwater-derived actinomycete metabolites described to date.[85, 86] Further *in vitro* profiling suggested that this group of diaza-anthracene antibiotics selectively targets *M. tuberculosis* over other bacteria, and is active against several forms of drug-resistant TB. Herein we present the identification and *in vitro* biological characterization of this unique antibiotic class with explorations of their elusive mechanism of action and their testing *in vivo*.

2.2 Results and discussion.

2.2.1 Isolation and identification of diazaquinomycins H (1) and J (2).

Screening of our actinomycete secondary metabolite library against *M. tuberculosis* in the microplate alamar blue assay (MABA) and low-oxygen-recovery assay (LORA) led to the

---

[†]Portions of this chapter are reproduced with permission from Mullowney, M. W.; Hwang, C. H.; Newsome, A. G.; Wei, X.; Tanouye, U.; Wan, B.; Carlson, S.; Barranis, N. J.; Ó hAinmhire, E.; Chen, W.-L.; Krishnamoorthy, K.; White, J.; Blair, R.; Lee, H.; Burdette, J. E.; Rathod, P. K.; Parish, T.; Cho, S.; Franzblau, S. G.; Murphy, B. T. Diaza-anthracene antibiotics from a freshwater-derived actinomycete with selective antibacterial activity toward *Mycobacterium tuberculosis. ACS Infect. Dis.* **2015**, *1*, 168-174. Copyright 2015 American Chemical Society.

selection of Lake Michigan-derived strain B026 for further chemical investigation. A 28 L fermentation of B026 was performed, and following extraction of secondary metabolites from the fermentation broth and several chromatographic steps using bioassay-guided fractionation, 0.3 mg each of **1** and **2** were purified using RP-C_{18} semi-preparative HPLC (2.4 mL • min^{-1}, gradient of 50% aqueous ACN to 100% ACN for 25 min, followed by an isocratic flow of 100% ACN for 15 min; t_R 18.6 min, 22.0 min, respectively).

2.2.2 Structure elucidation of diazaquinomycins H (1) and J (2).

Following a series of chromatographic steps, **1** was obtained as red powder. Combined NMR and high resolution IT-TOF MS experiments of **1** established the molecular formula as $C_{22}H_{26}N_2O_4$, which was indicative of eleven degrees of unsaturation. The UV absorption profile of **1** displayed characteristics of the diazaquinomycins as previously reported.[89] Analysis revealed that **1** lacked the symmetry of the previously reported DAQA (**3**) or DAQC (see Chapter 3).[90-92] A resonance at δ_H 7.00 (2H, H-3, H-6) observed in the ^{1}H NMR spectrum, determined by integration to represent two hydrogens, indicated a less substituted anthraquinone compound when compared to known DAQs. A triplet signal at δ_H 3.13 (2H, H-12) indicated one β-substituted methylene group and a singlet at δ_H 2.77 (3H, H-11) revealed one aromate-bound, β-substituted methyl group. A doublet with an integration of six at δ_H 0.87 (6H, H-19, H-20) and a methine multiplet resonance at δ_H 1.53 (1H, H-18) provided evidence of the isononyl group. Multiplet signals at δ_H 1.60 (2H, H-13), δ_H 1.47 (2H, H-14), δ_H 1.35 (2H, H-15), δ_H 1.31 (2H, H-16) and δ_H 1.19 (2H, H-17) were indicative of the methylene groups that constituted the remainder of the aliphatic side chain.

Analysis of ^{13}C NMR data suggested the presence of two quinone carbonyls (δ_C 180.1, C-10; 172.9, C-9), two near overlapping lactam carbonyls (δ_C 163.2 and 163.0; C-2 and C-7), two methine alkene carbons (δ_C 127.6, C-6; 128.6, C-3), six quaternary carbons, two of which were interchangeable (δ_C 160.1, C-5; 155.6, C-4; 136.3 and 136.8, C-8a and C-9a; 118.0, C-4a; 117.5,

C-10a), six methylene carbons, three of which were overlapping (δ_C 39.1, C-17; 35.0, C-12; 29.7, C-15; 29.7, C-14; 29.7, C-13; 27.4, C-16), and three methyl carbons (δ_C 23.1, C-11; 22.8, C-19 and C-20) (Table 2). Given that the molecular formula afforded 11 degrees of unsaturation and the molecule contained 4 carbonyls, 6 quaternary alkene carbons, and 2 methine alkene carbons, the remaining degrees were satisfied by the fused ring system. Key HMBC, COSY, and 1D-TOCSY correlations are given in Figure 4. Interpretation of COSY and 1D-TOCSY data defined one distinct aliphatic spin system (H_2-12 to H_3-20). Connectivity of the aliphatic side chain and the methyl group to opposing β-substituted positions of the core ring system was established using HMBC correlations (Figures 4 and A23).

HMBC correlations between H_3-11 and C-3, C-4 and C-4a, as well as correlations between the H_2-12 and C-5, C-6, C-10a gave evidence for the connectivity of the alkyl groups to opposing sides of the anthracene core skeleton of **1**. Two lactam carbonyl resonances, C-2 and C-7, were observed in the ^{13}C DEPTQ spectrum; due to overlap it was not possible to distinguish between them in an HMBC experiment (Table 2). Similarly, two quaternary carbon resonances, C-8a and C-9a, were observed in the ^{13}C DEPTQ spectrum but were indistinguishable by an HMBC experiment. This NMR data, coupled with MS data, confirmed the presence of methyl and isononyl β-substituents on either lactam ring confirming the structure of **1** is as shown (Figures 3 and 4).

Following a series of chromatographic steps, **2** was obtained as red powder. Combined NMR and high resolution IT-TOF MS experiments of **2** established the molecular formula as $C_{23}H_{28}N_2O_4$, which was indicative of eleven degrees of unsaturation. Analysis of the UV absorption profile and ^{1}H NMR data of **2** indicated that it was also an asymmetric diazaquinomycin analog similar to **1**.[89] Additional structure elucidation of **2** was executed in the same fashion as **1**, using a similar series of MS and one- and two-dimensional NMR experiments, including

1D-TOCSY, to identify the 14 Da increase in molecular weight as an additional methylene in the aliphatic side chain (Figures A27-33).

Table 2. ^{1}H and ^{13}C NMR chemical shift data ($CDCl_3$–1% CF_3CO_2D) of **1** and **2**.

Position	**1**		**2**	
	^{13}C [a]	^{1}H mult. (J, Hz) [b]	^{13}C [a]	^{1}H mult. (J, Hz) [b]
1		8.05 s		8.03 s
2	163.2 [d]		161.0	
3	128.6	7.00 s	128.9 [c]	6.93 s
4	155.6		154.6	
4a	118.0		118.3	
5	160.1		160.2 [c]	
6	127.6	7.00 s	128.0 [c]	6.93 s
7	163.0 [d]		160.9 [c]	
8		8.05 s		8.03 s
8a	136.3 [e]		136.2	
9	172.9		173.0	
9a	136.8 [e]		136.8	
10	180.1		180.0	
10a	117.5		117.8	
11	23.1	2.77 s	23.0	2.74 s
12	35.0	3.13 t (7.7)	35.0	3.10 t (7.0)
13	29.7 [f]	1.60 p (7.5)	29.9	1.59 m
14	29.7 [f]	1.47 p (7.4)	29.8	1.45 m
15	29.7 [f]	1.35 m	29.7	1.35 m
16	27.4	1.31 m	29.6	1.31 m
17	39.1	1.19 q (6.9)	27.5	1.28 m
18	28.1	1.53 m	39.1	1.17 m
19	22.8	0.87 d (6.6)	28.1	1.52 m
20	22.8	0.87 d (6.6)	22.8	0.86 d (6.6)
21			22.8	0.86 d (6.6)

[a] 226.2 MHz; [b] 900 MHz; [c] shifts obtained through HMBC and/or HSQC NMR experiments; [d, e, f] shifts indistinguishable by HMBC and HSQC NMR experiments. s = singlet; t = triplet; q = quartet; p = pentet; m = multiplet.

Figure 3. Structures of diazaquinomycins H (**1**), J (**2**), and A (**3**).

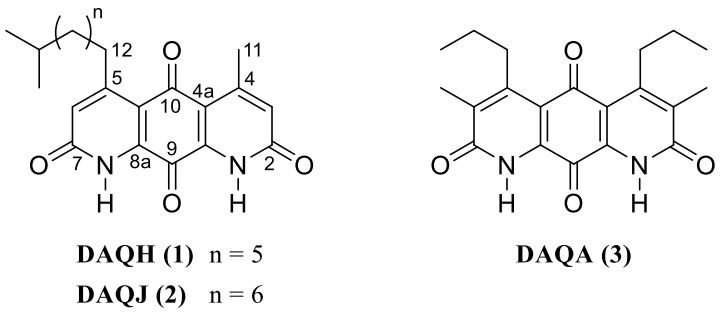

Figure 4. Key 2D NMR Correlations of **1** and **2**.

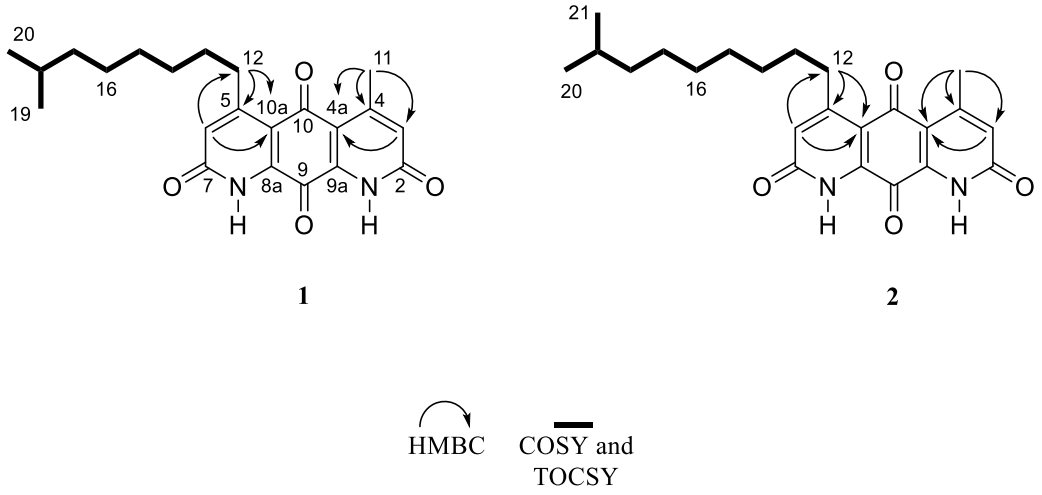

2.2.3 *In vitro* evaluation of diazaquinomycins H (1), J (2), and A (1) in TB whole-cell assays.

Once compounds **1** and **2** were identified, Chang Hwa Hwang in the ITR tested their ability to inhibit replicating *M. tuberculosis in vitro* using the MABA. The MABA is a phenotypic whole cell-based microplate dilution assay that employs a fluorometric readout, relying on the correlation of resazurin dye reduction to bacterial proliferation.[93, 94] Compounds **1** and **2** exhibited minimum inhibitory concentrations (MICs; defined as the lowest concentration resulting in ≥90% growth

inhibition of $H_{37}Rv$, and averaged from triplicates) of 0.10 μM and 0.18 μM, respectively. A luminescence reporter gene assay (LuxABCDE driven by P_{hsp60}) was used to confirm that activity of **1** and **2** was not readout dependent. Further biological characterization of **1** and **2** was difficult, since a 28 L fermentation afforded only 0.3 mg of each. Fortunately, in a separate study discussed in Chapter 3, we isolated and identified four analogs of the diazaquinomycin antibiotic class from a marine-derived *Streptomyces* sp.[89] DAQs F and G were a co-eluting isomeric mixture but DAQA (**3**) and DAQE were purified and screened in the MABA, exhibiting MICs of 0.28 μM and 0.10 μM, respectively. From this strain, compound **3** was produced in relatively large amounts, thus all further biological experiments were carried out using this molecule. Moving forward, the solubility of **3** was an important consideration in all biological testing. DAQA exhibited a maximum room temperature concentration of 0.42 μM in water in a previous study and 1.7 mM in DMSO in the current study.[95]

Compound **3** was also tested for its ability to inhibit non-replicating *M. tuberculosis* in the LORA.[96] Low-oxygen adapted *M. tuberculosis* carrying the luxABCDE plasmid was exposed for 10 days to serially diluted **3** in 96-well microplates in a low oxygen environment created with an Anoxomat commercial system. After 28 hours normoxic "recovery," activity was assessed using the ability to block recovery of the production of a luminescent signal. The MIC value of **3** was 2.03 μM.

As a confirmatory approach for its anti-TB activity, the minimum bactericidal concentration (MBC_{99}; defined as the lowest concentration that reduces CFU by 99% relative to the zero-time inoculum) was determined for **3** by subculture onto 7H11 agar just prior to addition of the Alamar Blue and Tween™ 80 for MABA MBC_{99}, and reading of luminescence on Day 10 from a lux reporter strain for LORA MBC_{99}. Compound **3** exhibited an MBC_{99} of 1.04 μM under normoxic conditions, but did not exhibit a significant MBC_{99} under hypoxic conditions.

2.2.4 Cytotoxicity evaluation of diazaquinomycins H (1), J (2), and A (1).

To assess the cytotoxicity of the DAQ class, compounds **1**-**3** were tested *in vitro* against Vero cells (ATCC CRL-1586) in the ITR by Baojie Wan. They did not exhibit cytotoxicity at 10 μg/mL, the highest testing concentration. Insufficient yields of **1** and **2** prevented further cytotoxicity screening of these compounds, however compound **3** exhibited a range of LC_{50} values when screened against a panel of human cancerous [MDA-MB-435 (0.09 μM), MDA-MB-231 (3.6 μM), HT-29 (5.7 μM), OVCAR3 (0.48 μM), OVCAR4 (4.3 μM), Kuramochi (9.4 μM)], and non-cancerous cell lines [MOSE (7.8 μM), MOE (>28 μM)] in the Joanna Burdette lab by Wei-Lun Chen. Compound **3** was also tested in a previous study against ovarian cancer cell line OVCAR5 and exhibited an LC_{50} value of 8.8 μM.[89] After further investigation, we determined that the moderate cytotoxicity in this cell line was due to DNA damage followed by the induction of apoptosis.[89] A previous report indicated that compound **3** and DAQC exhibited no significant inhibition when screened for anti-fungal activity against *Mucor miehei* and *Candida albicans*.[90] We also assessed the ability of **3** to inhibit the growth of *Candida albicans* (ATCC 90028) in the ITR, but no significant activity was exhibited when tested at the highest concentration of 28.24 μM.

2.2.5 Antibiotic specificity of diazaquinomycin A (3) toward *M. tuberculosis*.

In order to assess the ability of DAQA to overcome antibiotic resistance in TB and to gain potential insight into the mechanism of action (MOA) for this compound class, we screened **3** against a panel of mono-drug-resistant strains using the MABA (Table 3). Compound **3** maintained potency across the panel, which suggested the absence of cross-resistance with current anti-TB agents.

Table 3. In vitro activity of **3** against a drug-resistant *M. tuberculosis* panel.

		MIC (μg/mL)					
		3	**RMP** [a]	**INH** [b]	**SM** [c]	**KM** [d]	**PA824** [e]
$H_{37}Rv$	MABA	0.10	<0.08	0.05	0.12	0.65	0.01
	LORA	0.72	0.85	>13.7	1.10	–	–
Drug-resistant *M. tuberculosis* strains	rRMP	0.27	>2.00	0.02	0.27	0.92	0.03
	rINH	0.13	0.01	>2.00	0.46	0.95	0.03
	rSM	0.17	0.03	0.02	>2.00	0.95	0.11
	rKM	0.06	<0.01	0.03	1.20	>2.00	0.19
	rCS	0.14	<0.01	0.01	0.41	0.98	0.12

[a] RMP = Rifampin; [b] INH = Isoniazid; [c] SM = Streptomycin; [d] KM = Kanamycin; [e] PA824 = nitroimidazole antibiotic pretomanid. rRIF (ATCC 35838); rINH (ATCC 35822); rSTR (ATCC 35820); rCS (cycloserine; ATCC 35826); rKM (ATCC 35827).

In order to assess the specificity of **3** toward *M. tuberculosis*, the compound was screened in the ITR by Baojie Wan and Sang Hyun Cho against a panel of non-tuberculosis mycobacteria using broth microdilution with a spectrophotometric readout at A_{570} (Table 4). Interestingly, **3** exhibited selectivity toward *M. tuberculosis* and the closely related *M. bovis* BCG (MIC of 0.34 μM).

In the first reports of the diazaquinomycin class, screening of **3** and its 9,10-dihydro derivative, DAQB, against a panel of bacteria revealed a relatively weak MIC of 6.25 μg/mL against three *Staphylococcus aureus* strains (FDA209P, ATCC 6538P, KB199) and *Streptococcus faecium* IFO3181, while exhibiting a MIC of 1.13 μg/mL against *Micrococcus luteus*.[91, 92] In the current study, screenings in our own lab by Skylar Carlson as well as collaborations with the labs of Larry Dangizer and Hyunwoo Lee allowed us to determine the MICs of **3** against a diverse panel of Gram-negative and Gram-positive pathogens.[97] Compound **3** did not exhibit significant inhibitory activity toward Gram-negative bacteria and showed weak inhibitory activity against the

Gram-positive bacteria tested. The results of this study and of previous reports indicate that **3** possesses a narrow spectrum of activity, and shows greatest inhibition toward the pathogen *M. tuberculosis*.

Table 4. Antimicrobial spectrum of **3**.[a]

		MIC (μg/mL)
		3
Mycobacteria	*M. abscessus*	> 7.5
	M. chelonae	> 7.5
	M. marinum	> 7.5
	M. kansasii	> 7.5
	M. avium	3.85
	M. smegmatis	4.56
	M. bovis	0.12
G+ [e]	MSSA[b]	4
	MRSA[c]	16
	E. faecalis	8
	E. faecium	8
	VRE[d]	32
	S. pyogenes	> 25
	S. pneumoniae	> 10
	B. thuringiensis	25
	B. cereus 14579	25
	B. cereus 10987	12.5
	B. anthracis	6.25
	B. subtilis	100
G- [f]	*A. baumannii*	128
	E. coli	128
	E. cloacae	64
	K. pneumoniae	128
	P. aeruginosa	128
	P. mirabilis	64

[a] ATCC designations are listed in the Supporting Information; [b] methicillin-sensitive *S. aureus*; [c] methicillin-resistant *S. aureus*; [d] vancomycin-resistant *E. faecium*; [e] Gram-positive bacteria; [f] Gram-negative bacteria.

2.2.6 Caco-2 permeability and liver microsome stability of diazaquinomycin A (3).

Compound 3 was incubated at 1 μM for 30 min with 0.5 mg/mL of human and mouse liver microsomes and resulted in 96% and 98% of the parent compound remaining, respectively. In addition, to predict absorption via oral administration, Caco-2 bi-directional permeability was performed by incubating 5 μM of **3** (with vinblastine and propranolol controls) and measuring apical and basolateral concentrations using tandem LCMS. Compared to control compounds, **3** exhibited moderate absorption showing a permeability of 44 nm/s with 82% recovery (from apical to basolateral), and 9 nm/s with 98% recovery (from basolateral to apical), and no efflux substrate potential (0.2 efflux ratio).

2.2.7 *In vivo* evaluation of diazaquinomycin A (3).

Yuehong Wang of the ITR collaborated with the Toxicology Research Laboratory (TRL) at UIC to perform a tolerance assessment of **3** as our first *in vivo* study. It was previously published that **3** deposited solid residues and exhibited acute toxicity when dosed at 100 mg/kg intraperitoneally (IP),[91, 95] though in our study the compound exhibited no qualitatively detectable ill effect and was well tolerated when dosed daily by oral gavage at 100 mg/kg for five days in uninfected mice. While it is possible this difference was due to limited oral bioavailability, our Caco-2 data predicted otherwise.

A subsequent study also in collaboration with the TRL aimed to assess pharmacokinetics (PK) of **3** in mouse lungs and plasma. Dosing twenty-four seven- to ten-week old male Balb/c mice with **3** followed by analysis at half-, one-, two-, and four-hour time points resulted in observation of DAQA in lungs and plasma by LC-MS. The greatest concentrations were seen at two hours, though none of the time points resulted in concentrations that could be observed above the LC-MS limit of quantitation (LOQ). Interestingly, the internal standard, tetramethyl-diazaquinomycin (**4**), was also frequently below the LOQ when extracted from matrices but not

when injected in clean ACN indicating that DAQ solubility was likely a cause. In addition to dosing of 100 mg/kg in 10 µL/kg vehicle by oral gavage, half of the mice were dosed at 50 mg/kg in 5 µL/kg vehicle intraperitoneally. Similar to the toxicity study, mice dosed by oral gavage remained healthy throughout all PK time points, while acute toxicity evidenced by hunched posture, closed eyes, decreased activity, and a rough coat followed dosing by IP, which was in accord with the earlier mentioned reports.[91, 95]

Despite the lack of conclusive data in the PK study, we progressed to *in vivo* studies of **3** to examine efficacy in TB-infected mice in collaboration with Carolyn Shoen in the lab of Michael Cynamon. Unfortunately, the vehicle was found to be toxic when two control mice died after four days, so the experiment failed to produce conclusive results.

2.2.8 Optimization of diazaquinomycin A (3) for increased solubility and potency against *M. tuberculosis*.

Stocks of **3** purified from strain F001 had been greatly depleted in the course of our extensive biological screening campaign, justifying synthesis of the compound. Dr. Larry Klein of the ITR at UIC optimized the published diazaquinomycin A total synthesis to increase the supply of compound for future biological studies and synthetic derivative generation (Figure A34).[98] Along with production of **3**, two novel analogs with α- and β-modifications were generated, resulting in tetramethyl-diazaquinomycin (**4**) and bis-normethyl-diazaquinomycin A (**5**; Figure 5).

Figure 5. Structures of tetramethyl-diazaquinomycin (**4**) and bis-normethyl-diazaquinomycin A (**5**).

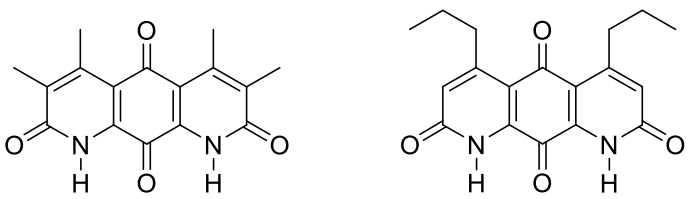

4 **5**

From the renewed DAQA stock, a series of analogs were generated based on published syntheses with the aim of exploring structure-activity relationships (SAR) and investigating positions for 'clickable' and photo-reactive moieties for target capture and pull-down. These studies also had the goal of improving the solubility and anti-tuberculosis activity of **3** (Figures 6 and 7).[92, 95] Bismorpholino DAQA (**6**) was the synthetic target for the generation of a DAQ analog

Figure 6. Synthesis of α-substituted and O-methylated diazaquinomycin analogs.

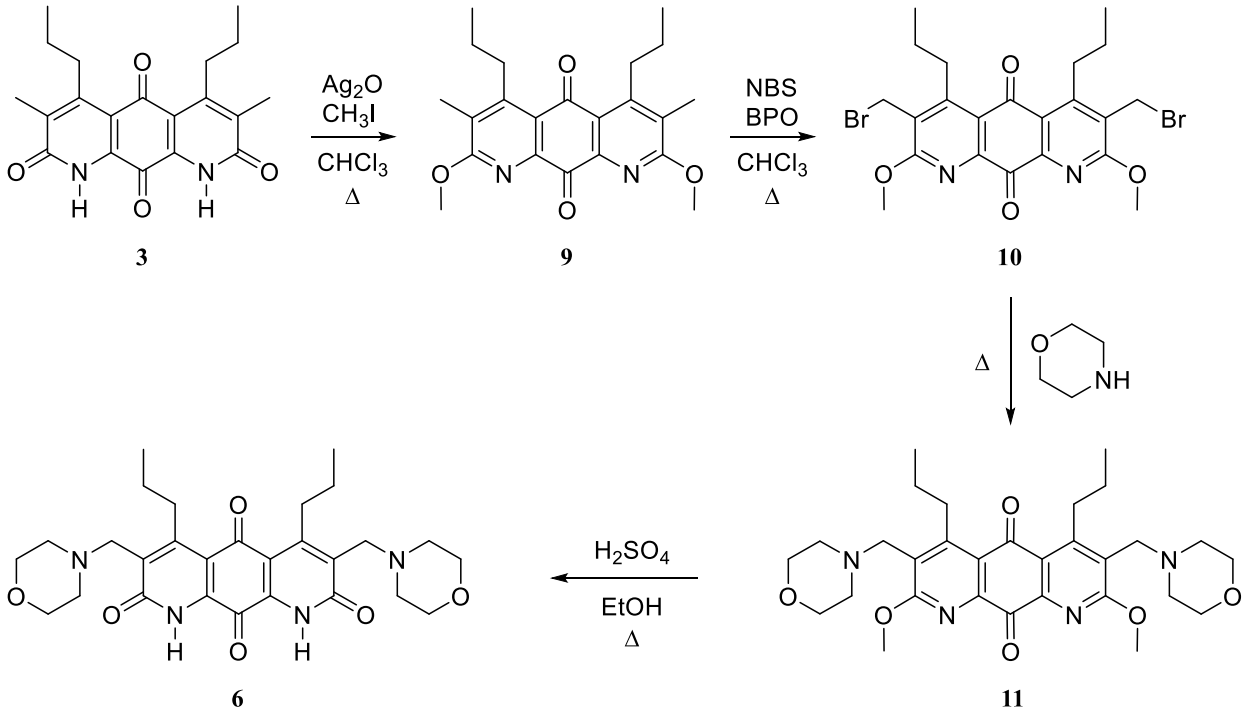

modified to add bulk to the α-position (NMR spectrum Figure A39). In a separate reaction, N,N'-bismethyl DAQA (**7**) was synthesized along with its side product N,O-bismethyl DAQA (**8**) in a 2:1 ratio in order to explore the role of the N-H groups in bioactivity (NMR spectra Figures A40 - A41). Compound **6**, its three synthetic precursors bismethoxy DAQA, **9**; bisbromo-bismethoxy DAQA, **10**; and bismethoxy-bismorpholino DAQA **11**; NMR spectra Figures A35 – A40), and the two methylated analogs all exhibited qualitatively greater organic solubility

but were orders of magnitude less active than DAQA against *M. tuberculosis* in the MABA. Both compounds **4** and **5** retained the activity exhibited by the isolated DAQ natural products (Table 5).

Figure 7. Synthesis of **7** and **8**.

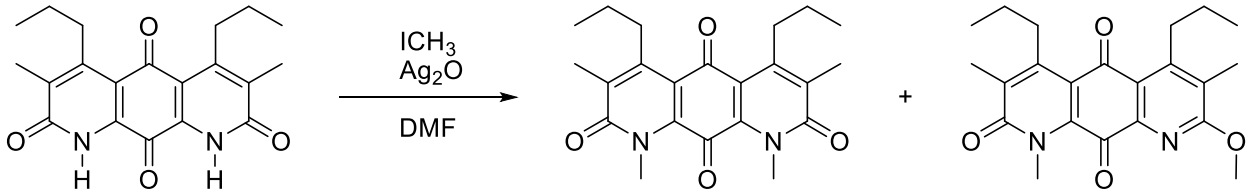

3 7 8

Table 5. In vitro anti-TB activity of **4**-**11**.

Compound	$H_{37}Rv$ MIC (μg/mL)
	MABA
4	0.06
5	0.07
6	2.69
7	>50
8	6.0
9	22.8
10	>10
11	8.63

Although modifications at the α-position were detrimental to DAQ activity, **4**, **5**, and the five actinomycete-derived DAQs provided evidence that the presence or absence of α-methyl groups and the number and length of carbons at the β-substituted side chains do not effect change in anti-TB activity. With this in mind, we set out to modify the β-substituted positions with groups other than variations in carbon bulk. Several failed attempts made it apparent that both the

published and Klein-optimized syntheses of **3** precluded the possibility of introducing reactive species to the β-substituted side chains due to a highly oxidative, high heat, H_2SO_4 penultimate synthetic step. Klein, in collaboration with Mr. Michael Tufano also of the ITR at UIC, attempted to circumvent this problematic step by developing an entirely new DAQA total synthesis that would facilitate modification of the DAQ core at the β-substituted positions, but was unsuccessful.

An alternative approach was attempted when observation that some hydroxylase enzymes, specifically those from *Pseudomonas putida* GPo1 and *Mycobacterium sp.* HXN-1500, had the ability to catalyze hydroxylation of terminal alkanes and might have potential for producing novel β-hydroxylated DAQA products.[99-101] To explore the possibility of a whole-cell biocatalysis method, plasmids containing hydroxylase genes from the aforementioned strains were acquired from Christian Willrodt of the Andreas Schmid lab and *E. coli* transformants were generated. Unfortunately, lack of evidence for biocatalysis products in the MS total ion chromatograms of the *E. coli* clone extracts and failed bioconversion of the positive control substrates indicated that the experiment was unsuccessful.

2.2.9 Studies toward elucidation of the diazaquinomycin mechanism of action.

Given its mild reported antibiotic activity in *E. faecium*, observation of potency against *M. tuberculosis* provided sufficient motivation for us to further explore the DAQA biological MOA. It was reported that the antibacterial activity of **3** was reversed when folate, dihydrofolate, leucovorin, and thymidine were added to the growth medium, suggesting that the target was within the folate pathway.[102] Shortly after its discovery, previous studies claimed that **3** inhibited thymidylate synthase competitively with its coenzyme 5,10-methylenetetrahydrofolate in both *E. faecium* and Ehrlich ascites carcinoma, with *Ki*'s of 36 μM and 14 μM, respectively.[102] Thymidylate synthase is an attractive target as it plays a crucial role in DNA replication and repair by synthesizing *de novo* deoxythymidine monophosphate (dTMP) from deoxyuridine

monophosphate (dUMP). *M. tuberculosis* encodes for two structurally and mechanistically unrelated thymidylate synthase enzymes, ThyA and ThyX. ThyA occurs across kingdoms, while ThyX has been found to occur only in bacteria and has been associated with survival of *Corynebacteriaceae* during the stationary growth phase.[103, 104] Thus, we attempted to determine which of these enzymes, is any, was the antibiotic target.

Through a collaboration with the Rathod lab at the University of Washington, we found that **3** did not significantly inhibit the activity of purified human ThyA (HsThyA), *M. tuberculosis* ThyA (MtThyA), or MtThyX when compared to the positive control – folate analog and known ThyA inhibitor 1843U89 – when tested in a cell-free enzyme assay (Figures A17-A18).[105] To rule out the possibility of **3** being metabolized to a biologically active species within the cell, we collaborated with the Tanya Parish lab at the Infectious Disease Research Institute (IDRI) to perform *in vitro* testing against *M. tuberculosis thyA* and *thyX* overexpression (OE) mutants. We did not observe a significant differential in the MIC when **3** was screened against *M. tuberculosis thyA* and *thyX* OE mutants under induced (+anhydrotetracycline) and uninduced (-anhydrotetracycline) conditions, compared to the H_{37}Rv wild-type strain (Figure A19). Additionally, we observed no reversal of the antibiotic properties of **3** when the culture media was supplemented with thymine or thymidine, indicating that there was likely no disruption in the thymidylate synthase related enzymatic processes of the folate pathway.

Figure 8. Summary of experiments performed to determine DAQA mechanisms of action.

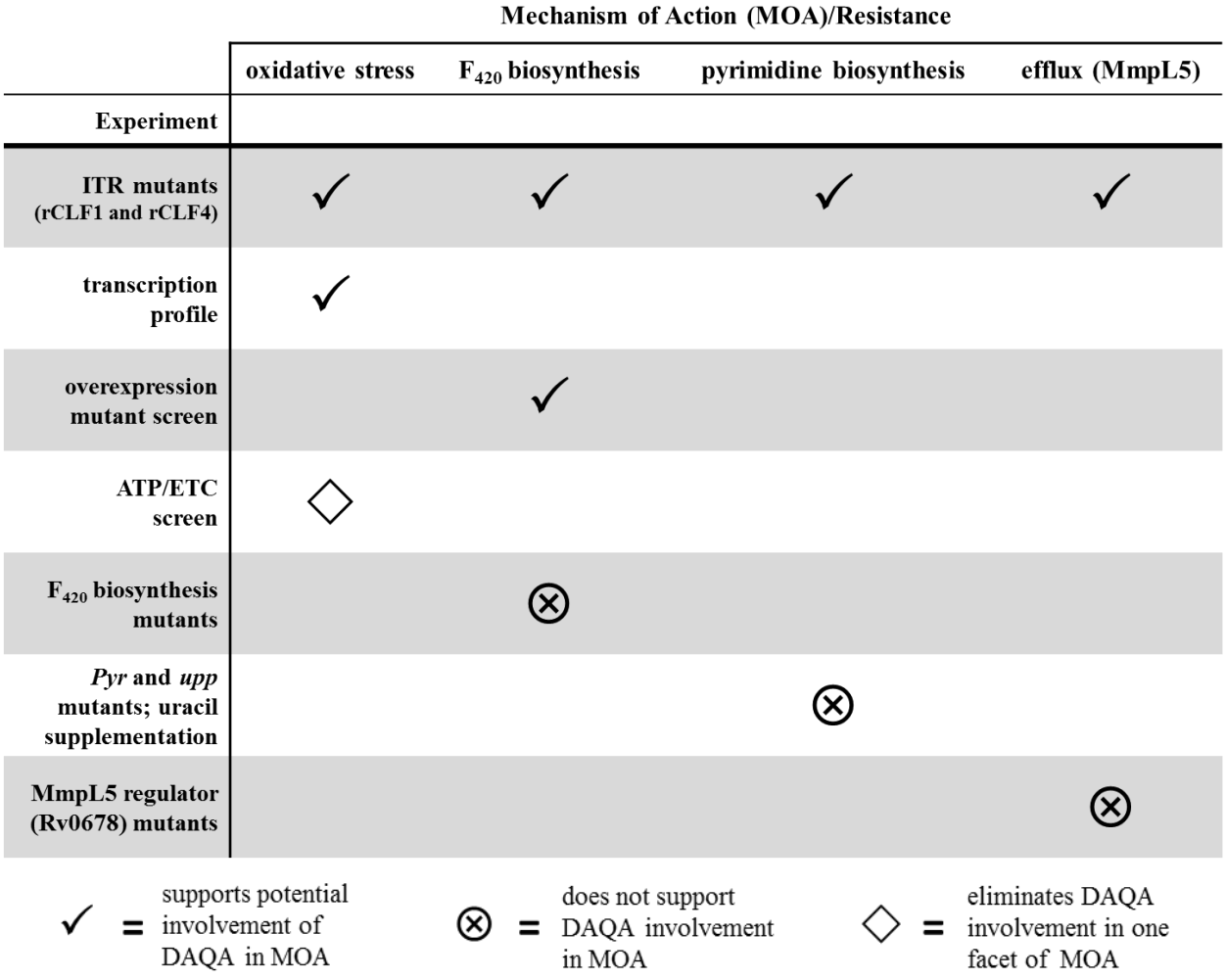

Having eliminated the possibility that DAQA targets thymidylate synthase as it had been reported for other organisms, we set out to establish the mechanism of inhibition in *M. tuberculosis*. Initially, we attempted to directly capture a molecular target of **3** using the DARTS method, but that proved unfruitful (Appendix A2.1.1).[106, 107] Later, approaches using overexpression mutant screening, transcription profiling, and a screening against clofazimine-resistant mutant strains (rCLF1 and rCLF4) revealed potential mechanisms of action involving oxidative stress, F_{420} biosynthesis, pyrimidine biosynthesis, and MmpL5 efflux. We set out to confirm each of these with additional targeted experiments. Aside from gaining a minimal

understanding of a potential inhibition by oxidative stress, we were unable to confidently identify a singular molecular target using the experiments as detailed herein (Figure 8).

2.2.9.1 diazaquinomycin A (3) activity against a library of *M. tuberculosis* overexpression mutants.

Following elimination of a Thy mechanism, we decided to use the broad approach of screening against the remainder of the *M. tuberculosis* OE mutant library at the IDRI. The *M. tuberculosis* OE mutant library screen is designed to identify the targets of novel compounds or the mechanism of resistance to compounds in *M. tuberculosis*. This approach is based on the concept that if the target of a compound is over-expressed, the bacteria will be more resistant to that compound. By screening a library of clones that over-express individual proteins, it is possible to identify the target or the mode of resistance of that compound. DAQA was screened against a library of approximately 1700 recombinant *M. tuberculosis* clones that each over-express an individual protein under the control of an anhydrotetracycline (ATc) responsive promoter. The mutant library included predicted essential proteins [the majority predicted by transposon site hybridization (TraSH)], as well as efflux pumps, regulatory proteins, and other proteins of interest.

The entire library was treated with DAQ-A at 2.75 µM, five times the MIC of 0.55 µM determined at the IDRI against *M. tuberculosis* H_{37}Rv wild-type (London Pride strain) in the presence and absence of ATc.[108] Growth was estimated by measuring the OD_{590} at day five with compound and DMSO vehicle only and calculating the ratio. Clones that exhibited increased growth over the mean and sufficient growth with DMSO were considered to express potential targets and were selected for further study. Resistant clones were defined as those with a growth ratio of ≥ 3 standard deviations above the mean or ≥ 0.41. Following treatment with DAQA, three clones were selected for investigation. MICs were determined under both uninduced and induced conditions (±150 ng/mL ATc).

Table 6. Resistance of Rv0953c, Rv2486, and Rv3500c *M. tuberculosis* OE mutants to **3**.

Strain	Rifampin MIC (μM)		DAQ-A MIC (μM)		Fold change from WT[a]	
	Uninduced	Induced	Uninduced	Induced	Uninduced	Induced
Wild-type	0.0026	0.00	0.24	0.20	1.0	1.0
TOE Rv0953c	0.0044	0.01	0.91	1.3	3.8	6.5
TOE Rv2486	0.0017	0.00	0.40	0.42	1.7	2.1
TOE Rv3500c	0.0016	*nd*	1.4	*nd*	5.8	*nd*

[a] fold change as compared to wild-type is given as a measure of resistance. *nd* – not determined; the growth of the Rv3500c OE strain was insufficient to determine MIC in the presence of ATc.

Following screening, the Rv0953c OE mutant exhibited a shift toward resistance to DAQA, which was more pronounced after induction of expression. A second clone overexpressing Rv3500c showed resistance in uninduced conditions but induction of expression was detrimental to growth. The third clone selected for follow-up, a Rv2486 OE mutant, only showed a two-fold shift in MIC. This was deemed insignificant and the mutant deprioritized (Table 6).

Rv3500c (*yrbE4B*) encodes a putative ABC transporter predicted to be involved in lipid catabolism. It is in the *kstR* regulon, which contains some 74 genes involved in the utilization of diverse lipids for energy.[109] YrbE4B is predicted to be required for growth on cholesterol.[110] Rv0953c is predicted to be an F_{420}-dependent oxidoreductase and is also in the *kstR* regulon.[109] While Rv0953c is not yet characterized, F_{420}-bearing enzymes of this class are absent in humans, not well represented in prokaryotes, but present extensively in mycobacteria, including the reduced genome of *M. leprae*, providing an attractive, although non-essential, target.[111]

2.2.9.2 *M. tuberculosis* transcription profile following diazaquinomycin A (3) treatment.

With the aim of uncovering the DAQA MOA, we collaborated with the Clifton Barry lab of the National Institute of Allergy and Infectious Diseases at the NIH to generate a transcription profile of *M. tuberculosis* following treatment with the compound. This profile was generated

Figure 9. Transcription profile of *M. tuberculosis* following treatment with **3**.

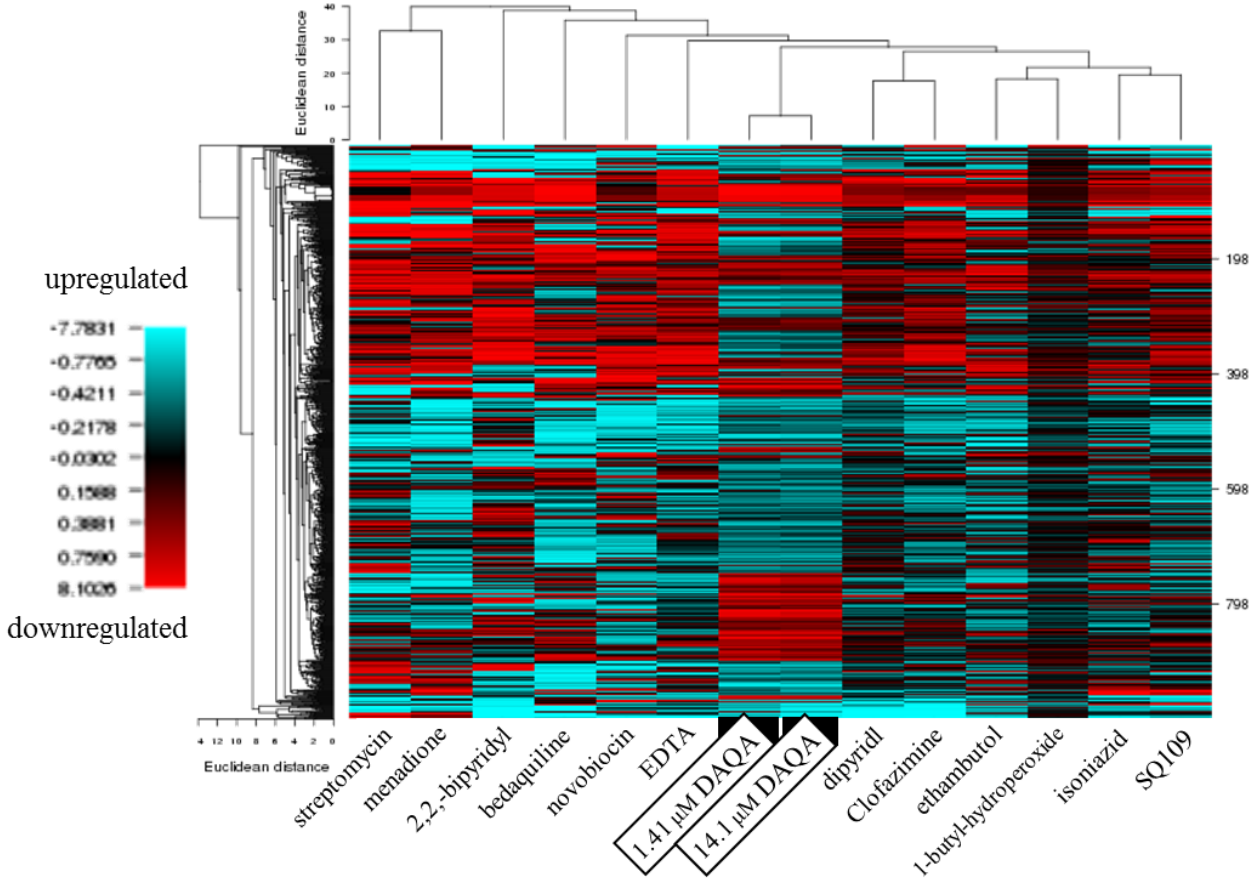

concurrently with those of well-studied TB inhibitors with the purpose of gaining insight into the DAQA MOA by comparison. The transcription pattern revealed for DAQA was consistent at the two tested concentrations, but without a close match from the known anti-TB compounds (Figure 9). Thus, no definitive conclusions about a mechanism could be inferred from these results, but some general characteristics of the DAQA mechanism could be inferred. Twenty-seven of the

thirty-two most down-regulated genes were transposases, while the most highly up-regulated genes were those coding for the peroxidase katG (Rv1908c), iron-sulfur cluster restoration, and the biosynthesis of two siderophores, mycobactin and exochelin. This combination of upregulated genes is indicative of oxidative stress while the implications of downregulated transposases are unknown.[112] In general, there was a massive oxidative stress response implicated by DAQA that was similar to that observed for known TB drugs CLF and BDQ (TMC207).[113, 114] Despite these similarities, DAQA did not have a similar effect on electron transport as CLF when tested in a separate experiment (Appendix 2.1.2).

2.2.9.3 Institute for Tuberculosis Research (ITR) clofazimine-resistant mutants are cross-resistant to diazaquinomycin A (3).

Following observation of an oxidative stress response in the microarray study, we tested whether the mechanism was iron-dependent by screening strains of *M. tuberculosis* with DAQA first on iron-depleted GAS media, then on GAS media supplemented with a range of iron concentrations from 0 to 800 μg/L. Two clofazimine resistant mutants and a bedaquiline-resistant mutant were selected for testing along with wild type in order to further assess commonality between the DAQA mechanism and that of clofazimine or bedaquiline (Table 7). While no connection between iron concentration and activity was observed, two additional observations were made.

We first observed that *M. tuberculosis* strains were more susceptible to DAQA when they were grown on GAS media at any iron concentration than when grown on 7H12 media. This phenomenon had one exception in the bedaquiline-resistant strain rTMC207 (BK12), which has a *atpE* subunit c mutation. Why DAQA activity remains consistent between media types only in this mutant is as of yet unexplained. We subsequently investigated this difference in activities between

media types for the other strains by substituting the glycerol carbon source in GAS media with the palmitic acid carbon source from 7H12 media, but were unable to identify a significant trend.

Table 7. Effect of iron concentration and nutrient composition on anti-TB activity of **3**.

		Media (ferric ammonium citrate conc., µg/L)				
Compound	**Mtb strain**	**7H12 (40)**	**GAS (0)**	**GAS (50)**	**GAS (200)**	**GAS (800)**
DAQA	$H_{37}Rv$	0.30	< 0.10	< 0.10	< 0.10	< 0.10
	rCLF1	3.00	0.50	0.33	0.38	0.37
	rCLF4	2.26	0.48	0.45	0.42	0.36
	rTMC207(BK12)	0.16	0.16	0.17	0.18	0.16
RMP	$H_{37}Rv$	0.03	0.04	0.05	0.06	0.03
	rCLF1	0.08	0.10	0.05	0.03	0.01
	rCLF4	0.03	0.03	0.03	0.01	0.01
	rTMC207(BK12)	0.01	0.03	0.01	0.01	0.02
INH	$H_{37}Rv$	0.19	0.15	0.15	0.15	0.14
	rCLF1	0.15	0.15	0.12	0.18	0.14
	rCLF4	0.29	0.12	0.52	0.29	0.20
	rTMC207(BK12)	0.15	0.08	0.13	0.14	0.13
PA-824	$H_{37}Rv$	0.10	0.22	0.54	0.72	0.39
	rCLF1	> 26	> 26	> 26	> 26	> 26
	rCLF4	> 26	> 26	> 26	> 26	> 26
	rTMC207(BK12)	0.10	0.14	0.38	0.42	0.29
TMC207	$H_{37}Rv$	0.73	0.86	0.83	0.85	0.65
	rCLF1	1.86	1.24	1.25	1.67	1.58
	rCLF4	1.59	1.81	1.58	1.70	1.64
	rTMC207(BK12)	5.97	3.29	3.28	3.21	3.09
CLF	$H_{37}Rv$	0.26	0.28	0.08	0.14	0.11
	rCLF1	2.00	1.95	1.19	1.97	1.81
	rCLF4	1.37	2.10	1.74	1.86	1.54
	rTMC207(BK12)	0.14	0.29	0.15	0.15	0.14

The second observation was that mutant strains rCLF1 and rCLF4, products of an unpublished spontaneous clofazimine-resistant mutant generation study in the ITR, exhibited a cross-resistance to DAQA with a nine-fold increase in MIC on all media types. This was a welcome discovery as we have yet to achieve generation of spontaneous *M. tuberculosis* $H_{37}Rv$ mutants resistant to DAQA for genome sequencing. Thus far, each attempt results in an abundance of phenotypically resistant colonies rather than a few truly resistant strains. These rCLF mutant strains also exhibit marked cross-resistance to PA-824 and other nitroimidazoles due to mutations

in F_{420} cofactor biosynthesis genes, which are involved in the pro-drug activation mechanism of these compounds, as well as cross-resistance to bedaquiline (TMC207) due to mutations in the MmpL5 efflux suppressor gene. [115, 116]

2.2.9.4 Diazaquinomycin A (3) activity against *M. tuberculosis* strains with efflux regulator, pyrimidine biosynthesis, and F_{420} biosynthesis gene mutations.

Upon discovery of the DAQA cross-resistant mutants rCLF1 and rCLF4, we compared the genomes of each strain with the aim of identifying a common mutation responsible for resistance. Of the eight total mutations between them, those shared were present in the MmpL5 efflux pump transcriptional repressor gene (Rv0678) and the orotate phosphoribotransferase gene (Rv0382c; *pyrE*) from the pyrimidine biosynthesis pathway, while two others were mutations in separate

Table 8. Genes and their descriptions from DAQA-resistant strains rCLF1 and rCLF4.

Gene Name		
rCLF1	**rCLF4**	**Enzyme function**
Rv0382c	Rv0382c	orotate phosphoribosyltransferase (PyrE); pyrimidine biosynthesis
Rv0678	Rv0678	MmpL5 efflux pump transcriptional repressor
	Rv3261 [a]	probable F_{420} biosynthesis protein (FbiA)
Rv1173 [a]		probable FO synthase (FbiC)
Rv2932		phenolpthiocerol synthesis type-I polyketide synthase (PpsB)
Rv0552		hypothetical amidohydrolase
	Rv0050	involved in peptidoglycan biosynthesis (PonA1)
	Rv1392	probable S-adenosylmethionine synthetase (MetK)

[a] Rv3261 and Rv1173 are separate genes but code for enzymes in the same pathway. Gray rows indicate mutations shared between ITR strains rCLF1 and rCLF4.

genes (Rv1173; *fbiC* and Rv3261; *fbiA*) within the F_{420} biosynthetic pathway (Table 8). The mutation in the Rv0678 transcription repressor allows for efflux of clofazimine and bedaquiline by the MmpL5 pump, orotate phosphoribosyltransferase (PyrE) is involved in catalyzing the synthesis of pyrimidine biosynthesis intermediate orotidine 5'-monophosphate (OMP), and F_{420} is

a flavin derivative cofactor involved in numerous bacterial redox reactions.[112,116, 117] The Rv0678 repressor and *fbiA* genes are classified as non-essential by Himar1-based transposon mutagenesis but *pyrE* and *fbiC* were found to be essential.[109, 118]

We identified strains with single-mutations of each mutation shared between the rCLF mutants. These were screened in order to confirm the role of each mutation in DAQA resistance (Table 9). Our first bioassay revealed that *M. tuberculosis* Rv0678 mutant strains from the Stewart

Table 9. Susceptibility of *M. tuberculosis* mutant strains to **3**.

	MIC (μg/mL)			
Strain	**3**	**PA824**	**CLF**	**RIF**
'Wild type' $H_{37}Rv$ [a]	0.19	0.10	0.11	0.04
efflux (Rv0678); pyrimidine biosynthesis (*pyrE*); F_{420} biosynthesis [a]				
rCLF1	2.23	> 26	2.04	0.05
rCLF4	1.25	> 26	1.17	0.04
MmpL5 efflux pump repressor (Rv0678) [a]				
$H_{37}Rv_{CFZ\text{-}R1}$	0.18	0.11	0.20	0.02
$H_{37}Rv_{CFZ\text{-}R2}$	0.09	0.13	0.24	0.04
pyrimidine biosynthesis [b]				
$H_{37}Rv$ (Mizrahi)	0.8			
MTBSRM1 [c]	0.8			
MTBSRM2 [d]	0.8			
upp::Tn [e]	0.8			
F_{420} biosynthesis [f]				
7A2 (*fbiAB*-)	0.3	>50		
5A1 (*fbiC*-)	0.2	>50		
control strains [f]				
14A1 (Rv3547-) [g]	0.3	>50		
T3 (fgd-) [g]	0.3	>50		
rRIF-BJ [h]	0.2	0.4		

[a] screened at the ITR; [b] screened in the Mizrahi lab; [c] 5-flourouracil-resistant mutant; Δa74 in *upp* causing a frameshift mutation; [d] 5-flourouracil-resistant mutant, nsSNP in pyrR, Asp91Asn; [e] transposon insertion in *upp* 5-flourouracil-resistant mutant; [f] screened in the Barry lab; [g] PA824-resistant controls; [h] rifampin-resistant Beijing strain.

Cole lab, $H_{37}Rv_{CFZ\text{-}R1}$ and $H_{37}Rv_{CFZ\text{-}R2}$,[116] were susceptible to DAQA. This all but completely nullifies the possibility that DAQA is a substrate of the MmpL5 efflux system since rCFL4 and $H_{37}Rv_{CFZ\text{-}R1}$ share gene sequence mutations while mutations in rCLF1 and $H_{37}Rv_{CFZ\text{-}R2}$ are unique.

We also screened for inhibition of the pyrimidine biosynthesis pathway in collaboration with the Mizrahi lab at The University of Cape Town. An *M. tuberculosis* strain with anhydrotetracycline-inducible expression (*pyrE* Tet-ON) was developed according to published methods to facilitate exploration of this enzyme and it's potential as a target for anti-tuberculosis treatment.[119] Interestingly, no sensitivity was observed in the *pyrE* Tet-ON mutant when it was treated with DAQA in the absence of anhydrotetracycline. Importantly, this strain is unstable and so far, not validated for PyrE conditional expression level. These negative results were supported when 0.39 to 100 µM concentrations of uracil, a downstream product of the PyrE enzyme, were unable to rescue H_{37}Rv treated with DAQA. In a previous report, the Mizrahi lab described the anti-tuberculosis activity of 5-flourouracil (5-FU) and its MOA within the pyrimidine biosynthesis salvage pathway.[119] With this in mind, we screened DAQA and 5-FU in combination against TB with the aim of identifying synergy that would suggest pyrimidine biosynthesis inhibition, but no synergy was observed between the tested 5-FU concentrations of 0.39 to 100 µM. Pyrimidine salvage pathway mutant strains, MTBSRM1 and MTBSRM2, were also screened and both were susceptible. The observed MICs in all Mizrahi lab screenings were slightly greater than the reported MIC (0.1 µg/ml) possibly due to the strain difference and/or precipitation of the compound, which was observed in test wells containing the highest concentrations of 6.4 and 3.2 µg/ml. Together, these studies eliminate the possibility that the DAQA mechanism involves disruption of pyrimidine biosynthesis despite the *pyrE* gene mutation presence in both of the ITR rCLF mutant strains. This left one remaining possibility.

Having nearly eliminated the shared mutations between rCLF1 and rCLF4 in Rv0678 and *pyrE* as target candidates, we then decided to explore whether mutations shared in F_{420} biosynthesis were indicative of inhibition of that pathway by **3**. Possible additional support for F_{420} involvement was found when the gene for the putative F_{420}-dependent Rv0953c protein was a target candidate

revealed in the aforementioned OE panel screening at the IDRI. Surprisingly, these final mutations were also eliminated as possible target candidates when DAQA was able to inhibit *M. tuberculosis* strains 7A2 (*fbiAB*-) and 5A1 (*fbiC*-) with the same potency as the wild type when tested through a collaboration with the Clifton Barry lab at the NIH. Additional screenings against environmental actinomycetes based on the recognition that these microbes also utilize biochemical pathways dependent on F_{420} show some promise of assisting with MOA studies but were incomplete and inconclusive regarding the role of F_{420} (Appendix A2.1.3).

2.3 Methods.

2.3.1 General experimental procedures for the isolation and characterization of diazaquinomycins H (1) and J (2).

UV spectra were measured on a Shimadzu Pharma Spec UV-1700 spectrophotometer. NMR spectra were obtained on a Bruker 600 MHz DRX NMR spectrometer equipped with an inverse 5 mm TXI cryogenic probe with z-axis pfg and XWINNMR version 3.5 operating software, and a 900 (226.2) MHz Bruker AVANCE NMR spectrometer equipped with an inverse 5 mm TCI cryogenic probe with z-axis pfg and TopSpin version 1.3 operating software at the University of Illinois at Chicago Center for Structural Biology. Chemical shifts (δ) are given in ppm and coupling constants (*J*) are reported in Hz. ^{1}H and ^{13}C NMR resonances of **1** and **2** are reported in Table 2. ^{1}H and ^{13}C NMR chemical shifts were referenced to the $CDCl_3$ with vapor TFA solvent signals (δ_H 7.26 ppm and δ_C 77.0 ppm, respectively). High resolution mass spectra (HRMS) were obtained on a Shimadzu IT-TOF LC-MS spectrometer at the University of Illinois at Chicago Research Resources Center. High-performance liquid chromatography (HPLC-UV) data were obtained using a Hewlett-Packard series 1100 system controller and pumps with a Model G1315A diode array detector (DAD) equipped with a reversed-phase C18 column (Phenomenex Luna, 100 × 4.6 mm, 5 μm) at a flow rate of 0.5 mL • min^{-1}. Semi-preparative scale HPLC separations were performed using a Hewlett Packard Series 1050 system with a Phenomenex Luna

semi-preparative C18 column (250 × 10 mm, 5 μm) at a flow rate of 2.4 mL • min^{-1}. Preparative scale HPLC separations were performed using a Waters LC4000 System equipped with a Phenomenex Luna preparative C18 column (250 × 21.2 mm, 5 μm) at a flow rate of 16 mL • min^{-1}. Silica gel column chromatography was conducted using Bonna-Angela Technologies Cleanert® silica gel with an average particle size of 40-60 μm and an average pore size of 60 Å.

2.3.2 Collection and identification of actinomycete strain B026.

Strain B026 was isolated from a sediment sample collected by PONAR at a depth of 56 m, from ca. 16.5 miles off the coast north of Milwaukee, WI in Lake Michigan (43°13′27″ N, 87°34′12″ W) on August 23, 2010. Strain B026 (GenBank accession number KP009553) shared 100% 16S rRNA gene sequence identity with the type strain *Micromonospora maritima* strain D10-9-5 (GenBank accession number NR109311).[120]

2.3.3 Fermentation and extraction.

Strain B026 was grown in 28 × 1 L portions in Fernbach flasks containing high nutrient A1 medium (0.5 L of filtered Lake Michigan water, 0.5 L DI water, 10 g starch, 4 g yeast extract, 2 g peptone, 1 g calcium carbonate, 100 mg potassium bromide, and 40 mg iron sulfate) for 5 days at 21 °C while shaking at 220 rpm. Sterilized Amberlite XAD-16 resin (15 g·L−1) was added to each flask to absorb the extracellular secondary metabolites. The culture medium and resin were shaken for 8 h and filtered using cheesecloth to remove the resin. The resin, cell mass, and cheesecloth were extracted with acetone overnight, concentrated under vacuum, and partitioned between water and ethyl acetate. The organic layer was dried under vacuum to afford 1.1 g of extract.

2.3.4 Isolation and characterization of diazaquinomycin H (1) and diazaquinomycin J (2) from strain B026 fermentation broth.

Strain B026 was grown in 28 L for 5 days at 21 °C while shaking at 220 rpm. The extracellular secondary metabolites were absorbed from the fermentation broth using Amberlite

XAD-16 resin, followed by extraction with acetone, and partitioning between water and ethyl acetate. The organic layer was dried under vacuum to afford 1.1 g of extract.

The organic layer from the liquid-liquid partition was fractionated using silica gel flash column chromatography (100 g of silica) eluting with an isocratic 95% chloroform ($CHCl_3$):5% methanol (MeOH) solvent system to afford 15 fractions. Using bioassay-guided fractionation, it was determined that fraction 2 contained the bioactive constituents, thus it was separated using RP-C_{18} preparative HPLC (16 mL • min^{-1}, gradient of 50% aqueous acetonitrile (ACN) to 100% ACN for 20 min, followed by an isocratic flow of 100% ACN for 10 min) to afford five fractions. Compounds **1** and **2** were observed in fractions 3 and 4, respectively.

To further isolate **1**, fraction 3 was separated using RP-C_{18} semi-preparative HPLC (2.4 mL • min^{-1}, gradient of 50% aqueous ACN to 100% ACN for 25 min, followed by an isocratic flow of 100% ACN for 15 min) to afford 4 fractions. Fraction 4 was determined to contain **1** and was further purified using RP-C_{18} semi-preparative HPLC (2.4 mL • min^{-1}, gradient of 50% aqueous ACN to 100% ACN for 25 min, followed by an isocratic flow of 100% ACN for 15 min) to afford diazaquinomycin H (**1**, t_R 18.6 min, 0.3 mg, 0.00026% yield).

To further isolate **2**, fraction 4 was separated further using RP-C_{18} semi-preparative HPLC (2.4 mL • min^{-1}, gradient of 50% aqueous ACN to 100% ACN for 25 min, followed by an isocratic flow of 100% ACN for 15 min) to afford 5 fractions. Fraction 3 was separated further using RP-C_{18} semi-preparative HPLC (2.4 mL • min^{-1}, gradient of 50% aqueous ACN to 100% ACN for 25 min, followed by an isocratic flow of 100% ACN for 15 min) to afford 5 fractions. Fraction 4 was determined to contain **2** and was further purified using RP-C_{18} semi-preparative HPLC (2.4 mL • min^{-1}, gradient of 50% aqueous ACN to 100% ACN for 25 min, followed by an isocratic flow of 100% ACN for 15 min) to afford diazaquinomycin J (**2**, t_R 22.0 min, 0.3 mg, 0.00026% yield).

Diazaquinomycin H (1): Red solid (0.3 mg). UV (MeOH) λ_{max} (log ε) = 278 (3.83), 301 (3.72), 357 (3.26) and a broad absorption with maximum at 472 (2.59) nm. ^{1}H NMR (900 MHz, $CDCl_3$ - 1% CF_3CO_2D) and ^{13}C NMR (226.2 MHz, $CDCl_3$ - 1% CF_3CO_2D), see Table 2. HR-ESI-IT-TOF MS *m*/*z* 383.1993 $[M + H]^+$ (calcd. for $C_{22}H_{27}N_2O_4$: 383.1971), *m*/*z* 381.1771 $[M - H]^-$ (calcd. for $C_{22}H_{25}N_2O_4$: 381.1820), *m*/*z* 765.3778 $[2M + H]^+$ (calcd. for $C_{44}H_{53}N_4O_8$: 765.3863) and *m*/*z* 763.3639 $[2M - H]^-$ (calcd. for $C_{44}H_{51}N_4O_8$: 763.3712).

Diazaquinomycin J (2): Red solid (0.3 mg). UV (MeOH) λ_{max} (log ε) = 278 (3.37), 300 (3.26), 356 (2.90) and a broad absorption with maximum at 472 (2.44) nm. ^{1}H NMR (900 MHz, $CDCl_3$ - 1% CF_3CO_2D) and ^{13}C NMR (226.2 MHz, $CDCl_3$ - 1% CF_3CO_2D), see Table 2. HR-ESI-IT-TOF MS *m*/*z* 397.2162 $[M + H]^+$ (calcd. for $C_{23}H_{29}N_2O_4$: 397.2127), *m*/*z* 395.1924 $[M - H]^-$ (calcd. for $C_{23}H_{27}N_2O_4$: 395.1976), *m*/*z* 793.4129 $[2M + H]^+$ (calcd. for $C_{46}H_{57}N_4O_8$: 793.4176) and *m*/*z* 791.3825 $[2M - H]^-$ (calcd. for $C_{46}H_{55}N_4O_8$: 791.4025).

2.3.5 *M. tuberculosis* fermentation for determination of minimum inhibitory concentration (MIC).

M. tuberculosis H_{37}Rv (ATCC 27294) was purchased from American Type Culture Collection (ATCC) while the derivative *M. tuberculosis* strain mc^{2}7000 (H_{37}Rv ΔRD1 Δ*panCD*) was acquired from the laboratory of Dr. William R. Jacobs Jr. at the Howard Hughes Medical Institute, Department of Microbiology and Immunology, Albert Einstein College of Medicine, Bronx, NY.[121] These strains were cultured to late log phase in the 7H12 media, Middlebrook 7H9 broth supplemented with 0.2% (vol/vol) glycerol, 0.05% Tween™ 80, and 10% (vol/vol) oleic acid-albumin-dextrose-catalase (OADC). The culture was harvested and resuspended in phosphate-buffered saline. Suspensions were then filtered through 8 μm filter membranes and frozen at 80 °C. Prior to use of bacterial stocks for the anti-TB assay, CFUs were determined by plating on 7H11 agar media. The MIC is defined here as the lowest concentration resulting in

≥90% growth inhibition of the bacteria relative to untreated controls. MIC against replicating *M. tuberculosis* was measured by the Microplate Alamar Blue Assay (MABA).[93, 94]

2.3.6 Low oxygen recovery assay (LORA).

The luciferase reporter gene luxABCDE-recombinant *M. tuberculosis* was prepared as previously reported.[96] The bacteria were adapted to low oxygen conditions during culture in a BioStatQ fermenter. The low oxygen-adapted culture was exposed to test samples in a 96-well microplate for 10 days at 37 °C in a hypoxic environment created with an Anoxomat (WS-8080, MART Microbiology). The cultures were then transferred to a normoxic environment at 37 °C for 28 hours. Viability was assessed by the measurement of luciferase-mediated luminescence. The LORA MIC was defined as the lowest concentration effecting a reduction of luminescence of ≥90% relative to untreated cultures.

2.3.7 Determination of cytotoxicity.

Vero (ATCC CRL-1586) cells were cultivated in 10% fetal bovine serum (FBS) in Eagle minimum essential medium.[122, 123] The culture was incubated at 37 °C under 5% CO_2 in air and then diluted with phosphate-buffered saline to 106 cells/mL. Two-fold serial dilutions of testing samples with a final volume of 200 μL cell culture suspension were prepared in a transparent 96-well plate (Falcon Microtest 96). After 72 h incubation at 37 °C, the medium was removed and monolayers were washed twice with 100 μL of warm Hanks balanced salt solution (HBSS). 100 μL of medium and 20 μL of MTS-PMS (Promega) were added to each well. Plates were then incubated for 3 hours and cytotoxicity was determined by the measurement of absorbance at 490 nm.

Human melanoma MDA-MB-435 cancer cells, human breast MDA-MB-231 cancer cells, human ovarian OVCAR3 cancer cells and human colon HT-29 cancer cells were purchased from the ATCC (Manassas, VA). The cell line was propagated at 37 °C in 5% CO_2 in RPMI 1640 medium, supplemented with fetal bovine serum (10%), penicillin (100 units/ml), and streptomycin

(100 µg/ml). Cells in log phase growth were harvested by trypsinization followed by two washings to remove all traces of enzyme. A total of 5,000 cells were seeded per well of a 96-well clear, flat-bottom plate (Microtest 96®, Falcon) and incubated overnight (37 °C in 5% CO_2). Samples dissolved in DMSO were then diluted and added to the appropriate wells (concentrations: 20 µg/mL, 4 µg/mL, 0.8 µg/mL, 0.16 µg/mL, 0.032 µg/mL; total volume: 100 µL; DMSO: 0.5%). The cells were incubated in the presence of test substance for 72 h at 37 °C and evaluated for viability with a commercial absorbance assay (CellTiter 96® AQ_{ueous} One Solution Cell Proliferation Assay, Promega Corp, Madison, WI) that measured viable cells. LC_{50} values are expressed in µg/mL relative to the solvent (DMSO) control.

Human ovarian OVCAR4 and Kuramochi cancer cells were maintained in RPMI 1640 (11875-093, Life-technologies) supplemented with 10% FBS (16000-044, Life-technologies) and 1% penicillin/streptomycin. Non-cancerous murine ovarian surface epithelium (MOSE) and murine oviductal epithelium (MOE) cells were maintained as previously reported.[124] Concentration-response experiments were performed as previously described for 72 hours.[89]

2.3.8 Minimum inhibitory concentration (MIC) determination against drug-resistant *M. tuberculosis* isolates.

M. tuberculosis strains individually resistant to rifampin (RMP, ATCC 35838), isoniazid (INH, ATCC 35822), streptomycin (SM, ATCC 35820), cycloserine (CS, ATCC 35826) and kanamycin (KM, ATCC 35827) were obtained from the American Type Culture Collection (ATCC). *M. tu*berculosis strains resistant to clofazimine ($H_{37}Rv_{CFZ\text{-}R1}$ and $H_{37}Rv_{CFZ\text{-}R2}$) were obtained from the lab of Stewart Cole at the École Polytechnique Fédérale de Lausanne in Switzerland. Bedaquiline-resistant *M. tuberculosis* strain rTMC207 (BK12) was obtained from the Belgian Coordinated Collections of Microorganisms (BCCM). Cultures were prepared and MICs

against drug-resistant *M. tuberculosis* isolates were determined by the MABA as described above for *M. tuberculosis* $H_{37}Rv$.

M. tuberculosis mutant strains 7A2 (*fbiAB*-), 5A1 (*fbiC*-), 14A1 (Rv3547-), and T3 (fgd-) were generated in a previous study,[125] while rRIF-BJ was a rifampin-resistant strain with a Ser531Leu *rpoB* mutation (confirmed by PCR of *rpoB*) generated in the Barry lab from strain K04b00DS.[126] Screening against these strains took place in the Barry lab. DMSO stocks of **3** and PA824 were diluted in 7H9/ADC/Tw as a two-fold serial dilution series in duplicate at 50 µL per well in clear round-bottom 96-well plates (Thermo Scientific #163320) leaving a drug-free medium control in column 12. *M. tuberculosis* $H_{37}Rv$ (ATCC 27294) and the aforementioned strains were cultured in 7H9/ADC/Tw to an OD_{650} of 0.2 and diluted 1:1000 in the same medium followed by addition of 50 µL of the diluted cell suspension to each well. The plates were incubated at 37 °C in sealed bags for one week after which growth was recorded using an inverted enlarging mirror. The MIC was taken as the concentration that completely inhibited all visible growth.

M. tuberculosis mutant strains MTBSRM1d, MTBSRM2e, and upp::Tnf were generated by the Mizrahi lab in a previous study,[119] while $H_{37}Rv$ (ATCC 27294) was acquired from the ATCC, and *pyrE* Tet-ON is as yet unpublished. Screening of **3** against these strains, along with the uracil supplementation experiment, and the 5-FU synergy experiment were performed in the Mizrahi lab following previously published methods.[119]

2.3.9 Minimum inhibitory concentration (MIC) determination against non-tuberculous mycobacteria (NTM).

Mycobacterium smegmatis (mc^2155), *Mycobacterium abscessus* (ATCC 19977), *Mycobacterium chelonae* (ATCC 35752), *Mycobacterium avium* (ATCC 15769), *Mycobacterium marinum* (ATCC 927), *Mycobacterium kansasii* (ATCC 12478), and *Mycobacterium bovis* BCG

(ATCC 35734) were obtained from the American Type Culture Collection (ATCC). Cultures were prepared and MICs against these mycobacteria were determined by the MABA as described above for *M. tuberculosis* H_{37}Rv. *M. abscessus* was incubated with 7H12 medium at 37 °C for 3 days and for an additional 4 hours after adding 12 μL of 20% Tween™ 80 and 20 μL of Alamar blue dye. *M. bovis* was incubated with 7H12 medium at 37 °C for 7 days, and an additional 1 day of incubation after adding 12 μL of 20% Tween™ 80 and 20 μL of Alamar blue dye. *M. chelonae* was incubated with 7H9 medium at 30 °C for 3 days, plus an additional 6 days of incubation after adding 12 μL of 20% Tween™ 80 and 20 μL of Alamar blue dye. *M. marinum* was incubated with 7H9 medium at 30 °C for 5 days, and an additional 1 day of incubation after adding 12 μL of 20% Tween™ 80 and 20 μL of Alamar blue dye. *M. avium* and *M. kansasii* were incubated with 7H9 media at 37 °C for 6 days, plus an additional day of incubation after adding 12 μL of 20% Tween™ 80 and 20 μL of Alamar blue dye. Viability was assessed by measuring fluorescence at 530 nm excitation/590 nm emission with a Victor^3 multilabel reader (PerkinElmer).

2.3.10 Minimum inhibitory concentration (MIC) determination against Gram-positive and Gram-negative bacteria.

The following Gram-positive and Gram-negative reference organisms were obtained from the ATCC: Methicillin-sensitive *Staphylococcus aureus* (ATCC 29213), methicillin-resistant *Staphylococcus aureus* (ATCC 33591), *Enterococcus faecalis* (ATCC 29212), *Enterococcus faecium* (ATCC 19434), vancomycin-resistant *Enterococcus faecium* (ATCC 51559), *Streptococcus pneumoniae* (ATCC49619), *Streptococcus pyogenes* Rosenbach (ATCC BAA-1633), *Bacillus cereus* (ATCC 14579), *Bacillus cereus* (ATCC 10987), *Bacillus thuringiensis* serovar konkukian str. 97-27, *Acinetobacter baumannii* (ATCC 19606), *Escherichia coli* (ATCC 25922), *Enterobacter cloacae* (ATCC 13047), *Klebsiella pneumoniae* (ATCC 13883), *Pseudomonas aeruginosa* (ATCC 27853), and *Proteus mirabilis* (ATCC 29906). *Bacillus subtilis* subsp. subtilis 168 is a laboratory strain and *Bacillus anthracis* Sterne was

obtained from Philip C. Hanna at the University of Michigan, Ann Arbor. Positive controls piperacillin, ampicillin, vancomycin and gentamicin were obtained from Sigma-Aldrich, while daptomycin was obtained from Fisher Scientific; each was used to prepare a stock solution of at least 1280 µg/mL on the same day of each experiment. Inocula for MSSA, MRSA, *E. faecalis*, *E. faecium*, VRE, *A. baumannii*, *E. coli*, *E. cloacae*, *K. pneumoniae*, *P. aeruginosa*, and *P. mirabilis* consisted of 5 x 10^5 CFU/mL of each bacterial species with determination of MICs by broth microdilution in duplicate according to Clinical Laboratory Standards Institute (CLSI) guidelines with growth scored by visual observation of turbidity.[97] The MIC against *S. pneumoniae* (ATCC 49619) was determined by broth microdilution method using a 4 x 10^5 CFU/mL inoculum as described in the National Committee on Clinical Laboratory Standards (NCCLS)[127, 128] with viability assessed by spectrophotometric readout at 490 nm using a Victor^3 multilabel reader (PerkinElmer). Inocula for *S. pyogenes* consisted of approximately 5 x 10^6 CFU/mL with determination of MICs by broth microdilution with growth scored by optical density (OD) at 625 nm using a Biotek Synergy 2 Microplate Reader. Each *Bacillus* inoculum consisted of 1 x 10^5 to 2 x 10^5 CFU/mL, with determination of MICs by broth microdilution and growth scored by visual observation of turbidity.

2.3.11 Characterization of diazaquinomycin A (3) *in vivo*.

Approval for animal studies was provided by the Office of Animal Care and Institutional Biosafety (OACIB) Institutional Biosafety Committee (IBC), case no. 12-183. Compound **3** was prepared in a dosing vehicle of 10% polyethylene glycol 400 (PEG 400), 10% polyoxyl 35 castor oil (Kolliphor® EL, BASF), and 80% oleic acid for all *in vivo* studies. To test tolerance of the compound, the formulation was administered by oral gavage at 100 mg/kg of **3** to a pair of female BALB/c mice once daily for five days followed by observation for qualitative indicators of toxicity (e.g. weight loss, ragged fur, huddling).

For PK assessment of **3**, Twenty-four 7 - 10 week old male Balb/c mice were separated into two groups; one group of twelve for dosing 100 mg/kg in 10 µL/kg by oral gavage and the other group of twelve for dosing 50 mg/kg in 5 µL/kg by intraperitoneal injection. Body weight was measured on the first day of dosing. Regular rodent chow and autoclaved tap water was provided to all animals *ad libitum*. From three animals at each of four time points of 0.5, 1, 2, and 4 hours, blood samples (>500 µL) were collected post dosing through terminal orbital bleeds using CO_2/O_2 and collected in K_2EDTA microtainers before being placed on wet ice. The microtainers were centrifuged at 3000 rpm for 15 min at 4 °C after which plasma samples were aliquoted and stored frozen at -80 °C until further analysis. Following blood collection, all animals were euthanized first by carbon dioxide asphyxiation then cervical dislocation. Both lobes of the lung were removed, washed clean with saline, flash frozen in liquid nitrogen, transferred on dry ice, and stored at -80 °C until transport on dry ice for further analysis.

Plasma aliquots of 100 µL were mixed with 5 µL 100 µM **4** internal standard stock solution, then mixed with 395 µL acetonitrile at 27 °C (0.5% formic acid, 1% DMSO). The mixtures were centrifuged at 10K g for 30 min at 22 °C. 100 µL supernatants were frozen at -80 °C overnight and analyzed by LC-MS^2 on the Agilent triple-quad 6410 (QQQ) the following day.

Lung samples were washed in phosphate-buffered saline (PBS), dried with paper towel, and weighed. To each sample, 3 mL PBS per gram of tissue was added and sample was homogenized by probe sonication. The homogenates were centrifuged at 10K g (9800 RPM on Eppendorf 5417R) for 30 min at 4 °C. Resulting supernatant aliquots of 100 µL of were mixed with 5 µL 100 µM **4** internal standard stock solution, then mixed with 395 µL of acetonitrile at 27 °C (0.5% formic acid, 1% DMSO), The mixtures were then centrifuged at 10K g for 30 min at 22 °C. 100 µL supernatants were frozen at -80 °C overnight and analyzed by LC-MS^2 on the QQQ the following day.

All samples were analyzed using RP-C_{18} analytical HPLC (10 µL injection, 0.3 mL • min^{-1}, isocratic 50% aqueous acetonitrile (ACN) for 1 min followed by a gradient of 50% aqueous ACN to 100% ACN over two min, and an isocratic 95% aqueous ACN wash for three min) followed by selected ion monitoring on an Agilent triple-quad 6410 (QQQ). DAQA (t_R = 1.5 min) was observed at the quantitative ion transition of 355.3 *m/z* → 297.2 *m/z* and the qualitative ion transitions of 355.3 *m/z* → 323.1 *m/z* and 355.3 *m/z* → 270.1 *m/z*. Compound **4** (t_R = 1.0 min) was the internal standard and was monitored at the quantitative ion transition of 299.2 *m/z* → 271.1 *m/z* and the qualitative transitions of 299.2 *m/z* → 253.0 *m/z* and 299.2 *m/z* → 228.1 *m/z*.

In vivo efficacy studies were performed in the lab of Michael Cynamon at the VA Medical Center in Syracuse, NY. Mice were contained in microisolator cages (Lab Products inc. Maywood, NJ) and provided water and Prolab RMH 3000 rodent chow (Purina, St. Louis, MO). *M. tuberculosis* str. Erdman (ATCC 35801) was obtained from the ATCC (Manassas, VA). Mice were anesthetized by intramuscular injection with a telazol (45 mg/kg)/xylazine (7.5mg/kg) cocktail (Lederle Parenterals, Carolina, Puerto Rico and Bayer Corp., Shawnee Mission, Kansas, respectively) to facilitate the infection procedure. Treatment of six 6-week-old female Balb/c mice (Charles River Laboratories, Wilmington, DE) was initiated 21 days after intranasal infection with ~3.12×10^2 CFU of *M. tuberculosis* str. Erdman per mouse. A volume of 0.2 ml of the aforementioned formulation of **3** was delivered by oral gavage for five days per week for two weeks. In addition, there were six early control mice that were euthanized at the commencement of DAQA treatment to determine baseline infection CFUs and four late control mice that were treated with 0.2 ml of the formulation vehicle only by oral gavage in parallel with the experimental group to determine final infection CFUs and confirm virulence. As a positive control, eight additional mice were administered 10 mg/kg RIF dissolved in 20% DMSO and 80% ddH_2O orally by gavage using the same schedule as DAQA. The mice were all euthanized by CO_2 asphyxiation.

Right lungs were removed aseptically and frozen at -70 °C until processing. Lungs were thawed and homogenized in saline with Tween™ 80 using a sealed tissue homogenizer (IdeaWorks! Laboratory Devices, Syracuse, NY), then diluted further in sterile water with Tween™ 80. The homogenate was plated on 7H10 agar (BD Diagnostic Systems, Sparks, MD) with 10% OADC (BBL Microbiology Systems, Cockeysville, MD) and 0.2% glycerol followed by incubation for four weeks at 37 °C in ambient air before counting.

2.3.12 Synthesis of diazaquinomycin derivatives.

Chemical reagents benzoyl peroxide, methyl iodide, silver(I) oxide, carbon tetrachloride, chloroform, dichloromethane, N,N-dimethylformamide, morpholine, N-bromosuccinimide, sodium carbonate, and sulfuric acid were all purchased from Sigma-Aldrich (St. Louis, MO), while ethanol and methanol were purchased from Fisher Scientific. All reagents were used without additional purification. Preparative thin layer chromatography was performed following reactions using EMD Millipore PLC silica gel 60 F_{254} 20 cm × 20 cm × 0.5 mm glass plates and Phenomenex Strata SI-1 silica (55µm, 7Å) 1000mg/6mL SPE cartridges unless noted otherwise. ^{1}H NMR spectra were acquired on a Bruker 600 MHz DRX NMR spectrometer equipped with an inverse 5 mm TXI cryogenic probe with z-axis pfg and XWINNMR version 3.5 operating software. ^{1}H NMR chemical shifts were referenced to $CDCl_3$ solvent signals (δ_H 7.26 ppm and δ_C 77.0 ppm, respectively). Synthesis of bis(morpholino)diazaquinomycin A and its three intermediates was achieved using methods described by Tsuzuki, et al. with modifications to the chromatography steps to accommodate use of preparative thin layer chromatography.[95] Purification of the bis(methoxy)diazaquinomycin A intermediate was achieved by silica gel column chromatography eluting with a 1:6 ratio of ethyl acetate : hexanes to result in 68.5 mg (42.3% yield). Purification of the bis(bromo)bis(methoxy)diazaquinomycin A intermediate was achieved by silica gel SPE eluting with 100 % methylene chloride to result in 60.8 mg (63% yield).

Purification of the bis(methoxy)bis(morpholino)diazaquinomycin A intermediate was achieved by preparative thin layer chromatography using 3.5% methanol in 100 mL methylene chloride to result in 14.7 mg (23.6% yield). Finally, purification of the bis(morpholino)diazaquinomycin A product was achieved using silica gel column chromatography as previously reported to result in 6.3 mg (45.1% yield).[95] Synthesis of **7** and **8** was achieved using methods described by Omura, et al.[92] Purification of **7** and **8** was achieved by RP-C_{18} preparative HPLC (16 mL·min−1, gradient of 50% aqueous acetonitrile (ACN) to 100% ACN for 20 min, followed by an isocratic flow of 100% ACN for 10 min) to afford 5.4 mg and 2.2 mg (46.0% and 18.7% yield) of each product, respectively.

2.3.13 Attempt at whole-cell biocatalysis of hydroxy-diazaquinomycin A analogs.

Dicyclopropyl ketone (DCPK; > 95% purity) was purchased from TCI Chemicals (Portland, OR), while aminolevulinic acid hydrochloride (ALA; ≥ 98%), (S)-(–)-limonene (96% purity), and nonanoic acid methyl ester (NAME; ≥ 99.8% purity), were purchased from Sigma-Aldrich (St. Louis, MO). The plasmids used in this study were the previously published pCom8-PFR1500, pCom8-PFR1500L, and pBTL10 and were provided by the Andreas Schmid lab at The Helmholtz-Centre for Environmental Research GmbH – UFZ in Leipzig, Germany.[99-101] Chemically competent cells generated from *E. coli* W3110 were transformed with pCom8-PFR-1500, pCom8-PFR-1500L, and pBTL10 plasmids by heat shock.[129] Transformants were selected on LB medium containing the appropriate antibiotics and were then cultured with appropriate antibiotics (10 µg/mL gentamicin for pCom8-PFR-1500 and pCom8-PFR-1500L and 50 µg/mL kanamycin for pBTL10).[130]

To determine the susceptibility of each transformant to **3**, a DMSO stock of the compound was diluted in LB media as a two-fold serial dilution series in triplicate at 100 µL per well in a clear polystyrene 96-well assay microplate (Corning™ 3370) in parallel with kanamycin and

tetracycline controls, leaving a drug-free media control in column 12. All three W3110 transformants and an untransformed W3110 control were fermented in LB media overnight followed by addition of 100 µL of the culture to each well. The plates were sealed and incubated at 22 °C for 24 hours after which growth was scored and MICs determined by visual observation of turbidity.

A 10 µL inoculum of each *E. coli* W3110 transformant was grown in 3 mL LB media with the necessary antibiotic (50 µg/mL kanamycin; 10 µg/mL gentamicin) at 37 °C and ~200 rpm for 16 hours. A 1 mL aliquot of this culture was used to inoculate 100 mL modified M9 media (M9*) supplemented with 1 mL/L US^{Fe} trace element solution containing 0.5% (wt/vol) glucose and appropriate antibiotic in a 500 mL Erlenmeyer flask.[131, 132] Cultures were grown to an OD_{450} of 0.3. Induction of enzymes was performed by incubation at ~200 RPM for an additional 4 hours following addition of 0.025% (v/v) DCPK to all transformant cultures with the addition of 1 mM ALA (5-aminolevulinic acid) to the pCom8-PFR1500 and pCom8-PFR1500L transformants only. Cells were harvested by centrifugation for 20 min at 4,600 × *g* at 4 °C. The supernatant was discarded and the cells were resuspended in 100 mM potassium phosphate buffer (pH 7.4) containing 1% (w/v) glucose to an OD_{450} of 6.0. Resting cells were aliquoted to 1 mL total volume in sealed tubes and shaken at 37 °C and ~200 RPM for approximately 5 min. The resting cell assay was then initiated with the addition of **3** in DMSO to a final concentration of 110 µM, and NAME and (S)-(–)-limonene in ethanol to final concentrations of 133 µM and 2 mM, respectively. The reaction was terminated after eight hours by the addition of 1 mL DCM containing the **4** internal standard at 0.2 mM for test cultures.

2.3.14 Cell-free ThyA and ThyX enzyme inhibition assay.

Over-expression and purification of *M. tuberculosis* ThyA and ThyX were performed as detailed in Hunter, et al.[105] Human thymidylate synthase A gene (commonly referred to as TYMS)

in pET17xb was transformed into BL21(DE3)pLysS. The enzyme was over-expressed in LB media supplemented with 40 µg/mL chloramphenicol and 100 µg/mL ampicillin at 37 °C until OD_{600} 0.6, when the culture was inoculated with 1 mM IPTG and incubated further at 18 °C for 18 h. Cultures were spun down and the cell-pellet from a 1.5 L culture was lysed in 30 mL of 20 mM potassium phosphate, 500 mM NaCl, 10 mM $MgCl_2$, 0.1 mM EDTA, and 1 mM 2-mercaptoethanol at pH 7.9 on ice by sonication (5 cycles, 1 min, 90 W). The crude extract was spun down at 4 °C and 30,597 RCF. 27.5 mL clarified lysate was obtained. 5.4 g ammonium sulfate (around 35% saturation) was added in three parts and allowed to dissolve at 4 °C. The precipitate obtained was spun-down at 4 °C and 11,952 RCF. 30 mL supernatant was obtained, to which 10.75 g of ammonium sulfate (approximately 80% saturation) was added slowly at 4 °C and allowed to dissolve. The precipitate obtained was again spun-down at 4 °C and 11,952 RCF. It was re-dissolved in 15 mL of 20 mM Tris, 100 mM NaCl, 2 mM 2-mercaptoethanol, and 10% glycerol at pH 7.8, concentrated to 7 mL, and buffer exchanged into 20 mM Tris, 100 mM NaCl, 2 mM 2-mercaptoethanol, and 10% glycerol at pH 7.8. The sample was purified on a 5 mL HiTrap Q column (Low-salt buffer: 20 mM Tris, 100 mM NaCl, 2 mM 2-mercaptoethanol, and 10% glycerol at pH 7.8, High-salt buffer: 20 mM Tris, 1 M NaCl, 2 mM 2-mercaptoethanol, and 10% glycerol at pH 7.8). The protein eluted out before 40% high-salt buffer. Further purification was carried out using Hiload 16/200 superdex 200 pg size-exclusion column using 20 mM Tris, 100 mM NaCl, 2 mM 2-mercaptoethanol, and 10% glycerol at pH 7.8. HsThyA containing fractions were pooled and buffer exchanged into 50 mM Tris, 150 mM NaCl, 2 mM TCEP, and 30% glycerol at pH 7.8 and stored at -80 °C until further use.

MtThyA (562.8 ng), MtThyX (8.4 µg), and HsThyA (638.4 ng) were pre-incubated with inhibitors (13 µM) for 15 min at room-temperature in 125 mM TES, 60 mM $MgCl_2$, 2.5 mM EDTA, and 2 mM 2-mercaptoethanol at pH 7.9. The control contained DMSO without inhibitors.

FAD (10.5 µM) was included in the pre-incubation in the case of MtThyX. The total reaction volume was 151 µL for MtThyA and HsThyA, and 160 µL for MtThyX.

Radiolabeled dUMP solution was made by mixing 20 µL 5'-^{3}H-dUMP and 5 µL of 10 mM dUMP in 475 µL of water. After 15 min, mTHF (67 µM for MtThyA, 5.1 µM for MtThyX, and 5.5 µM for HsThyA) and radiolabeled dUMP (5 µL) were added to 18 µL of the enzyme/inhibitor samples. NADPH at 145 µM was also added to the MtThyX samples. All samples were incubated at room-temperature for 30 min. Total reaction volume in all cases was 26 µL. Reaction was stopped after 30 min by addition of 20 µL stop solution (1.5 N TCA, 1.1 mM non-radioactive dUMP). A volume of 200 µL 10% charcoal (w/v) was added and samples were incubated on ice for 15 min before being spun-down at 4 °C and 14,100 RCF for 15 min. A 100 µL aliquot of the supernatant was assayed by liquid scintillation counting to determine the amount of tritium-containing water produced by the reaction.

2.3.15 *In vitro* screening of diazaquinomycin A (3) against *M. tuberculosis* overexpression (OE) mutants.

Recombinant strains were constructed in which each gene (thyA or thyX) was under the control of a tetracycline inducible promoter.[133] Plasmids were transformed into *M. tuberculosis* by electroporation.[134] Recombinant and wild-type strains were grown to late log phase in roller bottles with the presence of inducer (150 ng/mL anhydrotetracycline). The MIC of compound **3** was determined by measuring bacterial growth after 5 days in the presence of the test compound and inducer.[135] Compounds were prepared as a 10-point two-fold serial dilution in DMSO and diluted into 7H9-Tw-OADC medium in 96-well plates with a final DMSO concentration of 2%. Each plate included assay controls for background (medium/DMSO only, no bacterial cells), zero growth (2% 100 µM rifampin), and maximum growth (DMSO only), as well as a rifampin dose response curve. Cultures were filtered through a 5 µm filter and inoculated to a starting OD_{590}

0.02. Plates were incubated for 5 days and growth was measured by OD_{590}. The percent growth was calculated and fitted to the Gompertz model.[136] MIC was defined as the minimum concentration at which growth was completely inhibited and was calculated from the inflection point of the fitted curve to the lower asymptote (zero growth).

2.3.16 Transcription profile of *M. tuberculosis* following *in vitro* treatment with diazaquinomycin A (3).

Treatment of *M. tuberculosis* H_{37}Rv (ATCC 27294), RNA extraction, and RNA labeling methods described by Boshoff, et al. were followed toward the generation of transcriptional profiles for **3** and known TB inhibitors.[137] Custom-designed oligonucleotide microarray chips were synthesized by Agilent. RNA (2 μg) extracted from vehicle control (DMSO) treated cells were labeled with cyanine dye Cy5 and used as the reference, while RNA (2 μg) from inhibitor-treated cells screened in parallel were labeled with cyanine dye Cy3. The ratios of Cy5/Cy3 (DMSO/test compound) were extracted as $log_2 n$. For visualization of transcription profiles, genes from the data that were unidentified, uncharacterized, or were deferentially expressed at a < ± 0.2 ratio after exposure to **3** were eliminated to reduce the number for display to the 1,000 most relevant. A heat map was then constructed from the trimmed data using the CIMminer (Clustered Image Maps) online application available from The Genomic and Bioinformatics Group in the Developmental Therapeutics Branch of the NCI at the NIH (http://discover.nci.nih.gov/cimminer).[138]

2.3.17 Minimum inhibitory concentration (MIC) determination against *M. tuberculosis* strains grown in varying media conditions.

Cultures were prepared in standard glycerol-alanine-salts (GAS) media; four separate GAS media, each supplemented with either 0, 50, 200, or 800 μg/mL ferric ammonium citrate; GAS media supplemented with 5 mg/mL albumen; and GAS media supplemented with 5 mg/mL albumen, and 5.6 μg/mL palmitic acid, but without glycerol. MICs were determined by the MABA as described previously for *M. tuberculosis* H_{37}Rv.

2.4 Conclusions.

Despite decades of research into actinomycete small molecules from terrestrial and marine environments, to the best of our knowledge identification of secondary metabolites from freshwater Actinobacteria has been virtually absent from the peer-reviewed literature. The unique structures and activity of the diazaquinomycins provide first evidence that the Great Lakes, and more broadly freshwater environments, are a relatively unexplored resource for novel biologically active molecules.

From a *Micromonospora* sp. in Lake Michigan sediment, we isolated novel antibiotic molecules of the diazaquinomycin class. An analog, compound **3**, displayed an *in vitro* activity profile similar or superior to clinically used TB agents and maintained potent inhibitory activity against a panel of drug-resistant TB strains. This compound displayed a selectivity profile targeted toward *M. tuberculosis*, even within the genus *Mycobacterium*. Since the 1980's, other research groups reported that members of the diazaquinomycin class exhibited weak antibacterial activity by targeting thymidylate synthase, though no reports of their anti-TB activity existed and our studies have suggested an alternate MOA in TB. Preliminary *in vitro* analysis of **3** predicts that it will exhibit high metabolic stability, and therefore a long predicted serum half-life *in vivo*. Though **3** was well tolerated in a dedicated five-day *in vivo* tolerance test, subsequent pharmacokinetics and efficacy experiments revealed toxicity that was suspected to be caused by the highly viscous vehicle. Additionally, **3** was not observed above the LOQ in the PK study. This might indicate that compound exhibits poor bioavailability but the presence of the **4** internal standard below the LOQ suggests an incompatibility of the PK methods with the poorly soluble DAQs.

Exhaustive attempts at a new DAQ total synthesis and whole cell biocatalysis methods were both aimed at facilitating the modification of the DAQ structure at the β-substituted position, but neither were successful. Reasons for the failed synthesis are uncertain. The biocatalysis

experiment likely failed because of the limited solubility of **3** in aqueous media added to potential difficulty of its penetration through the lipopolysaccharide outer membrane of *E. coli*.

In the *M. tuberculosis* OE mutant screen, both Rv0953c oxidoreductase and Rv3500c transporter OE mutants exhibited a six-fold MIC increase and are predicted to be involved with lipid metabolism as part of the *kstR* regulon.[110] The fact that both mutants were resistant and contained mutations within the same regulon lends support to the potential of this pathway as a mechanism of resistance to **3**. Importantly, the basal levels of the Rv0953c and Rv3500c genes' expression exhibited four-and two-fold increases in MIC, respectively, in the uninduced mutants. Continually overexpressed genes could lead to global metabolic pathway changes that might hinder interpretation of results such as identification of the exact site targeted in the pathway. But since these enzymes have been identified as non-essential, they are likely not targets of **3**.[109, 118, 139] Instead, they may be involved in resistance by redox inactivation (Rv0953c) and efflux (Rv3500c) of the compound from the cell. Additionally, the oxidoreductase may protect against general ROS or DAQ-related active derivatives involved in the oxidative stress evidenced in the microarray results. Interestingly, Rv0953c and Rv3500c were not up- or down-regulated significantly in the transcription profiling study, suggesting that though some protective effect can be gained by engineering strains that upregulate these genes, *M. tuberculosis* H_{37}Rv does not innately respond to oxidative stress or DAQ treatment by this mechanism.

Though differing overall patterns in the transcription profiles suggest separate mechanisms between **3** and other TB inhibitors, the oxidative stress response observed for the compound was similar to that from dipyridyl, menadione, and CLF.[140] Interestingly, we were able to disprove the possibility that inhibition of respiration similar to that of CLF was a part of the DAQA MOA (See Appendix 2.1.2). Because of the potential role of iron chelation in oxidative stress and a small level of resistance observed when culturing in 7H12, [141-144] we tested the effects of iron and a

palmitic acid carbon source on the activity of **3**. We found no correlation between iron concentration in media and DAQA inhibition of *M. tuberculosis* and were unable to identify a protective effect using the alternate carbon source.

Though we found potential MOA leads when two clofazimine-resistant strains exhibited cross-resistance to **3**, we were unable to identify a singular target following screening of additional mutants. These experiments suggested that **3** was not a substrate of the MmpL5 efflux system and that it did not have an effect on pyrimidine or F_{420} cofactor biosynthesis.

Also, attempts at isolating a protein target for **3** using the DARTS assay were unsuccessful. This may be because the DAQs have a many faceted mechanism that may not include direct interaction with a singular protein target (See Appendix 2.1.3).

In general, the major challenges of developing **3** as an anti-tuberculosis drug lead have been tied to the compound's limited solubility. Harsh conditions in the total synthesis have been prohibitive to derivatization aimed at improving solubility, exploring SAR, and embarking on additional MOA studies. The culmination of the aforementioned experiments saw the elimination of specific targets and pathways within a set of potential mechanisms established either through previous reports or by OE library screen and transcription profiling. More global approaches to target identification will be required in future studies to generate additional potential target leads.

2.5 Future directions.

If the DAQs are without a future as a tuberculosis therapy, additional studies into the remarkably selective mechanism still hold potential of revealing a novel target for future TB treatments. Thus, there is a continued focus on the characterization and eventual elucidation of the MOA in our laboratories. The most immediate goal is to generate mutant strains resistant to **3** for full genome sequencing using the avirulent *M. tuberculosis* strain mc^27000.[121] Mutations

identified to confer resistance will be prioritized as genes for potential molecular targets worthy of further investigation. The $mc^2$7000 strain has mutations allowing for its safe use in the convenience of BSL-2 containment and is a sufficient replacement for H_{37}Rv with its similar susceptibility to **3** at an MIC of 0.14 μM in the MABA.[121]

Additionally, many of the findings described in the previous chapter could be explored in greater depth. To test the specificity of the MOA of **3** in *M. tuberculosis*, synthetic DAQ derivatives inactive in the MABA could be tested against DAQA-susceptible cancer cell lines. A similar loss of activity would suggest that the pharmacophore and possibly the MOA is shared between *M. tuberculosis* and mammalian cells, while retention of activity would suggest the opposite. Additionally, the substructure of the **3** central quinone coupled with results from the microarray profile suggest that extensive redox chemistry might be responsible for cell damage in *M. tuberculosis*. The selectivity of the compound opposes the assumption of such a typically promiscuous mechanism, but testing the generation of ROS by **3** using appropriate ROS-sensitive dyes would confirm whether this suspected activity is valid.[145] Target candidates revealed from the OE mutant panel could be further investigated as well, though this would likely involve more resource-intensive molecular genetics experiments. For example, screenings of **3** against a double Rv0953c/Rv3500c OE mutant resulting in increased resistance and tests in Rv0953c and Rv3500c transposon mutants resulting in increased susceptibility would greatly support that this lipid catabolism pathway is part of a mechanism of resistance. In a more bioinformatic approach, discovery of the DAQ biosynthetic gene cluster may reveal closely associated resistance genes that could guide studies toward a mechanism in *M. tuberculosis*.[146]

Biocatalytic derivatization of the DAQ core to hydroxylate the β-position might be facilitated if one of the more soluble synthetic DAQ analogs was used as the substrate. Since these previously described α, O-, and N- modified derivatives tend to lack significant activity, the core

of the hydroxylated product could be converted back into the more active DAQA-like structure. Once a hydroxy-DAQA was achieved, further derivatizations could be made at the reactive hydroxyl group to include photo-reactive probe moieties for target capture and pull-down.

In the absence of better-informed approaches to understanding the DAQ MOA, a systematic approach to eliminating the possibility of the canonical antibiotic mechanisms of action would be a logical step. As Walsh has eloquently described in his book *Antibiotics: Actions, Origins, Resistance*, nearly without exception, antibiotics act by one of four general modes of action: 1) inhibition of peptidoglycan synthesis in the membrane, 2) protein synthesis inhibition, 3) inhibition of DNA or RNA synthesis, or 4) inhibition of DNA/RNA precursor synthesis.[147] Studies of DAQA in these areas could identify a target or serve to further support that this class acts by a novel mechanism.

Unfortunately, attempts at determining the efficacy of **3** in mice were unsuccessful due to deaths related to the highly viscous vehicle necessitated by the poor solubility of the compound. In the absence of a more soluble analog with retained potency, the continuation of *in vivo* evaluation for this antibiotic class is dependent on the determination of a better tolerated formulation. Use of the recently described intrapulmonary aerosol delivery method may be the ideal administration route for such an insoluble compound.[148] Following optimization of an administration method, **3** should be tested against an acute infection model in addition to retesting in the chronic infection model. This would allow the assessment of DAQA as a companion to bactericidal drugs *in vivo* if it is bacteriostatic. Importantly, a second attempt at quantitative pharmacokinetic data acquisition would greatly inform efficacy and additional *in vivo* experiments. These studies aim to identify a possible novel molecular target of the diazaquinomycins in TB and test the *in vivo* potential of this class as a part of further assessing their potential as anti-TB drug leads.

3. DIAZAQUINOMYCINs E–G, NOVEL DIAZA-ANTHRACENE ANALOGS FROM A MARINE-DERIVED *STREPTOMYCES* SP.‡

3.1 Introduction

Interestingly, in a separate study using bioassay-guided fractionation of strain F001 extract against the ovarian cancer cell line OVCAR5, we serendipitously isolated additional molecules of the diazaquinomycin class. The observed activity led to the selection of this strain for further chemical investigation. Of these, diazaquinomycin E (DAQE; **12**) and the isomeric mixture of diazaquinomycins F and G (DAQF, **13**; DAQG, **14**) were new, while the known analog diazaquinomycin A (DAQA; **3**) was also isolated in the process. The three new compounds are mono-normethyl analogs of the diazaquinomycin structural class. DAQE and DAQA inhibited the growth of OVCAR5 cells with moderate potency (LC_{50} = 9.0 and 8.8 μM, respectively). Further biological evaluation was performed on the most abundant analog, DAQA, while we were unable to evaluate the biological activity of the isomeric mixture of DAQF and DAQG due to their low mass yield. Details of the elucidation and anti-cancer biological activities are described herein.

3.2 Results and discussion.

3.2.1 Structure elucidation of diazaquinomycins E (12), F (13), and G (14).

Following a series of chromatographic steps, diazaquinomycin E (Figure 10) was obtained as red powder. The molecular formula was assigned as $C_{23}H_{28}N_2O_4$ on the basis of combined NMR and high-resolution MS experiments. This formula demanded 11 degrees of unsaturation. The unique chromophore of a fused diaza-anthracene ring system consistent with the diazaquinomycin structural class was observed in the UV spectrum of **12**. Analysis of the ^{1}H NMR spectrum of **12** suggested the presence of an isolated aromatic hydrogen (δ_H 6.94, s, H-6). Integration of the H-6,

---

‡Reproduced with permission from Mullowney, M. W.; Ó hAinmhire , E.; Shaikh, A.; Wei, X.; Tanouye, U.; Santarsiero, B. D.; Burdette, J. E.; Murphy, B. T. Diazaquinomycins E-G, novel diaza-anthracene analogs from a marine-derived *Streptomyces* sp. *Mar. Drugs* **2014**, *12*, 3574-3586. Utilized under the Creative Commons license. More information available via the Internet at: creativecommons.org/licenses/by/4.0/

H_3-11, H_2-12, H_2-17, H_3-16, and H_3-21 resonances in the ^1H spectrum further supported a mono-normethylated DAQ core skeleton, revealing an integration value of three for the α-substituted methyl hydrogens (δ_H 2.32, H_3-11) rather than the typical integration value of 6 for this resonance in previously reported symmetric DAQs. This mono-normethylation afforded an asymmetry to **12**.

Figure 10. Structures of diazaquinomycins E (**12**), F (**13**), G (**14**), and A (**3**).

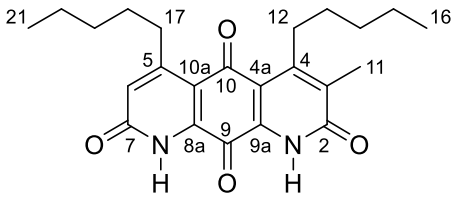

DAQE (12)

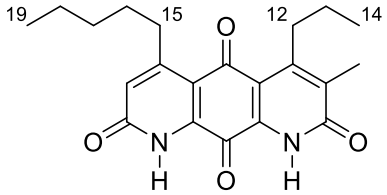

DAQF (13)

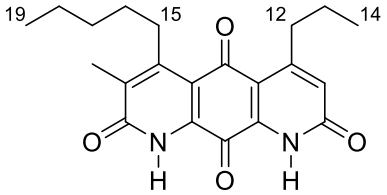

DAQG (14)

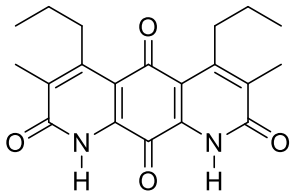

DAQA (3)

Analysis of ^{13}C NMR data suggested the presence of two quinone carbonyls (δ_C 180.82, C-10; 173.09, C-9), two lactam carbonyls (δ_C 162.98, C-2; 162.93, C-7), one methine alkene carbon (δ_C 127.49, C-6), seven quaternary carbons (δ_C 159.68, C-5; 154.17, C-4; 137.77, C-3; 136.51, C-8a; 134.12, C-9a; 118.03, C-4a; 117.79, C-10a), eight methylene carbons (δ_C 34.91, C-17; 32.32, C-14; 31.80, C-19; 30.70, C-12; 29.62, C-18; 28.81, C-13; 22.47, C-15; 22.45, C-20), and three methyl carbons (δ_C 14.12, C-16; 14.07, C-21; 13.05, C-11) (Table 10). Given that the molecular formula afforded 11 degrees of unsaturation and the molecule contained four carbonyls and eight quaternary alkene carbons, the remaining degrees were satisfied by the fused ring system.

Key HMBC, COSY, and 1D-TOCSY correlations are given in Figure 11. Since the molecule is asymmetric, we could employ proton-based spectroscopic experiments to distinguish between resonances of the β-substituted alkyl groups. Interpretation of COSY and 1D-TOCSY data defined two distinct spin systems (Figure 12), which were then connected to the core ring system using

Figure 11. Key 2D NMR correlations of **12**.

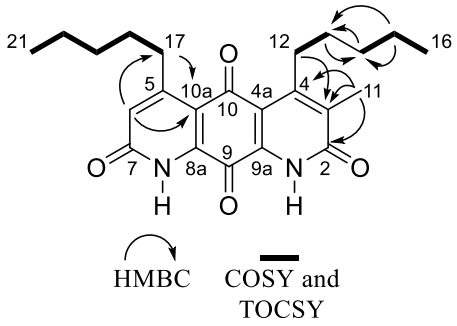

12

HMBC correlations. In HMBC correlation from H_2-17 to C-10a, and of H-6 to C-17 and C-10a, positioned the spin system of C-17–C-18–C-19–C-20–C-21 on the normethyl half of the diaza-anthracene core. Similarly, an HMBC correlation from H_2-12 to C-3 positioned the spin system of C-12–C-13–C-14–C-15–C-16 on the α-methylated ring of the diaza-anthracene core. The ^{13}C resonances of the lactam carbonyl carbons were distinguished from one another based on an HMBC correlation from H_3-11 to C-2, placing C-2 on the α-methylated ring. The remaining quinone carbons C-8a, C-9, C-9a, and C-10 were assigned based on comparison with reported values of other diazaquinomycin analogs;[90, 92] our assignments were highly consistent with reported values. Therefore, the structure of **12** was determined as shown and named diazaquinomycin E.

Table 10. ^{1}H and ^{13}C NMR data ($CDCl_3$/1% CF_3CO_2D) of **12**.

Position	^{13}C [a]	^{1}H mult. (*J*, Hz) [b]
2	162.98	
3	137.77	
4	154.17	
4a	118.03	
5	159.68	
6	127.49	6.94 s
7	162.93	
8a	136.51	
9	173.09	
9a	134.12	
10	180.82	
10a	117.79	
11	13.05	2.32 s
12	30.70	3.12 bt (6.4)
13	28.81	1.52 m
14	32.32	1.51 m
15	22.47	1.42 m
16	14.12	0.96 t (7.3)
17	34.91	3.11 t (7.7)
18	29.62	1.60 p (7.6)
19	31.80	1.43 m
20	22.45	1.40 m
21	14.07	0.94 t (7.3)

[a] 226.2 MHz; [b] 900 MHz.

Following a series of chromatographic steps, the co-eluting isomeric mixture of **13** and **14** (Figure 10) was obtained as red powder. The molecular formula for the mixture of constitutional isomers was assigned as $C_{21}H_{24}N_2O_4$ on the basis of combined NMR and high-resolution MS experiments. This formula demanded 11 degrees of unsaturation. A chromophore of a fused diaza-anthracene ring system consistent with **12** was observed in the UV spectrum of the compound mixture. The diaza-anthracene core of DAQF and DAQG was determined to be mono-methylated as was previously described for **12**. This was evidenced by the presence of an aromatic hydrogen in the ^{1}H NMR spectrum (δ_H 6.98, s, H-6 of **13** or **14**). Evidence for a second minor isomer was

observed adjacent to the resonance at δ_H 6.98 (δ_H 6.95, s, H-6 of **13** or **14**) (Figures A53 and A56). Integration of the major aromatic hydrogen and the n-pentyl and n-propyl group resonances in the ^{1}H spectrum further supported a mono-normethylated DAQ core skeleton. Distinguishing separate,

Figure 12. 1D-TOCSY correlations of **12.**

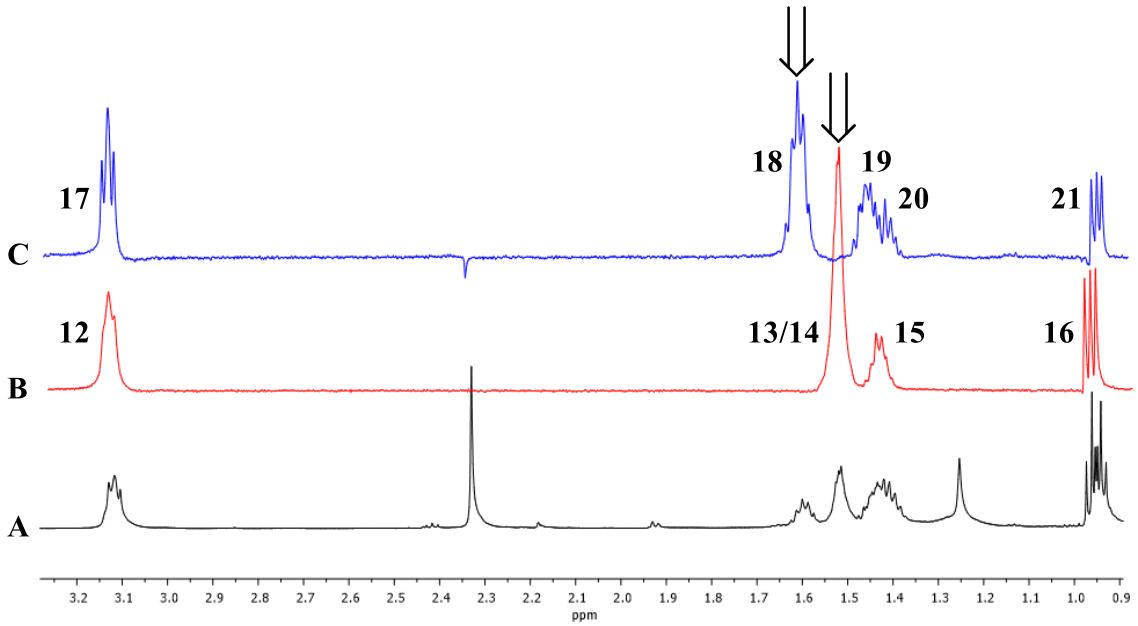

Arrows indicate irradiated resonances. (A) Expansion of ^{1}H NMR spectrum (600 MHz) of **12**; (B) Expansion of 1D-TOCSY spectrum of **12** (irradiation of 1.51 ppm); (C) Expansion of 1D-TOCSY spectrum of **12** (irradiation of 1.62 ppm).

complete sets of ^{13}C shifts from DEPTQ and HMBC experiments was not possible due to the structural similarity and inability to separate **13** and **14**. Partial carbon shift data shared by the isomers was extracted from an HSQC experiment (Supplemental Information, Table A5). Interpretation of COSY data defined two distinct spin systems, one n-pentyl group and one n-propyl group.

To confirm the structural features observable by NMR analysis and to determine the remaining connectivity of the structures, an X-ray structure determination was attempted. The mixture of **13** and **14** was co-crystallized from methanol using a slow evaporation technique. Compounds **13** and **14** occupied the same molecular site, crystallizing in the monoclinic space

group $P2_1/m$ (No. 11), with a mirror plane bisecting the molecules through the central carbonyl atoms C9-O9 and C10-O10. The major isomer (**13**), present as 52.6% of the crystal, is defined with a methyl group carbon atom, C11, on atom C3 adjacent to the propyl-substituted C4 atom, and a methine group carbon atom, C6, adjacent to the pentyl-substituted C5 atom. A constitutional

Figure 13. Co-crystal structure of **13** and **14.**

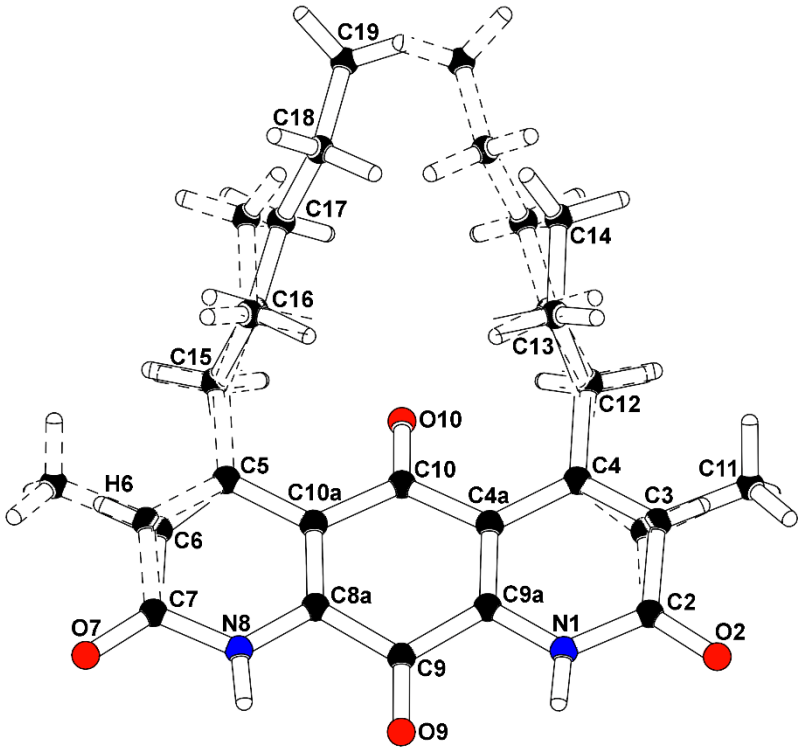

Structure numbered to emphasize DAQF occupancy in the co-crystal.

isomer (**14**), present as 47.4 % of the crystal, is modeled with the methyl group carbon atom, C11, on atom C3 adjacent to the pentyl-substituted C4 atom, and a methine group carbon atom, C6, adjacent to the propyl-substituted C5 atom. Partially occupied water molecules are evident from the electron density maps, and near the methyl groups. The C3(methyl)-C6(H):C3(H)-C6(methyl) fragment occupancy was refined to a ratio of 0.704(8):0.296(8), and the C4(n-propyl):C4(n-pentyl) fragment occupancy ratio was 0.566(9):0.434(9). The molecules are packed in the crystal through

hydrogen bonding with the amide hydrogen atoms and adjacent carbonyls. The intensity data was collected at experimental station 21-ID-D, LS-CAT, at Advanced Photon Source, Argonne National Laboratory, and processed with XDS.[149] The structure was solved and refined with SHELX.[150] The final R-factor was 0.0799 for 1525 intensities greater than 2σ, and 0.0961 for all 2030 unique data. The X-ray analysis supports the proposed structures of **13** and **14** (Figures 13, A59, and A60). Therefore, **13** and **14** were determined as shown and named diazaquinomycin F and diazaquinomycin G, respectively. Crystallographic data for the structure of **13** and **14** were deposited under accession number CCDC 996646 and can be obtained free of charge from The Cambridge Crystallographic Data Centre. The ratio of **13** and **14** in the co-crystal does not necessarily reflect the weight percentage in the compound mixture, as evidenced by uneven H-6 resonances in the ^{1}H NMR spectrum (Supplemental Figure A53 and A56).

The known metabolite DAQA (**3**) was isolated and characterized based on comparison of ^{1}H NMR and HRMS data with those appearing in literature.[91, 92]

3.2.2 Diazaquinomycin A (3) induces DNA damage, cell cycle arrest, and apoptosis through cleaved-PARP.

Compounds **12** and **3** were tested for *in vitro* cytotoxicity against the ovarian cancer cell line OVCAR5 by Eoghainín Ó hAinmhire in the lab of Joanna Burdette. Dose response analysis of the isolated compounds revealed an LC_{50} of 9.0 μM for **12** and 8.8 μM for **3** after treatment of cells for 96 hours (Figure 14). Further cell-based experiments were performed on **3** due to its high yield. Western blot analysis of OVCAR5 cells treated with 17.6 μM (LC_{100}) of **3** showed increased levels of p21 (a cell cycle inhibitor) after 8 hours (Figure 15). Interestingly, levels of p21 decreased after 24 hours when compared to solvent control. Reduction of p21 protein after 24 hours correlated with an increase in cleaved-PARP, an indication of apoptosis. The induction of cell cycle arrest, leading to apoptosis suggests significant DNA damage. To address this possibility,

immunofluorescence for phospho-histone H2A.X was performed on OVCAR5 cells treated with **3** at 17.6 μM. Enhanced DNA damage, as monitored by increased phospho-histone H2A.X staining, was seen after 8 hour and 24-hour treatment with 17.6 μM of **3** when compared to solvent control (Figure 16a and b). In summary, because cleaved PARP is the final stage of apoptosis and no significant increase in cleaved PARP was observed after the same 8-hour time frame that p21 and H2aX staining were increased, we concluded that the DNA damage was occurring prior to apoptosis.

Figure 14. Dose response analysis of **12** and **3** in OVCAR5 cells.

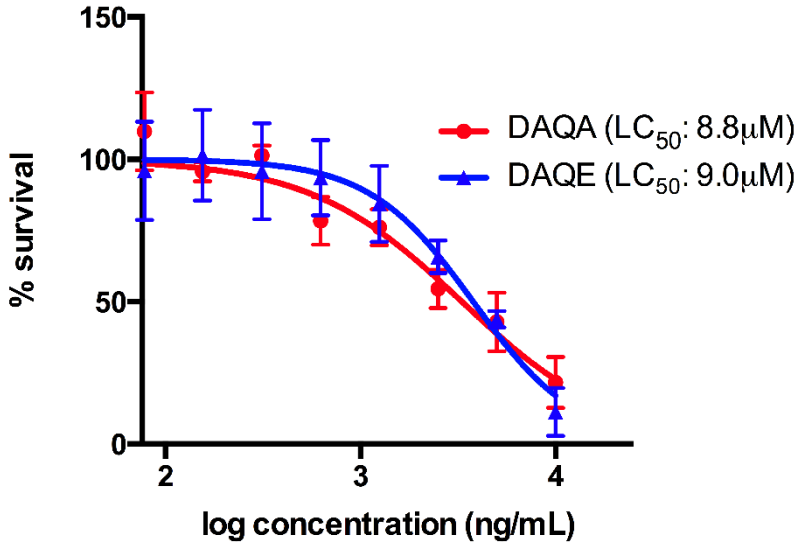

Concentrations represented as log of nanogram/mL. The LC_{50} value was determined using a non-linear curve fit on prism 6 GraphPad. These data represents average +/- SEM from three replicates.

Figure 15. Compound **3** induces cell cycle arrest followed by apoptosis.

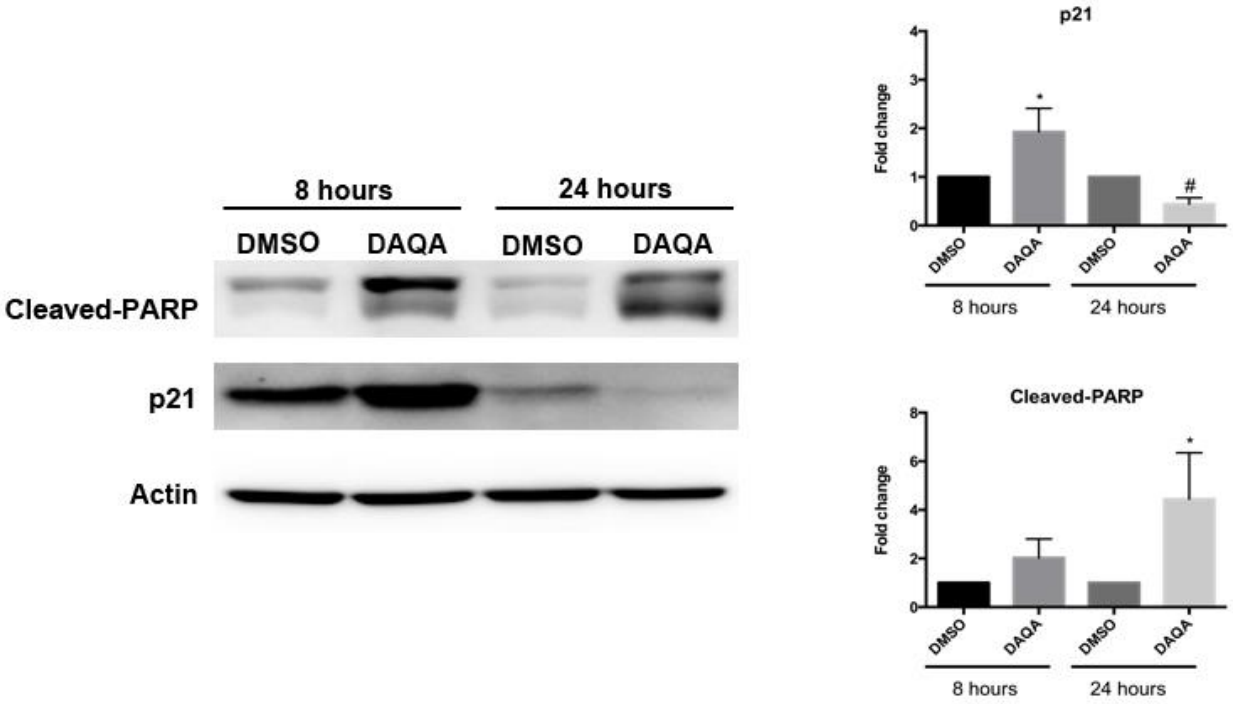

OVCAR5 cells treated with 17.6 μM of **3** showed induction of cell cycle arrest through increased p21 after 8 hours, and induction of apoptosis through increased cleaved-PARP after 24 hours. Increased expression of p21 in the DMSO control at 8 hours is due to mild cytotoxicity of the solvent, which is overcome after 24 hours. Densitometry of westerns was performed from three replicates. Statistical significance is denoted by * for increased expression, and # for decreased expression. Student t-test was performed for all statistics and are represented as SEM +/-, * and # $p \leq 0.05$.

Figure 16. Compound **3** induces DNA damage in OVCAR5 cells.

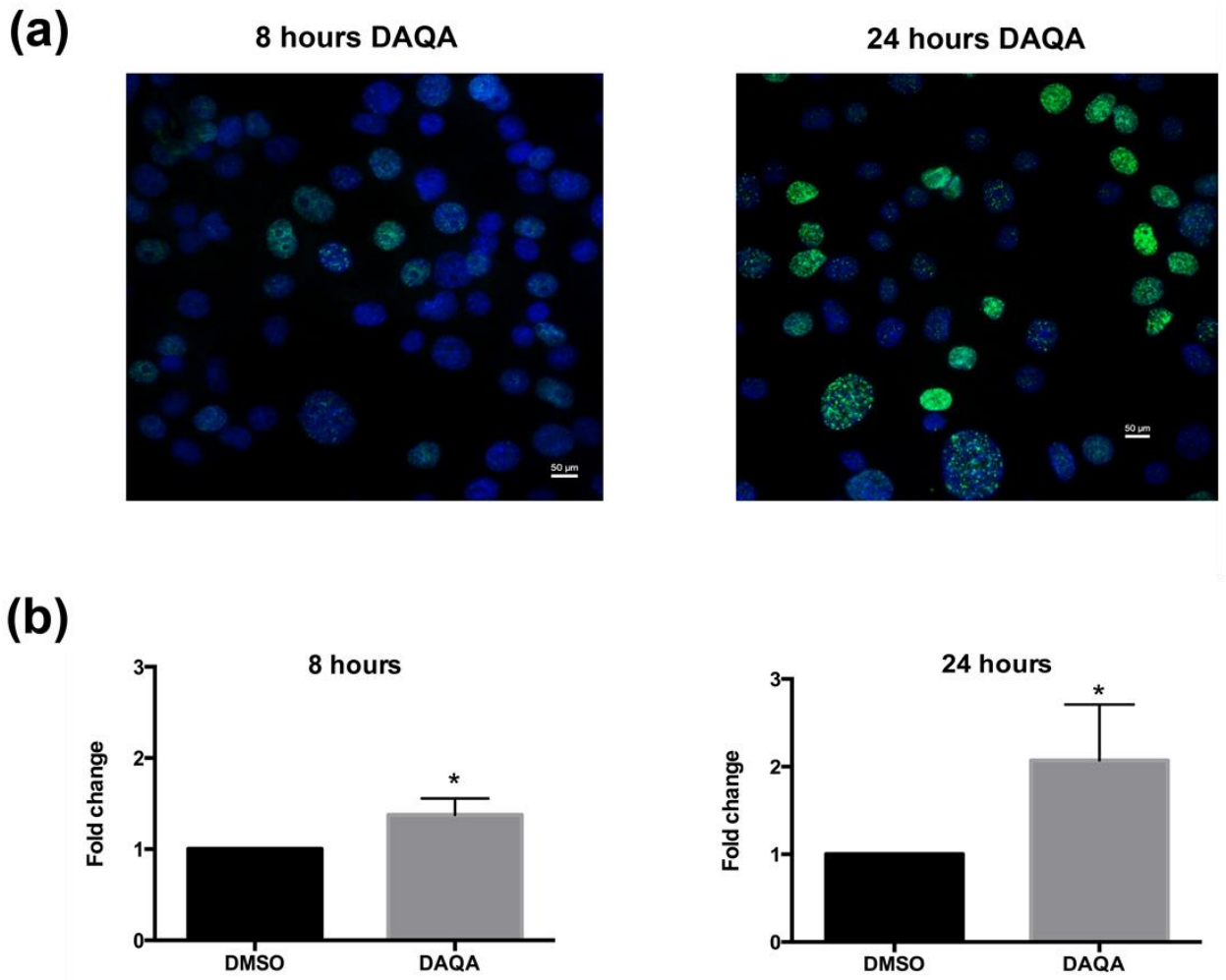

(a) H2A.X foci images taken after treatment of OVCAR5 cells with DAQA at 17.6 µM 8 hrs and 24 hours (b) Quantification of phospho-histone H2A.X foci as a fold increase over DMSO solvent control. Statistical significance is donated by * using student t-test. *$p \leq 0.05$.

Diazaquinomycins A and B were originally isolated from a *Streptomyces* sp. after exhibiting moderate inhibitory activity against four Gram-positive bacteria (three *Staphylococcus aureus* and one *Streptococcus faecium* IFO 3181 strains) in agar-based assays.[91, 92] A follow-up publication by the same group reported that **3** exhibited cytotoxicity against Vero and Raji cell lines, while also inhibiting thymidylate synthase in Ehrlich ascites carcinoma.[102] Additional studies were carried out in order to increase the solubility and bioactivity of **3**, and some success was achieved through modification of the C-3 and C-6 methyl groups to short chain ester and ether derivatives.[95] Nearly 15 years later, DAQC was isolated from a *Streptomyces* sp.; this report was

also the first mention of DAQD, though the metabolite was only observed through (-)-ESI MS experiments and was never fully characterized.[90] The observation of an aromatic resonance in the ^{1}H spectrum (H-6) of **12** is a feature unique among existing diazaquinomycin analogs; previously reported structures of this class contain a methyl group at this position.[90-92] In the current study, though four secondary metabolites were isolated and characterized from strain F001, we observed ten additional diazaquinomycin analogs (based on the presence of characteristic UV spectra and MS^2 fragmentation patterns) in LCMS data of our bioactive fractions. Positive ion values ranged from *m*/*z* 355.1 $[M + H]^+$ to 425.2 $[M + H]^+$, and given that UV spectra remained consistent among derivatives, structural modifications likely occurred in the α-substituted methyl and β-substituted alkyl groups. Finally, although **12** and **3** exhibited moderate cytotoxicity toward OVCAR5 cells by inducing apoptosis and enhancing DNA damage, these metabolites are currently under investigation in our laboratory for their selective antibiotic activity.

3.3 Methods.

3.3.1 General experimental procedures.

UV spectra were measured on a Shimadzu Pharma Spec UV-1700 spectrophotometer. NMR spectra were obtained on a Bruker 600 MHz DRX NMR spectrometer equipped with an inverse 5mm TXI cryogenic probe with z-axis pfg and XWINNMR version 3.5 operating software, and a 900 (226.2) MHz Bruker AVANCE NMR spectrometer equipped with an inverse 5 mm TCI cryogenic probe with z-axis pfg and TopSpin version 1.3 operating software at the University of Illinois at Chicago Center for Structural Biology. Chemical shifts (δ) are given in ppm and coupling constants (*J*) are reported in Hz. ^{1}H and ^{13}C NMR resonances of **12** are reported in Table 10. High resolution mass spectra were obtained on a Shimadzu IT-TOF spectrometer at the University of Illinois at Chicago Research Resources Center. High-performance liquid chromatography (HPLC-UV) data were obtained using a Hewlett-Packard series 1100 system

controller and pumps with a Model G1315A diode array detector (DAD) equipped with a reversed-phase C_{18} column (Phenomenex Luna, 100 × 4.6 mm, 5 μm) at a flow rate of 0.5 mL·min^{-1}. Semi-preparative HPLC scale separations were performed using a Hewlett Packard Series 1050 system with a Phenomenex Luna semi-preparative C_{18} column (250 × 10 mm, 5 μm) at a flow rate of 2.4 mL·min^{-1}. Preparative HPLC scale separations were performed using a Waters LC4000 System equipped with a Phenomenex Luna semi-preparative C_{18} column (250 × 21.2 mm, 5 μm) at a flow rate of 16 mL·min^{-1}.

3.3.2 Selection of actinomycete strain F001 for further investigation.

We screened our library of ca. 2,000 secondary metabolite fractions (from ca. 500 aquatic-derived actinomycete strains) in an in vitro single dose screen (20 μg/mL) against OVCAR5 and identified strain F001 as a promising bioactive lead, among other strains. Strain F001 (GenBank accession number KJ656126) shared 98% 16S rRNA gene sequence identity with the most closely related type strains *Streptomyces coacervatus* (GenBank accession number AB500703),[151] *Streptomyces hygroscopicus* subsp. *jinggangensis* (GenBank accession number NC_017765),[152] and *Streptomyces roseochromogenes* subsp. *oscitans* (GenBank accession number NZ_CM002285).[153]

3.3.3 Fermentation and extraction.

Strain F001 was cultured under two different media conditions. The culture that yielded **12** and **3** was grown in 44 × 1 L portions in Fernbach flasks containing high nutrient A1 medium (filtered ocean water, 10 g starch, 4 g yeast, 2 g peptone, 1 g calcium carbonate, 100 mg potassium bromide, and 40 mg iron sulfate) for 5 days at 21 °C while shaking at 220 rpm. The culture that yielded **13** and **14** was grown in 5 × 1 L portions in Fernbach flasks containing high nutrient CGS medium (filtered ocean water, 4 g casamino acids, 10 mL glycerol, and 5 g soy peptone) for 5 days at 21 °C while shaking at 220 rpm. Extraction methods for each growth condition were the same.

Sterilized Amberlite XAD-16 resin (15 $g \cdot L^{-1}$) was added to each flask to absorb the extracellular secondary metabolites. The culture medium and resin were shaken for 8 h and filtered using cheesecloth to remove the resin. The resin, cell mass, and cheesecloth were extracted with acetone overnight, concentrated under vacuum, and partitioned between water and ethyl acetate. The organic layer of the A1 fermentation was dried under vacuum to afford 6.3 g of extract. The organic layer of the CGS fermentation was dried under vacuum to afford 1.1 g of extract.

3.3.4 Isolation and characterization of diazaquinomycins E (12), F (13), and G (14).

DAQE was isolated from the fermentation broth (A1 media) of strain F001. The organic layer from the liquid-liquid partition was fractionated using silica gel flash column chromatography (100 g of silica) eluting with an isocratic 95% chloroform ($CHCl_3$):5% methanol (MeOH) solvent system to afford eight fractions. Using bioassay-guided fractionation, it was determined that fractions 2 and 3 contained the bioactive constituents, thus they were combined and separated using RP-C_{18} preparative HPLC (16 $mL \cdot min^{-1}$, gradient of 50% aqueous acetonitrile (ACN) to 100% ACN for 20 min, followed by an isocratic flow of 100% ACN for 10 min) to afford nine fractions. Fraction 8 (t_R 17.2 min, 14 mg) was separated using RP-C_{18} semi-preparative HPLC (2.4 $mL \cdot min^{-1}$, gradient of 50% aqueous ACN to 100% ACN for 25 min, followed by an isocratic flow of 100% ACN for 15 min) to afford diazaquinomycin E (**12**, t_R 22.1 min, 0.9 mg, 0.014% yield).

DAQF and DAQG were isolated from the fermentation broth (CGS media) of strain F001. The organic layer from the liquid-liquid partition of the culture extract was fractionated using silica gel flash column chromatography (100 g of silica) eluting with an isocratic 95% $CHCl_3$:5% MeOH solvent system to afford eight fractions. Using bioassay-guided fractionation, it was determined that fraction 8 contained the bioactive constituents, thus it was separated using normal phase silica gel (NP-Si) semi-preparative HPLC (2.0 $mL \cdot min^{-1}$, gradient of 99% $CHCl_3$:1% MeOH to 90%

$CHCl_3$:10% MeOH for 10 min, followed by an isocratic flow of 90% $CHCl_3$:10% MeOH for 15 min) to afford 7 fractions. Fraction 4 (t_R 18.1 min, 2.2 mg) was separated using NP-Si semi-preparative HPLC (2.0 $mL \cdot min^{-1}$, gradient of 99% $CHCl_3$:1% MeOH to 90% $CHCl_3$:10% MeOH for 10 min, followed by an isocratic flow of 90% $CHCl_3$:10% MeOH for 10 min) to afford 7 fractions. Fraction 5 (t_R 19.3 min, 0.4 mg) was separated using NP-Si semi-preparative HPLC (2.0 $mL \cdot min^{-1}$, gradient of 99% $CHCl_3$:1% MeOH to 90% $CHCl_3$:10% MeOH for 10 min, followed by an isocratic flow of 90% $CHCl_3$:10% MeOH for 10 min) to afford the co-eluting isomeric mixture of **13** and **14** (t_R 19.3 min, 0.28 mg, 0.025% yield).

Diazaquinomycin E (12): Red solid (0.9 mg). UV (MeOH) λ_{max} (log ε) = 282.5 (3.90), 362.5 (3.24), and a broad peak with maximum at 486.0 (2.56) nm. ^1H NMR (900 MHz, $CDCl_3$ - 1% CF_3CO_2D) and ^{13}C NMR (226.2 MHz, $CDCl_3$ - 1% CF_3CO_2D), see Table 10. HR-ESI-IT-TOF MS *m*/*z* 397.2198 $[M + H]^+$ (calcd. for $C_{23}H_{29}N_2O_4$: 397.2127), *m*/*z* 395.1943 $[M - H]^-$ (calcd. for $C_{23}H_{27}N_2O_4$: 395.1971), *m*/*z* 419.1997 $[M + Na]^+$ (calcd. for $C_{23}H_{28}N_2O_4Na$: 419.1947), *m*/*z* 793.4211 $[2M + H]^+$ (calcd. for $C_{46}H_{57}N_4O_8$: 793.4176), and *m*/*z* 815.3997 $[2M + Na]^+$ (calcd. for $C_{46}H_{56}N_4O_8Na$: 815.3996).

Diazaquinomycin F (13) and diazaquinomycin G (14): Red solid (0.28 mg). For UV, partial NMR, and HRMS data, see Appendix (Table S1; Figures A53-A60).

3.3.5 OVCAR5 cytotoxicity assay.

OVCAR5 cells were cultured in minimum essential media (Life Technologies, 11090-081) and supplemented with 10% fetal bovine serum (Gibco, 16000-044), 1% L-glutamine (Gibco, 25030-081), 1% nonessential amino acids (Gibco, 11140-050), 1% sodium pyruvate (Gibco, 11360-050) and 1% penicillin/streptomycin (Gibco, 15140-122). OVCAR5 cells (5000/well) were plated in a 96-well plate one day prior to treatment. The next day, cells were treated with varying doses of the given compound in regular culture media. The doses tested were 10 μg/mL, 5 μg/mL,

2.5 μg/mL, 1.25 μg/mL, 0.625 μg/mL, 0.3125 μg/mL, 0.15625 μg/mL and 0.078125 μg/mL. Doses higher than 10 μg/mL could not be tested due to compound insolubility in DMSO. Test plates were incubated at 37 ˚C with 5% CO_2 for 96 hours. After 96 hours, media was removed from the cells and washed with cold PBS. Cells were permanently fixed to the culture plate using 5% trichloroactetic acid (TCA). A sulforhodamine B (SRB) assay was performed as previously reported.[154] Percent survival was calculated by comparing samples treated with **12** or **3**, and samples treated with the relevant volume of DMSO solvent control. Prism 6 GraphPad was used to graph the results and determine the LC_{50} in μM concentrations.

3.3.6 Western blot analysis.

Cells were plated at a density of 50,000 cells in a 6-well plate one day before treatment. Cells were treated with 17.6 μM **3** for 8 hours and 24 hours. DMSO was used as a solvent control. Western blot gels were run as previously described.[124] 30 μg cell lysate was run for each sample. p21 (#9247) and cleaved-PARP (#9541) from Cell Signaling were used to probe protein membranes at concentrations of 1:1000 in 5% milk/TBS-T. Actin (Sigma-Aldrich) was used as a loading control at a concentration of 1:1000. Anti-rabbit HRP-linked antibody (cell signaling) was used for all blots at 1:1000. Densitometry was performed using ImageJ software. All samples were performed in triplicate.

3.3.7 Immunofluorescence.

Cells were plated at a density of 25,000 cells in a chamber slide (Millipore, PEZGS0816) one day before treatment. After one day, cells were treated with 17.6 μM of **3** for 8 hours and 24 hours. After the treatment, cells were washed with 1X cold PBS and fixed with 4% paraformaldehyde, and permeabilized with 0.2% Triton-X100 in PBS for 10 min. Cells were then washed twice with 1X PBS and blocked with 10% goat serum in PBS. Phospho-histone H2A.X (cell signal, #9178) was incubated on the cells for 1 hour at room temperature in 10% goat

serum/PBS at a concentration of 1/100. After two PBS washes, cells were incubated with anti-rabbit AlexaFluor 488 for 30 min at room temperature and mounted using Vectashield Mounting Medium with DAPI (Vector Laboratories). Images were taken on a Nikon E600 Microscope with a DS-Ri1 Digital Camera and NIS Elements Software. ImageJ software was used to count cells. The number of DAPI positive cells that were also positive for phosphor-histone H2A.X were expressed as a percentage of total DAPI stained cells. Only cells with defined foci were counted as positive. At least three random fields from three independent experiments were counted.

3.4 Conclusions.

Three new diaza-anthracene analogs were identified, diazaquinomycin E (**12**), F (**13**), and G (**14**) from the culture broth of a marine-derived *Streptomyces* sp. DAQE and its known analog DAQA exhibited moderate cytotoxicity toward OVCAR5 cells (LC_{50} of 9.0 and 8.8 μM, respectively). At lethal concentrations of **3**, evidence of DNA damage was seen with induction of apoptosis through cleaved-PARP. Among existing diazaquinomycins, **12**–**14** are the first reported members of the class to exhibit a variation in the diaza-anthracene core skeleton. Though this class of metabolites was initially identified from this strain based on moderate cytotoxicity toward OVCAR5 cells, additional studies in our laboratory have revealed that the DAQs exhibit promising antibiotic activity against TB. Detailed analysis of this bioactivity and the drug-lead potential of this class is described thoroughly in Chapter 1.

Cytotoxic evaluation is important in any rigorous characterization of a pre-clinical antibiotic drug-lead. In the case of a promising antibiotic lead, selectivity for bacterial growth inhibition over cytotoxicity is desirable and cancer cell line screenings are often read as a proxy for potential general cytotoxicity. While **3** was inactive against the non-cancerous Vero cell line, consideration of cytotoxicity towards cancer cell lines is important. While a moderate cytotoxicity LC_{50} value of 8.8 μM was observed in this study, **3** exhibited a remarkably potent and selective

inhibition of *M. tuberculosis* at an MIC of 0.28 μM. This amounts to an approximate 30-fold increase in bioactivity over OVCAR5 inhibition. Note that the LC_{50} value is the concentration at which **3** kills 50% of OVCAR5 cells, while the MIC value is the concentration at which **3** inhibits growth of 90% of mycobacteria. Considering the differences in inhibition percentage used to generate each data value, it becomes clear – a concentration that could kill *M. tuberculosis in vitro* is ever farther outside the window of relevant OVCAR5 cytotoxicity. This selectivity justified our extensive study of this class for its potential as an anti-TB drug candidate. However, through our later biological characterization of **3** in Chapter 1, two cancer cell lines, MDA-MB-435 (0.09 μM) and OVCAR3 (0.48 μM) were inhibited to levels closer to DAQ antibiotic activity. The lack of generalized cytotoxicity remains promising but these values beg for future investigation both for continued assessment of **3** as a viable drug lead and for the potential that a cytotoxic mechanism might inform the anti-tuberculosis mechanism.

4. A PIMARANE DITERPENE AND CYTOTOXIC ANGUCYCLINES FROM A MARINE-DERIVED *MICROMONOSPORA* SP. IN VIETNAM'S EAST SEA.[1]

4.1. Introduction.

The terpene class is a structurally diverse group of natural products with approximately 60,000 members. A recent study unveiled that the capacity of actinomycetes to produce the diterpene subclass has been significantly underestimated, where 25 of 100 randomly selected strains were identified as potential diterpene producers.[155] Despite this, only an estimated twenty diterpenes of actinomycete origin have been reported to date.[156] This is an exceedingly scarce fraction of the nearly 12,000 diterpenes described in the peer-reviewed literature, which are predominantly plant- and fungal-derived. In the current study, we report the rare isolation of a diterpene from an actinomycete strain.

As part of our program to explore the potential of marine and fresh water-derived actinomycete secondary metabolites to serve as antibiotic and anticancer drug leads, we have partnered with the Vietnam Academy of Science and Technology to explore Vietnam's East Sea to provide such leads.[89, 157] The East Sea in Vietnam covers an area of approximately three-million km^2 and traces 3000 km of coastline. This stretch is comprised of a multitude of microenvironments covering depths from 200 m to 5000 m. The marine biodiversity within the East Sea is considered to be some of the most extensive in the world, yet it remains poorly understood and explored. In the current study, through a screening of our fraction library against *M. tuberculosis* in the LORA which revealed a fraction with an MIC of 1.0 μg/mL, we identified an actinomycete isolated from sediment collected off the Cát Bà peninsula in the East Sea of

---

[1]Reproduced with permission from Mullowney, M.; Ó hAinmhire, E.; Tanouye, U.; Burdette, J.; Pham, V.; Murphy, B. A Pimarane Diterpene and Cytotoxic Angucyclines from a Marine-Derived *Micromonospora* sp. in Vietnam's East Sea. *Marine drugs* **2015**, *13*, 5815. Utilized under the Creative Commons license. More information available via the Internet at: creativecommons.org/licenses/by/4.0/

Vietnam. From this strain we isolated and characterized the novel diterpene isopimara-2-one-3-ol-8,15-diene (**15**) and lagumycin B (**16**), an angucycline that had yet to receive full structural characterization in the peer-reviewed literature (Figure 17).[158] In addition, we identified the previously reported angucyclines dehydrorabelomycin (**17**),[159, 160] phenanthroviridone (**18**),[161, 162] and WS-5995 A (**19**).[163, 164] Upon purification, these compounds were found to exhibit varying levels of cytotoxicity against a panel of ovarian cancer cell lines, indicating a toxicity not specific to the anti-TB activity observed when screening the parent fraction. Herein we present the structure elucidation and biological activity of these compounds.

4.2. Results and discussion.

4.2.1 Structure elucidation of isopimara-2-one-3-ol-8,15-diene (15) and lagumycin B (16).

Following a series of chromatographic experiments, **15** was obtained as a colorless solid (Figure 17). Combined HRMS and NMR experiments allowed for the assignment of the molecular formula as $C_{20}H_{30}O_2$, indicative of six degrees of unsaturation. ^{1}H and ^{13}C NMR data are shown in Table 11. In the ^{1}H NMR spectrum, we observed evidence for four sp^3 quaternary carbon-bound methyl groups, one vinyl group, an oxymethine geminal to a hydroxy group, a pair of geminal

Table 11. ^{1}H and ^{13}C NMR data ($CDCl_3$) of **15**.

Position	^{13}C, Type [a]	^{1}H, Mult. (*J*, Hz) [b,c]
1_{ax}	49.8, CH_2	2.25, d (12.3)
1_{eq}		2.58, d (12.3)
2	211.8,C	
3	83.0, CH	3.91, d (4.0)
3-OH		3.44, d (4.0)
4	45.3, C	
5	50.3, CH	1.78, m
6	18.8, CH_2	1.58, m
		1.80, m
7	32.3, CH_2	2.03, m
8	126.4, C	
9	134.3, C	
10	43.8, C	
11_{ax}	21.4, CH_2	1.76, m
11_{eq}		1.88, m
12_{eq}	34.8, CH_2	1.33, m
12_{ax}		1.53, m
13	35.3, C	
14	41.6, CH_2	1.76, m
		1.88, m
15	145.9, CH	5.72, dd (17.5, 10.7)
16	111.2, CH_2	4.85, dd (17.5, 1.4)
		4.92, dd (10.7, 1.4)
17	28.3, CH_3	0.98, s
18	20.6, CH_3	0.93, s
19	29.3, CH_3	1.21, s
20	16.5, CH_3	0.72, s

[a] 226.2 MHz; [b] 600 MHz; [c] s = singlet; d = doublet; dd = doublet of doublets; m = multiplet.

hydrogens adjacent to a carbonyl, and additional methylene and methine groups on **15** that constituted the remainder of a pimarane diterpene core skeleton.

Analysis of ^{13}C- DEPTQ and HSQC NMR data for **15** indicated the presence of one carbonyl carbon (δ_C 211.8, C-2), two fully-substituted endocyclic alkene carbons (δ_C 126.4, C-8; 134.3, C-9), one vinyl methylene carbon (δ_C 111.2, C-16), one vinyl methine carbon (δ_C 145.9, C-15), one oxymethine carbon (δ_C 83.0, C-3), and fourteen additional sp^3 carbons. Given that the molecular formula of **15** afforded six degrees of unsaturation and the molecule contained one carbonyl, one vinyl, and one endocyclic alkene group, the remaining three degrees were satisfied by the tricyclic pimarane ring system. Key HMBC, COSY, and 1D-TOCSY correlations are given in Figure 18.

Figure 17. Structures of compounds **15-19**.

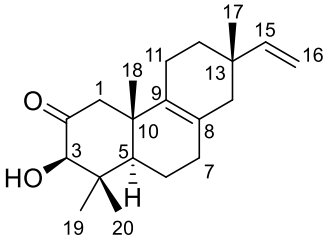

isopimara-2-one-3-ol-8,15-diene (15)

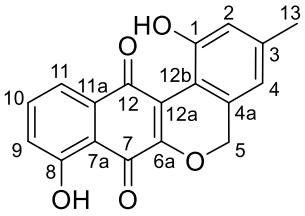

lagumycin B (16)

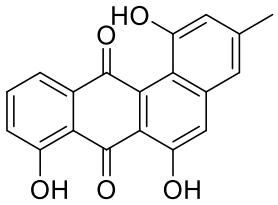

dehydrorabelomycin (17)

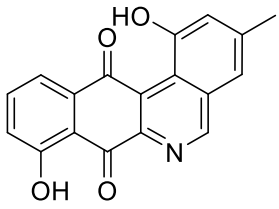

phenanthroviridone (18)

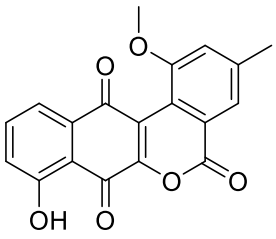

WS-5995 A (19)

Figure 18. Key 2D NMR correlations of **15** and **16**.

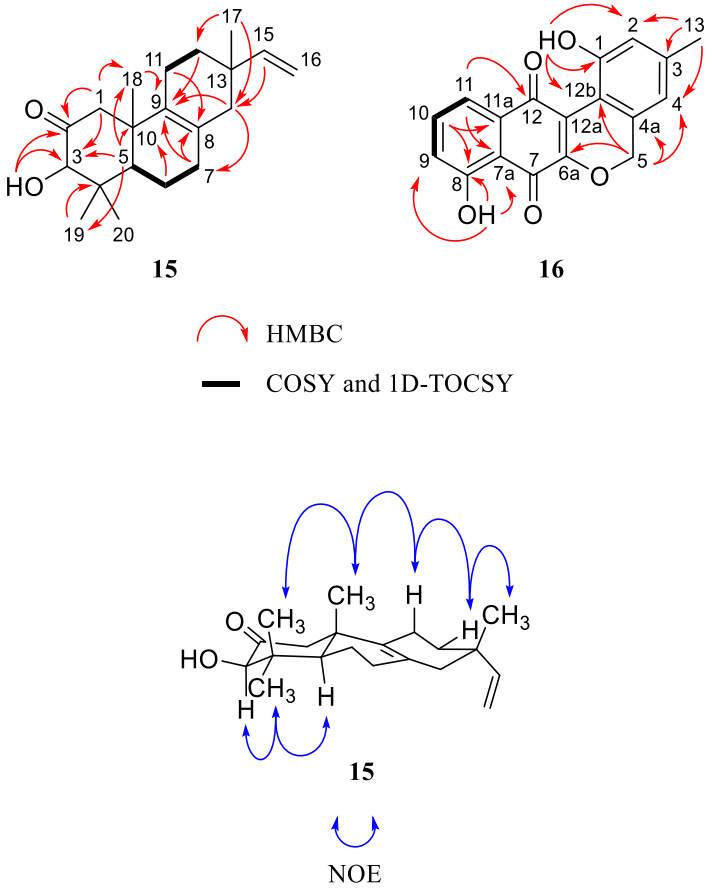

The connectivity of the two distinct spin systems of C-11–C-12 and C-5–C-6–C-7 was determined by interpretation of the COSY NMR spectrum. Confirmation of these assignments was supported by a series of 1D-TOCSY experiments that exploited the solvent effect of C_6D_6 on lower frequency chemical shifts, which served to deconvolute the signal overlap observed when ^{1}H NMR experiments were run in $CDCl_3$ (Table A6 and Figures A66–A70).[165] At this point in the elucidation process, we used HMBC correlations of methyl groups in **15** to piece together the tricyclic diterpene core. Geminal methyl groups were confirmed at C-4 based on HMBC correlations from H_3-19 and H_3-20 to C-3, C-4, and C-5. Signal H_3-18 exhibited correlations to C-1, C-9, and C-10, suggesting a bond to the quaternary C-10. The connectivity of ring A was further established by observation of HMBC correlations from H_2-1 to C-3, C-5, C-9, C-10, and C-18,

suggesting that this methylene was between the C-2 carbonyl and C-10. Additionally, the oxymethine signal (H-3) showed HMBC couplings to C-2, C-4, C-19, and C-20, while the hydroxy signal (3-OH) displayed correlations to C-2 and C-3. This supported that H-3 and 3-OH were connected to the same carbon, which was positioned between the carbonyl at C-2 and the quaternary C-4. Couplings were also observed from H-5 to C-4 and C-10, solidifying the fusion of rings A and B. The connectivity of the C-5–C-6–C-7 spin system from ring A to the remainder of the core was established by observation of HMBC correlations from H_2-7 to C-8 and C-9. Correlations from H_2-14 to C-7, C-8, C-9, C-12, C-15, and C-17 placed it between the alkene C-8 and quaternary C-13. Resonance H_3-17 showed HMBC correlations to C-12, C-13, C-14, and C-15, placing it at position 13. HMBC correlations between the vinyl methine hydrogen (H-15) and C-13, C-14, and C-17 supported this, while correlations from H_2-16 to C-15 and C-13 provided further evidence for connectivity of the vinyl group to C-13. The remaining connectivity of ring C was satisfied by HMBC correlations from H_2-11 to C-8, C-9, and C-13.

A 2D-NOESY NMR experiment was employed to determine the relative stereochemistry of **15**, revealing correlations between H_3-20 and H_3-18, H_3-18 and H-11_{ax}, H-11_{ax} and H-12_{eq}, and H-12_{eq} and H_3-17; this suggested that these hydrogens projected out from the same face of the molecule. This orientation was supported by the observation of NOESY correlations between hydrogens H-3 and H_3-19, and H_3-19 and H-5, projecting from the opposite face of the molecule (Figure 18).

To identify the absolute configuration of centers in **15**, a CD spectrum was acquired and analyzed (Figure A73). Compound **15** exhibited a positive Cotton effect at the $n \rightarrow \pi^*$ carbonyl transition of 290 nm, indicating that the β-axial methyl group (C-18) was in the rear upper left octant when the octant rule was applied.[166] Thus, the absolute configuration of stereocenters in **15** was elucidated as 3*R*, 5*R*, 10*S*, and 13*S*, establishing the structure of **15** as (3R,5R,10S,13S)-3-

hydroxy-4,4,10,13-tetramethyl-13-vinyl-1,4,5,7,8,10,11,12,13,14-decahydrophenanthren-2(3H)-one, which was given the simplified name of isopimara-2-one-3-ol-8,15-diene.

Following a series of chromatographic steps, **16** was obtained as a pale orange solid. Combined HRMS and NMR experiments allowed for the assignment of the molecular formula as $C_{18}H_{12}O_5$, indicative of thirteen degrees of unsaturation. The UV absorption profile (maxima of 204, 280, 310, and 410 nm) of **16** displayed characteristics of an extended aromatic ring system similar to the previously reported angucycline isolates **17**, **18**, and **19**. ^{1}H and ^{13}C NMR data are shown in Table 12. A singlet resonance at δ_H 5.19 (2H, H-5) observed in the ^{1}H NMR spectrum indicated the presence of oxygenated methylene protons. Two highly deshielded resonances at δ_H 10.45 (1H,

Table 12. ^{1}H and ^{13}C NMR data **(**$CDCl_3$) of **16**.

Position	**^{13}C, Type** [a]	**^{1}H, Mult. (*J*, Hz)** [b,c]
1	154.5, C	
1-OH		10.45, s
2	121.1, CH	6.85, s
3	143.7, C	
4	118.2, CH	6.54, s
4a	130.3, C	
5	70.7, CH_2	5.19, s
6a	157.0, C	
7	183.4, C	
7a	113.5, C	
8	161.7, C	
8-OH		11.70, s
9	125.2, CH	7.30, d (8.1)
10	137.2, CH	7.66, t (8.1)
11	121.3, CH	7.81, d (8.1)
11a	132.2, C	
12	186.6, C	
12a	124.4, C	
12b	109.9, C	
13	21.3, CH_3	2.33, s

[a] 226.2 MHz; [b] 600 MHz; [c] s = singlet; d = doublet; t = triplet.

1-OH) and δ_H 11.70 (1H, 8-OH) gave evidence of two hydroxy peri-protons. The observation of three aromatic signals at δ_H 7.30 (1H, H-9), δ_H 7.81 (1H, H-11), and δ_H 7.66 (1H, H-10) indicated the presence of a tri-substituted aromatic ring. Additionally, two singlet resonances were observed in the aromatic region at δ_H 6.54 (1H, H-4) and δ_H 6.85 (1H, H-2), indicating the presence of isolated hydrogens on a separate, tetrasubstituted aromatic system. Finally, a singlet resonance at δ_H 2.33 (3H, H_3-13) evidenced one aromate-bound methyl group.

Analysis of ^{13}C-DEPTQ NMR data suggested the presence of two quinone carbonyls (δ_C 186.6, C-12; 183.4, C-7), two hydroxy-substituted aromatic carbons (161.7, C-8; 154.5, C-1), one oxygenated methylene carbon (δ_C 70.7, C-5), one methyl carbon (δ_C 21.3, H_3-13), and an additional twelve aromatic carbons. Given that the molecular formula afforded thirteen degrees of unsaturation and the molecule contained two carbonyls and seven double bonds, the remaining degrees were satisfied by the fused angucycline ring system.

Interpretation of COSY NMR data defined one distinct aromatic spin system that connected C-9–C-10–C-11, supporting the aforementioned evidence for a 1,2,3-trisubstitued benzene moiety. A phenolic hydroxy peri-proton at δ_H 11.70 showed HMBC correlations to C-7a, C-8, and C-9, establishing hydroxy connectivity to C-8. An aromatic hydrogen at H-10 exhibited an HMBC correlation to C-11a, completing assignments for the 1,2,3-trisubstitued benzene. An HMBC correlation observed between aromatic hydrogen H-11 and the carbonyl C-12 was critical to establishment of the phenol position relative to the central quinone ring. The positions of the C-7 and C-12 relative to the oxygenated carbon at C-6a were based on comparison to previously reported ^{13}C chemical shift values of similarly substituted paraquinones.[167, 168] The 1-OH peri-proton showed HMBC correlations to C-1, C-12b, and C-2, providing evidence for connectivity of the hydroxy group to C-1. The singlet aromatic methyl signal at H_3-13 exhibited correlations to

C-3, C-2, and C-4 in the HMBC spectrum, placing it *meta* to the hydroxy group at C-1. HMBC correlations from the oxygenated methylene at H_2-5 to C-4a, C-4, C-12b, and C-6a established connectivity of the naphthoquinone fragment to the phenol moiety. Key COSY and HMBC correlations are given in Figure 18. Thus, the structure of **16** is as shown with the name lagumycin B, following the structure and nomenclature established in the 1995 dissertation by Balk-Bindseil and Laatsch.[158]

The characterization of known compounds **17**–**19** was based on comparison of ^{1}H NMR and HRMS data with those appearing in literature (Figures A80–A86).[159-164]

4.2.2 Antibiotic activity evaluation of isopimara-2-one-3-ol-8,15-diene (15), lagumycin B (16), dehydrorabelomycin (17), phenanthroviridone (18), and WS 5995 A (19) against *M. tuberculosis* in the MABA.

Following their identification, the MABA was used in the ITR by Sang Hyun Cho to test the ability of compounds **1-5** to inhibit replicating *M. tuberculosis* H_{37}Rv (ATCC 27294) *in vitro*

Table 13. *In vitro* anti-TB activity of **15-19**.

Compound	H_{37}Rv MIC (μg/mL)	
	MABA	LORA
15	19.4	> 50
16	2.01	25.7
17	1.01	19.6
18	0.72	17.8
19	22.7	> 50

as previously described.[93, 94, 157] Compounds **16**–**18** exhibited minimum inhibitory concentrations of 2.01 μg/mL, 1.01 μg/mL, and 0.72 μg/mL (MICs; defined as the lowest concentration resulting in ≥90% growth inhibition of H_{37}Rv, and averaged from triplicates), respectively, while compounds **15** and **19** lacked significant activity. Additionally, none of the compounds were

significantly active when tested for their ability to inhibit non-replicating *M. tuberculosis* $H_{37}Rv$ (ATCC 27294) in the LORA (Table 13).[93, 94, 96, 157] The potent MIC first observed in the parent fraction from our library was not reproduced by any of these compounds, indicating that either the large-scale strain regrow did not afford production of the active component or the compound responsible for the activity was not isolated.

4.2.3 Cytotoxicity evaluation of isopimara-2-one-3-ol-8,15-diene (15), lagumycin B (16), dehydrorabelomycin (17), phenanthroviridone (18), and WS 5995 A (19).

To further characterize the bioactivity profile of compounds **15**–**19**, assessment of cytotoxicity was performed using two high-grade ovarian cancer cell lines, OVCAR4 and Kuramochi.[169] Potential for selective cytotoxicity was evaluated using two non-cancerous mouse cell lines representing the putative progenitor cells of ovarian cancer, murine ovarian surface epithelial (MOSE) and murine oviductal epithelial (MOE). Screening of **15**–**19** against this panel

Table 14. *In vitro* cytotoxicity of **15-19**.

Compound	Cytotoxicity LC_{50} (µM) [a]			
	Kuramochi	**OVCAR4**	**MOSE**	**MOE**
15	>33.1	>33.1	>33.1	>33.1
16	>32.5	>32.5	9.80	10.8
17	6.72	11.0	3.50	28.5
18	1.11	4.82	2.85	6.20
19	18.6	127	>149	>149

[a] doxorubicin was used as the positive control and was lethal at the lowest concentration tested (0.078 µM).

by Eoghainín Ó hAinmhire in the lab of Joanna Burdette revealed **17** and **18** to be non-specifically cytotoxic, which was in accord with their previously reported bioactivities.[159, 161, 162, 170-172] Compound **16** exhibited up to 14-fold enhanced cytotoxicity against non-cancerous murine cell lines MOSE and MOE, with LC_{50} values of 9.80 µM and 10.8 µM, respectively. Generally speaking, this para-quinone scaffold is not an attractive lead, as higher toxicity in non-tumorigenic

cell lines confers serious overall toxicity. In contrast, compound **19** showed approximately seven-fold greater activity toward Kuramochi ovarian cancer cells with an LC_{50} of 18.6 μM (Table 14). Previous studies indicated that **19** inhibits tumor cell proliferation and viability in L1210 lymphocytic leukemia cells *in vitro* with an IC_{50} range of 0.24–0.65 μM.[173] Compound **15** was not significantly active in all bioassays in the current study. The antibiotic activity observed in the initial screening was determined not to be specific to TB given the cytotoxic nature of compounds **16**-**18**.

Compounds **16**–**19** are classified as angucyclines, which are among the largest class of type II PKS natural products and are known to exhibit a wide variety of biological activities.[174] Compound **16** was initially isolated from marine *Streptomyces* sp. B8245 and reported in a dissertation, but it has yet to receive formal characterization.[158] Both **17** and **18** have previously been identified as intermediates in kinamycin biosynthesis;[175, 176] this product was not detected in our fermentation extracts. Similarly, compound **17** was proven to be a biosynthetic intermediate of jadomycin and gilvocarcin in a *Streptomyces lividans* strain,[177] though these were also not observed in secondary metabolite fractions produced by our *Micromonospora* strain. In previous reports, **17** exhibited no detectable activity when screened against a panel of Gram-negative and Gram-positive bacteria,[178] but inhibited a wide range of cancer cell lines at micromolar potency. Compound **18** was reported to have a variety of antibiotic and cytotoxic properties and our data support these non-specific biological activities.[161, 162, 172] Finally, compound **19** was first isolated from a *Streptomyces auranticolor* strain and was reported to exhibit anticoccidial activity against the apicomplexan poultry parasite *Eimeria tenella*, while exhibiting no significant biological activity when screened against a panel that included two fungal species, a human parasite, and several Gram-negative and Gram-positive bacteria.[163, 164] This compound was also studied more recently for its aforementioned antileukemic activity, where it inhibited proliferation leading to

apoptosis through DNA cleavage, blockage of nucleoside transport and inhibition of DNA, RNA, and protein synthesis.[173] To our knowledge, this study is the first to report cytotoxicity of compound **19** in carcinomas. In most cases, **18** is significantly more cytotoxic than **17** and **19**. Presumably, this may be due to structural differences including the pyridine function in **18** that is absent in the others. Additionally, a contributing factor to reduced cytotoxicity may be the loss of aromaticity in the adjacent anthraquinone ring (**19**), though further biological testing and structure activity analyses are required to support this.

4.3 Methods.

4.3.1 General experimental procedures.

Optical rotation measurement was performed in MeOH using a 10.0 cm cell on a PerkinElmer 241 polarimeter at 25 °C. The UV spectra were measured on a Shimadzu Pharma Spec UV-1700 spectrophotometer. NMR spectra were obtained on a Bruker 600 MHz DRX NMR spectrometer equipped with an inverse 5 mm TXI cryogenic probe with z-axis pfg and XWINNMR version 3.5 operating software, and a 900 (226.2) MHz Bruker AVANCE NMR spectrometer equipped with an inverse 5 mm TCI cryogenic probe with z-axis pfg and TopSpin version 1.3 operating software at the University of Illinois at Chicago Center for Structural Biology. Chemical shifts (δ) are given in ppm and coupling constants (*J*) are reported in Hz. ^{1}H and ^{13}C NMR resonances of **15** and **16** are reported in Tables 11 and 12, respectively. ^{1}H and ^{13}C NMR chemical shifts were referenced to the $CDCl_3$ (δ_H 7.26 ppm and δ_C 77.0 ppm, respectively) and C_6D_6 solvent signals (δ_H 7.16 ppm and δ_C 128.1 ppm, respectively). High resolution mass spectra were obtained on a Waters Synapt Q-TOF mass spectrometer at the University of Illinois at Chicago Research Resources Center (UIC RRC). High-performance liquid chromatography (HPLC-UV) data were obtained using a Hewlett-Packard series 1100 system controller and pumps with a Model G1315A diode array detector (DAD) equipped with a reversed-phase C_{18} column (Phenomenex Luna,

100 mm × 4.6 mm, 5 μm; Torrance, CA, USA) at a flow rate of 0.5 mL·min^{-1}. Semi-preparative HPLC scale separations were performed using a Hewlett Packard Series 1050 system with a Phenomenex Luna semi-preparative C_{18} column (250 mm × 10 mm, 5 μm) at a flow rate of 2.4 mL·min^{-1}. Preparative HPLC scale separations were performed using a Waters LC4000 System equipped with a Phenomenex Luna preparative C_{18} column (250 mm × 21.2 mm, 5 μm) at a flow rate of 16 mL·min^{-1}. Silica gel column chromatography was conducted using Bonna-Angela Technologies Cleanert® silica gel (Wilmington, DE, USA) with an average particle size of 40–60 μm and an average pore size of 60 Å.

4.3.2 Collection and identification of actinomycete strain G039.

Strain G039 was isolated from a sediment sample collected by PONAR at a depth of 22 m, from *ca*. 3.3 miles off the coast southeast of Cát Bà Peninsula in Vietnam (20°41′30″ N, 107°05′58″ E) in July of 2011. Strain G039 (GenBank accession number KR703606) shared 99% 16S rRNA gene sequence identity with the type strain *Micromonospora haikouensis* (GenBank accession number NR117442).[179]

4.3.3 Fermentation and extraction.

Strain G039 was grown in 38 × 1 L portions in Fernbach flasks containing high nutrient media components in artificial seawater (10 g starch, 4 g yeast extract, 2 g peptone, 1 g calcium carbonate, 100 mg potassium bromide, 40 mg iron sulfate, and 33.3 g Instant Ocean® per liter of dH_2O) for 7 days at 21 °C while shaking at 220 rpm. Sterilized Amberlite XAD-16 resin (15 g·L^{-1}) was added to each flask to absorb the extracellular secondary metabolites. The culture medium and resin were shaken for 10 h and filtered using cheesecloth to remove the resin. The resin, cell mass, and cheesecloth were extracted with acetone overnight, concentrated under vacuum, and partitioned between water and ethyl acetate. The organic layer was dried under vacuum to afford 3.52 g of extract.

4.3.4 Isolation and characterization of isopimara-2-one-3-ol-8,15-diene (15), lagumycin B (16).

The organic layer from the liquid-liquid partition was fractionated using silica gel flash column chromatography (23 cm × 3.5 cm, 85 g silica) eluting with a step gradient solvent system of 200 mL 100% hexanes (HEX), 200 mL 90% HEX:10% dichloromethane (DCM), 200 mL 70% HEX:30% DCM, 200 mL 100% DCM, 200 mL 70% DCM:30% ethyl acetate (EtOAc), 200 mL 70% EtOAc:30% DCM, 200 mL 100% ethyl acetate, 200 mL 95% EtOAc:5% 2-propanol, 200 mL 90% EtOAc:10% methanol (MeOH), 200 mL 50% EtOAc:50% MeOH, 400 mL 95 % MeOH:5% ammonium hydroxide (NH_4OH) to afford eleven fractions. Upon re-screening, it was determined that fraction 3 contained the bioactive constituents, thus, it was further separated using RP-C_{18} preparative HPLC (16 mL·min^{-1}, gradient of 50% aqueous MeOH to 100% MeOH over 25 min, followed by an isocratic flow of 100% MeOH for 15 min), to afford 13 fractions. Fractions 6 and 11 exhibited biological activity so they were further separated.

Fraction 6 was further purified using RP-C_{18} semi-preparative HPLC (2.4 mL·min^{-1}, gradient of 70% aqueous MeOH to 80% MeOH for 37.5 min, followed by an isocratic flow of 100% ACN for 10 min) to afford phenanthroviridone (**18**, t_R 37.5 min, 0.66 mg, 0.019% yield), lagumycin B (**16**, t_R 40.2 min, 0.9 mg, 0.026% yield) and WS-5995 A (**19**, t_R 42.0 min, 1.2 mg, 0.034% yield).

Fraction 11 was further separated using RP-C_{18} semi-preparative HPLC (2.4 mL·min^{-1}, gradient of 80% aqueous MeOH to 90% MeOH for 37.5 min, followed by an isocratic flow of 100% ACN for 10 min) to afford 8 fractions. Fraction 2 was further purified using two iterations of RP-C_{18} semi-preparative HPLC (2.4 mL·min^{-1}, gradient of 80% aqueous MeOH to 90% MeOH for 37.5 min, followed by an isocratic flow of 100% ACN for 10 min) to afford dehydrorabelomycin (**17**, t_R 26.7 min, 0.4 mg, 0.011% yield). Purification of compound **17** also afforded isopimara-2-one-3-ol-

8,15-diene (**15**, t_R 27.5 min, 0.9 mg, 0.026% yield), eluting as a neighboring peak observable at 220 nm.

Isopimara-2-one-3-ol-8,15-diene (**15**): Colorless solid (0.9 mg). $[\alpha]_D^{25}$ = +20.7 (*c* = 0.00053, MeOH). UV (MeOH) λ_{max} (log ε) = 204 (3.67) and shoulders at 228 (3.39) and 242 (3.30) nm (Figure A72). CD (*c* = 0.0031, MeOH): λ_{max} (Δε) = 225 (+65.2), 250 (−4.4), 290 (+54.4) nm (Figure A73). ^{1}H NMR (900 MHz, $CDCl_3$) and ^{13}C NMR (226.2 MHz, $CDCl_3$), see Table 11. HR-ESI-Q-TOF MS *m*/*z* 303.2338 $[M + H]^+$ (calcd. for $C_{20}H_{31}O_2$: 303.2319), and *m*/*z* 325.2141 $[M + Na]^+$ (calcd. for $C_{20}H_{30}O_2Na$: 325.2138).

Lagumycin B (**16**): Pale orange solid (0.9 mg). UV (MeOH) λ_{max} (log ε) = broad absorptions with maxima at 204 (3.57), 280 (2.86), 310 (2.73) and 410 (2.27) nm. ^{1}H NMR (600 MHz, CDCl3) and ^{13}C NMR (226.2 MHz, $CDCl_3$), see Table 12. HR-ESI-Q-TOF MS *m*/*z* 309.0773 $[M + H]^+$ (calcd. for $C_{18}H_{13}O_5$: 309.0757).

4.3.5 OVCAR4, Kuramochi, MOSE, MOE, and Vero cytotoxicity assays.

Human ovarian OVCAR4 and Kuramochi cancer cells were maintained in RPMI 1640 (11875-093, Life-technologies; Carlsbad, CA, USA) supplemented with 10% FBS (16000-044, Life-technologies; Carlsbad, CA, USA) and 1% penicillin/streptomycin. Non-cancerous murine ovarian surface epithelium (MOSE) and murine oviductal epithelium (MOE) cells were maintained as previously reported.[124] Concentration-response experiments were performed as previously described for 72 h.[89]

4.4 Conclusions.

Of the five compounds isolated in this study, two were previously unreported. Compound **15** represents a relatively rare example of the isolation of a diterpene from an actinomycete strain. Since a previous report that mined the genomes of a small population of actinomycete strains

suggested that this phylum has a far greater capacity to produce diterpenes (25 of 100 strains) than is represented in the peer reviewed literature, it is possible that this discrepancy is a product of these pathways remaining silent under laboratory growth conditions, or of the methods used to isolate natural products from bacteria, namely bioassay-guided fractionation.[155] One possible explanation of the latter phenomenon is that specific classes of diterpenes are conserved within Actinobacteria, and that these classes are not biologically active in the typical barrage of assays used to discover small molecule leads, though in the absence of extensive genome mining and subsequent structure identification-bioactivity experiments, this will remain speculation.

The novel diterpene isopimara-2-one-3-ol-8,15-diene (**15**) was isolated along with the angucycline lagumycin B (**16**), and three other angucyclines from a *Micromonospora* sp. collected in the East Sea of Vietnam. The angucyclines exhibited varying degrees of TB inhibition in addition to cytotoxicity against a panel of cancerous and non-cancerous cell lines, with the notable exception of WS-5995 A (**19**), which showed enhanced cytotoxicity against the Kuramochi cell line when compared to non-tumorigenic cell lines. Though not significantly active in our bioassays, the discovery of isopimara-2-one-3-ol-8,15-diene contributes to the growing but still relatively small number of diterpenes identified from actinomycetes. This study highlights our collaborative efforts to discover novel biologically active molecules from the large, underexplored, and biodiversity-rich waters of Vietnam's East Sea.

5. CONCLUSIONS.

The pathogen *M. tuberculosis* is the deadliest of infectious agents, its annual death toll having surpassed HIV in 2015. Fortunately, millions of years of evolution have afforded microorganisms with the chemical arsenal necessary to target specific biological molecules in other organisms for their inhibition. Modern analytical, chemical, and biochemical techniques allow the application of these chemical weapons from nature to therapeutic roles for treatment of disease. The investigations presented herein give evidence for the importance of natural products drug discovery from aquatic derived actinomycete bacteria and include the novel approach of utilizing freshwater environments as a source for new strains with novel chemistry. In seeking novel molecules with anti-tuberculosis properties, several known compounds with somewhat promiscuous activity were discovered, while a series of novel diazaquinomycin analogs were identified that revealed a remarkable selectivity of this antibiotic class for TB inhibition.

In the first two studies, novel diazaquinomycin analog antibiotics were discovered from actinomycete strains collected in Lake Michigan and the marine environment. Various analytical and spectroscopic techniques were employed to elucidate the unique structures of these compounds. The potent and selective inhibition of *M. tuberculosis* by **3** was described and efforts to elucidate the anti-TB MOA were undertaken as a large, international collaborative effort. Despite the testing of **3** in a barrage of biochemical tests and whole-cell bioassays against a variety of *M. tuberculosis* mutants, a definitive mechanism of action remains to be discovered. Study of **3** *in vivo* has been troublesome due largely to the compound's poor solubility, but optimization for new studies are currently underway. The full potential of this class as an anti-TB treatment remains to be explored.

A separate study in Chapter 4 also aimed at identifying novel anti-TB agents described the rare discovery of a novel pimarane diterpene from an actinomycete strain collected in the East Sea

of Vietnam. Though neither this compound nor the angucyclines from the same strain show promise as drug-leads, this project establishes a collaboration aimed at searching the underexplored aquatic environments around Vietnam for novel drug-leads while also educating a generation of new researchers from that country who are typically not as involved in drug discovery as other Asian countries or their Western counterparts.

Despite being humanity's most deadly bacterial pathogen, much about *M. tuberculosis* and its treatment remain to be understood. Current therapies can cure patients of the disease, but the process is inefficient, with the use of multi-drug combination therapy regimens spanning months if not years. Additionally, the incidence of tuberculosis resistant to all forms of treatment are increasing.[43] More responsible, consistent, monitored therapy is needed so that current therapies don't become obsolete with rising resistance and so that new therapies have endurance in the clinic. With a need for new treatments comes a need for more researchers involved in discovery. Populations tend to favor funding of health initiatives that are self-beneficial. Though TB research efforts are mostly in the developed world they are still relatively sparse. Unfortunately, resources for study of the disease in communities afflicted by the disease are far more scarce. Thus, new efforts need to be made to involve those affected by TB in this biomedical research. Initiatives to grow TB discovery labs in these communities can be found within the TB alliance (Kenya, South Africa, Zambia, China, India) and even through the small collaboration between the Murphy lab and VAST in Vietnam which resulted in the work described in Chapter 4 and elsewhere.[30, 180, 181]

Novel sources for chemical diversity could also greatly enhance the pursuit for new drug leads. In the Murphy lab, we have successfully expanded the marine drug discovery paradigm to include freshwater-derived actinomycetes,[86, 157] and even more recently to explore the drug-lead potential of molecules produced by freshwater sponges and their associated microbial communities.[182-189] To date, the only reports of metabolites unique to freshwater sponges are

discoveries of novel lipids and sterols[182-188] and to our knowledge, the therapeutic potential of compounds from their associated microbes is virtually unexplored.[189, 190] This is surprising since the microbial diversity in freshwater sponges suggest a competition for resources that may elicit the production of antibiotics.[189-192] We are currently collaborating with a community of "citizen scientist" volunteer SCUBA divers from across the Great Lakes to engage in freshwater sponge collection. Sponge tissues are currently being extracted in our lab while sponge-associated bacteria and fungi are being isolated and grown for determination of the drug-lead potential of these communities.

Data rich comprehensive approaches to characterization of secondary metabolism from these new environmental sources are needed. We are advancing at an accelerated pace toward elucidation of all small molecules in nature and at present, we are making profound transitional leaps toward this end. Laboratories working to elucidate novel biosynthetic gene clusters concurrently with identification of their products aim to accelerate comprehensive characterization of individual secondary metabolites.[193, 194] Other efforts are aimed at social media-style collaborative engagement of researchers around the world for the characterization of large swaths of chemical space by LC-MS and molecular networking.[195] In conjunction with the rush to describe natural products chemical space comes the ultimate purpose of identifying secondary metabolite drug lead potential. Combining the aforementioned technologies with high-throughput bioassay would result in high-definition multidimensional plots describing structure, biosynthesis, and activity at once.

As we aim for a comprehensive elucidation of secondary metabolite space, advancements in synthetic biology will meet along the way. Currently, there are simplified microbial cell chassis being developed with the eventual aim of factory-scale production of molecules by only expressing the most essential genes,[196] custom rewriting of genetic code for the facilitation of a fully-

programmable microbe,[197] and cell-free biosynthetic systems that do away with the microbe altogether for a focus on *in vitro* enzymatic molecule production.[198] Though swapping, removing, or inserting modules in gene clusters is quite challenging today, soon these aforementioned advances may allow for coding of custom proteins to reliably produce designer molecules more safely, faster, and in greater abundance than is possible using synthetic chemistry.

Natural products remain viable and critical to the future of medicine. Continued exploration of new small molecule resources coupled with development of new analytical and biological engineering technologies will allow greater access to nature's treasure trove of defenses in the decades ahead. With concurrent research to greater understand disease, these efforts hold promise for success in the arms race against drug resistance.

CITED LITERATURE.

1. Donoghue, H. D.; Spigelman, M.; Greenblatt, C. L.; Lev-Maor, G.; Bar-Gal, G. K.; Matheson, C.; Vernon, K.; Nerlich, A. G.; Zink, A. R. Tuberculosis: From prehistory to Robert Koch, as revealed by ancient DNA. *Lancet Infect. Dis.* **2004**, *4*, 584-592.
2. Comas, I.; Coscolla, M.; Luo, T.; Borrell, S.; Holt, K. E.; Kato-Maeda, M.; Parkhill, J.; Malla, B.; Berg, S.; Thwaites, G.; Yeboah-Manu, D.; Bothamley, G.; Mei, J.; Wei, L.; Bentley, S.; Harris, S. R.; Niemann, S.; Diel, R.; Aseffa, A.; Gao, Q.; Young, D.; Gagneux, S. Out-of-africa migration and Neolithic coexpansion of *Mycobacterium tuberculosis* with modern humans. *Nature Genet.* **2013**, *45*, 1176-1182.
3. Wilson, L. G. Commentary: Medicine, population, and tuberculosis. *Int. J. Epidemiol.* **2005**, *34*, 521-524.
4. Riva, M. A. From milk to rifampicin and back again: History of failures and successes in the treatment for tuberculosis. *J. Antibiot.* **2014**, *67*, 661-665.
5. Clark, J., *The influence of climate in the prevention and cure of chronic disease, more particularly of the chest and digestive organs*. Thomas and George Underwood: London, 1829.
6. Russell, D. G.; Barry, C. E.; Flynn, J. L. Tuberculosis: what we don't know can, and does, hurt us. *Science* **2010**, *328*, 852-856.
7. Schatz, A.; Bugie, E.; Waksman, S. A. Streptomycin, a substance exhibiting antibiotic activity against Gram-positive and Gram-negative bacteria. 1944. *Proc. Soc. Exp. Biol. Med.* **1944**, *55*, 66–69.
8. Streptomycin treatment of pulmonary tuberculosis: A medical research council investigation. *Br. Med. J.* **1948**, *2*, 769-782.
9. Musser, J. M. Antimicrobial agent resistance in mycobacteria: Molecular genetic insights. *Clin. Microbiol. Rev.* **1995**, *8*, 496-514.
10. Fox, W.; Sutherland, I.; Daniels, M. A five-year assessment of patients in a controlled trial of streptomycin in pulmonary tuberculosis. *Report to the Tuberculosis Chemotherapy Trials Committee of the Medical Reasearch Council* **1954**, *23*, 347-366.
11. Treatment of pulmonary tuberculosis with streptomycin and *para*-amino-salicylic acid: A medical research council investigation. *Br. Med. J.* **1950**, *2*, 1073-1085.
12. Treatment of pulmonary tuberculosis with isoniazid: A medical research council investigation. *Br. Med. J.* **1952**, *2*, 735-746.
13. Various combinations of isoniazid with streptomycin or with P.A.S. in the treatment of pulmonary tuberculosis; seventh report to the Medical Research Council by their Tuberculosis Chemotherapy Trials Committee. *Br. Med. J.* **1955**, *1*, 435-445.
14. *An international investigation of the efficacy of chemotherapy in previously untreated patients with pulmonary tuberculosis*; International Union again Tuberculosis: 1964; 1-191.
15. Lehmann, J. Twenty years afterward: Historical notes on the discovery of the antituberculosis effect of *para*-aminosalicylic acid (PAS) and the first clinical trials. *Am. Rev. Respir. Dis.* **1964**, *90*, 953-956.
16. Fox, W.; Sutherland, I. A. N. A five-year assessment of patients in a controlled trial of streptomycin, para-aminosalicylic acid, and streptomycin plus *para*-aminosalicylic acid, in pulmonary tuberculosis. *Q. J. Med.* **1956**, *25*, 221-244.
17. Mitchison, D.; Davies, G. The chemotherapy of tuberculosis: past, present and future. *Int. J. Tuberc. Lung Dis.* **2012**, *16*, 724-732.
18. Maggi, N.; Pasqualucci, C. R.; Ballotta, R.; Sensi, P. Rifampicin: A new orally active rifamycin. *Chemotherapy* **1966**, *11*, 285-292.

19. Doster, B.; Murray, F. J.; Newman, R.; Woolpert, S. F. Ethambutol in the initial treatment of pulmonary tuberculosis. U. S. Public health service tuberculosis therapy trials. *Am. Rev. Respir. Dis.* **1973**, *107*, 177-190.
20. Hong Kong Chest Service/British Medical Research Council. Controlled trial of 6-month and 8-month regimens in the treatment of pulmonary tuberculosis: The results up to 24 months. *Tubercle* **1979**, *60*, 201-210.
21. East African/British Medical Research Councils. Controlled clinical trial of four short-course (6-month) regimens of chemotherapy for treatment of pulmonary tuberculosis. *Lancet* **1974**, *304*, 237-240.
22. *Who treatment guidelines for drug-resistant tuberculosis – 2016 update*; World Health Organization: Geneva, 2016.
23. *Treatment of tuberculosis: Guidelines for national programmes*; World Health Organization: Geneva, 2010.
24. Beena; Rawat, D. S. Antituberculosis drug research: a critical overview. *Medicinal Research Reviews* **2013**, *33*, 693-764.
25. Bayer, R.; Wilkinson, D.; Bayer, R. Directly observed therapy for tuberculosis: history of an idea. *Lancet* **1995**, *345*, 1545-1548.
26. *What is DOTS? A guide to understanding the whorecommended TB control strategy known as dots*; World Health Organization: Geneva, 1999.
27. *An expanded DOTS framework for effective tuberculosis control*; World Health Organization: Geneva, 2002.
28. Moonan, P. K.; Quitugua, T. N.; Pogoda, J. M.; Woo, G.; Drewyer, G.; Sahbazian, B.; Dunbar, D.; Jost, K. C.; Wallace, C.; Weis, S. E. Does directly observed therapy (DOT) reduce drug resistant tuberculosis? *BMC Public Health* **2011**, *11*, 1-8.
29. Karumbi, J.; Garner, P. Directly observed therapy for treating tuberculosis. *Cochrane Database of Systematic Reviews* **2015**, *5*, 1-56.
30. *Scientific blueprint for tuberculosis drug development.*; New York, 2001.
31. *The global plan to stop TB*; 2001; http://www.stoptb.org/global/plan/plan0105.asp.
32. Schito, M.; Migliori, G. B.; Fletcher, H. A.; McNerney, R.; Centis, R.; D'Ambrosio, L.; Bates, M.; Kibiki, G.; Kapata, N.; Corrah, T.; Bomanji, J.; Vilaplana, C.; Johnson, D.; Mwaba, P.; Maeurer, M.; Zumla, A. Perspectives on advances in tuberculosis diagnostics, drugs, and vaccines. *Clin. Infect. Dis.* **2015**, *61*, S102-S118.
33. *Introduction of bedaquiline for the treatment of multidrug-resistant tuberculosis at country level - implementation plan*; World Health Organization: Geneva, 2015.
34. *The use of delamanid in the treatment of multidrug-resistant tuberculosis - interim policy guidance*; World Health Organization: Geneva, 2014.
35. Li, K.; Schurig-Briccio, L. A.; Feng, X.; Upadhyay, A.; Pujari, V.; Lechartier, B.; Fontes, F. L.; Yang, H.; Rao, G.; Zhu, W.; Gulati, A.; No, J. H.; Cintra, G.; Bogue, S.; Liu, Y.-L.; Molohon, K.; Orlean, P.; Mitchell, D. A.; Freitas-Junior, L.; Ren, F.; Sun, H.; Jiang, T.; Li, Y.; Guo, R.-T.; Cole, S. T.; Gennis, R. B.; Crick, D. C.; Oldfield, E. Multitarget drug discovery for tuberculosis and other infectious diseases. *J. Med. Chem.* **2014**, *57*, 3126-3139.
36. Clinicaltrials.gov. https://clinicaltrials.gov/ (accessed 07/08/2016).
37. Cole, S. T. Learning from the genome sequence of *Mycobacterium tuberculosis* H_{37}Rv. *FEBS Lett.* **1999**, *452*, 7-10.
38. Ghosh, S.; Baloni, P.; Mukherjee, S.; Anand, P.; Chandra, N. A multi-level multi-scale approach to study essential genes in *Mycobacterium tuberculosis*. *BMC Syst. Biol.* **2013**, *7*, 1-21.

39. Zhang, Y. The magic bullets and tuberculosis drug targets. *Annu. Rev. Pharmacol. Toxicol.* **2005**, *45*, 529-564.
40. Ashforth, E. J.; Fu, C. Z.; Liu, X. Y.; Dai, H. Q.; Song, F. H.; Guo, H.; Zhang, L. X. Bioprospecting for antituberculosis leads from microbial metabolites. *Nat. Prod. Rep.* **2010**, *27*, 1709-1719.
41. Tuberculosis: a global emergency. *World health forum* **1993**, *14*, 438.
42. *Global tuberculosis report — 2015*; World Health Organization: Geneva, 2015.
43. Dorman, S. E.; Chaisson, R. E. From magic bullets back to the magic mountain: The rise of extensively drug-resistant tuberculosis. *Nat. Med.* **2007**, *13*, 295-298.
44. Fischbach, M. A.; Walsh, C. T. Antibiotics for emerging pathogens. *Science* **2009**, *325*, 1089-1093.
45. Parida, S. K.; Axelsson-Robertson, R.; Rao, M. V.; Singh, N.; Master, I.; Lutckii, A.; Keshavjee, S.; Andersson, J.; Zumla, A.; Maeurer, M. Totally drug-resistant tuberculosis and adjunct therapies. *J. Intern. Med.* **2015**, *277*, 388-405.
46. Glaziou, P.; Falzon, D.; Floyd, K.; Raviglione, M. Global epidemiology of tuberculosis. *Semin. Respir. Crit. Care Med.* **2013**, *34*, 3-16.
47. *The end TB strategy - global strategy and targets for tuberculosis prevention, care and control after 2015*; World Health Organization: Geneva, 2014.
48. McGann, P.; Snesrud, E.; Maybank, R.; Corey, B.; Ong, A. C.; Clifford, R.; Hinkle, M.; Whitman, T.; Lesho, E.; Schaecher, K. E. *Escherichia coli* harboring mcr-1 and blaCTX-M on a novel IncF plasmid: first report of mcr-1 in the United States. *Antimicrob. Agents Chemother.* **2016**, *60*, 4420-4421.
49. Cragg, G. M.; Newman, D. J., Biodiversity: A continuing source of novel drug leads. In *Pure Appl. Chem.*, 2005; Vol. 77, pp 7-24.
50. Fabricant, D. S.; Farnsworth, N. R. The value of plants used in traditional medicine for drug discovery. *Environ. Health Perspect.* **2001**, *109*, 69-75.
51. Gould, K. Antibiotics: From prehistory to the present day. *J. Antimicrob. Chemother.* **2016**, *71*, 572-575.
52. Nelson, M. L.; Dinardo, A.; Hochberg, J.; Armelagos, G. J. Brief communication: Mass spectroscopic characterization of tetracycline in the skeletal remains of an ancient population from Sudanese Nubia 350–550 ce. *Am. J. Phys. Anthropol.* **2010**, *143*, 151-154.
53. Newman, D. J.; Cragg, G. M. Natural products as sources of new drugs from 1981 to 2014. *J. Nat. Prod.* **2016**, *79*, 629-661.
54. Fenical, W.; Jensen, P. R. Developing a new resource for drug discovery: marine actinomycete bacteria. *Nat. Chem. Biol.* **2006**, *2*, 666-673.
55. Copp, B. R.; Pearce, A. N. Natural product growth inhibitors of *Mycobacterium tuberculosis*. *Nat. Prod. Rep.* **2007**, *24*, 278-297.
56. Evans, B. E.; Rittle, K. E.; Bock, M. G.; DiPardo, R. M.; Freidinger, R. M.; Whitter, W. L.; Lundell, G. F.; Veber, D. F.; Anderson, P. S. Methods for drug discovery: Development of potent, selective, orally effective cholecystokinin antagonists. *J. Med. Chem.* **1988**, *31*, 2235-2246.
57. Lipinski, C. A.; Lombardo, F.; Dominy, B. W.; Feeney, P. J. Experimental and computational approaches to estimate solubility and permeability in drug discovery and development settings. *Adv. Drug Del. Rev.* **2001**, *46*, 3-26.
58. Pauli, G. F.; Case, R. J.; Inui, T.; Wang, Y.; Cho, S.; Fischer, N. H.; Franzblau, S. G. New perspectives on natural products in TB drug research. *Life Sci.* **2005**, *78*, 485-494.
59. Murphy, B. T.; Maloney, K.; Fenical, W., "Marine microorganisms". In *Phytochemistry and Pharmacognosy*, Eolss Publishers: Oxford, UK, 2011.

60. Waksman, S. A. Successes and failures in the search for antibiotics. *Adv. Appl. Microbiol.* **1969**, *11*, 1-16.
61. Olivera, B. M.; Cruz, L. J.; de Santos, V.; LeCheminant, G. W.; Griffin, D.; Zeikus, R.; McIntosh, J. M.; Galyean, R.; Varga, J.; Gray, W. R.; Rivier, J. Neuronal calcium channel antagonists. Discrimination between calcium channel subtypes using ω-conotoxin from *Conus magus* venom. *Biochemistry* **1987**, *26*, 2086-2090.
62. Rinehart, K. L.; Holt, T. G.; Fregeau, N. L.; Stroh, J. G.; Keifer, P. A.; Sun, F.; Li, L. H.; Martin, D. G. Ecteinascidins 729, 743, 745, 759a, 759b, and 770: Potent antitumor agents from the caribbean tunicate *Ecteinascidia turbinata*. *J. Org. Chem.* **1990**, *55*, 4512-4515.
63. Pettit, G. R.; Herald, C. L.; Boyd, M. R.; Leet, J. E.; Dufresne, C.; Doubek, D. L.; Schmidt, J. M.; Cerny, R. L.; Hooper, J. N.; Rützler, K. C. Isolation and structure of the cell growth inhibitory constituents from the western Pacific marine sponge *Axinella* sp. *J. Med. Chem.* **1991**, *34*, 3339-3340.
64. Pettit, G. R.; Herald, C. L.; Boyd, M. R.; Leet, J. E.; Dufresne, C.; Doubek, D. L.; Schmidt, J. M.; Cerny, R. L.; Hooper, J. N.; Rutzler, K. C. Isolation and structure of the cell growth inhibitory constituents from the western Pacific marine sponge *Axinella* sp. *J. Med. Chem.* **1991**, *34*, 3339-3340.
65. El Sayed, K. A.; Bartyzel, P.; Shen, X. Y.; Perry, T. L.; Kjawiony, J. K.; Hamann, M. T. Marine natural products as antituberculosis agents. *Tetrahedron* **2000**, *56*, 949-953.
66. Chlipala, G., E.; Mo, S.; Orjala, J. Chemodiversity in freshwater and terrestrial cyanobacteria – a source for drug discovery. *Curr. Drug Targets* **2011**, *12*, 1654-1673.
67. Du, L.; Risinger, A. L.; King, J. B.; Powell, D. R.; Cichewicz, R. H. A potent HDAC inhibitor, 1-alaninechlamydocin, from a *Tolypocladium* sp. induces G2/M cell cycle arrest and apoptosis in MIA PaCa-2 cells. *J. Nat. Prod.* **2014**, *77*, 1753-1757.
68. Cross, T. Aquatic actinomycetes: A critical survey of the occurrence, growth and role of actinomycetes in aquatic habitats. *J. Appl. Bacteriol.* **1981**, *50*, 397-423.
69. Goodfellow, M.; Williams, S. T. Ecology of actinomycetes. *Annu. Rev. Microbiol.* **1983**, *37*, 189-216.
70. de Menezes, A. B.; Lockhart, R. J.; Cox, M. J.; Allison, H. E.; McCarthy, A. J. Cellulose degradation by micromonosporas recovered from freshwater lakes and classification of these actinomycetes by DNA gyrase B gene sequencing. *Appl. Environ. Microbiol.* **2008**, *74*, 7080-7084.
71. de Menezes, A. B.; McDonald, J. E.; Allison, H. E.; McCarthy, A. J. Importance of *Micromonospora* spp. as colonizers of cellulose in freshwater lakes as demonstrated by quantitative reverse transcriptase PCR of 16S rRNA. *Appl. Environ. Microbiol.* **2012**, *78*, 3495-3499.
72. Erikson, D. Studies on some lake-mud strains of *Micromonospora*. *J. Bacteriol.* **1941**, *41*, 277-300.
73. Kollner, K. E.; Carstens, D.; Keller, E.; Vazquez, F.; Schubert, C. J.; Zeyer, J.; Burgmann, H. Bacterial chitin hydrolysis in two lakes with contrasting trophic statuses. *Appl. Environ. Microbiol.* **2012**, *78*, 695-704.
74. Newton, R. J.; Jones, S. E.; Eiler, A.; McMahon, K. D.; Bertilsson, S. A guide to the natural history of freshwater lake bacteria. *Microbiol. Mol. Biol. Rev.* **2011**, *75*, 14-49.
75. Glockner, F. O.; Zaichikov, E.; Belkova, N.; Denissova, L.; Pernthaler, J.; Pernthaler, A.; Amann, R. Comparative 16S rRNA analysis of lake bacterioplankton reveals globally distributed phylogenetic clusters including an abundant group of Actinobacteria. *Appl. Environ. Microbiol.* **2000**, *66*, 5053-5065.

76. Hahn, M. W. Description of seven candidate species affiliated with the phylum Actinobacteria, representing planktonic freshwater bacteria. *Int. J. Syst. Evol. Microbiol.* **2009**, *59*, 112-117.
77. Hahn, M. W.; Lünsdorf, H.; Wu, Q.; Schauer, M.; Höfle, M. G.; Boenigk, J.; Stadler, P. Isolation of novel ultramicrobacteria classified as Actinobacteria from five freshwater habitats in Europe and Asia. *Appl. Environ. Microbiol.* **2003**, *69*, 1442-1451.
78. Newton, R. J.; Jones, S. E.; Helmus, M. R.; McMahon, K. D. Phylogenetic ecology of the freshwater Actinobacteria acI lineage. *Appl. Environ. Microbiol.* **2007**, *73*, 7169-7176.
79. Warnecke, F.; Amann, R.; Pernthaler, J. Actinobacterial 16S rRNA genes from freshwater habitats cluster in four distinct lineages. *Environ. Microbiol.* **2004**, *6*, 242-253.
80. Zwart, G.; Crump, B. C.; Kamst-van Agterveld, M. P.; Hagen, F.; Han, S.-K. Typical freshwater bacteria: An analysis of available 16S rRNA gene sequences from plankton of lakes and rivers. *Aquat. Microb. Ecol.* **2002**, *28*, 141-155.
81. Fenical, W.; Jensen, P. R.; Palladino, M. A.; Lam, K. S.; Lloyd, G. K.; Potts, B. C. Discovery and development of the anticancer agent salinosporamide A (NPI-0052). *Bioorg. Med. Chem.* **2009**, *17*, 2175-2180.
82. Hirata, Y.; Uemura, D. Halichondrins – antitumor polyethers macrolides from a marine sponge. *Pure Appl. Chem.* **1986**, *58*, 701-710.
83. Riedlinger, J.; Reicke, A.; Zahner, H.; Krismer, B.; Bull, A. T.; Maldonado, L. A.; Ward, A. C.; Goodfellow, M.; Bister, B.; Bischoff, D.; Sussmuth, R. D.; Fiedler, H. P. Abyssomicins, inhibitors of the *para*-aminobenzoic acid pathway produced by the marine *Verrucosispora* strain AB-18-032. *J. Antibiot. (Tokyo)* **2004**, *57*, 271-279.
84. Uemura, D.; Takahashi, K.; Yamamoto, T.; Katayama, C.; Tanaka, J.; Okumura, Y.; Hirata, Y. Norhalichondrin A: an antitumor polyether macrolide from a marine sponge. *J. Am. Chem. Soc.* **1985**, *107*, 4796-4798.
85. Carballeira, N. M.; Pagan, M.; Shalabi, F.; Nechev, J. T.; Lahtchev, K.; Ivanova, A.; Stefanov, K. Two novel iso-branched octadecenoic acids from a *Micrococcus* species. *J. Nat. Prod.* **2000**, *63*, 1573-1575.
86. Carlson, S.; Tanouye, U.; Ómarsdóttir, S.; Murphy, B. T. Phylum-specific regulation of resistomycin production in a *Streptomyces* sp. via microbial coculture. *J. Nat. Prod.* **2015**, *78*, 381-387.
87. Parker, B. C.; Ford, M. A.; Gruft, H.; Falkinham III, J. O. Epidemiology of infection by nontuberculous mycobacteria. Iv. Preferential aerosolization of *Mycobacterium intracellulare* from natural waters. *Am. Rev. Respir. Dis.* **1983**, *128*, 652-656.
88. Falkinham III, J. O. Surrounded by mycobacteria: Nontuberculous mycobacteria in the human environment. *Journal of Applied Microbiology* **2009**, *107*, 356-367.
89. Mullowney, M. W.; Ó hAinmhire , E.; Shaikh, A.; Wei, X.; Tanouye, U.; Santarsiero, B. D.; Burdette, J. E.; Murphy, B. T. Diazaquinomycins E-G, novel diaza-anthracene analogs from a marine-derived *Streptomyces* sp. *Mar. Drugs* **2014**, *12*, 3574-3586.
90. Maskey, R. P.; Grun-Wollny, I.; Laatsch, H. Isolation and structure elucidation of diazaquinomycin C from a terrestrial *Streptomyces* sp. and confirmation of the akashin structure. *Nat. Prod. Res.* **2005**, *19*, 137-142.
91. Omura, S.; Iwai, Y.; Hinotozawa, K.; Tanaka, H.; Takahashi, Y.; Nakagawa, A. OM-704 A, a new antibiotic active against Gram-positive bacteria produced by *Streptomyces* sp. *J. Antibiot.* **1982**, *35*, 1425-1429.
92. Omura, S.; Nakagawa, A.; Aoyama, H.; Hinotozawa, K.; Sano, H. The structures of diazaquinomycins A and B, new antibiotic metabolites. *Tetrahedron Lett.* **1983**, *24*, 3643-3646.

93. Collins, L.; Franzblau, S. G. Microplate alamar blue assay versus BACTEC 460 system for high-throughput screening of compounds against *Mycobacterium tuberculosis* and *Mycobacterium avium*. *Antimicrob. Agents Chemother.* **1997**, *41*, 1004-1009.
94. Franzblau, S. G.; Witzig, R. S.; McLaughlin, J. C.; Torres, P.; Madico, G.; Hernandez, A.; Degnan, M. T.; Cook, M. B.; Quenzer, V. K.; Ferguson, R. M.; Gilman, R. H. Rapid, low-technology MIC determination with clinical *Mycobacterium tuberculosis* isolates by using the microplate alamar blue assay. *J. Clin. Microbiol.* **1998**, *36*, 362-366.
95. Tsuzuki, K.; Yokozuka, T.; Murata, M.; Tanaka, H.; Omura, S. Synthesis and biological activity of analogues of diazaquinomycin A, a new thymidylate synthase inhibitor. *J. Antibiot.* **1989**, *42*, 727-737.
96. Cho, S. H.; Warit, S.; Wan, B.; Hwang, C. H.; Pauli, G. F.; Franzblau, S. G. Low-oxygen-recovery assay for high-throughput screening of compounds against nonreplicating *Mycobacterium tuberculosis*. *Antimicrob. Agents Chemother.* **2007**, *51*, 1380-1385.
97. Performance standards for antimicrobial susceptibility testing; 24th informational supplement. CLSI document M100-S24. In *Clinical and Laboratory Standards Institute (CLSI)*, (CLSI), C. a. L. S. I., Ed. CLSI: Wayne, PA, 2014.
98. Kelly, T. R.; Field, J. A.; Li, Q. Synthesis of diazaquinomycin A and B: The first double Knorr cyclization. *Tetrahedron Lett.* **1988**, *29*, 3545-3546.
99. van Beilen, J. B.; Holtackers, R.; Lüscher, D.; Bauer, U.; Witholt, B.; Duetz, W. A. Biocatalytic production of perillyl alcohol from limonene by using a novel *Mycobacterium* sp. cytochrome P450 alkane hydroxylase expressed in *Pseudomonas putida*. *Appl. Environ. Microbiol.* **2005**, *71*, 1737-1744.
100. Cornelissen, S.; Julsing, M. K.; Volmer, J.; Riechert, O.; Schmid, A.; Buhler, B. Whole-cell-based CYP153A6-catalyzed (S)-limonene hydroxylation efficiency depends on host background and profits from monoterpene uptake via AlkL. *Biotechnol. Bioeng.* **2013**, *110*, 1282-1292.
101. Julsing, M. K.; Schrewe, M.; Cornelissen, S.; Hermann, I.; Schmid, A.; Buhler, B. Outer membrane protein AlkL boosts biocatalytic oxyfunctionalization of hydrophobic substrates in *Escherichia coli*. *Appl. Environ. Microbiol.* **2012**, *78*, 5724-5733.
102. Murata, M.; Miyasaka, T.; Tanaka, H.; Omura, S. Diazaquinomycin A, a new antifolate antibiotic, inhibits thymidylate synthase. *J. Antibiot.* **1985**, *38*, 1025-1033.
103. Myllykallio, H.; Lipowski, G.; Leduc, D.; Filee, J.; Forterre, P.; Liebl, U. An alternative flavin-dependent mechanism for thymidylate synthesis. *Science* **2002**, *297*, 105-107.
104. Chernyshev, A.; T., F.; Kohen, A. Thymidyl biosynthesis enzymes as antibiotic targets. *Appl. Microbiol. Biotechnol.* **2007**, *74*, 282-289.
105. Hunter, J. H.; Gujjar, R.; Pang, C. K.; Rathod, P. K. Kinetics and ligand-binding preferences of *Mycobacterium tuberculosis* thymidylate synthases, ThyA and ThyX. *PloS one* **2008**, *3*, e2237.
106. Lomenick, B.; Hao, R.; Jonai, N.; Chin, R. M.; Aghajan, M.; Warburton, S.; Wang, J.; Wu, R. P.; Gomez, F.; Loo, J. A.; Wohlschlegel, J. A.; Vondriska, T. M.; Pelletier, J.; Herschman, H. R.; Clardy, J.; Clarke, C. F.; Huang, J. Target identification using drug affinity responsive target stability (DARTS). *Proc. Natl. Acad. Sci. U. S. A.* **2009**, *106*, 21984-21989.
107. Pai, M. Y.; Lomenick, B.; Hwang, H.; Schiestl, R.; McBride, W.; Loo, J. A.; Huang, J. Drug affinity responsive target stability (DARTS) for small molecule target identification. *Methods Mol. Biol.* **2015**, *1263*, 287-298.
108. Ioerger, T. R.; Feng, Y.; Ganesula, K.; Chen, X.; Dobos, K. M.; Fortune, S.; Jacobs, W. R.; Mizrahi, V.; Parish, T.; Rubin, E.; Sassetti, C.; Sacchettini, J. C. Variation among genome

sequences of H_{37}Rv strains of *Mycobacterium tuberculosis* from multiple laboratories. *J. Bacteriol.* **2010**, *192*, 3645-3653.
109. Griffin, J. E.; Gawronski, J. D.; DeJesus, M. A.; Ioerger, T. R.; Akerley, B. J.; Sassetti, C. M. High-resolution phenotypic profiling defines genes essential for mycobacterial growth and cholesterol catabolism. *PLoS Pathog.* **2011**, *7*, e1002251.
110. Kendall, S. L.; Withers, M.; Soffair, C. N.; Moreland, N. J.; Gurcha, S.; Sidders, B.; Frita, R.; Ten Bokum, A.; Besra, G. S.; Lott, J. S.; Stoker, N. G. A highly conserved transcriptional repressor controls a large regulon involved in lipid degradation in *Mycobacterium smegmatis* and *Mycobacterium tuberculosis*. *Mol. Microbiol.* **2007**, *65*, 684-699.
111. Selengut, J. D.; Haft, D. H. Unexpected abundance of coenzyme F_{420}-dependent enzymes in *Mycobacterium tuberculosis* and other Actinobacteria. *J. Bacteriol.* **2010**, *192*, 5788-5798.
112. Voskuil, M.; Bartek, I.; Visconti, K.; Schoolnik, G. The response of *Mycobacterium tuberculosis* to reactive oxygen and nitrogen species. *Frontiers in Microbiology* **2011**, *2*, 105.
113. Hards, K.; Robson, J. R.; Berney, M.; Shaw, L.; Bald, D.; Koul, A.; Andries, K.; Cook, G. M. Bactericidal mode of action of bedaquiline. *J. Antimicrob. Chemother.* **2015**, *70*, 2028-2037.
114. Yano, T.; Kassovska-Bratinova, S.; Teh, J. S.; Winkler, J.; Sullivan, K.; Isaacs, A.; Schechter, N. M.; Rubin, H. Reduction of clofazimine by mycobacterial type 2 NADH:quinone oxidoreductase: a pathway for the generation of bactericidal levels of reactive oxygen species. *J. Biol. Chem.* **2011**, *286*, 10276-10287.
115. Singh, R.; Manjunatha, U.; Boshoff, H. I. M.; Ha, Y. H.; Niyomrattanakit, P.; Ledwidge, R.; Dowd, C. S.; Lee, I. Y.; Kim, P.; Zhang, L.; Kang, S.; Keller, T. H.; Jiricek, J.; Barry, C. E. PA-824 kills nonreplicating *Mycobacterium tuberculosis* by intracellular NO release. *Science* **2008**, *322*, 1392-1395.
116. Hartkoorn, R. C.; Uplekar, S.; Cole, S. T. Cross-resistance between clofazimine and bedaquiline through upregulation of MmpL5 in *Mycobacterium tuberculosis*. *Antimicrob. Agents Chemother.* **2014**, *58*, 2979-2981.
117. Zhang, S.; Chen, J.; Cui, P.; Shi, W.; Zhang, W.; Zhang, Y. Identification of novel mutations associated with clofazimine resistance in *Mycobacterium tuberculosis*. *J. Antimicrob. Chemother.* **2015**, *70*, 2507-2510.
118. Sassetti, C. M.; Boyd, D. H.; Rubin, E. J. Genes required for mycobacterial growth defined by high density mutagenesis. *Mol. Microbiol.* **2003**, *48*, 77-84.
119. Singh, V.; Brecik, M.; Mukherjee, R.; Evans, J. C.; Svetlikova, Z.; Blasko, J.; Surade, S.; Blackburn, J.; Warner, D. F.; Mikusova, K.; Mizrahi, V. The complex mechanism of antimycobacterial action of 5-fluorouracil. *Chem. Biol.* **2015**, *22*, 63-75.
120. Songsumanus, A.; Tanasupawat, S.; Igarashi, Y.; Kudo, T. *Micromonospora maritima* sp. nov., isolated from mangrove soil. *Int. J. Syst. Evol. Microbiol.* **2013**, *63*, 554-559.
121. Ojha, A. K.; Baughn, A. D.; Sambandan, D.; Hsu, T.; Trivelli, X.; Guerardel, Y.; Alahari, A.; Kremer, L.; Jacobs, W. R.; Hatfull, G. F. Growth of *Mycobacterium tuberculosis* biofilms containing free mycolic acids and harbouring drug-tolerant bacteria. *Mol. Microbiol.* **2008**, *69*, 164-174.
122. Falzari, K.; Zhu, Z.; Pan, D.; Liu, H.; Hongmanee, P.; Franzblau, S. G. *In vitro* and *in vivo* activities of macrolide derivatives against *Mycobacterium tuberculosis*. *Antimicrob. Agents Chemother.* **2005**, *49*, 1447-1454.

123. Cantrell, C. L.; Lu, T.; Fronczek, F. R.; Fischer, N. H.; Adams, L. B.; Franzblau, S. G. Antimycobacterial cycloartanes from *Borrichia frutescens*. *J. Nat. Prod.* **1996**, *59*, 1131-1136.
124. Ó hAinmhire, E.; Quartuccio, S. M.; Cheng, W.; Ahmed, R. A.; King, S. M.; Burdette, J. E. Mutation or loss of p53 differentially modifies TGFβ action in ovarian cancer. *PloS one* **2014**, *9*, e89553.
125. Manjunatha, U. H.; Boshoff, H.; Dowd, C. S.; Zhang, L.; Albert, T. J.; Norton, J. E.; Daniels, L.; Dick, T.; Pang, S. S.; Barry, C. E. Identification of a nitroimidazo-oxazine-specific protein involved in PA-824 resistance in *Mycobacterium tuberculosis*. *Proc. Natl. Acad. Sci. U. S. A.* **2006**, *103*, 431-436.
126. Song, T.; Park, Y.; Shamputa, I. C.; Seo, S.; Lee, S. Y.; Jeon, H.-S.; Choi, H.; Lee, M.; Glynne, R. J.; Barnes, S. W.; Walker, J. R.; Batalov, S.; Yusim, K.; Feng, S.; Tung, C.-S.; Theiler, J.; Via, L. E.; Boshoff, H. I. M.; Murakami, K. S.; Korber, B.; Barry, C. E.; Cho, S. N. Fitness costs of rifampicin resistance in *Mycobacterium tuberculosis* are amplified under conditions of nutrient starvation and compensated by mutation in the β' subunit of RNA polymerase. *Mol. Microbiol.* **2014**, *91*, 1106-1119.
127. Methods for dilution antimicrobial susceptibility tests for bacteria that grow aerobically—second edition: Approved standard M7-A2. In *National Committee for Clinical Laboratory Standards (NCCLS)*, NCCLS: Villanova, PA, 1990.
128. Performance standards for antimicrobial susceptibility testing; third informational supplement M100-S3. In *National Committee for Clinical Laboratory Standards (NCCLS)*, NCCLS: Villanova, PA, 1991.
129. Hayashi, K.; Morooka, N.; Yamamoto, Y.; Fujita, K.; Isono, K.; Choi, S.; Ohtsubo, E.; Baba, T.; Wanner, B. L.; Mori, H.; Horiuchi, T. Highly accurate genome sequences of Escherichia coli K-12 strains MG1655 and W3110. *Molecular Systems Biology* **2006**, *2*, 2006.0007.
130. Sambrook, J.; Fritsch, E. F.; Maniatis, T., *Molecular cloning: A laboratory manual*. 4th ed. ed.; Cold Spring Harbor Laboratory Press: Cold Spring Harbor, N.Y., 2012.
131. Panke, S.; Meyer, A.; Huber, C. M.; Witholt, B.; Wubbolts, M. G. An alkane-responsive expression system for the production of fine chemicals. *Appl. Environ. Microbiol.* **1999**, *65*, 2324-2332.
132. Bühler, B.; Bollhalder, I.; Hauer, B.; Witholt, B.; Schmid, A. Use of the two-liquid phase concept to exploit kinetically controlled multistep biocatalysis. *Biotechnol. Bioeng.* **2003**, *81*, 683-694.
133. Galagan, J. E.; Minch, K.; Peterson, M.; Lyubetskaya, A.; Azizi, E.; Sweet, L.; Gomes, A.; Rustad, T.; Dolganov, G.; Glotova, I.; Abeel, T.; Mahwinney, C.; Kennedy, A. D.; Allard, R.; Brabant, W.; Krueger, A.; Jaini, S.; Honda, B.; Yu, W. H.; Hickey, M. J.; Zucker, J.; Garay, C.; Weiner, B.; Sisk, P.; Stolte, C.; Winkler, J. K.; Van de Peer, Y.; Iazzetti, P.; Camacho, D.; Dreyfuss, J.; Liu, Y.; Dorhoi, A.; Mollenkopf, H. J.; Drogaris, P.; Lamontagne, J.; Zhou, Y.; Piquenot, J.; Park, S. T.; Raman, S.; Kaufmann, S. H.; Mohney, R. P.; Chelsky, D.; Moody, D. B.; Sherman, D. R.; Schoolnik, G. K. The *Mycobacterium tuberculosis* regulatory network and hypoxia. *Nature* **2013**, *499*, 178-183.
134. Goude, R.; Parish, T., *Electroporation of mycobacteria*. Humana Press: Totowa, NJ, 1998.
135. Ollinger, J.; Bailey, M. A.; Moraski, G. C.; Casey, A.; Florio, S.; Alling, T.; Miller, M. J.; Parish, T. A dual read-out assay to evaluate the potency of compounds active against *Mycobacterium tuberculosis*. *PloS one* **2013**, *8*, e60531.
136. Sirgel, F. A.; Wiid, I. J.; van Helden, P. D. Measuring minimum inhibitory concentrations in mycobacteria. *Methods Mol. Biol.* **2009**, *465*, 173-186.

137. Boshoff, H. I. M.; Myers, T. G.; Copp, B. R.; McNeil, M. R.; Wilson, M. A.; Barry, C. E. The transcriptional responses of *Mycobacterium tuberculosis* to inhibitors of metabolism: novel insights into drug mechanisms of action. *J. Biol. Chem.* **2004**, *279*, 40174-40184.
138. Weinstein, J. N.; Myers, T. G.; O'Connor, P. M.; Friend, S. H.; Fornace, A. J.; Kohn, K. W.; Fojo, T.; Bates, S. E.; Rubinstein, L. V.; Anderson, N. L.; Buolamwini, J. K.; van Osdol, W. W.; Monks, A. P.; Scudiero, D. A.; Sausville, E. A.; Zaharevitz, D. W.; Bunow, B.; Viswanadhan, V. N.; Johnson, G. S.; Wittes, R. E.; Paull, K. D. An information-intensive approach to the molecular pharmacology of cancer. *Science* **1997**, *275*, 343-349.
139. Lamichhane, G.; Zignol, M.; Blades, N. J.; Geiman, D. E.; Dougherty, A.; Grosset, J.; Broman, K. W.; Bishai, W. R. A postgenomic method for predicting essential genes at subsaturation levels of mutagenesis: application to *Mycobacterium tuberculosis*. *Proc. Natl. Acad. Sci. U. S. A.* **2003**, *100*, 7213-7218.
140. Barry, V. C.; Belton, J. G.; Conalty, M. L.; Denneny, J. M.; Edward, D. W.; O'Sullivan, J. F.; Twomey, D.; Winder, F. A new series of phenazines (rimino-compounds) with high antituberculosis activity. *Nature* **1957**, *179*, 1013-1015.
141. Niwa, Y.; Sakane, T.; Miyachi, Y.; Ozaki, M. Oxygen metabolism in phagocytes of leprotic patients: Enhanced endogenous superoxide dismutase activity and hydroxyl radical generation by clofazimine. *J. Clin. Microbiol.* **1984**, *20*, 837-842.
142. Smith, F.; Richter, F. P. Substituted 1,10-phenanthroline ferrous complex oxidation-reduction indicators potential determinations as a function of acid concentration. *Ind. Eng. Chem., Anal. Ed.* **1944**, *16*, 580-581.
143. Kohanski, M. A.; Dwyer, D. J.; Hayete, B.; Lawrence, C. A.; Collins, J. J. A common mechanism of cellular death induced by bactericidal antibiotics. *Cell* **2007**, *130*, 797-810.
144. Wang, X.; Zhao, X. Contribution of oxidative damage to antimicrobial lethality. *Antimicrob. Agents Chemother.* **2009**, *53*, 1395-1402.
145. Dwyer, D. J.; Belenky, P. A.; Yang, J. H.; MacDonald, I. C.; Martell, J. D.; Takahashi, N.; Chan, C. T. Y.; Lobritz, M. A.; Braff, D.; Schwarz, E. G.; Ye, J. D.; Pati, M.; Vercruysse, M.; Ralifo, P. S.; Allison, K. R.; Khalil, A. S.; Ting, A. Y.; Walker, G. C.; Collins, J. J. Antibiotics induce redox-related physiological alterations as part of their lethality. *Proc. Natl. Acad. Sci. U. S. A.* **2014**, *111*, E2100-E2109.
146. Johnston, C. W.; Skinnider, M. A.; Dejong, C. A.; Rees, P. N.; Chen, G. M.; Walker, C. G.; French, S.; Brown, E. D.; Berdy, J.; Liu, D. Y.; Magarvey, N. A. Assembly and clustering of natural antibiotics guides target identification. *Nat. Chem. Biol.* **2016**, *12*, 233-239.
147. Walsh, C., *Antibiotics: Actions, origins, resistance*. ASM Press: Washington, DC, 2003; p 345.
148. Gonzalez-Juarrero, M.; Woolhiser, L. K.; Brooks, E.; DeGroote, M. A.; Lenaerts, A. J. Mouse model for efficacy testing of antituberculosis agents via intrapulmonary delivery. *Antimicrob. Agents Chemother.* **2012**, *56*, 3957-3959.
149. Kabsch, W. XDS. *Acta Crystallogr. Sect. D* **2010**, *66*, 125-132.
150. Sheldrick, G. M. A short history of SHELX. *Acta Crystallogr. Sect. A* **2008**, *64*, 112-122.
151. Shibazaki, A.; Omoto, Y.; Kudo, T.; Yaguchi, T.; Saito, A.; Ando, A.; Mikami, Y.; Gonoi, T. *Streptomyces coacervatus* sp. nov., isolated from the intestinal tract of *Armadillidium vulgare*. *Int. J. Syst. Evol. Microbiol.* **2011**, *61*, 1073-1077.
152. Wu, H.; Qu, S.; Lu, C.; Zheng, H.; Zhou, X.; Bai, L.; Deng, Z. Genomic and transcriptomic insights into the thermo-regulated biosynthesis of validamycin in *Streptomyces hygroscopicus* 5008. *BMC Genomics* **2012**, *13*, 337.

153. Ruckert, C.; J., K.; Heide, L.; Apel, A. K. Draft genome sequence of *Streptomyces roseochromogenes* subsp. *oscitans* DS 12.976, producer of the aminocoumarin antibiotic clorobiocin. *Genome Announc.* **2014**, *2*, e01147-13.
154. Vichai, V.; Kirtikara, K. Sulforhodamine B colorimetric assay for cytotoxicity screening. *Nat. Protoc.* **2006**, *1*, 1112-1116.
155. Xie, P.; Ma, M.; Rateb, M. E.; Shaaban, K. A.; Yu, Z.; Huang, S.-X.; Zhao, L. X.; Zhu, X.; Yan, Y.; Peterson, R. M.; Lohman, J. R.; Yang, D.; Yin, M.; Rudolf, J. D.; Jiang, Y.; Duan, Y.; Shen, B. Biosynthetic potential-based strain prioritization for natural product discovery: A showcase for diterpenoid-producing actinomycetes. *J. Nat. Prod.* **2014**, *77*, 377-387.
156. Smanski, M. J.; Peterson, R. M.; Huang, S. X.; Shen, B. Bacterial diterpene synthases: New opportunities for mechanistic enzymology and engineered biosynthesis. *Curr. Opin. Chem. Biol.* **2012**, *16*, 132-141.
157. Mullowney, M. W.; Hwang, C. H.; Newsome, A. G.; Wei, X.; Tanouye, U.; Wan, B.; Carlson, S.; Barranis, N. J.; Ó hAinmhire, E.; Chen, W.-L.; Krishnamoorthy, K.; White, J.; Blair, R.; Lee, H.; Burdette, J. E.; Rathod, P. K.; Parish, T.; Cho, S.; Franzblau, S. G.; Murphy, B. T. Diaza-anthracene antibiotics from a freshwater-derived actinomycete with selective antibacterial activity toward *Mycobacterium tuberculosis*. *ACS Infectious Diseases* **2015**, *1*, 168-174.
158. Balk-Bindseil, W.; Laatsch, H. Neue naturstoffe aus dem screening mariner actinomyceten - isolierung und strukturaufklärung der lagumycine und des oceamycins. PhD thesis, University of Göttingen, Germany, 1995.
159. Yamashita, N. Manufacture of dehydrorabelomycin with *Streptomyces* species and use of the antibiotic agent as antitumor agent. JP 10201494 A, Aug 4, 1998.
160. Liu, W. C.; Parker, L.; Slusarchyk, S.; Greenwood, G. L.; Grahm, S. F.; Meyers, E. Isolation, characterization, and structure of rabelomycin, a new antibiotic. *J. Antibiot.* **1970**, *23*, 437-441.
161. Fendrich, G.; Zimmermann, W.; Gruner, J.; Auden, J. A. L. Phenanthridine derivatives, process for the preparation thereof, and compositions containing them. 1990.
162. Gore, M. P.; Gould, S. J.; Weller, D. D. Synthesis of putative intermediates in the biosynthesis of the kinamycin antibiotics: Total synthesis of phenanthroviridin aglycon and related compounds. *J. Org. Chem.* **1992**, *57*, 2774-2783.
163. Ikushima, H.; Iguchi, E.; Kohsaka, M.; Aoki, H.; Imanaka, H. *Streptomyces auranticolor* sp. nov., a new anticoccidial antibiotics producer. *J. Antibiot.* **1980**, *33*, 1103-1106.
164. Ikushima, H.; Okamoto, M.; Tanaka, H.; Ohe, O.; Kohsaka, M.; Aoki, H.; Imanaka, H. New anticoccidial antibiotics, WS-5995 A and B: I. Isolation and characterization. *J. Antibiot.* **1980**, *33*, 1107-1113.
165. Crews, P.; Rodríguez, J.; Jaspars, M., *Organic structure analysis*. 2nd ed.; Oxford University Press: New York, 2010; p 656.
166. Moffitt, W.; Woodward, R. B.; Moscowitz, A.; Klyne, W.; Djerassi, C. Structure and the optical rotatory dispersion of saturated ketones. *J. Am. Chem. Soc.* **1961**, *83*, 4013-4018.
167. Dawson, B. A.; Girard, M.; Kindack, D.; Fillion, J.; Awang, D. V. C. ^{13}C NMR of lapachol and some related naphthoquinones. *Magn. Reson. Chem.* **1989**, *27*, 1176-1177.
168. Yamashita, M.; Kaneko, M.; Tokuda, H.; Nishimura, K.; Kumeda, Y.; Iida, A. Synthesis and evaluation of bioactive naphthoquinones from the brazilian medicinal plant, *Tabebuia avellanedae*. *Bioorg. Med. Chem.* **2009**, *17*, 6286-6291.
169. Domcke, S.; Sinha, R.; Levine, D. A.; Sander, C.; Schultz, N. Evaluating cell lines as tumour models by comparison of genomic profiles. *Nat. Commun.* **2013**, *4*, 1-10.

170. Lombó, F.; Abdelfattah, M. S.; Braña, A. F.; Salas, J. A.; Rohr, J.; Méndez, C. Elucidation of oxygenation steps during oviedomycin biosynthesis and generation of derivatives with increased antitumor activity. *ChemBioChem* **2009**, *10*, 296-303.
171. Yamashita, N.; Takashi, H.; Kazuo, S.; Haruo, S. 6-hydroxytetrangulol, a new CPP32 protease inducer produced by *Streptomyces* sp. *J. Antibiot.* **1998**, *1*, 79-81.
172. Zhang, W.; Liu, Z.; Li, S.; Lu, Y.; Chen, Y.; Zhang, H.; Zhang, G.; Zhu, Y.; Zhang, G.; Zhang, W.; Liu, J.; Zhang, C. Fluostatins I–K from the South China Sea-derived *Micromonospora rosaria* SCSIO N160. *J. Nat. Prod.* **2012**, *75*, 1937-1943.
173. Perchellet, E. M.; Sperfslage, B. J.; Qabaja, G.; Jones, G. B.; Perchellet, J. P. Quinone isomers of the WS-5995 antibiotics: synthetic antitumor agents that inhibit macromolecule synthesis, block nucleoside transport, induce DNA fragmentation, and decrease the growth and viability of L1210 leukemic cells more effectively than ellagic acid and genistein *in vitro*. *Anticancer drugs* **2001**, *12*, 401-417.
174. Kharel, M. K.; Pahari, P.; Shepherd, M. D.; Tibrewal, N.; Nybo, S. E.; Shaaban, K. A.; Rohr, J. Angucyclines: biosynthesis, mode-of-action, new natural products, and synthesis. *Nat. Prod. Rep.* **2012**, *29*, 264-325.
175. Seaton, P. J.; Gould, S. J. Kinamycin biosynthesis. Derivation by excision of an acetate unit from a single-chain decaketide intermediate. *J. Am. Chem. Soc.* **1987**, *109*, 5282-5284.
176. Cone, M. C.; Hassan, A. M.; Gore, M. P.; Gould, S. J.; Borders, D. B.; Alluri, M. R. Detection of phenanthroviridin aglycon in a UV mutant of *Streptomyces murayamaensis*. *J. Org. Chem.* **1994**, *59*, 1923-1924.
177. Tibrewal, N.; Pahari, P.; Wang, G.; Kharel, M. K.; Morris, C.; Downey, T.; Hou, Y.; Bugni, T. S.; Rohr, J. Baeyer-Villiger C-C bond cleavage reaction in gilvocarcin and jadomycin biosynthesis. *J. Am. Chem. Soc.* **2012**, *134*, 18181-18184.
178. Cone, M. C.; Seaton, P. J.; Halley, K. A.; Gould, S. J. New products related to kinamycin from *Streptomyces murayamaensis* I. Taxonomy, production, isolation, and biological properties. *J. Antibiot.* **1989**, *42*, 179-188.
179. Xie, Q. Y.; Qu, Z.; Lin, H. P.; Li, L.; Hong, K. *Micromonospora haikouensis* sp. nov., isolated from mangrove soil. *Antonie Leeuwenhoek* **2012**, *101*, 649-655.
180. Thi, Q. V.; Tran, V. H.; Maia, H. D.; Le, C. V.; Hong Mle, T.; Murphy, B. T.; V.M., C.; Pham, V. C. Antimicrobial metabolites from a marine-derived actinomycete in Vietnam's East Sea. *Nat. Prod. Commun.* **2016**, *11*, 49-51.
181. Thi, Q. V.; Tran, V. H.; Maia, H. D.; Le, C. V.; Hong Mle, T.; Murphy, B. T.; V.M., C.; Pham, V. C. Secondary metabolites from an actinomycete from Vietnam's East Sea. *Nat. Prod. Commun.* **2016**, *11*, 401-404.
182. Dembitsky, V. M.; Rezanka, T.; Srebnik, M. Lipid compounds of freshwater sponges: family Spongillidae, class Demospongiae. *Chem. Phys. Lipids.* **2003**, *123*, 117-155.
183. Imbs, A. B.; Vereshchagin, A. L. Isolation and characteristic of super long-chain unsaturated aldehydes from the freshwater sponge *Lubomirskia baicalensis*. *Russ. J. Bioorg. Chem.* **2005**, *31*, 651-656.
184. Imbs, A. B.; Rodkina, S. A. Trans and positional ethylenic bonds in two dominant isomers of eicosapentaenoic acid from the freshwater sponge *Baicalospongia bacillifera*. *Lipids* **2005**, *40*, 963-968.
185. Řezanka, T.; Sigler, K.; Dembitsky, V. M. Syriacin, a novel unusual sulfated ceramide glycoside from the freshwater sponge *Ephydatia syriaca* (Porifera, Demospongiae, Spongillidae). *Tetrahedron* **2006**, *62*, 5937-5943.
186. Hu, J.; Zhao, Y.; Chen, J.; Miao, Z.; Zhou, J. A new spongilipid from the freshwater sponge *Spongilla lacustris*. *Bull. Korean Chem. Soc.* **2009**, *30*, 1170-1172.

187. Mazur, A. A new sponge sterol. *J. Am. Chem. Soc.* **1941**, *63*, 883-884.
188. Makarieva, T. N.; Bondarenko, I. A.; Dmitrenok, A. S.; Boguslavsky, V. M.; Stonik, V. A.; Chernih, V. I.; Efremova, S. M. Natural products from Lake Baikal organisms, I. Baikalosterol, a novel steroid with an unusual side chain, and other metabolites from the sponge *Baicalospongia bacilifera*. *J. Nat. Prod.* **1991**, *54*, 953-958.
189. Keller-Costa, T.; Jousset, A.; van Overbeek, L.; van Elsas, J. D.; Costa, R. The freshwater sponge *Ephydatia fluviatilis* harbours diverse *Pseudomonas* species (*Gammaproteobacteria*, *Pseudomonadales*) with broad-spectrum antimicrobial activity. *PloS one* **2014**, *9*, e88429.
190. Kaluzhnaya, O.; Krivich, A.; Itskovich, V. Diversity of 16S rRNA genes in metagenomic community of the freshwater sponge *Lubomirskia baicalensis*. *Russ. J. Genet.* **2012**, *48*, 855-858.
191. Taylor, M. W.; Radax, R.; Steger, D.; Wagner, M. Sponge-associated microorganisms: Evolution, ecology, and biotechnological potential. *Microbiol. Mol. Biol. Rev.* **2007**, *71*, 295-347.
192. Reiswig, H. M.; Frost, T. M.; Ricciardi, A., Ecology and classification of North American freshwater invertebrates. Third Ed. ed.; Thorp, J. H.; Alan, P. C., Eds. Academic Press: London, 2010; pp 91-124.
193. Goering, A. W.; McClure, R. A.; Doroghazi, J. R.; Albright, J. C.; Haverland, N. A.; Zhang, Y.; Ju, K.-S.; Thomson, R. J.; Metcalf, W. W.; Kelleher, N. L. Metabologenomics: Correlation of microbial gene clusters with metabolites drives discovery of a nonribosomal peptide with an unusual amino acid monomer. *ACS Cent. Sci.* **2016**, *2*, 99-108.
194. Duncan, K. R.; Crüsemann, M.; Lechner, A.; Sarkar, A.; Li, J.; Ziemert, N.; Wang, M.; Bandeira, N.; Moore, B. S.; Dorrestein, P. C.; Jensen, P. R. Molecular networking and pattern-based genome mining improves discovery of biosynthetic gene clusters and their products from *Salinispora* species. *Chem. Biol.* **2015**, *22*, 460-471.
195. Wang, M.; Carver, J. J.; Phelan, V. V.; Sanchez, L. M.; Garg, N.; Peng, Y.; Nguyen, D. D.; Watrous, J.; Kapono, C. A.; Luzzatto-Knaan, T.; Porto, C.; Bouslimani, A.; Melnik, A. V.; Meehan, M. J.; Liu, W.-T.; Crusemann, M.; Boudreau, P. D.; Esquenazi, E.; Sandoval-Calderon, M.; Kersten, R. D.; Pace, L. A.; Quinn, R. A.; Duncan, K. R.; Hsu, C.-C.; Floros, D. J.; Gavilan, R. G.; Kleigrewe, K.; Northen, T.; Dutton, R. J.; Parrot, D.; Carlson, E. E.; Aigle, B.; Michelsen, C. F.; Jelsbak, L.; Sohlenkamp, C.; Pevzner, P.; Edlund, A.; McLean, J.; Piel, J.; Murphy, B. T.; Gerwick, L.; Liaw, C.-C.; Yang, Y.-L.; Humpf, H.-U.; Maansson, M.; Keyzers, R. A.; Sims, A. C.; Johnson, A. R.; Sidebottom, A. M.; Sedio, B. E.; Klitgaard, A.; Larson, C. B.; Boya P, C. A.; Torres-Mendoza, D.; Gonzalez, D. J.; Silva, D. B.; Marques, L. M.; Demarque, D. P.; Pociute, E.; O'Neill, E. C.; Briand, E.; Helfrich, E. J. N.; Granatosky, E. A.; Glukhov, E.; Ryffel, F.; Houson, H.; Mohimani, H.; Kharbush, J. J.; Zeng, Y.; Vorholt, J. A.; Kurita, K. L.; Charusanti, P.; McPhail, K. L.; Nielsen, K. F.; Vuong, L.; Elfeki, M.; Traxler, M. F.; Engene, N.; Koyama, N.; Vining, O. B.; Baric, R.; Silva, R. R.; Mascuch, S. J.; Tomasi, S.; Jenkins, S.; Macherla, V.; Hoffman, T.; Agarwal, V.; Williams, P. G.; Dai, J.; Neupane, R.; Gurr, J.; Rodriguez, A. M. C.; Lamsa, A.; Zhang, C.; Dorrestein, K.; Duggan, B. M.; Almaliti, J.; Allard, P.-M.; Phapale, P.; Nothias, L.-F.; Alexandrov, T.; Litaudon, M.; Wolfender, J.-L.; Kyle, J. E.; Metz, T. O.; Peryea, T.; Nguyen, D. T.; VanLeer, D.; Shinn, P.; Jadhav, A.; Muller, R.; Waters, K. M.; Shi, W.; Liu, X.; Zhang, L.; Knight, R.; Jensen, P. R.; Palsson, B. O.; Pogliano, K.; Linington, R. G.; Gutierrez, M.; Lopes, N. P.; Gerwick, W. H.; Moore, B. S.; Dorrestein, P. C.; Bandeira, N. Sharing and community curation of mass spectrometry data with global natural products social molecular networking. *Nat. Biotech.* **2016**, *34*, 828-837.

196. Hutchison, C. A.; Chuang, R.-Y.; Noskov, V. N.; Assad-Garcia, N.; Deerinck, T. J.; Ellisman, M. H.; Gill, J.; Kannan, K.; Karas, B. J.; Ma, L.; Pelletier, J. F.; Qi, Z. Q.; Richter, R. A.; Strychalski, E. A.; Sun, L.; Suzuki, Y.; Tsvetanova, B.; Wise, K. S.; Smith, H. O.; Glass, J. I.; Merryman, C.; Gibson, D. G.; Venter, J. C. Design and synthesis of a minimal bacterial genome. *Science* **2016**, *351*, 1414.
197. Ostrov, N.; Landon, M.; Guell, M.; Kuznetsov, G.; Teramoto, J.; Cervantes, N.; Zhou, M.; Singh, K.; Napolitano, M. G.; Moosburner, M.; Shrock, E.; Pruitt, B. W.; Conway, N.; Goodman, D. B.; Gardner, C. L.; Tyree, G.; Gonzales, A.; Wanner, B. L.; Norville, J. E.; Lajoie, M. J.; Church, G. M. Design, synthesis, and testing toward a 57-codon genome. *Science* **2016**, *353*, 819-822.
198. Hodgman, C. E.; Jewett, M. C. Cell-free synthetic biology: thinking outside the cell. *Metab. Eng.* **2012**, *14*, 261-269.

APPENDIX.

A1.Dereplication of known compounds from aquatic actinomycete strains.

A1.1 Introduction.

A prime objective in natural products drug discovery is identifying whether the compounds responsible for observed preliminary bioactivity of a fraction or extract represent novelty. Novelty worth investigating may include unique chemical structure, new therapeutic application, and/or novel MOA. Ideally, compounds without novelty or drug-lead potential are identified early and the corresponding project deprioritized or abandoned for the sake of efficiency and conservation of resources. The process aimed at quickly identifying known compounds without interesting bioactivity is termed "dereplication." In the course of investigating microbial library fractions that exhibited anti-tuberculosis activity, a number of producing strains were deprioritized based on these criteria. These compounds are described in this chapter.

A1.2 Antibiotics from Vietnam strain G016 that inhibit TB.

As a part of our ongoing collaboration with the ITR, the Murphy lab fraction library was screened for inhibitors of non-replicating *M. tuberculosis* in the low oxygen recovery assay (LORA). Fraction 1 from strain G016, a putative actinomycete, exhibited an MIC of 4.0 μg/mL in this assay, justifying further analysis. The strain was isolated from a sediment sample collected by PONAR in Hạ Long Bay at a depth of 22 m, from *ca*. 2.7 miles off the coast southeast of the Cát Bà Peninsula in Vietnam (20°41′53″ N, 107°05′34″ E) in July of 2011 (Figure A1). This was a part of a larger collection effort in collaboration with the Vietnamese Academy of Science and Technology (VAST) that resulted in a series of samples collected across an ~ 8.5 km transect with depths ranging from 5 m to 23 m, including the sample that was the foundation for Chapter 4.

Figure A1. G016 source sediment location near He Long Bay, Cát Bà, Vietnam.

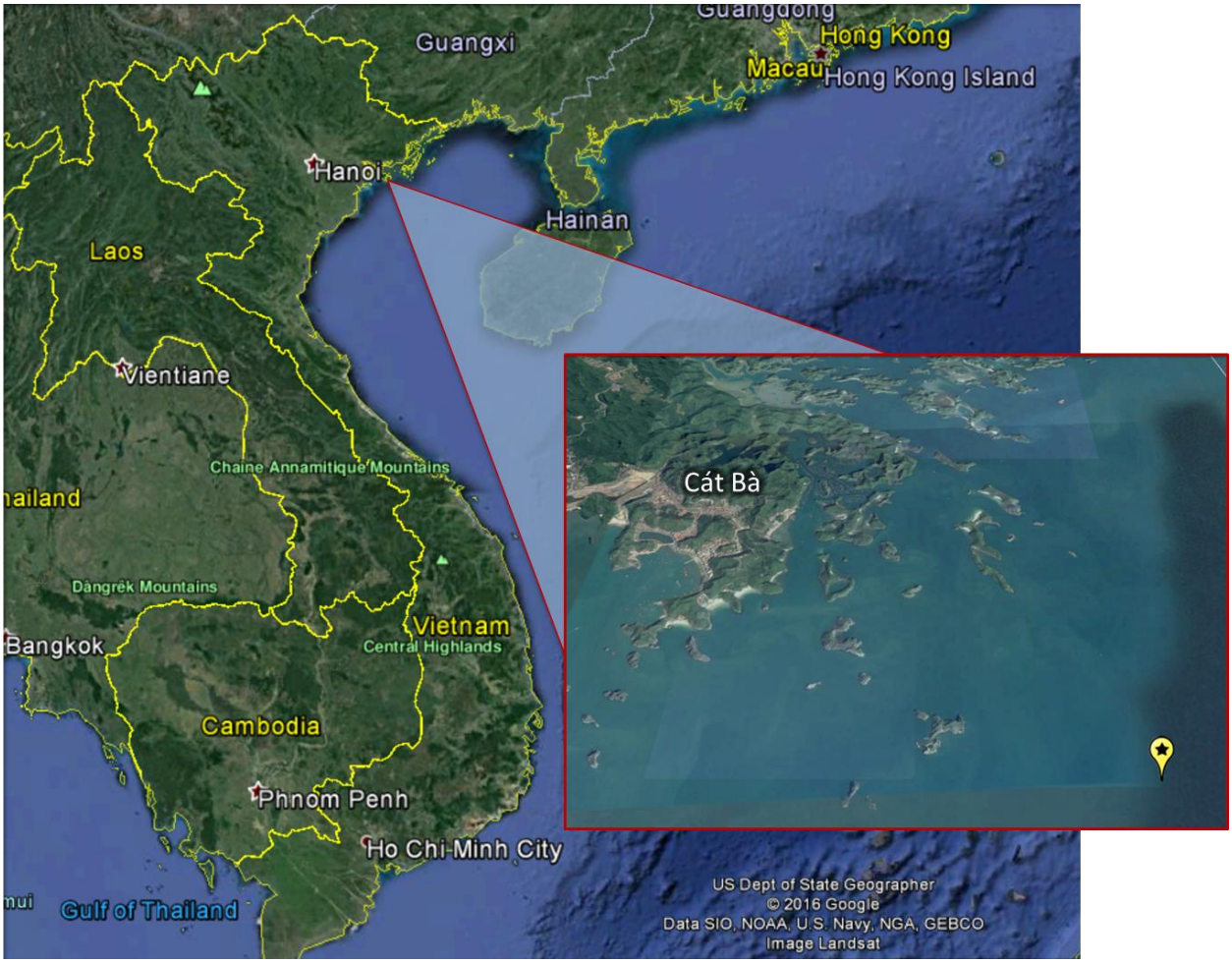

The star pin indicates the location of sediment (20°41′53″ N, 107°05′34″ E, 22 m) from which strain G016 was isolated.

Upon identification of its anti-TB bioactivity, fraction G016-F1 was analyzed by HPLC-UV, which led to the observation of three prominent chromatographic peaks for isolation (Figure A2). The 8.1 mg of G016-F1 was further were separated using RP-C_{18} preparative HPLC (5.0 mL·min^{-1}, gradient of 87% aqueous MeOH to 100% MeOH for 30 min, followed by an isocratic flow of 100% MeOH for 30 min) to afford seven fractions, among them the known compounds mansoquinone (**20**, G016-F1-2, t_R 16.8 min, 0.70 mg, 1.0% yield), hibarimicin HMP-M2 (**21**, G016-F1-3, t_R 19.5 min, 0.41 mg, 0.61% yield) and 1-methoxy-9-propyltetracene-6,11-dione (**22**, G016-F1-5, t_R 24.7 min, 0.36 mg, 0.56% yield).

Figure A2. HPLC-UV chromatogram of G016-F1 with UV profiles of **20**-**22**.

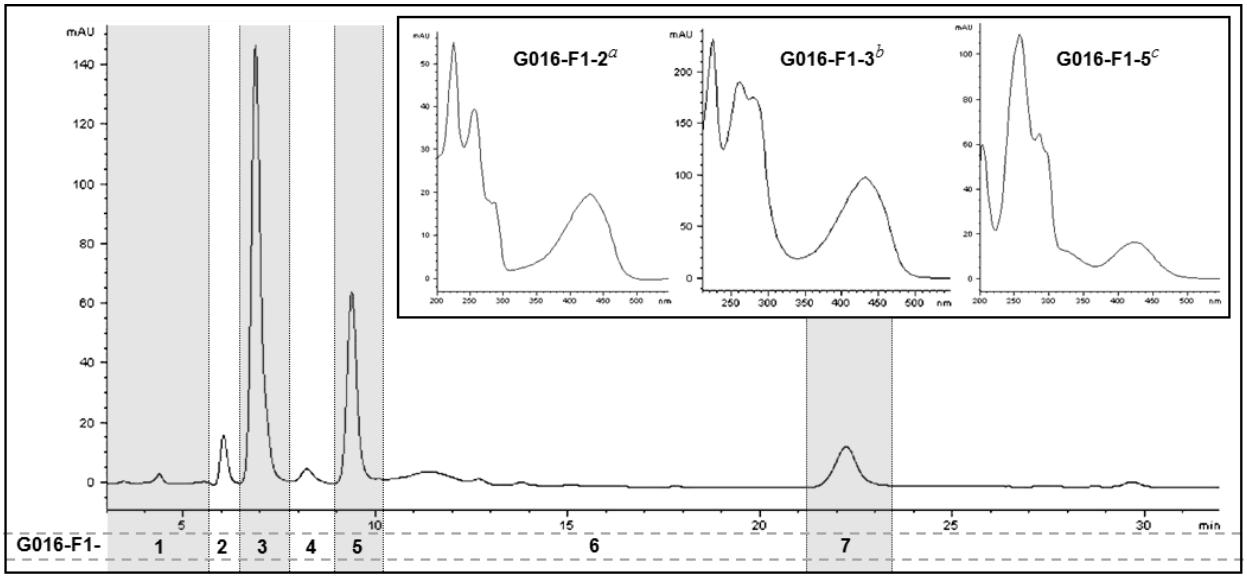

RP-HPLC-UV with a 100 x 4.6 mm 5 Å Luna C18 column. Method: 87% aqueous MeOH gradient to 100% MeOH over 15 min, then 100% MeOH wash for 15 min. [a]mansoquinone; [b]hibarimicin HMP-M2; [c]1-methoxy-9-propyltetracene-6,11-dione.

These seven fractions were rescreened at the ITR against replicating *M. tuberculosis* $H_{37}Rv$ in the MABA and the non-replicating form of the bacteria in the LORA to determine which were responsible for the activity observed in the parent fraction. Compounds **20** and **21** had moderate MIC values of 11.1 and 10.1, respectively, against replicating *M. tuberculosis*, while **22** was not active at the highest testing concentration of 50 μg/mL. None of the fractions significantly inhibited non-replicating *M. tuberculosis* in the LORA. The compounds were also screened by Eoghainín O hainmhire of the Burdette Lab at UIC in the OVCAR5 bioassay, which indicated that only **21** exhibited cytotoxicity at an LC_{50} of 22.4 μg/mL, while the others were inactive (Table A1).

Table A1. Antibiotic and cytotoxic activities of **20**-**22**.

Fraction / Compound	$H_{37}Rv$ MIC (µg/mL)		% inhib. at 50 µg/mL	LC_{50} (µg/mL)
	MABA	**LORA**	**Vero**	**OVCAR5**
G016-F1-1	>50 (12%)	>50 (20%)		
G016-F1-2 (**20**)	11.1	> 50	32.0	>100
G016-F1-3 (**21**)	10.1	45.7	19.8	22.4
G016-F1-4	>50	>50		
G016-F1-5 (**22**)	>50	>50	0.0	>100
G016-F1-6	12.28	>50		
G016-F1-7	48.03	46.9		

The ^{1}H NMR spectrum of G016-F1-2, putatively identified as containing mansoquinone (**20**) is shown with the chemical structure in Figure A3. This anthraquinone was previously reported to moderately inhibit the growth of *E. coli*, *B. subtilis*, and *S. aureus*.[1]

Figure A3. ^{1}H NMR spectrum (600 MHz) of **20** in $CDCl_3$.

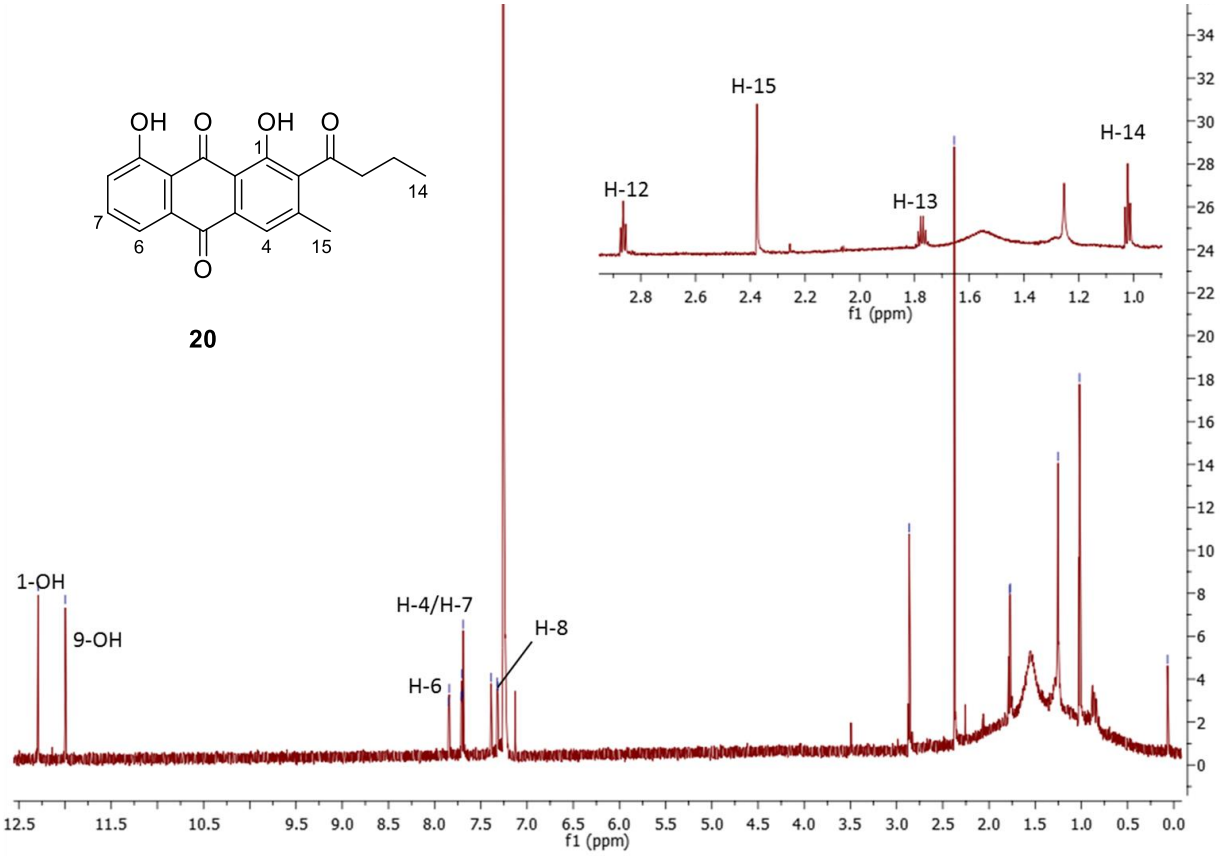

The ^{1}H NMR spectrum of G016-F1-3, putatively identified as containing hibarimicin HMP-M2 (**21**) is shown with its chemical structure in Figure A4. This anthraquinone was structurally very similar to mansoquinone except for its enol subgroup and ethane extension on the side chain. Compound **21** was isolated in 2002 from a chemically-mutagenized strain of *Microbispora rosea* subsp. *hibaria* TP-A0121 and was identified as a shunt metabolite arising from a biosynthetic precursor of hibarimicin B.[2] The hibarimicins were discovered in a screening for tyrosine kinase inhibitors, though in a follow-up study compound **21** did not exhibit significant influence on tyrosine kinase inhibition or HL-60 cell differentiation.[3, 4] To our knowledge, this report represents the first discovery of compound **21** from a non-mutagenized environmental actinomycete strain and the first screening of this compound for antibiotic activity.

Figure A4. ^{1}H NMR spectrum (600 MHz) of **21** in $CDCl_3$.

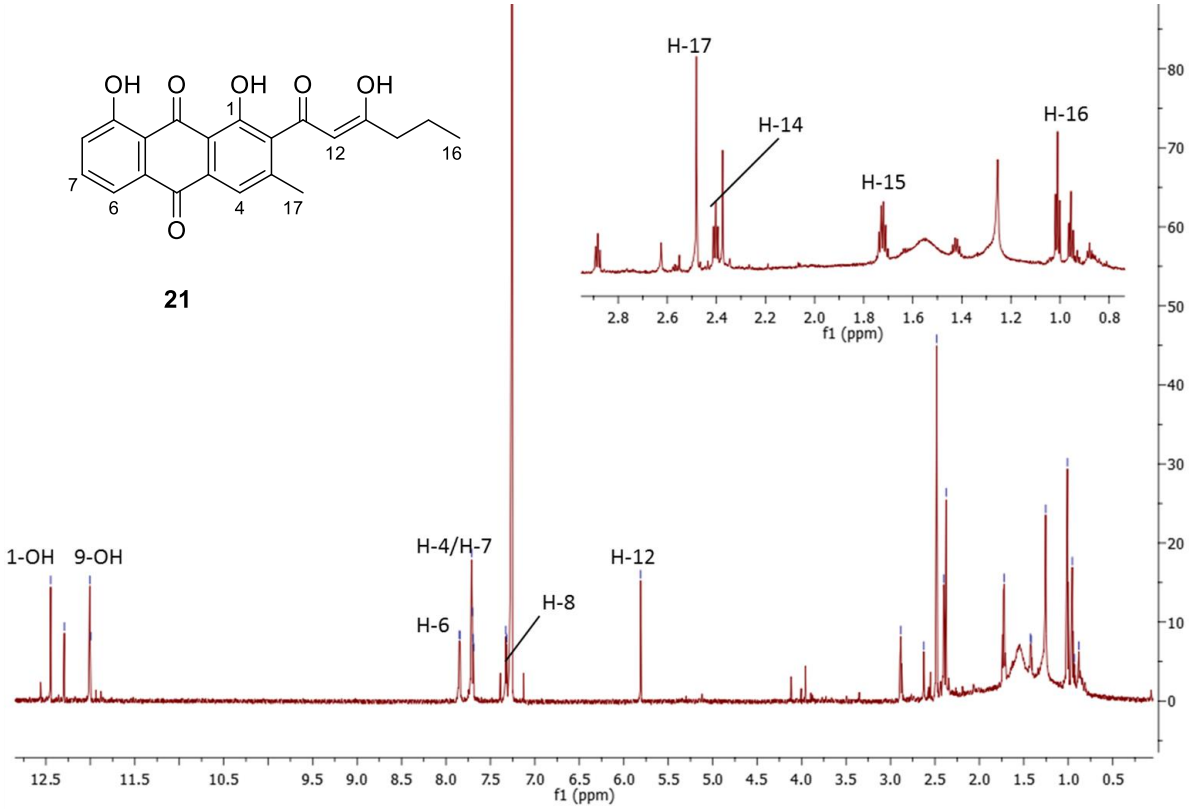

The ^{1}H NMR spectrum of fraction G016-F1-5 was putatively identified as containing 1-methoxy-9-propyltetracene-6,11-dione (**22**) and is shown with the chemical structure in Figure A5. This tetracene compound was reported in 2012 from a *Micromonospora* sp. extract that contained metabolites active against the HCT-8 human colon adenocarcinoma cell line.[5] Compound **22** was inactive against this cell line, which agrees with the absence of activity observed in our study (Table A1). These molecules were not prioritized for further exploration due their previous characterization and lack of significant activity in our bioassays.

Figure A5. ^{1}H NMR spectrum (600 MHz) of **22** in $CDCl_3$**.**

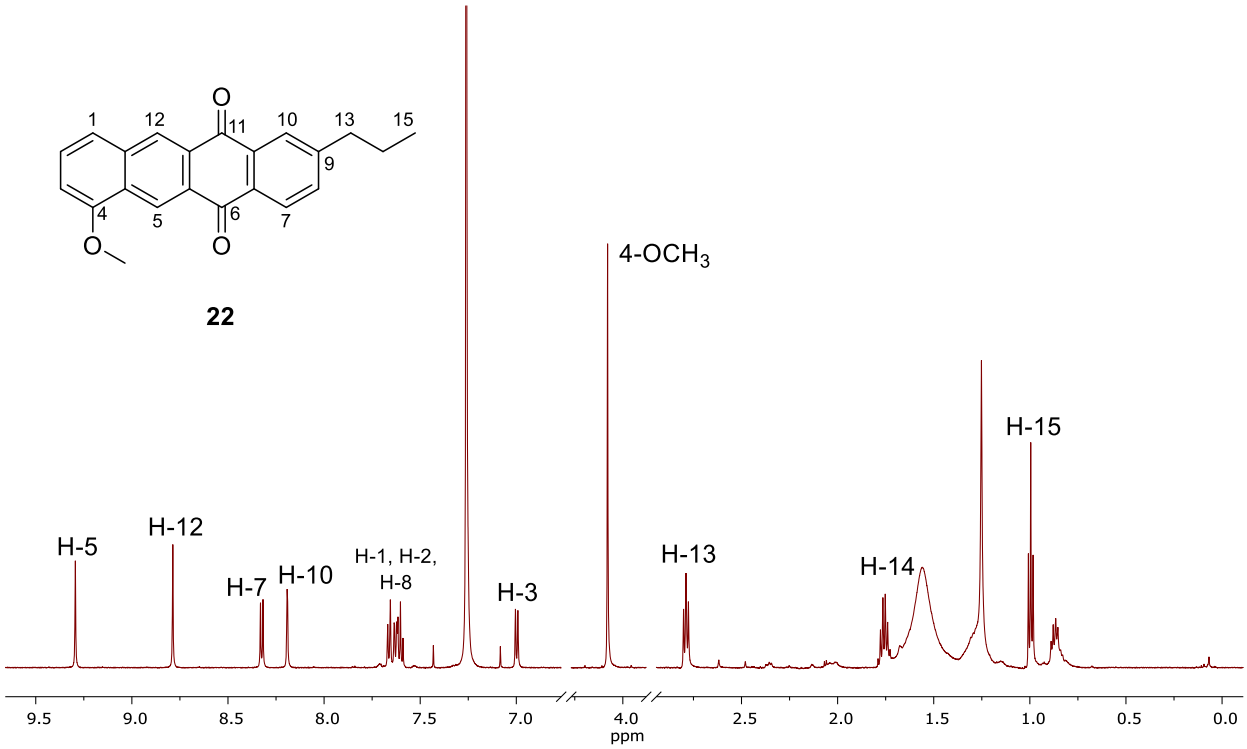

A1.3 Identification of tirandamycins from Icelandic sediment-derived strain K123.

We set out to identify the source of anti-TB activity observed in strain K123 fractions to further our limited knowledge of the chemical diversity and pharmacological potential of secondary metabolites from Icelandic marine-derived actinomycetes. To our knowledge, the bioactivity of molecules from these sources is completely unknown. Furthermore, the collection site of strain K123 is at a high latitude along the Icelandic coast and adjacent to geothermal features that may foster interesting microbial communities. This environment may provide selection pressures for interesting adaptations which could include novel biosynthetic pathways. The pharmacological activity of secondary metabolites from actinomycetes living in the unusual conditions of the island is also unexplored.[6]

Strain K123 was isolated from a sediment sample collected at a depth of 1 m near the shoreline of Reykjanestá, the southwestern-most tip of Iceland (63° 48' 40.33" N,

22° 42' 58.42" W) in March of 2013. Fraction K123-F4 inhibited *M. tuberculosis* with an MIC of 0.30 μg/mL in the MABA and 0.26 μg/mL in the LORA. Based on their molecular ions and UV profiles (Figure A6), compounds of MW 433.46 and 417.45 were quickly identified as tirandamycins A (**23**) and B (**24**), which were initially implicated in the activity for the fraction due to their prominence in the chromatogram. Fraction K123-F3 also contained these compounds, so it was combined with K123-F4 with the goal of increasing the yield of tirandamycins following subsequent chromatographic separation.

Figure A6. Representative tirandamycin UV profile.

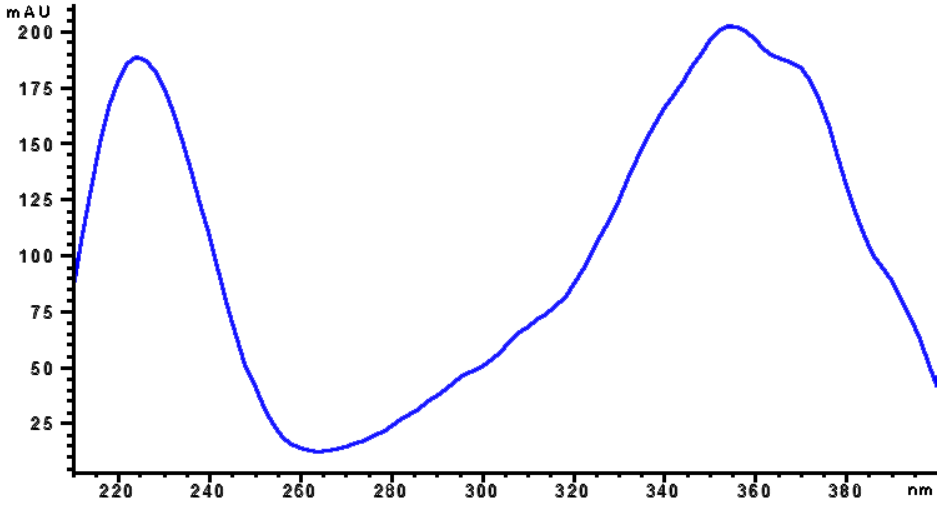

The tirandamyicins (TAMs) are tetramic acids and were first isolated and characterized in the early 1970s.[7-9] Interestingly, there is no report describing the screening of the tirandamycin class against TB. To date, this class has been reported to kill *B. malayi* parasites;[10] the protozoa *E. histolytica*;[11] pathogenic anaerobes *B. fragilis*, *B. vulgatus*, *B. thetaomicron*, *C. perfringens*, *P. anaerobius*, and *C. difficile*; and have been shown to exhibit moderate activity against the aerobe *S. pyogenes*,[12] and VRE;[13] without exhibiting cytotoxicity.[10] The class was reported to target RNA polymerase in bacteria but not eukaryotes in a cell-free assay.[14, 15] The mode of action of the

antibiotic was reported to be identical to streptolydigin in inhibition of the transcriptional process, though tirandamycin was reportedly 40 times less potent.[16] Interestingly, it has been reported that *M. tuberculosis* is resistant to streptolydigin.[17] Due to the TB-inhibition observed by this fraction that appeared to be composed predominantly of TAMs, we explored the possibility that the structural differences of the TAMs compared to streptolydigin might allow for circumvention of this resistance (Figure A7).

Figure A7. Structures of **23**, **24**, and streptolydigin.

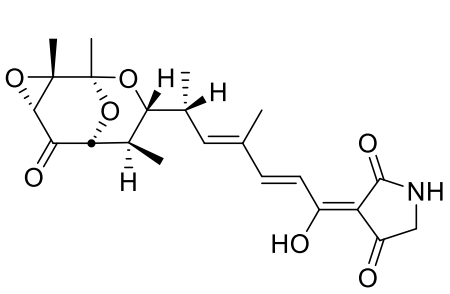

23

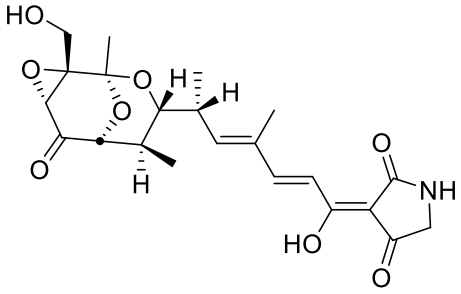

24

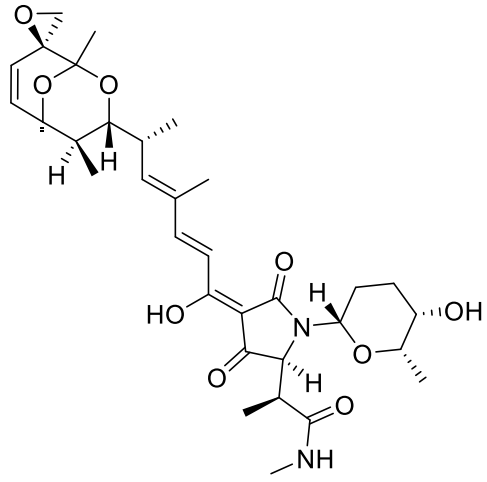

streptolydigin

A 26.1 mg portion of the total 51.4 mg K123-F3/4 was separated using RP-C_{18} preparative HPLC (16.0 mL·min^{-1}, gradient of 30% to 82% ACN for 26 min, followed by an isocratic flow of 100% ACN for 10 min) to afford seven fractions, including the known compounds tirandamycin B (**24**, K123-F3/4-2, t_R 19.7 min, 4.58 mg, 17.55% yield), and tirandamycin A (**23**, K123-F3/4-6, t_R 25.3 min, 2.42 mg, 9.27% yield). Structures were confirmed by ^{1}H NMR comparison (Figures A8 and A9).[8]

Figure A8. ^{1}H NMR spectrum (600 MHz) of **23** in $CDCl_3$.

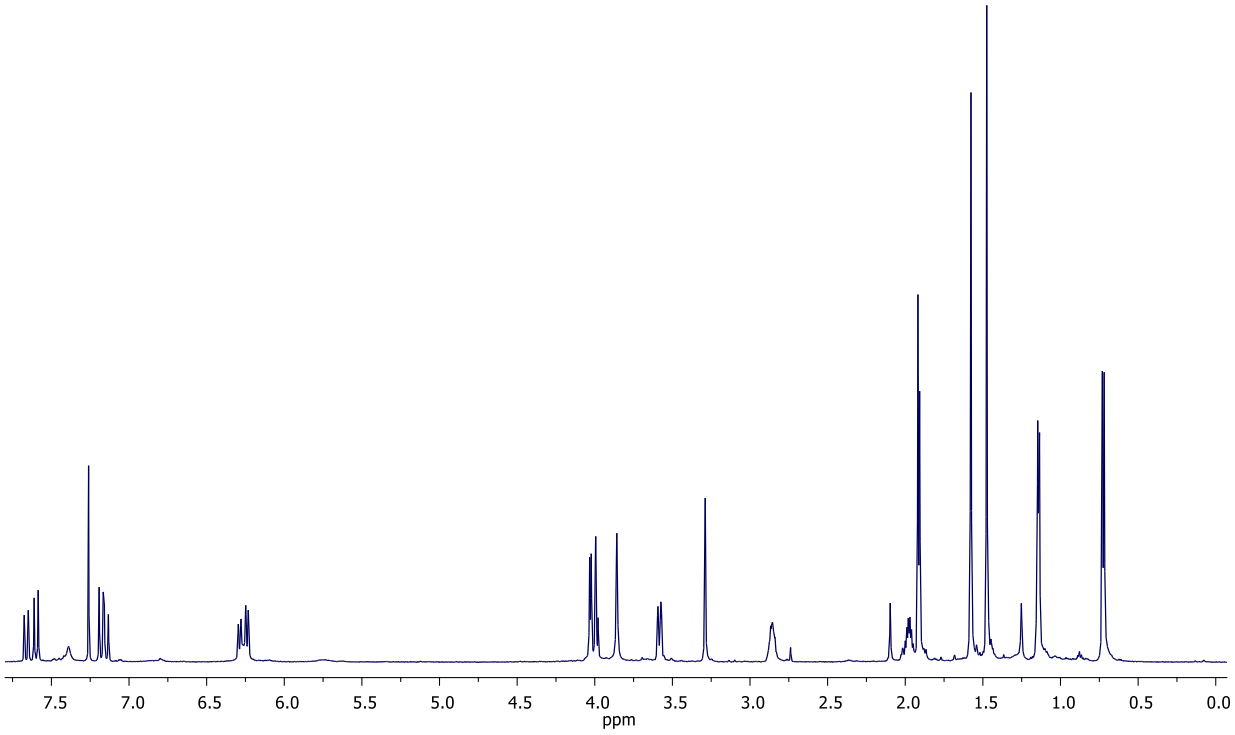

Figure A9. ^{1}H NMR spectrum (600 MHz) of **24** in $CDCl_3$.

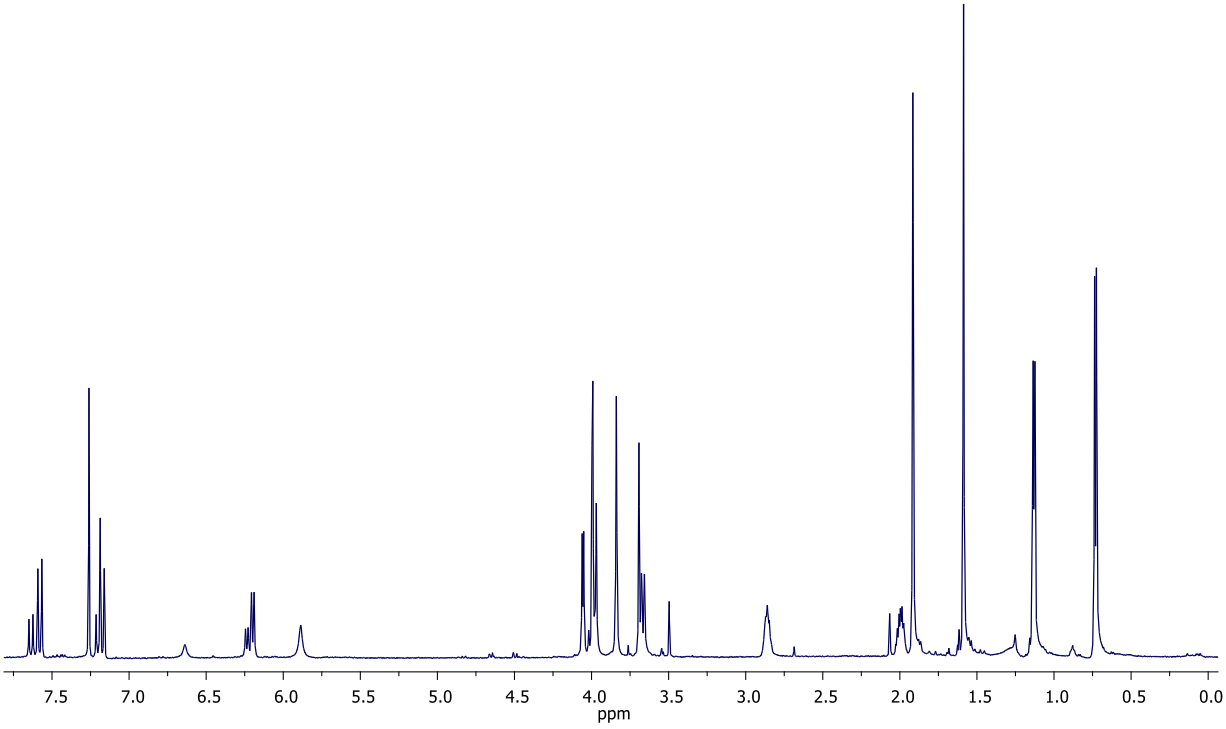

Table A2. Anti-TB activities of K123-F3/4 and subfractions.

Fraction	$H_{37}Rv$ MIC (µg/mL)
	MABA
K123-F3/4	6.0
K123-F3/4-1	> 50
K123-F3/4-2 (**24**)	> 50
K123-F3/4-3	> 50
K123-F3/4-4	> 50
K123-F3/4-5	24.6
K123-F3/4-6 (**23**)	> 50
K123-F3/4-7	> 50

Following submission to the ITR for screening in the MABA, the K123-F3/4 subfractions, including the tirandamycins, were found to lack the activity of the parent fraction (Table A2). This

was unexpected, so possible explanations for loss of material were explored. Interestingly, a group of non-UV absorbing analytes that were observable by MS in the methanol wash of an HPLC-MS run were absent when using an acetonitrile mobile phase for analysis of the same sample (Figures A10 and A11). This series of peaks had molecular weights in the high 700's and low 800's and are evidence to the fact that though MeOH is often a weaker eluent than ACN at lower concentrations, it can act as a stronger eluent than ACN at 100%.

Figure A10. K123-F3/4 UV and MS chromatograms with ACN organic mobile phase.

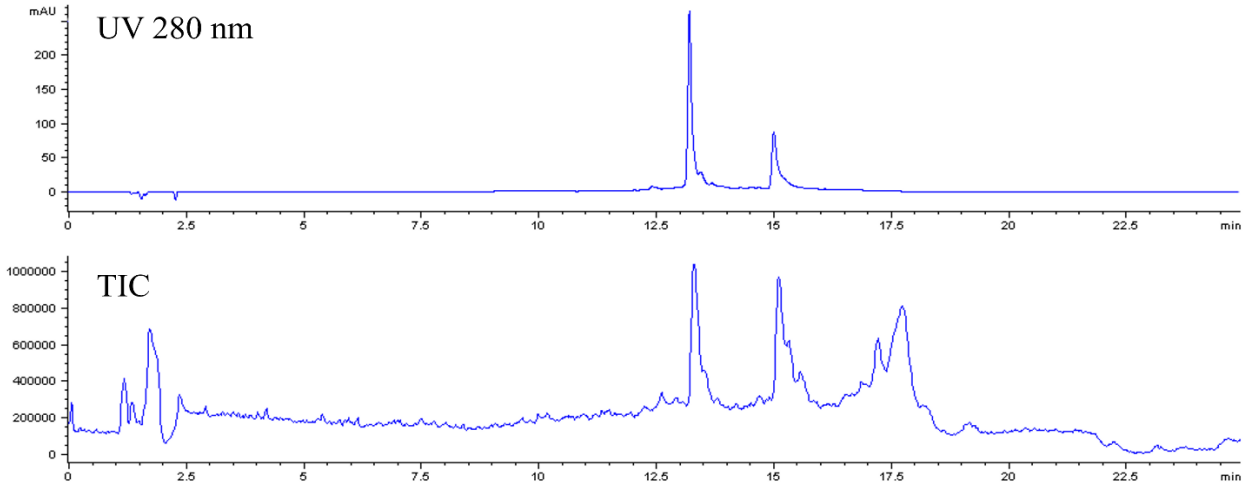

Luna C18 100 x 4.6 mm 5 µm 100 Å; 30% ACN 5 min, 30-100% ACN 10 min, 100% ACN 10 min. No MS peaks observed between 19 and 21 minutes.

Figure A11. K123-F3/4 UV and MS chromatograms with MeOH organic mobile phase.

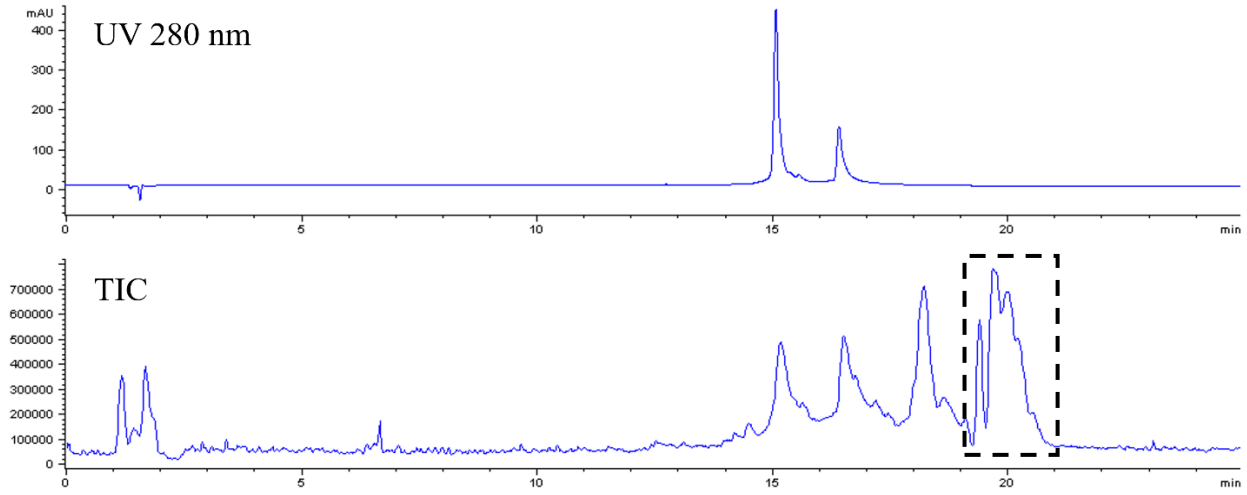

Luna C18 100 x 4.6 mm 5 µm 100 Å; 30% MeOH 5 min, 30-100% MeOH 10 min, 100% MeOH 10 min. At least five overlapping MS peaks observed between 19 and 21 minutes. Dotted line highlights peaks unique to MeOH wash.

These non-polar MeOH wash molecules are worth exploring further for their anti-TB activity. Unfortunately, a MeOH wash from the earlier separation was not collected and the material was not retrievable from the column. To explore the bioactive potential of the MeOH wash identified from MS, a 4.54 mg portion of remaining K123 F3/4 was eluted through 0.5 cm loose C18 in a 6" Pasteur pipette using acetonitrile. Following elution with 4 mL acetonitrile, the C18 resin retained a yellow hue, evidence for additional material remaining on the column. In accord with observations from the MS data, a wash of 100% MeOH was sufficient to elute this material. Two 3 mL fractions of the wash were collected resulting in 1.28 mg for the first fraction (MeOH W1) and 0.51 mg for the second (MeOH W2). These were included in a subsequent screening against *M. tuberculosis* in the MABA. Other samples that were also included in order to explore other possible explanations for the loss of bioactivity, included 1) fractions F3, F4, and combined fraction F3/4 from the fraction library to test for bioassay anomalies, cancelation of F4

activity by F3 (or vice versa), or degradation of material; 2) combined **23** and **24** to test for potential synergy between TAMs that would have been lost in the isolation process.

Bioassay supported the earlier observation of activity from K123-F3/4 and indicated that the first of the two methanol washes was responsible for the activity of the parent fraction with an MIC of 7.8 µg/mL. Interestingly, these washes did not exhibit cytotoxicity when screened against the Vero cell line. The combined TAMs and the second wash were not significantly active (Table A3).

Table A3. *In vitro* anti-TB activity and cytotoxicity of K123 fractions**.**

Sample	$H_{37}Rv$ MABA MIC (µg/mL)	Vero IC_{50} (µg/mL)
K123-F3	2.7	Not tested
K123-F4	3.0	Not tested
K123-F3/4	5.9	Not tested
TAMA / TAMB	>50	Not tested
K123-3/4 MeOH W1	7.8	> 50
K123-3/4 MeOH W2	22.2	> 50

Analysis of MS data collected for the first MeOH wash of combined fractions K123-F3/4 revealed six peaks (Figure A12). Four of these shared a common ion pattern that is putatively a Na^+ adduct of the $[M+H]^+$ ion following a loss of H_2O (Figure A13). The consistent pattern among these peaks suggested that they are a class of related analogs.

Figure A12. Selected ion chromatogram of K123-F3/4 MeOH W1.

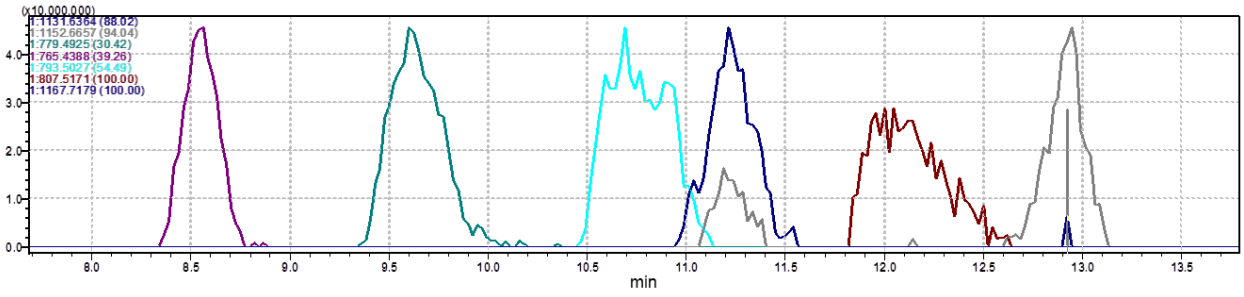

Kinetex C18 100 x 2.1 mm 2.6 µm 100 Å; 30% ACN 5 min, 30-100% ACN 10 min, 100% ACN 10 min.

Figure A13. Representative ion pattern for K123-F3/4 MeOH W1 selected ion peaks.

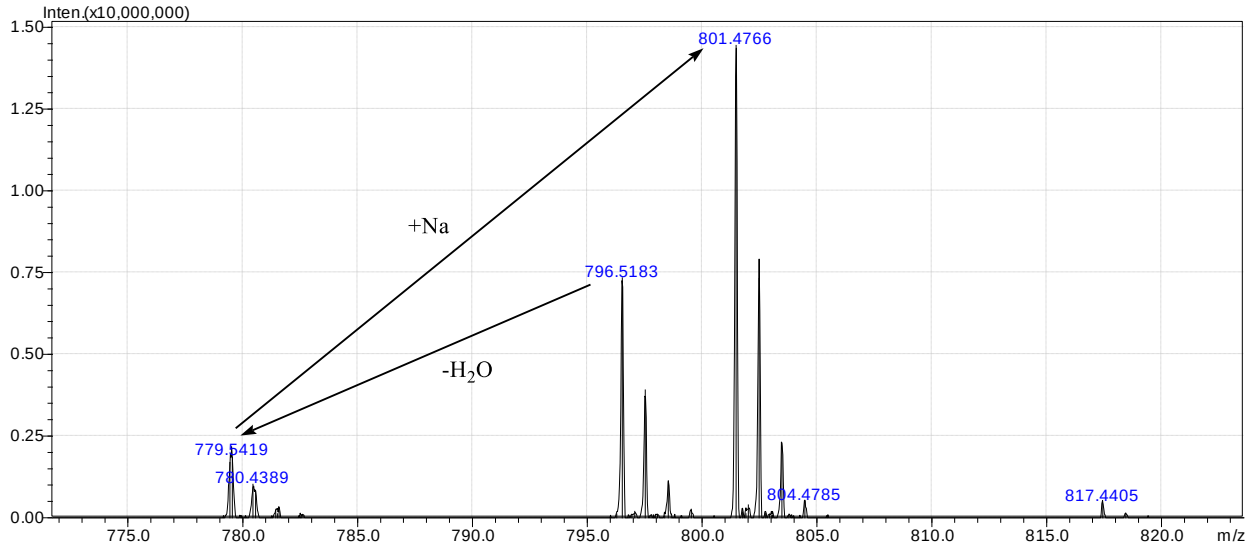

Figure A14. ^{1}H NMR spectrum (600 MHz) of K123-F3/4 MeOH W1 in $CDCl_3$.

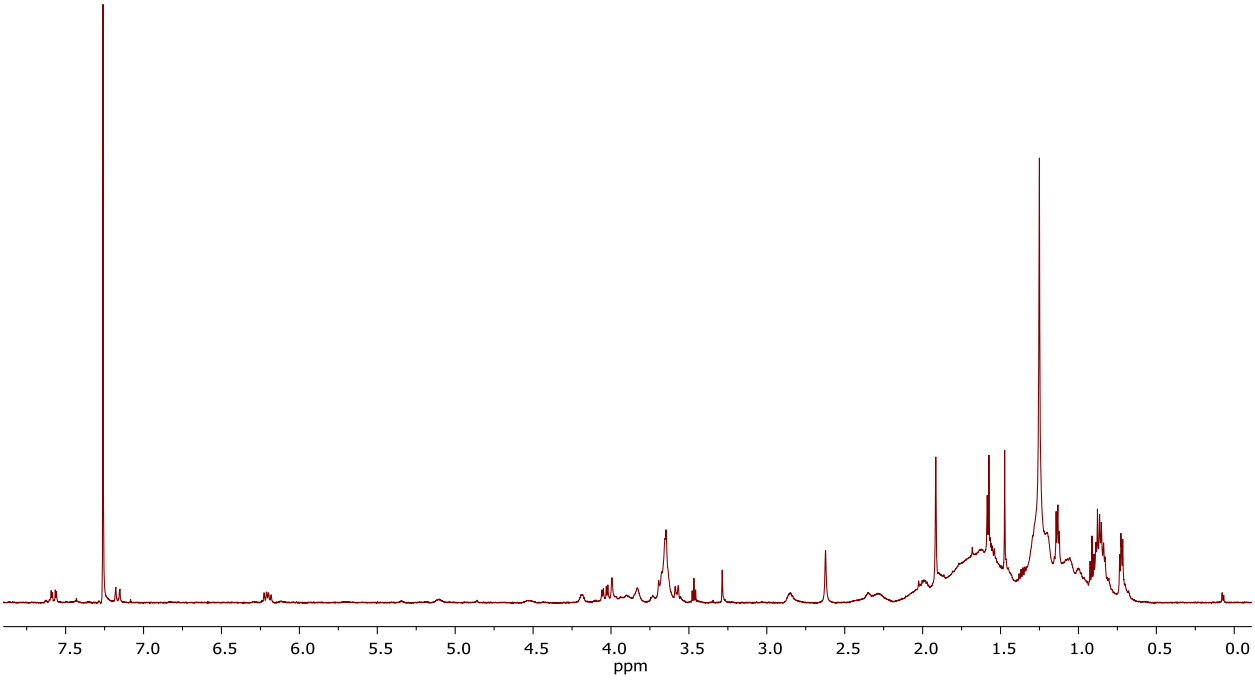

The molecular weights, absence of UV absorbance between 200 – 600 nm, and ^{1}H NMR spectrum (Figure A14) were used to dereplicate the compounds present in the MeOH W1 fraction. Potential compound matches were not found. Since this is a 1.28 mg combination of at least seven compounds, a greater abundance of each peak should be purified to more confidently assess their

potential novelty. Additional chromatographic steps are required to isolate greater amounts of each compound from the 25.3 mg remaining of K123-F3/4. A larger scale regrow of strain K123 would also be an option for generating more material for testing. Future studies would involve the isolation, dereplication, and characterization of novel compounds in this TB-active K123-F3/4 W1 wash fraction.

A1.4 CITED LITERATURE.

1. Abdelfattah, M. S. Mansoquinone: Isolation and structure elucidation of new antibacterial aromatic polyketides from terrestrial *Streptomyces* sp. Eg5. *Nat. Prod. Res.* **2009**, *23*, 212-218.
2. Igarashi, Y.; Kajiura, T.; Furumai, T.; Hori, H.; Higashi, K.; Ishiyama, T.; Uramoto, M.; Uehara, Y.; Oki, T. Biosynthesis of hibarimicins. III. Structures of new hibarimicin-related metabolites produced by blocked mutants. *J. Antibiot. (Tokyo)* **2002**, *55*, 61-70.
3. Cho, S. I.; Fukazawa, H.; Honma, Y.; Kajiura, T.; Hori, H.; Igarashi, Y.; Furumai, T.; Oki, T.; Uehara, Y. Effects of hibarimicins and hibarimicin-related compounds produced by Microbispora on v-Src kinase activity and growth and differentiation of human myeloid leukemia HL-60 cells. *J. Antibiot. (Tokyo)* **2002**, *55*, 270-278.
4. Kajiura, T.; Furumai, T.; Igarashi, Y.; Hori, H.; Higashi, K.; Ishiyama, T.; Uramoto, M.; Uehara, Y.; Oki, T. Biosynthesis of hibarimicins. II. Elucidation of biosynthetic pathway by cosynthesis using blocked mutants. *J. Antibiot. (Tokyo)* **2002**, *55*, 53-60.
5. Sousa, T. d. S.; Jimenez, P. C.; Ferreira, E. G.; Silveira, E. R.; Braz-Filho, R.; Pessoa, O. D. L.; Costa-Lotufo, L. V. Anthracyclinones from *Micromonospora* sp. *J. Nat. Prod.* **2012**, *75*, 489-493.
6. Omarsdottir, S.; Einarsdottir, E.; Ögmundsdottir, H. M.; Freysdottir, J.; Olafsdottir, E. S.; Molinski, T. F.; Svavarsson, J. Biodiversity of benthic invertebrates and bioprospecting in Icelandic waters. *Phytochem. Rev.* **2013**, *12*, 517-529.
7. Duchamp, D. J.; Branfman, A. R.; Button, A. C.; Rinehart, K. L. X-ray structure of tirandamycic acid p-bromophenacyl ester. Complete stereochemical assignments of tirandamycin and streptolydigin. *J. Am. Chem. Soc.* **1973**, *95*, 4077-4078.
8. Rinehart, K. L.; MacKellar, F. A.; Grostic, M. F.; Olson, E. C.; Wnuk, R. J.; Branfman, A. R. Tirandamycin. I. Structure assignment. *J. Am. Chem. Soc.* **1971**, *93*, 4943-4945.
9. Meyer, C. E. Tirandamycin, a new antibiotic isolation and characterization. *J. Antibiot.* **1971**, *24*, 558-560.
10. Rateb, M. E.; Yu, Z.; Yan, Y.; Yang, D.; Huang, T.; Vodanovic-Jankovic, S.; Kron, M. A.; Shen, B. Medium optimization of *Streptomyces* sp. 17944 for tirandamycin B production and isolation and structural elucidation of tirandamycins H, I and J. *J. Antibiot.* **2014**, *67*, 127-132.
11. Espinosa, A.; Socha, A. M.; Ryke, E.; Rowley, D. C. Antiamoebic properties of the actinomycete metabolites echinomycin A and tirandamycin A. *Parasitol. Res.* **2012**, *111*, 2473-2477.
12. Rosen, T.; Fernandes, P. B.; Marovich, M. A.; Shen, L.; Mao, J.; Pernet, A. G. Aromatic dienoyl tetramic acids. Novel antibacterial agents with activity against anaerobes and staphylococci. *J. Med. Chem.* **1989**, *32*, 1062-1069.
13. Carlson, J. C.; Li, S.; Burr, D. A.; Sherman, D. H. Isolation and characterization of tirandamycins from a marine-derived *Streptomyces* sp. *J. Nat. Prod.* **2009**, *72*, 2076-2079.
14. Reusser, F. Tirandamycin: Inhibition of ribonucleic acid polymerase. *Infect. Immun.* **1970**, *2*, 77-81.
15. Reusser, F. Tirandamycin, an inhibitor of bacterial ribonucleic acid polymerase. *Antimicrob. Agents Chemother.* **1976**, *10*, 618-622.
16. Reusser, F. Tirandamycin: Inhibition of oxidative phosphorylation in rat liver mitochondria. *Infect. Immun.* **1970**, *2*, 82-88.
17. Speer, A.; Rowland, J. L.; Niederweis, M. *Mycobacterium tuberculosis* is resistant to streptolydigin. *Tuberculosis (Edinb.)* **2013**, *93*, 401-404.

A2.SUPPLEMENTAL INFORMATION.

A2.1.Supplemental information for: DIAZA-ANTHRACENE ANTIBIOTICS FROM A FRESHWATER-DERIVED ACTINOMYCETE WITH SELECTIVE ANTIBACTERIAL ACTIVITY TOWARD *M. TUBERCULOSIS*.

A.2.1.1DARTS assay for identification of the molecular target of diazaquinomycin A in *M. tuberculosis* cell lysate.

Multiple unsuccessful attempts were made at directly isolating a protein target using the drug affinity responsive target stability (DARTS) assay method developed by the Huang lab at the University of California, Los Angeles.[1, 2] Multiple reagent concentrations, incubation times, and temperatures were attempted without success. This method primarily uses SDS-PAGE and mass spectrometry and relies on the ability of the test compound, in our case DAQA, to bind and stabilize a protein target in the presence of a protease mixture. There are numerous explanations why this method was unsuccessful, of them being the possibilities that 1) **3** binds or interacts with a non-protein target that would not be detected by this method, 2) **3** has multiple targets, 3) **3** does not bind covalently, strongly enough, or in such a conformation as to protect a protein target from protease degradation, 4) the protein target was in too low of abundance to be identified on an SDS-PAGE gel.

A2.1.2 Investigation of the ability of diazaquinomycin A (3) to inhibit cellular respiration.

Menaquinones are critical to electron transport, oxidative phosphorylation, and endospore formation in bacteria. We recognized that the anthraquinone structure of **3** has a similarity to the menaquinones (Vitamin K). Additionally, **3** exhibited an oxidative stress component similar to clofazimine, which interferes with menaquinones in the electron transport chain.[3] Thus, we reasoned that the DAQs may also inhibit electron transport. If **3** competed with menaquinones to affect electron transport, it would quickly affect ATP levels similar to bedaquiline (BDQ)[4] In collaboration with the Clifton Barry lab, we used a Promega BacTiter-Glo™ assay, which harnesses the bioluminescence signal from a luciferase-catalyzed reaction for the measurement of

ATP levels following incubation with test compound for 24 hours. The heatmap in Figure A15 illustrates that **3** had no direct effect on respiration that would result in depletion of ATP in *M. tuberculosis*. ATP increases over 24 hours in certain stress situations, which is seen following isoniazid and rifampin treatment. Conversely, BDQ, Q203, and carbonyl cyanide chlorophenylhydrazone (CCCP) are known inhibitors of respiration that deplete ATP in this timeframe.

Figure A15. *M. tuberculosis* ATP levels are unaffected following treatment with **3**.

concentration and compound	Luminescence (RLU)											
7 µM INH[a]	4542120	5075280	7521520	7593920	7525080	6586040	1769120	713880	696160	721320	666560	554240
5 µg/mL RIF[b]	488280	698480	669720	1146520	1174440	1207520	1271280	1328000	1439800	1656120	1890160	693080
25 µM SM[c]	317000	372520	590960	437040	692280	663040	578040	646840	556360	595920	644320	697920
10 µM BDQ[d]	14360	19600	22280	29240	56440	82160	121760	190320	280640	356200	402080	683360
0.5 µM Q203	65120	67360	72560	69280	110640	111720	115400	125760	147480	206520	229680	682880
25 µg/mL CCCP[e]	51920	70440	88680	104640	126600	223800	380160	629560	761600	785400	733600	653760
10 µg/mL DAQA[f]	305880	583880	787520	509560	530080	677040	653720	697440	725160	793320	732800	600840
10 µg/mL DAQA[f]	387160	549440	652040	508240	656920	724760	769920	844640	943000	945600	881280	701040

increase

decrease

[a]isoniazid; [b]rifampin; [c]streptomycin; [d]bedaquiline; [e]carbonyl cyanide chlorophenylhydrazone; [f]diazaquinomycin A. Compound and initial concentration in first well indicated in far left column. Subsequent wells to the right are 2-fold dilutions down to column 11. Column 12 is drug-free control.

Methods. DMSO stocks of each TB inhibitor were diluted in 7H9/ADC/Tw as two-fold serial dilution series in duplicate at 50 µL per well in clear round-bottom 96-well plates (Thermo Scientific #163320) leaving a drug-free media control in column 12. *M. tuberculosis* $H_{37}Rv$ (ATCC 27294) was cultured in 7H9/ADC/Tw to an OD of 0.2 and diluted 1:1000 in the same medium followed by addition of 50 µL of the diluted cell suspension to each well. The plates were incubated at 37 °C in sealed bags for 24 hours after which 20uL BacTiter Glo reagent (Promega) was added. Luminescence was recorded after 15 min incubation at room temperate in a Fluorostar Optima reader.

A2.1.3 Antibiotic activity of diazaquinomycin A (3) against a panel of environmental actinomycete bacteria.

In the interest of generating additional experimental options to aid in characterization of the DAQA MOA, we screened the compound against a series of aquatic-derived actinomycete bacteria from the Murphy lab strain library using a disk diffusion assay. Justification for the experiment was initially based upon the recognition that, as in *M. tuberculosis,* environmental actinomycetes such as *Streptomyces* and *Micromonospora* species share biochemical pathways dependent on F_{420}.[5] Though **3** activity has been incredibly selective thus far, there remains the possibility for susceptibility in other microorganisms. Surprisingly, there was a range of activities observed against these strains (Table A4). As many as ten of the seventeen environmental actinomycetes exhibited some degree of susceptibility to **3**. The zones of inhibition for four of the susceptible environmental strains were not devoid of colonies, but rather had an observably less dense lawn surrounding the paper disks, while another strain that was not susceptible in terms of viability underwent inhibition of the production of a red pigment. Though it is difficult to compare assays performed in solid agar with those in liquid media, this study adds to the understanding of DAQA selectivity. Based on activities observed in mycobacteria and these environmental isolates, this class of compound seems to have the greatest effect on biological processes in bacteria of the order *Actinomycetales*. These data suggest that resistant mutant strains could be generated from DAQ-susceptible environmental actinomycetes to aid in future MOA studies. These strains may be more amenable to mutant generation with less frequent occurrence of phenotypically resistant colonies and could serve as a substitute in the event of failed experiments using $mc^2$7000.

Table A4. Evaluation of the activity of **3** against environmental actinomycete bacteria.

Strain name	16S rRNA sequence identity	Zone of Inhibition (mm)				Notes
		Control (0 µg)	1 µg	10 µg	25 µg	
A001	*S. tendae*	0	0	0	0	
A003	*S. tendae*	0	0	0	0	red pigment production inhibited
A004	*S. koyangensis*	0	8	10	12	well defined zones of less dense colonies
A009	*S. flavogriseus*	0	0	8	10	
A019	*S. tendae*	0	8	8	10	well defined zones of less dense colonies
B007	*S. griseoflavus*	0	0	8	10	
B010	*S. mordarskii*	0	0	0	0	
D034	*S. tacrolimicus*	0	0	0	0	well defined zones of less dense colonies
D036	*S. erythrogriseus*	0	10	12	14	
D038	*S. lienomycini*	0	0	0	0	
D041	*S. griseoincarnatus*	0	10	13	18	forms sparse colonies – inhibition zones difficult to measure
D057	*S. jietaisiensis*	0	8	10	12	well defined zones of less dense colonies
D080	*S. xinghaiensis*	0	0	0	0	forms sparse colonies – inhibition zones difficult to measure
DAQ producer strains						
F001	*S. coacervatus*	0	0	0	0	
B006	*M. tulbaghiae*	0	9	11	16	
Negative control						
D012	*B. thuringiensis*	0	0	0	0	

Methods. Paper disks containing 1 µg, 10 µg, and 25 µg of **3** were made by applying 0.025 mg/mL, 0.250 mg/mL, and 0.625 mg/mL solutions of **3**, respectively, dissolved in 1:1 DCM:MeOH to 6 mm Whatman #1 filter paper disks in 5 µL increments dropwise, allowing for

solvent evaporation between drops. Solvent control blank disks soaked in the equivalent volume 1:1 DCM:MeOH without **3** and dried were also included. One of each of these four disks was then applied to plates with one of 15 strains identified as actinomycetes by 16S sequencing alongside a single *B. thuringiensis* strain as a negative control. These were incubated at room temperature for 11 days. Zones of inhibition were measured as the mm diameter surrounding each paper disk.

A2.1.4 CITED LITERATURE.

1. Lomenick, B.; Hao, R.; Jonai, N.; Chin, R. M.; Aghajan, M.; Warburton, S.; Wang, J.; Wu, R. P.; Gomez, F.; Loo, J. A.; Wohlschlegel, J. A.; Vondriska, T. M.; Pelletier, J.; Herschman, H. R.; Clardy, J.; Clarke, C. F.; Huang, J. Target identification using drug affinity responsive target stability (DARTS). *Proc. Natl. Acad. Sci. U. S. A.* **2009**, *106*, 21984-21989.
2. Pai, M. Y.; Lomenick, B.; Hwang, H.; Schiestl, R.; McBride, W.; Loo, J. A.; Huang, J. Drug affinity responsive target stability (DARTS) for small molecule target identification. *Methods Mol. Biol.* **2015**, *1263*, 287-298.
3. Yano, T.; Kassovska-Bratinova, S.; Teh, J. S.; Winkler, J.; Sullivan, K.; Isaacs, A.; Schechter, N. M.; Rubin, H. Reduction of clofazimine by mycobacterial type 2 NADH:quinone oxidoreductase: a pathway for the generation of bactericidal levels of reactive oxygen species. *J. Biol. Chem.* **2011**, *286*, 10276-10287.
4. Hards, K.; Robson, J. R.; Berney, M.; Shaw, L.; Bald, D.; Koul, A.; Andries, K.; Cook, G. M. Bactericidal mode of action of bedaquiline. *J. Antimicrob. Chemother.* **2015**, *70*, 2028-2037.
5. Choi, K. P.; Kendrick, N.; Daniels, L. Demonstration that *fbiC* is required by *Mycobacterium bovis* BCG for coenzyme F_{420} and FO biosynthesis. *J. Bacteriol.* **2002**, *184*, 2420-2428.

A2.1.5 Reference spectra and figures.

Figure A16. Fraction library generation scheme.

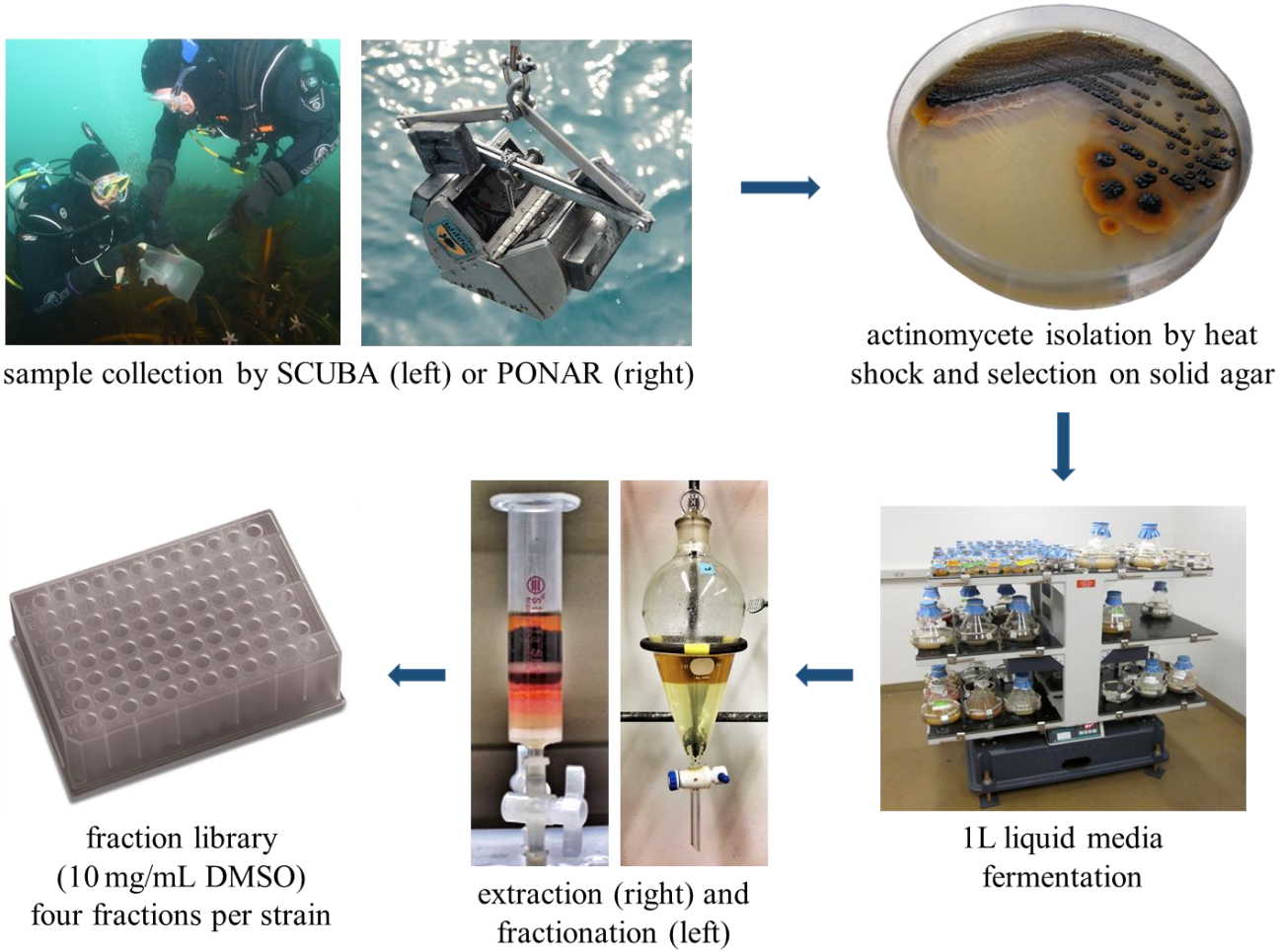

Figure A17. Activity of MtThyA, MtThyX, and HsThyA Enzymes in the Presence of 9 µM **3** and 9 µM 1843U89 (Positive Control).

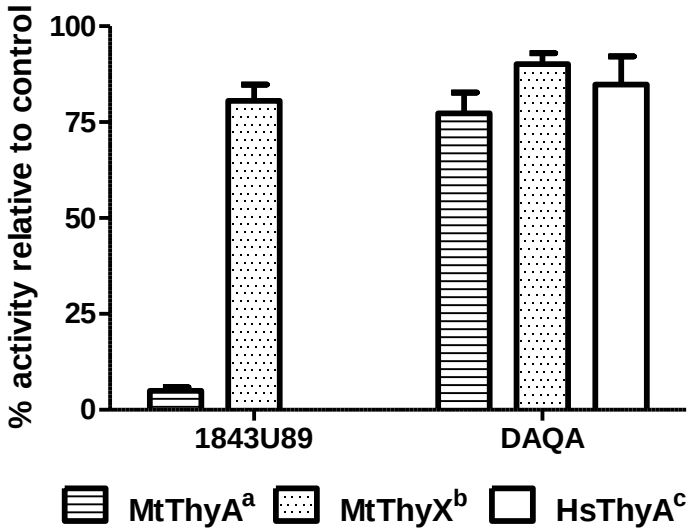

[a] *M. tuberculosis* thymidylate synthase A; [b] *M. tuberculosis* thymidylate synthase X; [c] human thymidylate synthase A

Figure A18. Purity of MtThyA, MtThyX, and HsThyA Enzymes.

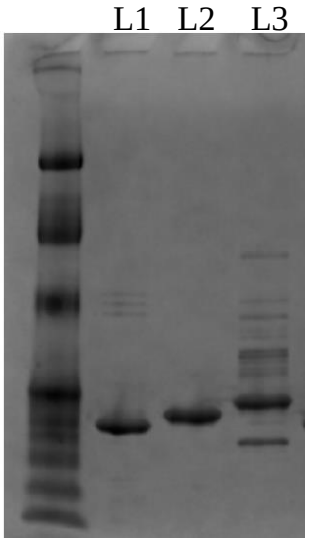

Lane 1: MtThyA
Lane 2: MtThyX
Lane 3: HsThyA

Figure A19. Concentration-response curves of **3** against *M. tuberculosis* anhydrotetracycline-inducible *thyA* and *thyX* overexpression mutants.

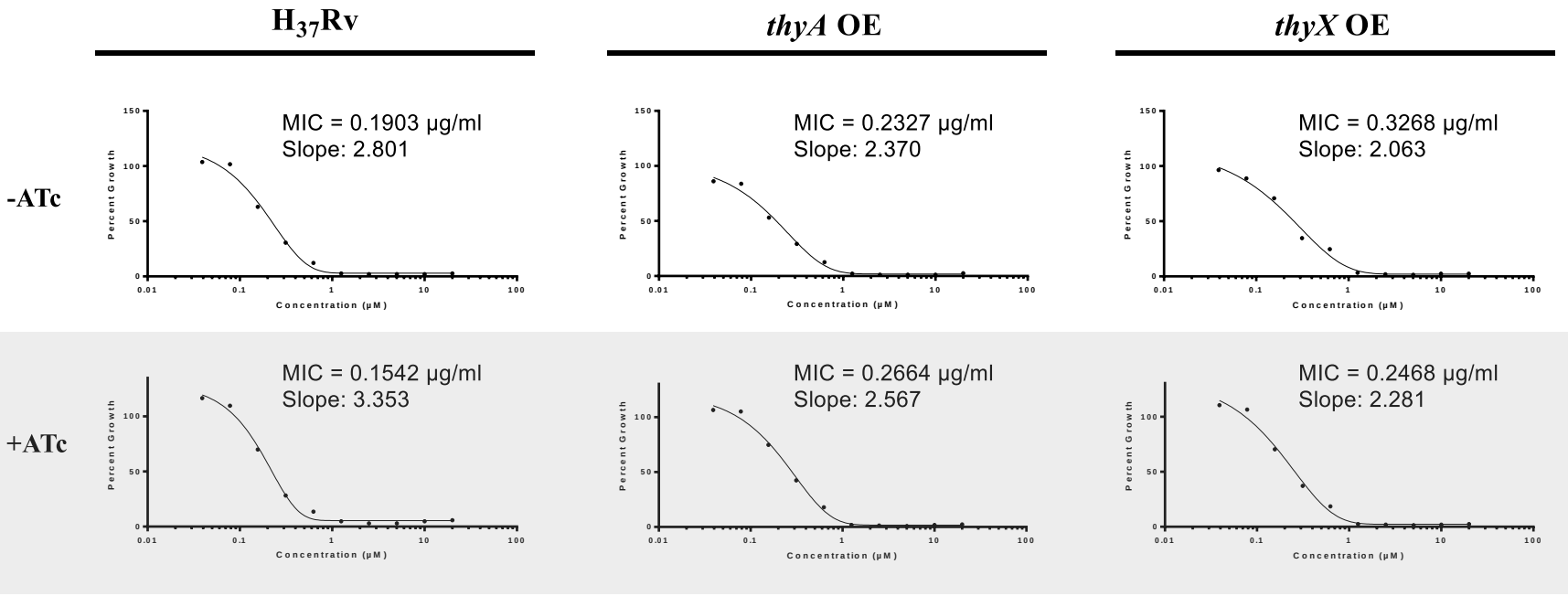

Figure A20. ^{1}H NMR spectrum (900 MHz) of **1** in $CDCl_3$–1% CF_3CO_2D.

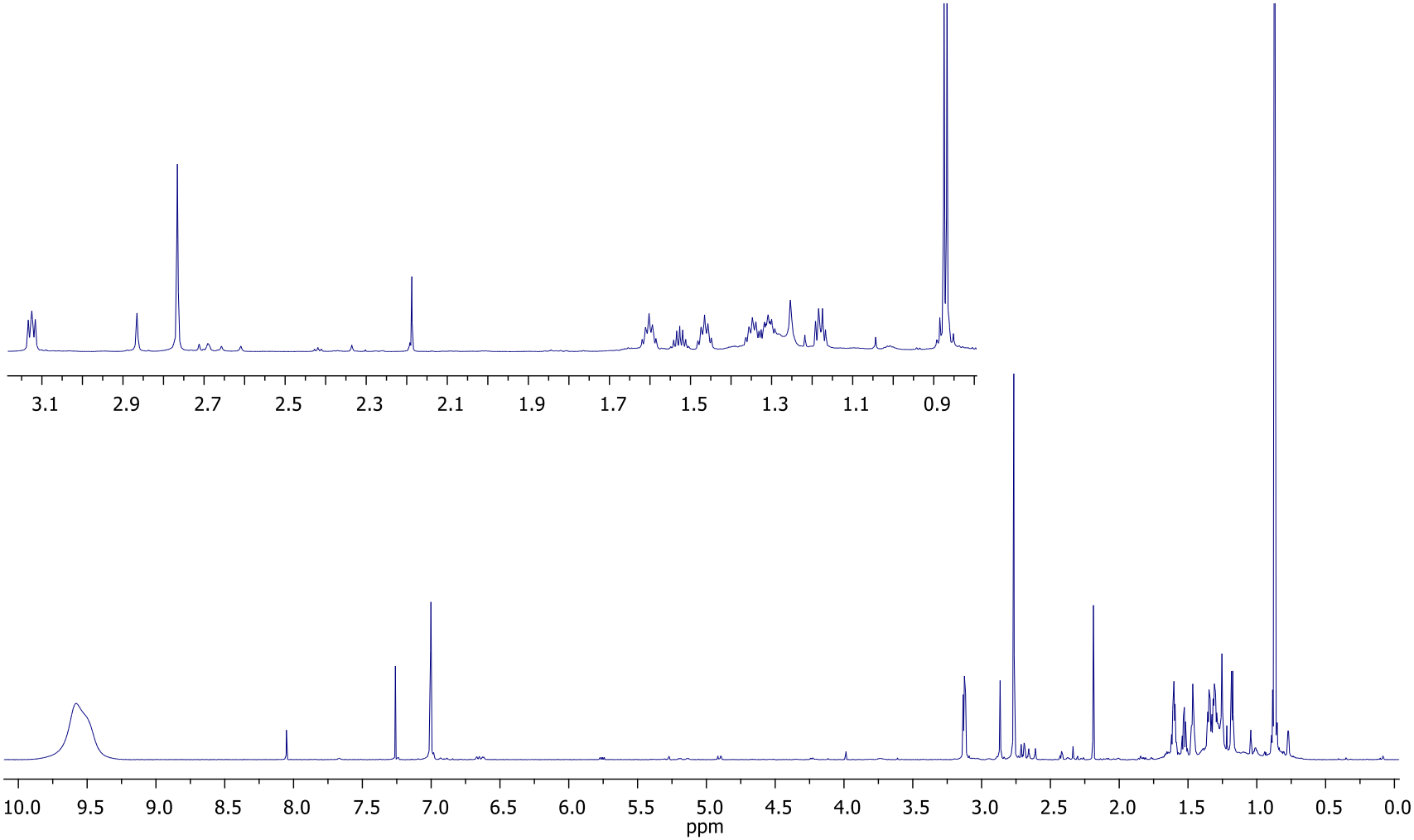

Figure A21. ^{13}C DEPTQ spectrum (226.2 MHz) of **1** in $CDCl_3$–1% CF_3CO_2D.

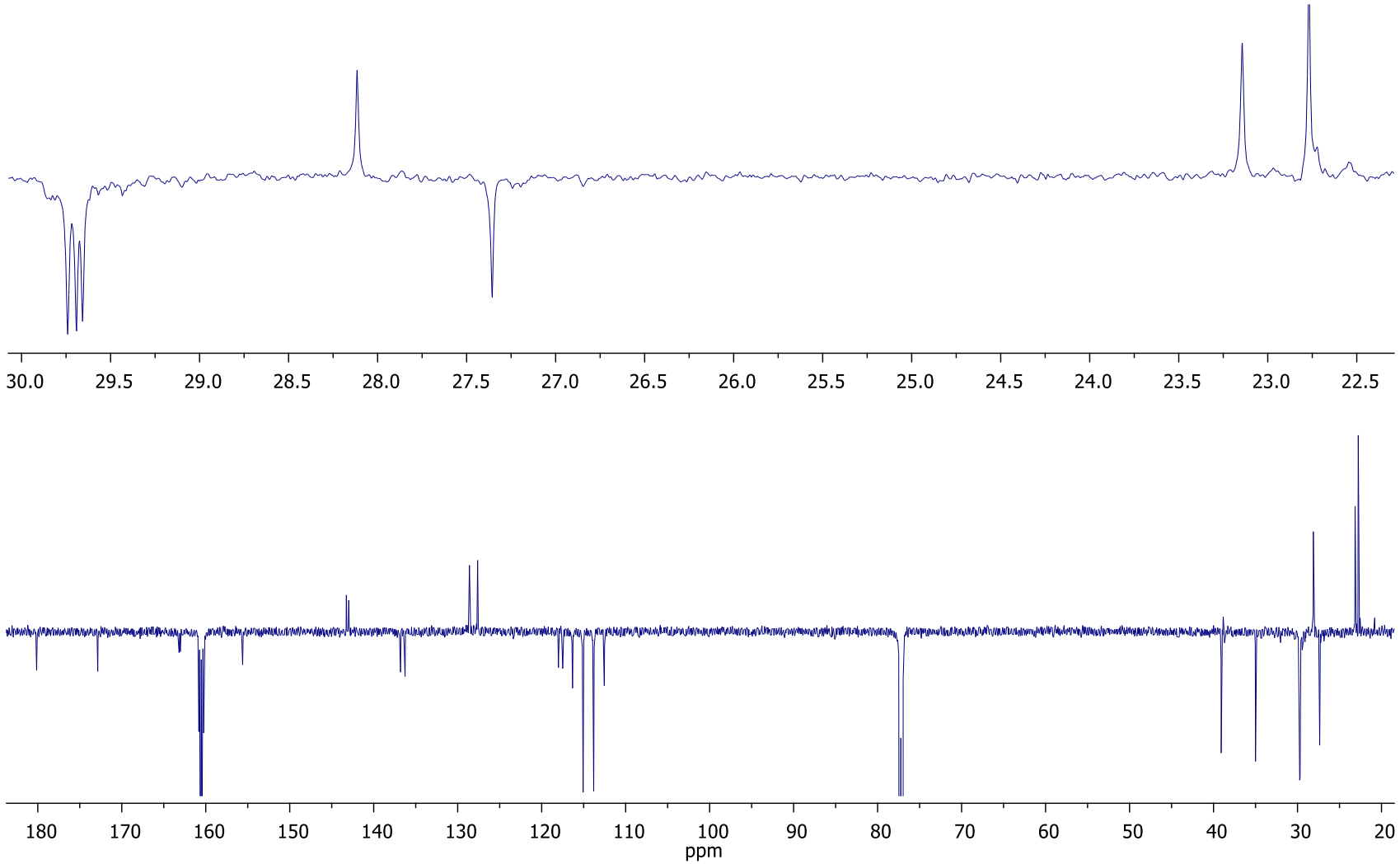

Figure A22. COSY spectrum (600 MHz) of **1** in $CDCl_3$–1% CF_3CO_2D.

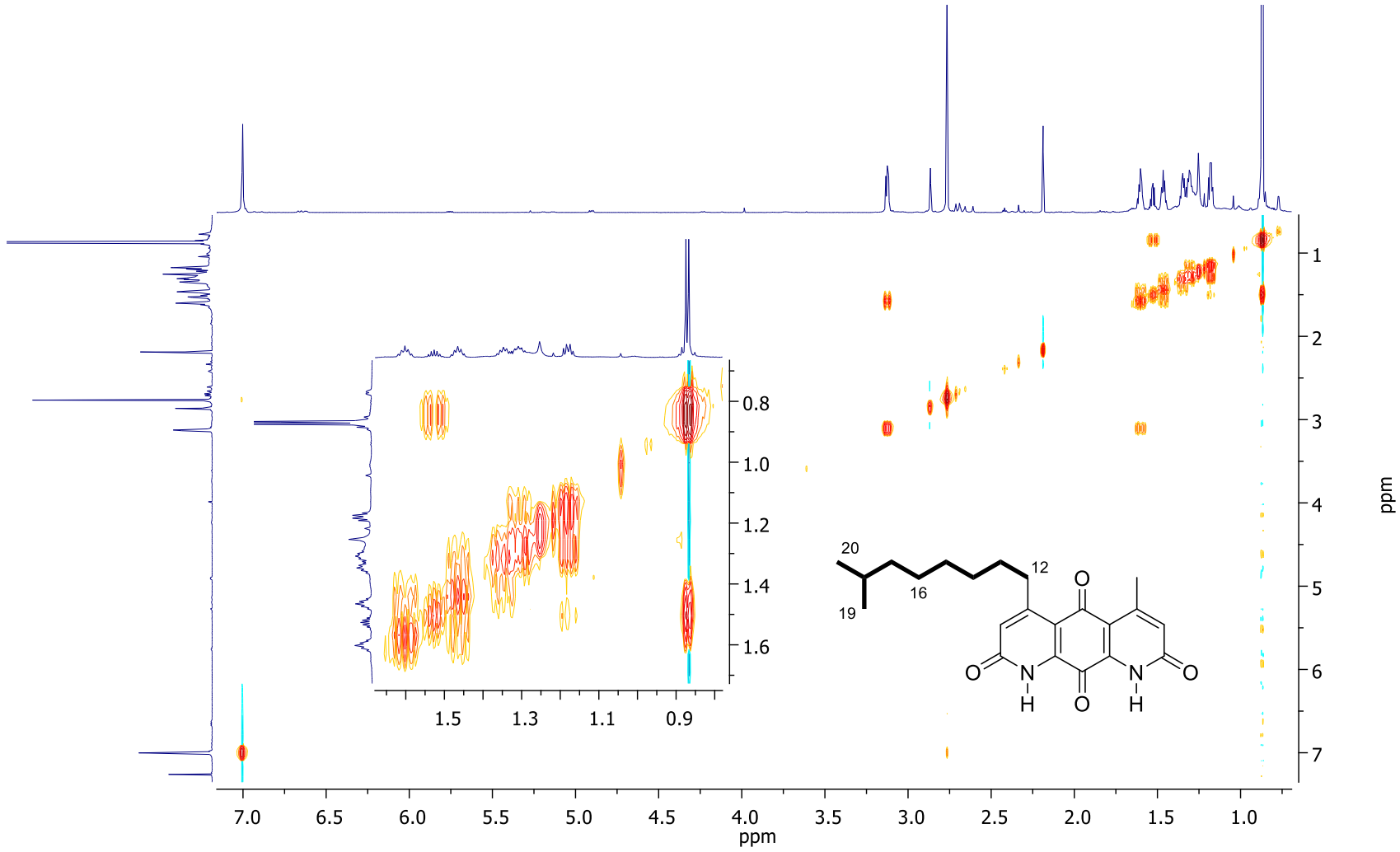

Figure A23. HMBC spectrum (600 MHz) of **1** in $CDCl_3$–1% CF_3CO_2D.

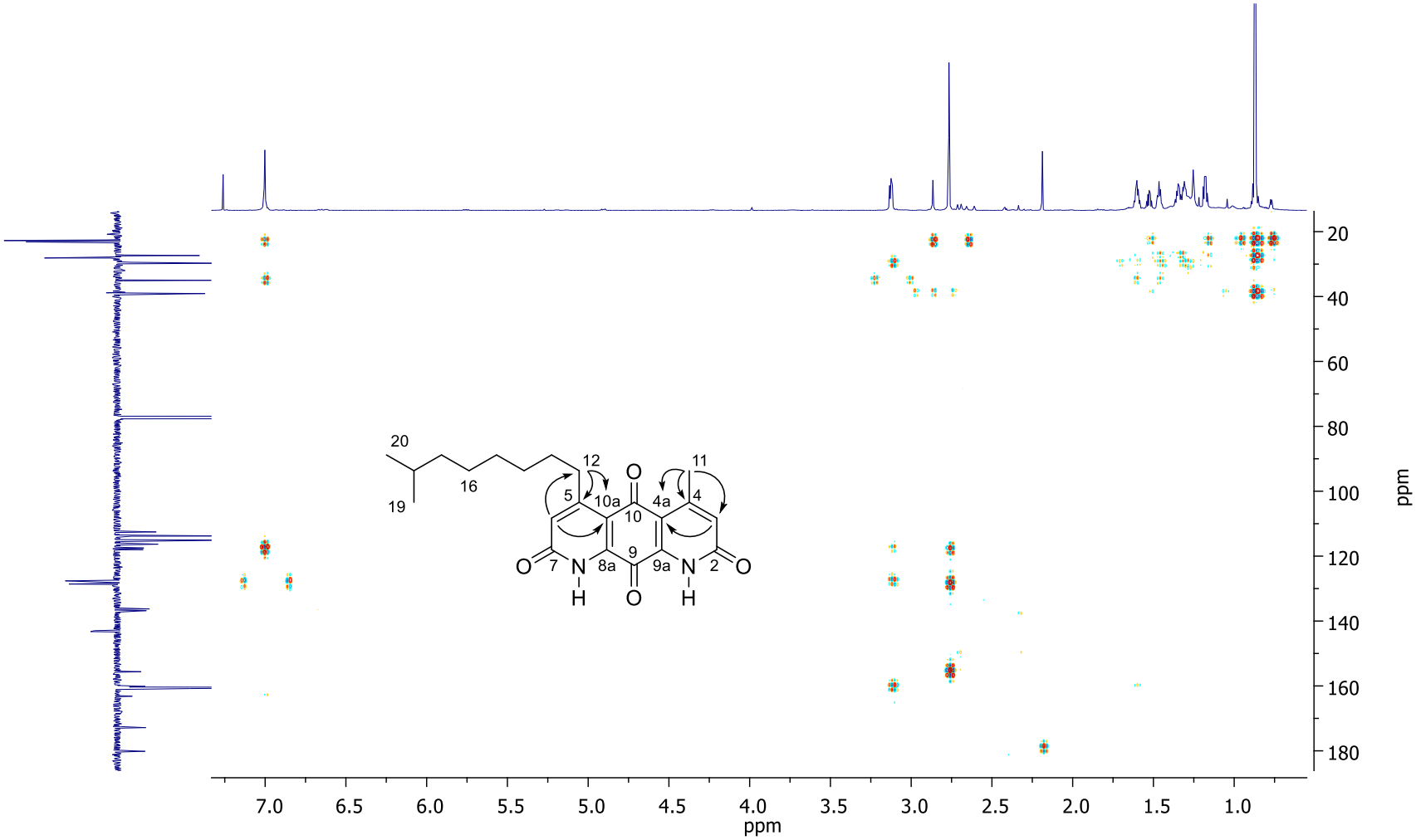

Figure A24. 1D-TOCSY spectra (600 MHz) of **1** in $CDCl_3$–1% CF_3CO_2D.

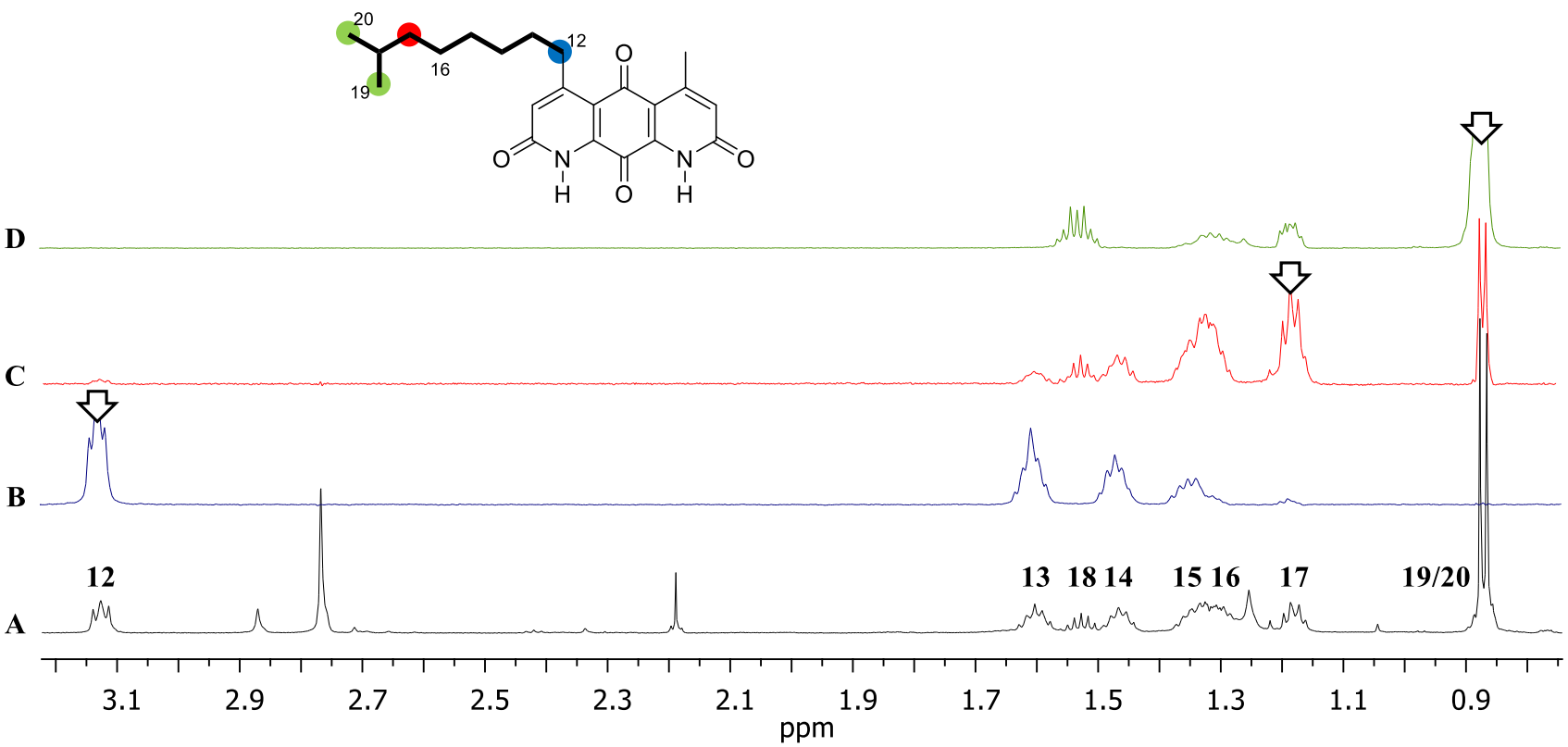

Arrows indicate irradiated resonances. (A) Expansion of ^{1}H NMR spectrum (600 MHz) of **1**; (B) Expansion of 1D-TOCSY spectrum of **1** (irradiation of δ_H 3.13); (C) Expansion of 1D-TOCSY spectrum of **1** (irradiation of δ_H 1.19); (D) Expansion of 1D-TOCSY spectrum of **1** (irradiation of δ_H 0.87).

Figure A25. Expanded HR-ESI-IT-TOF mass spectra of **1**.

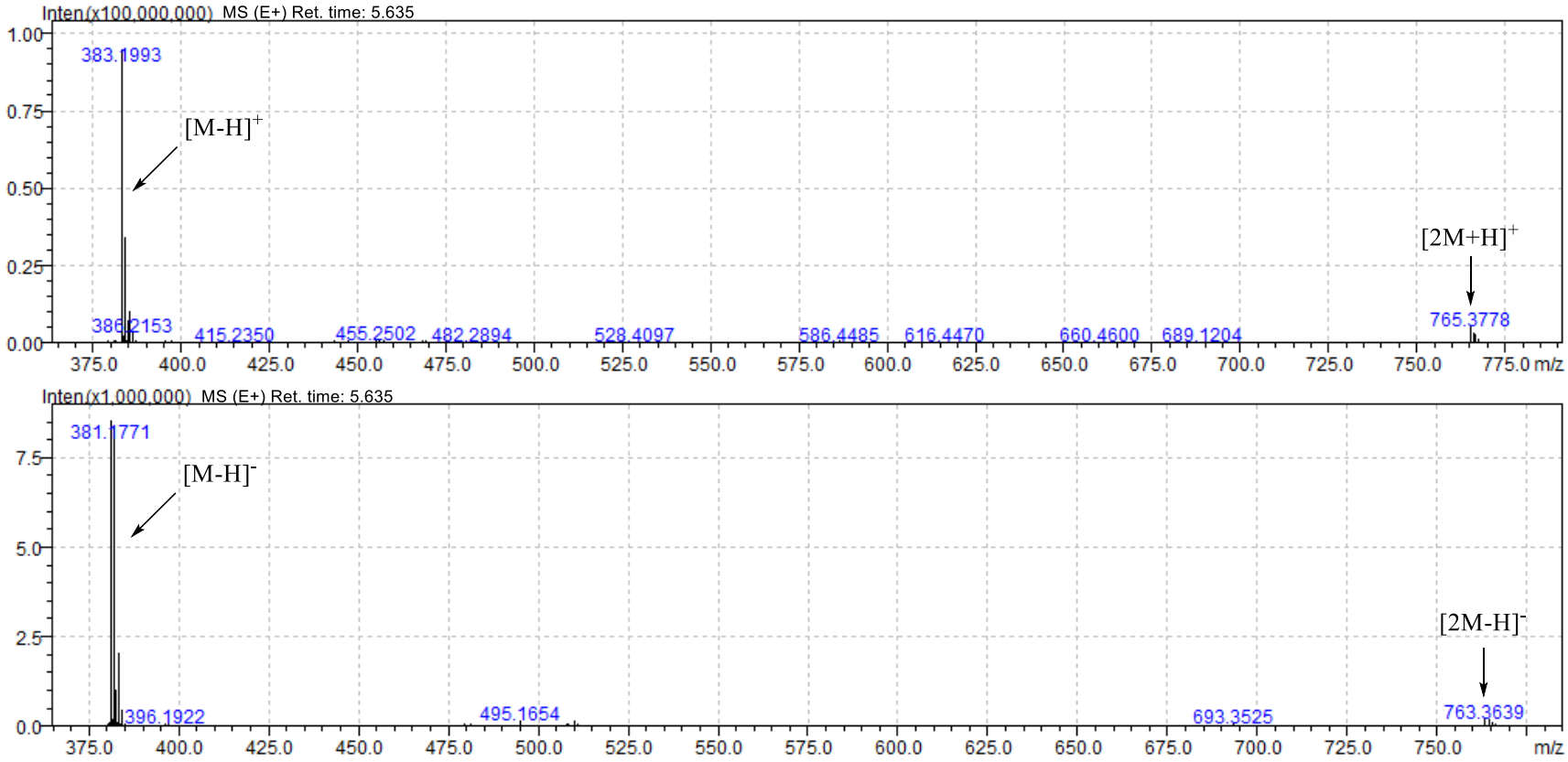

HR-ESI-IT-TOF MS *m/z* 383.1993 $[M + H]^+$ (calcd. for $C_{22}H_{27}N_2O_4$: 383.1971), *m/z* 381.1771 $[M - H]^-$ (calcd. for $C_{22}H_{25}N_2O_4$: 381.1820), *m/z* 765.3778 $[2M + H]^+$ (calcd. for $C_{44}H_{53}N_4O_8$: 765.3863), and *m/z* 763.3639 $[2M - H]^-$ (calcd. for $C_{44}H_{51}N_4O_8$: 763.3712).

Figure A26. UV spectrum of **1** in methanol.

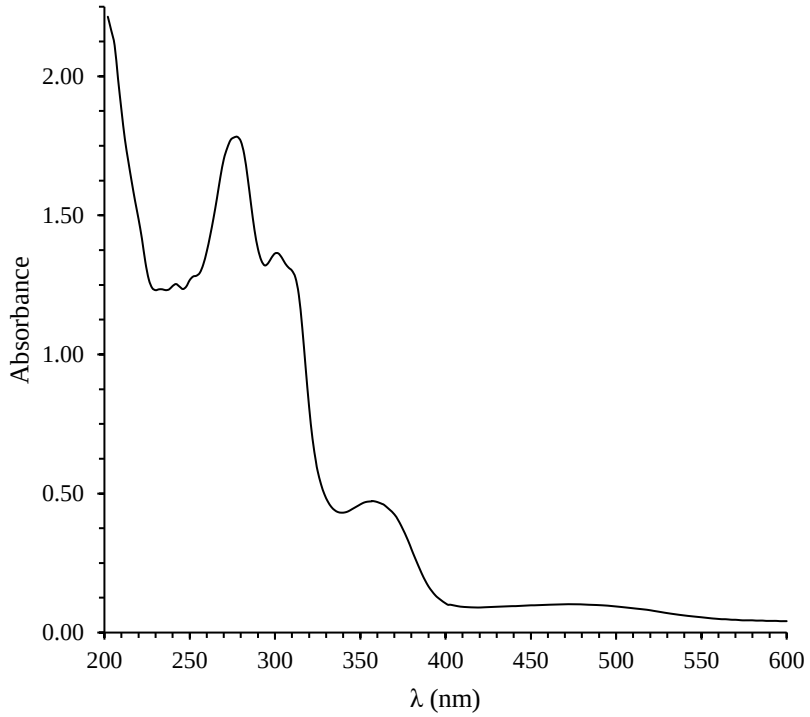

UV (MeOH) λ_{max} (log ε) = 278 (3.83), 301 (3.72), 357 (3.26) and a broad absorption with maximum at 472 (2.59) nm.

Figure A27. ^{1}H NMR spectrum (900 MHz) of **2** in $CDCl_3$–1% CF_3CO_2D.

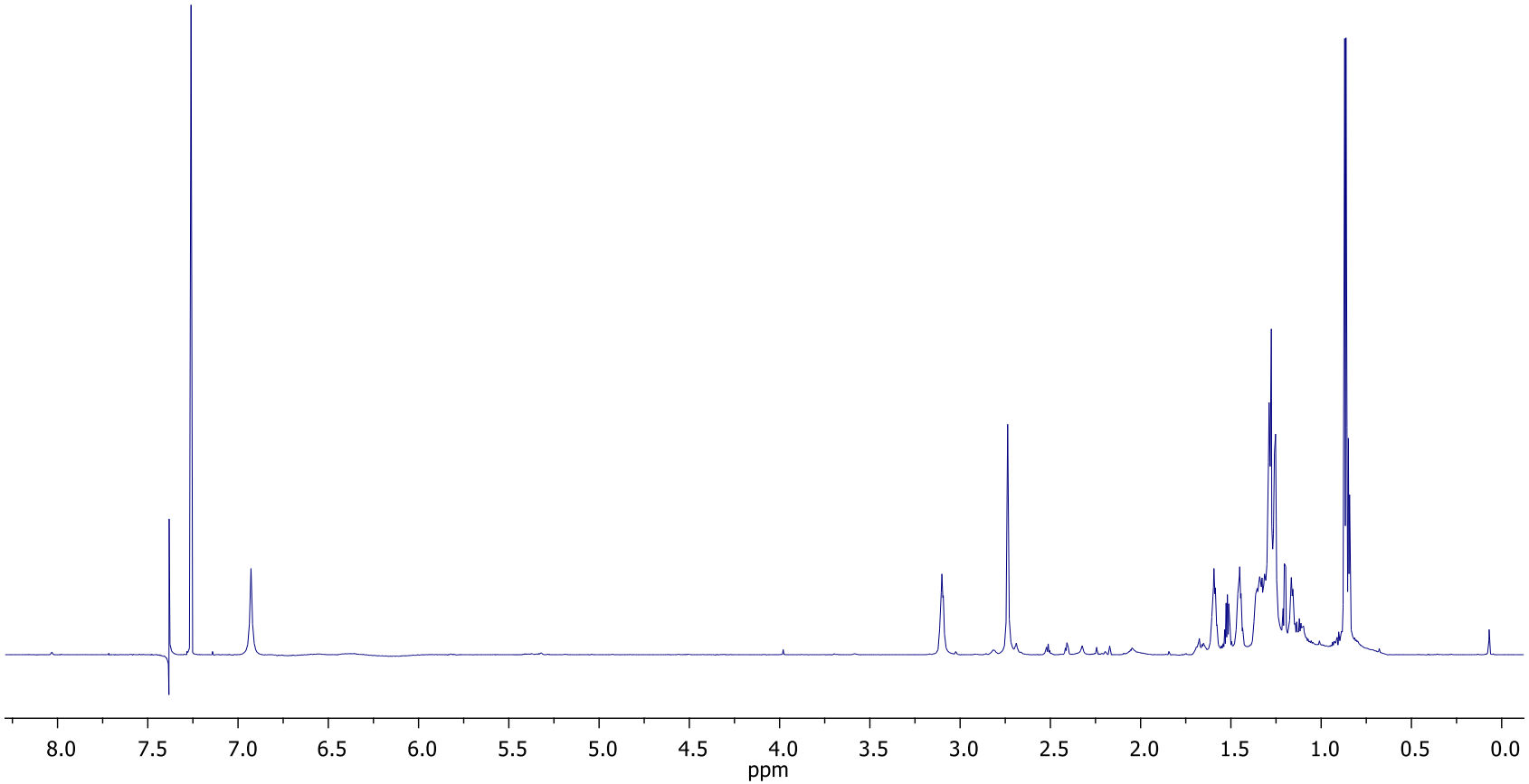

Figure A28. ^{13}C DEPTQ spectrum (226.2 MHz) of **2** in $CDCl_3$–1% CF_3CO_2D.

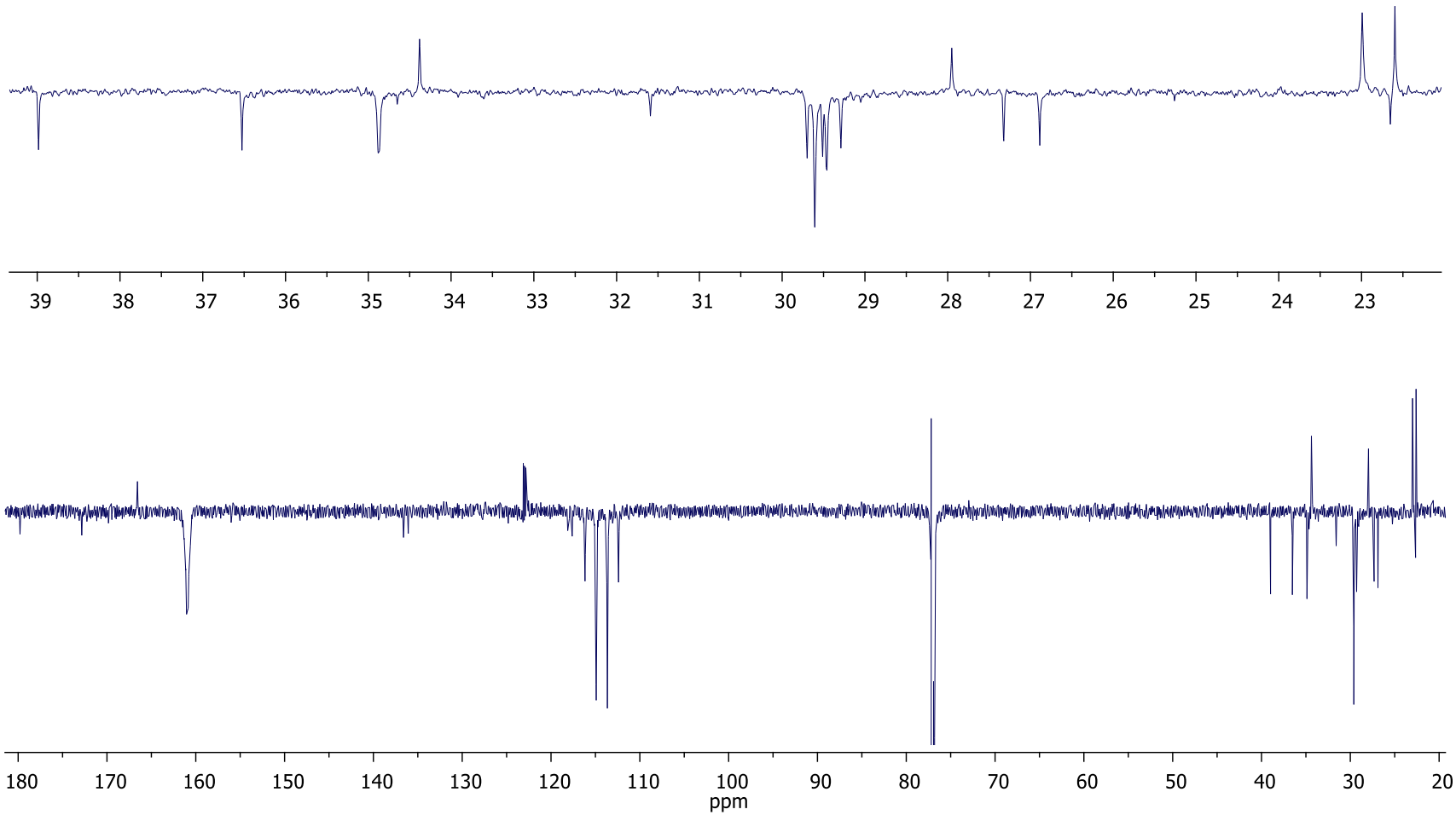

Figure A29. COSY spectrum (600 MHz) of **2** in $CDCl_3$–1% CF_3CO_2D.

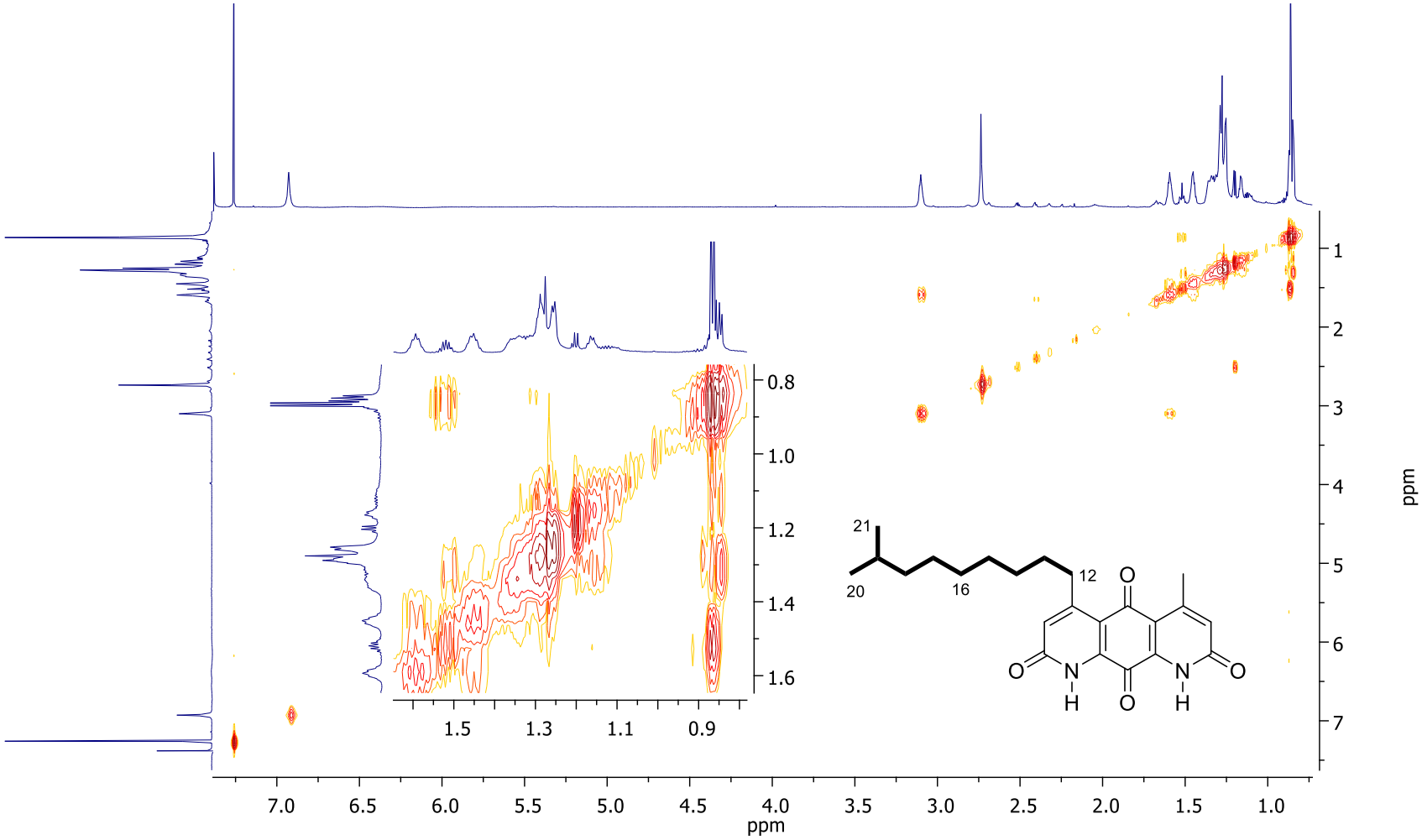

Figure A30. HMBC spectrum (600 MHz) of **2** $CDCl_3$–1% CF_3CO_2D.

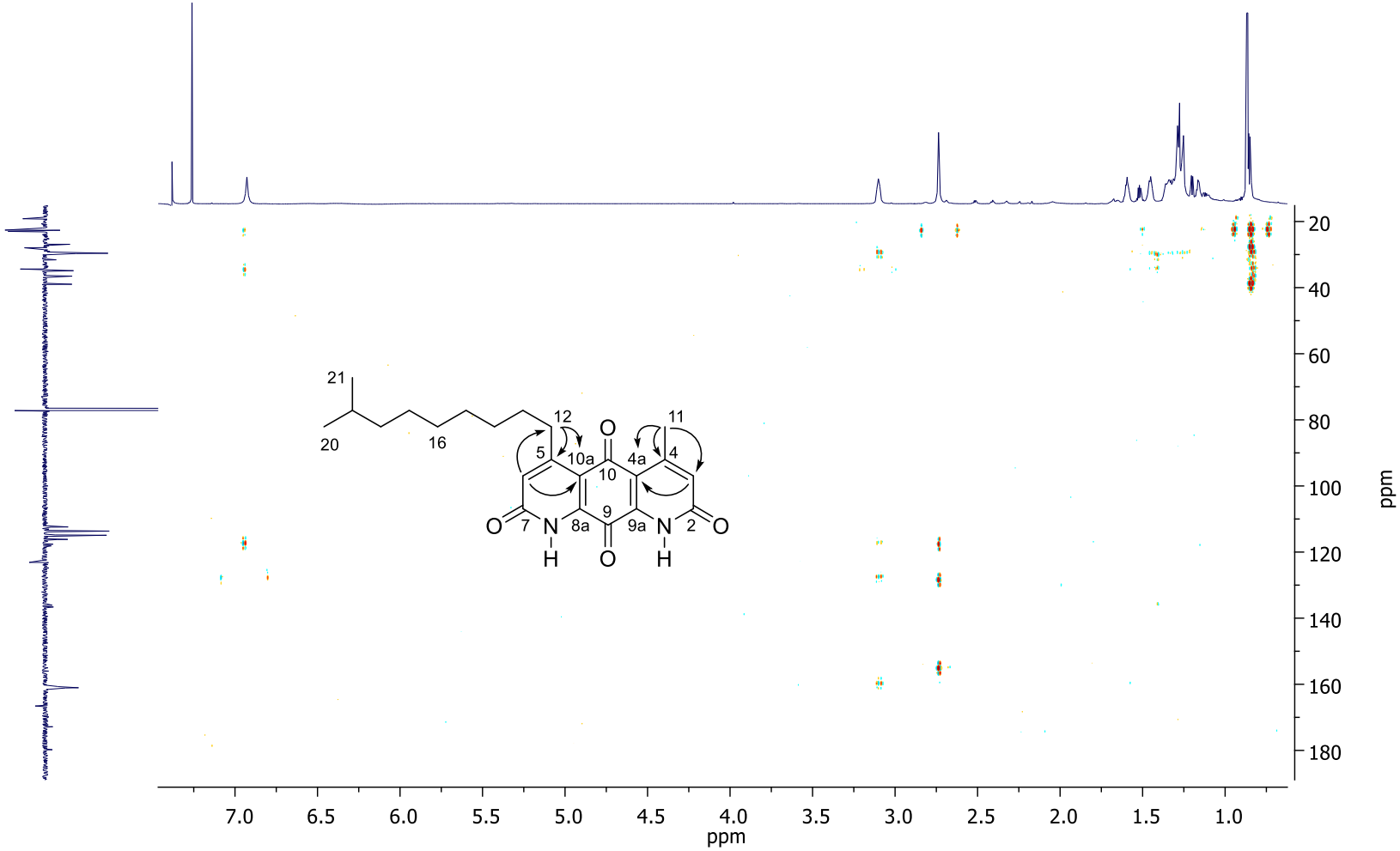

Figure A31. 1D-TOCSY spectra (600 MHz) of **2** in $CDCl_3$–1% CF_3CO_2D.

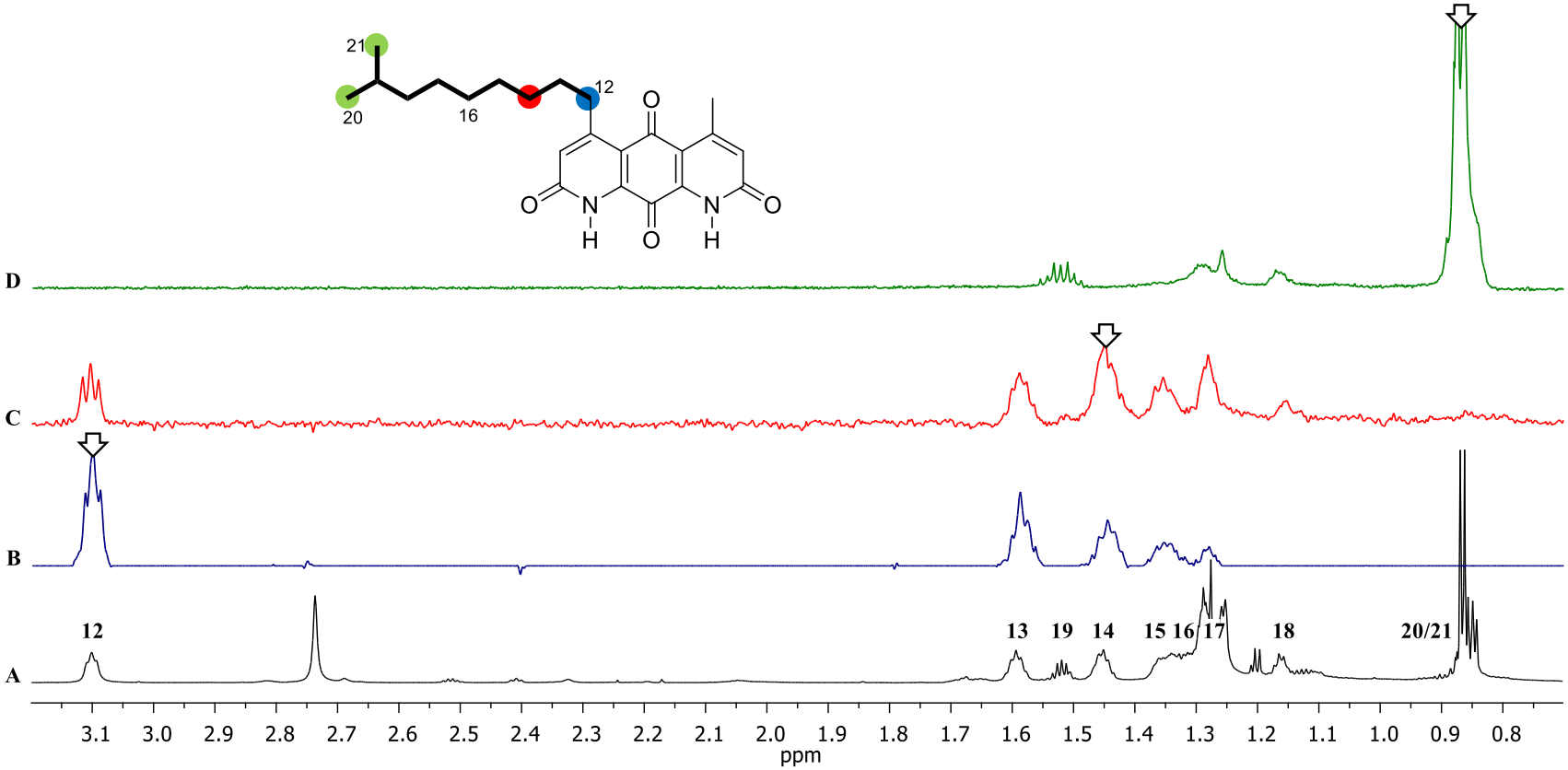

Arrows indicate irradiated resonances. (A) Expansion of ^{1}H NMR spectrum (600 MHz) of **2**; (B) Expansion of 1D-TOCSY spectrum of **2** (irradiation of δ_H 3.10); (C) Expansion of 1D-TOCSY spectrum of **2** (irradiation of δ_H 1.45); (D) Expansion of 1D-TOCSY spectrum of **2** (irradiation of δ_H 0.86).

Figure A32. Expanded HR-ESI-IT-TOF mass spectra of **2**.

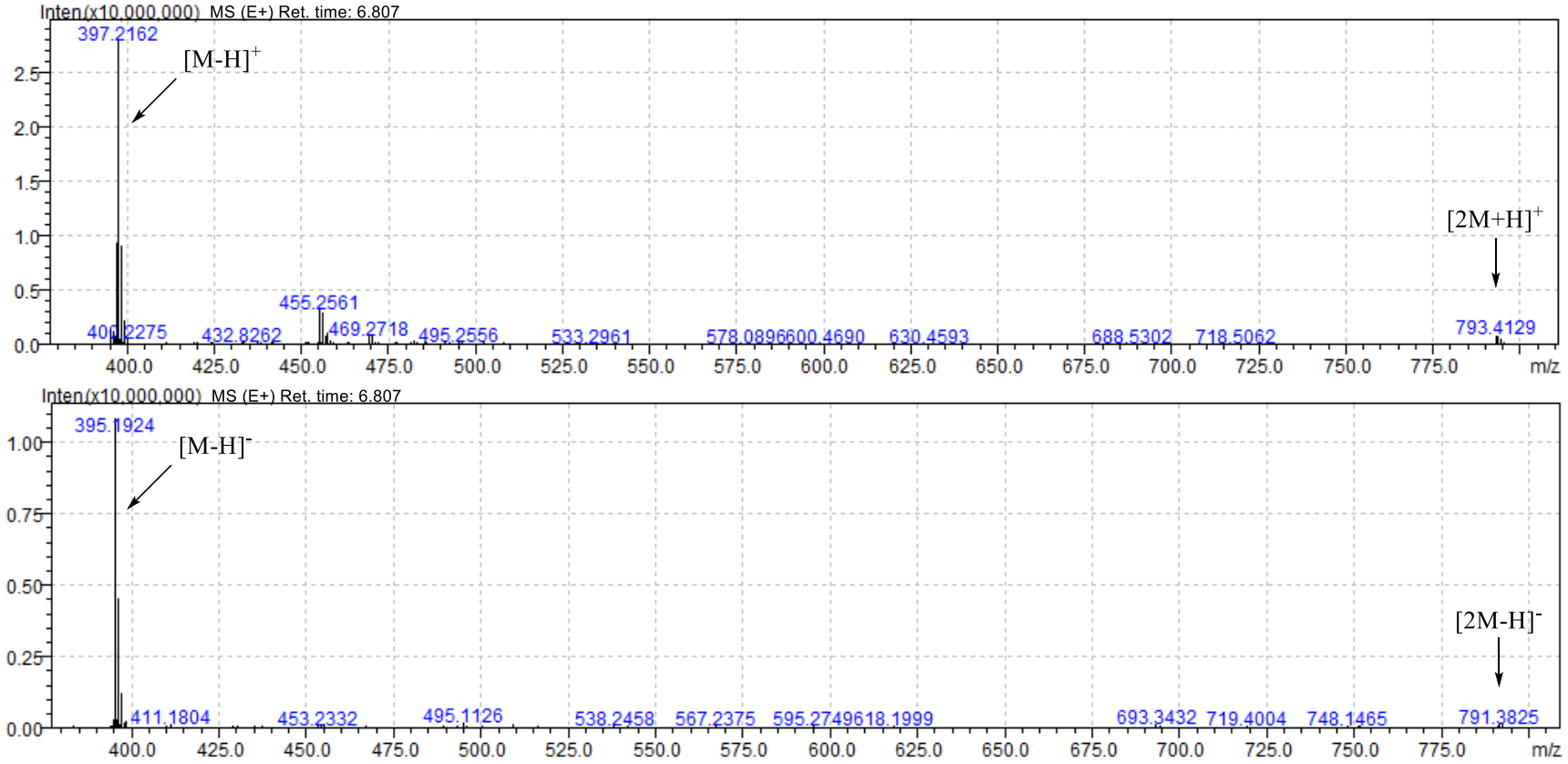

HR-ESI-IT-TOF MS *m/z* 397.2162 $[M + H]^+$ (calcd. for $C_{23}H_{29}N_2O_4$: 397.2127), *m/z* 395.1924 $[M - H]^-$ (calcd. for $C_{23}H_{27}N_2O_4$: 395.1976), *m/z* 793.4129 $[2M + H]^+$ (calcd. for $C_{46}H_{57}N_4O_8$: 793.4176), and *m/z* 791.3825 $[2M - H]^-$ (calcd. for $C_{46}H_{55}N_4O_8$: 791.4025).

Figure A33. UV spectrum of **2** in methanol.

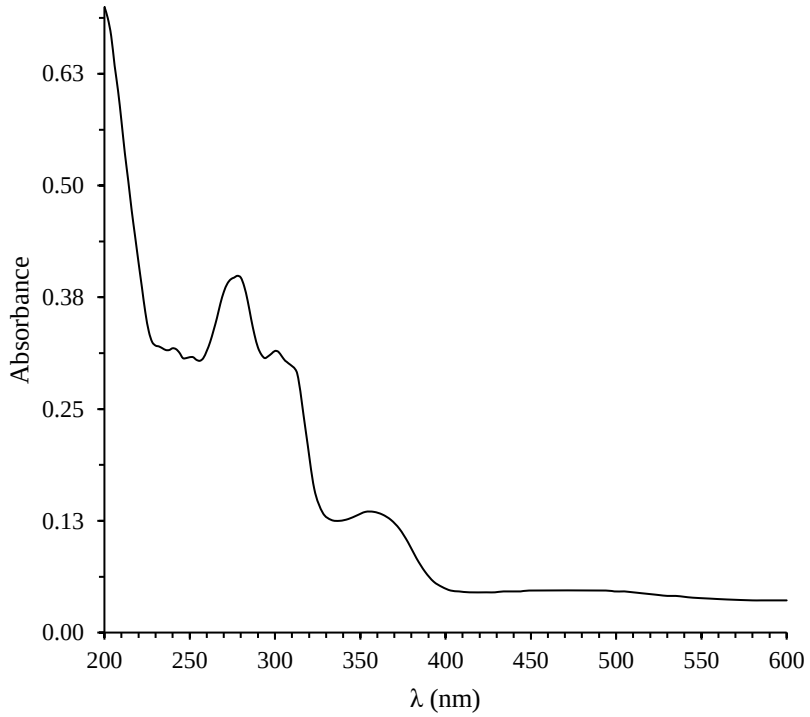

UV (MeOH) λ_{max} (log ε) = 278 (3.37), 300 (3.26), 356 (2.90) and a broad absorption with maximum at 472 (2.44) nm.

Figure A34. Optimized diazaquinomycin total synthesis.

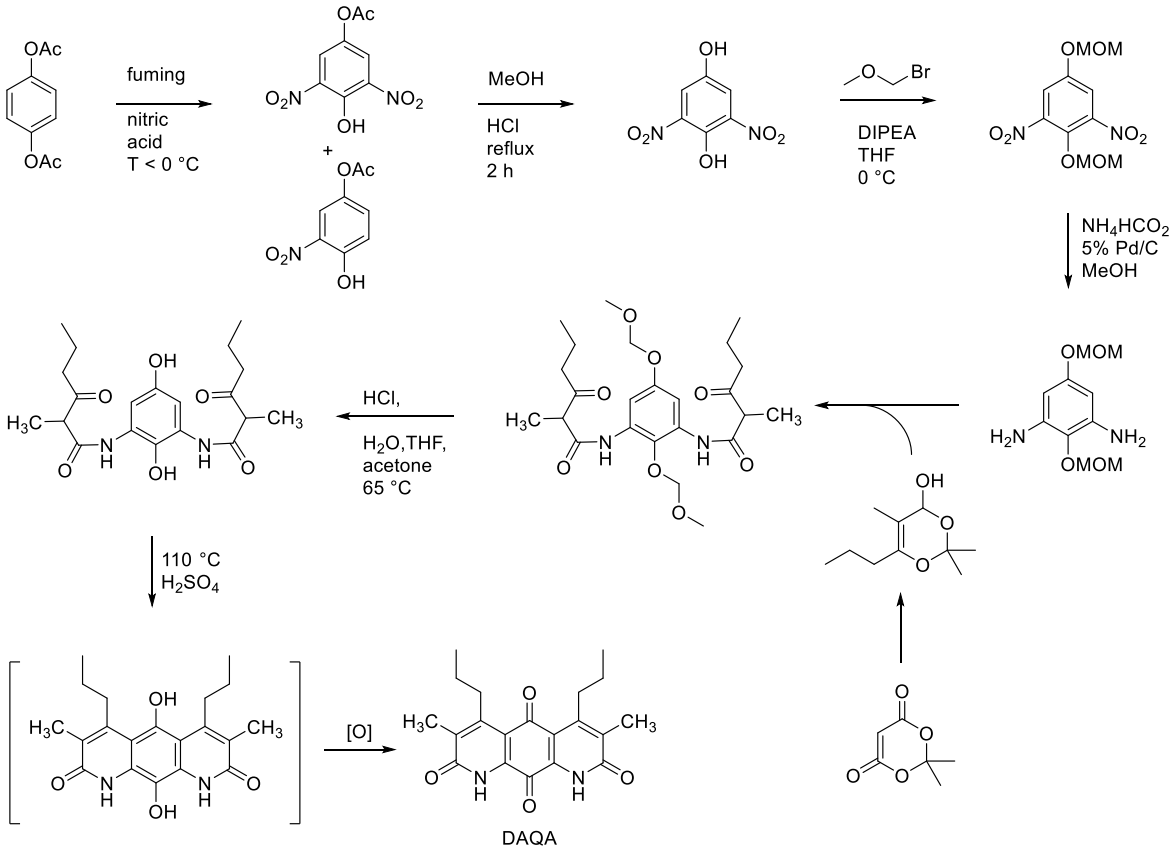

Figure A35. Expansion of ^{1}H NMR spectrum (600 MHz) of **6** in $CDCl_3$.

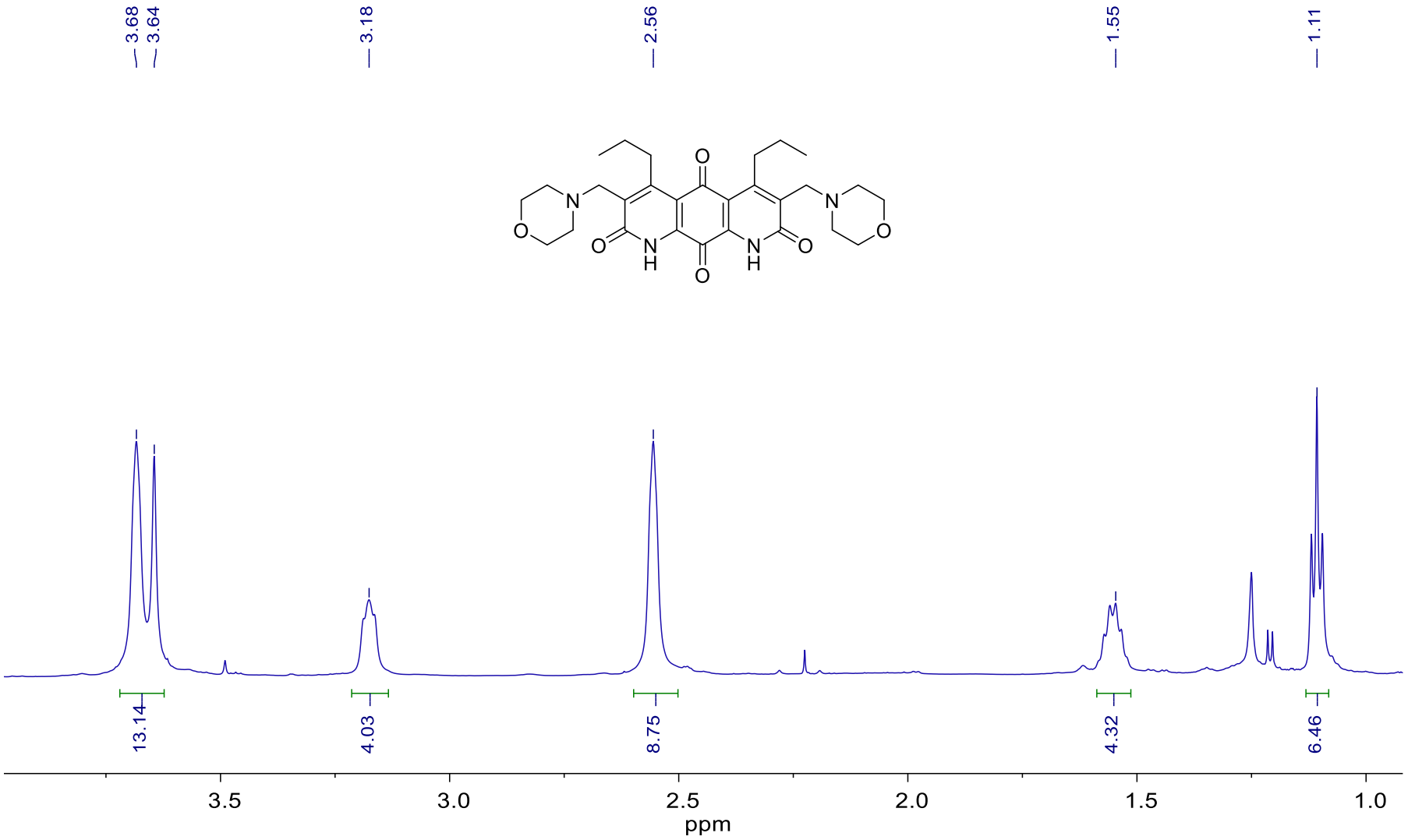

Figure A36. Expansion of ^{1}H NMR spectrum (600 MHz) of **9** in $CDCl_3$.

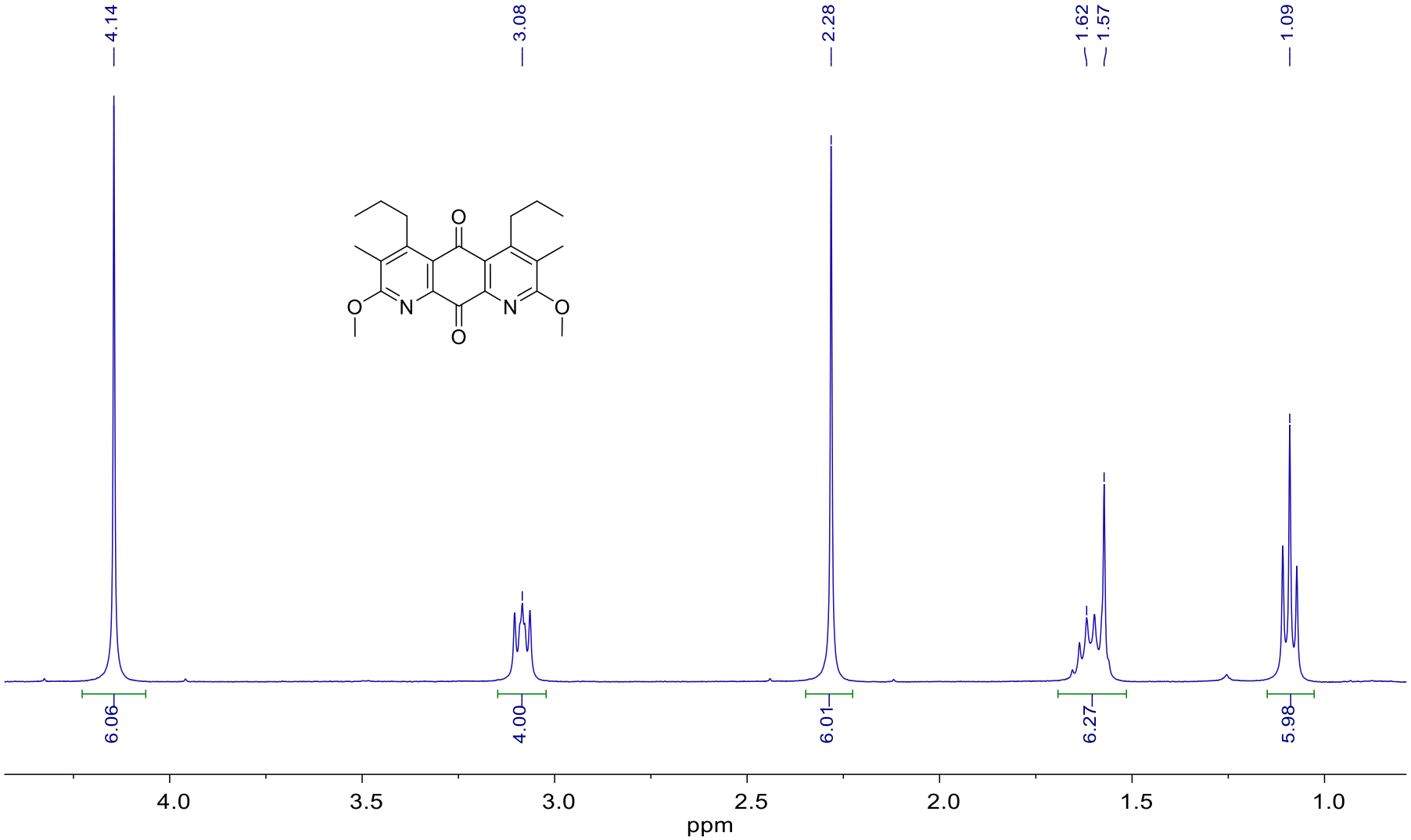

Figure A37. Expansion of ^{1}H NMR spectrum (600 MHz) of **10** in $CDCl_3$.

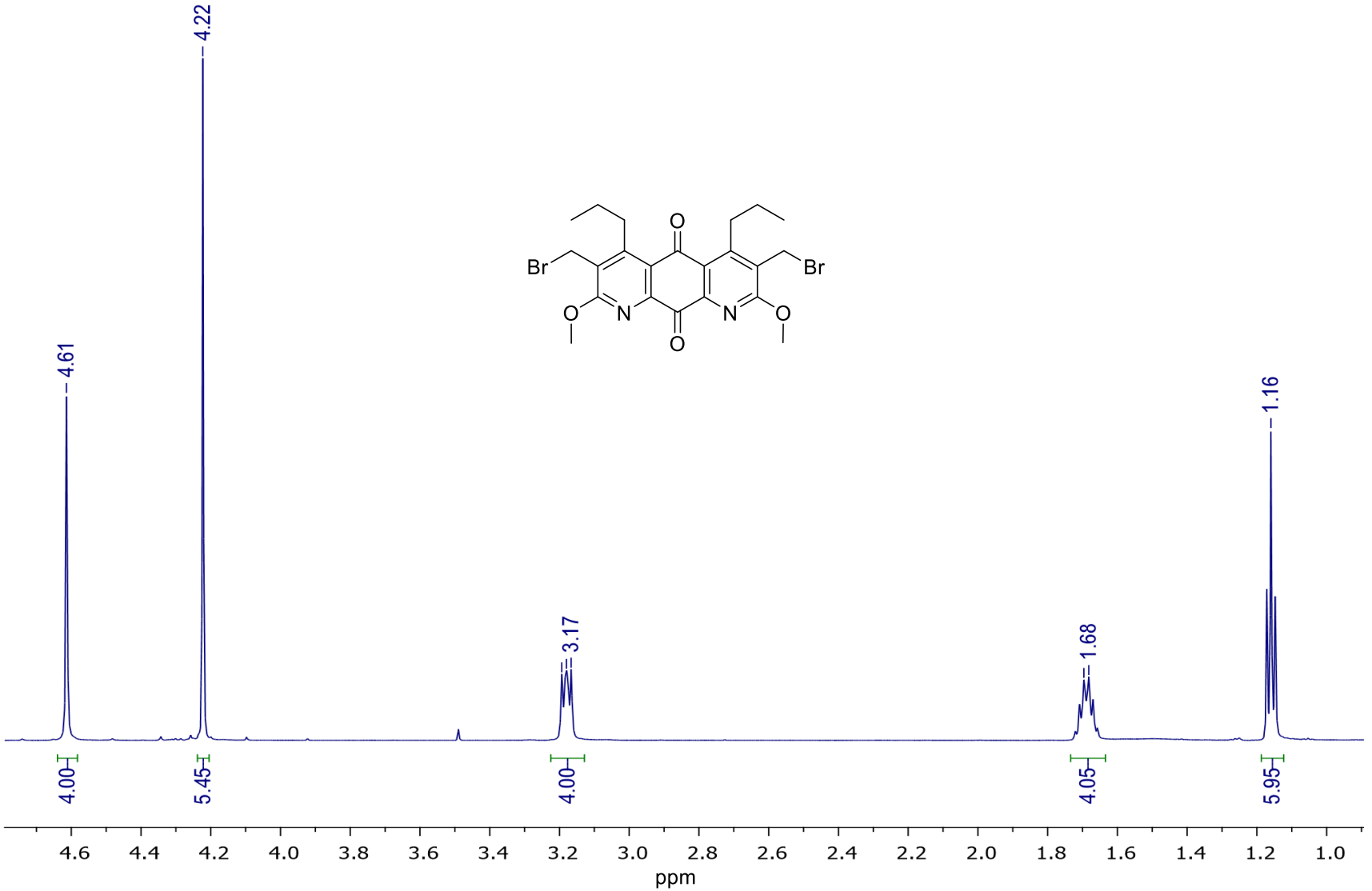

Figure A38. Expansion of ^{1}H NMR spectrum (600 MHz) of **11** in $CDCl_3$.

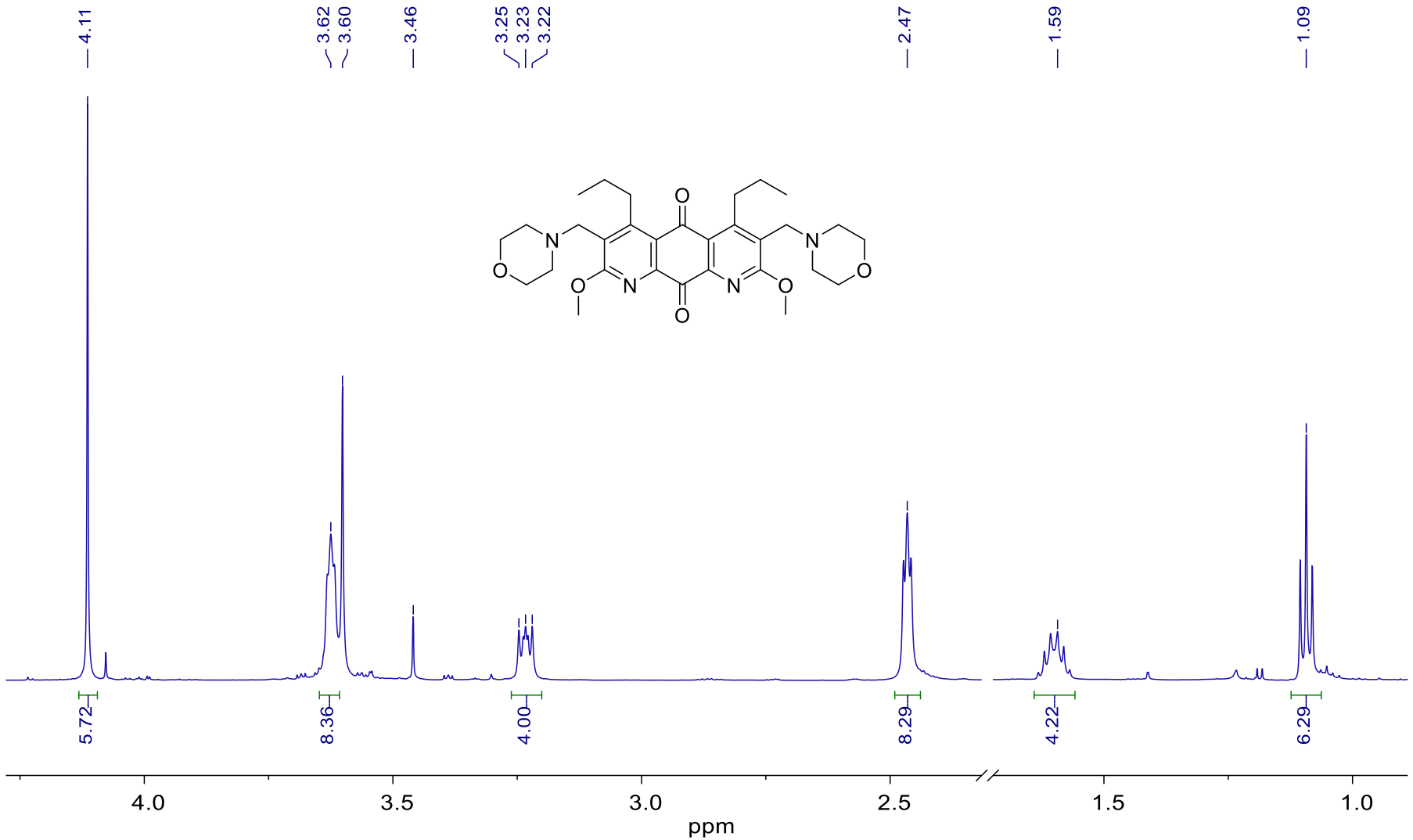

Figure A39. Expansion of ^{1}H NMR spectrum (600 MHz) of **7** in $CDCl_3$.

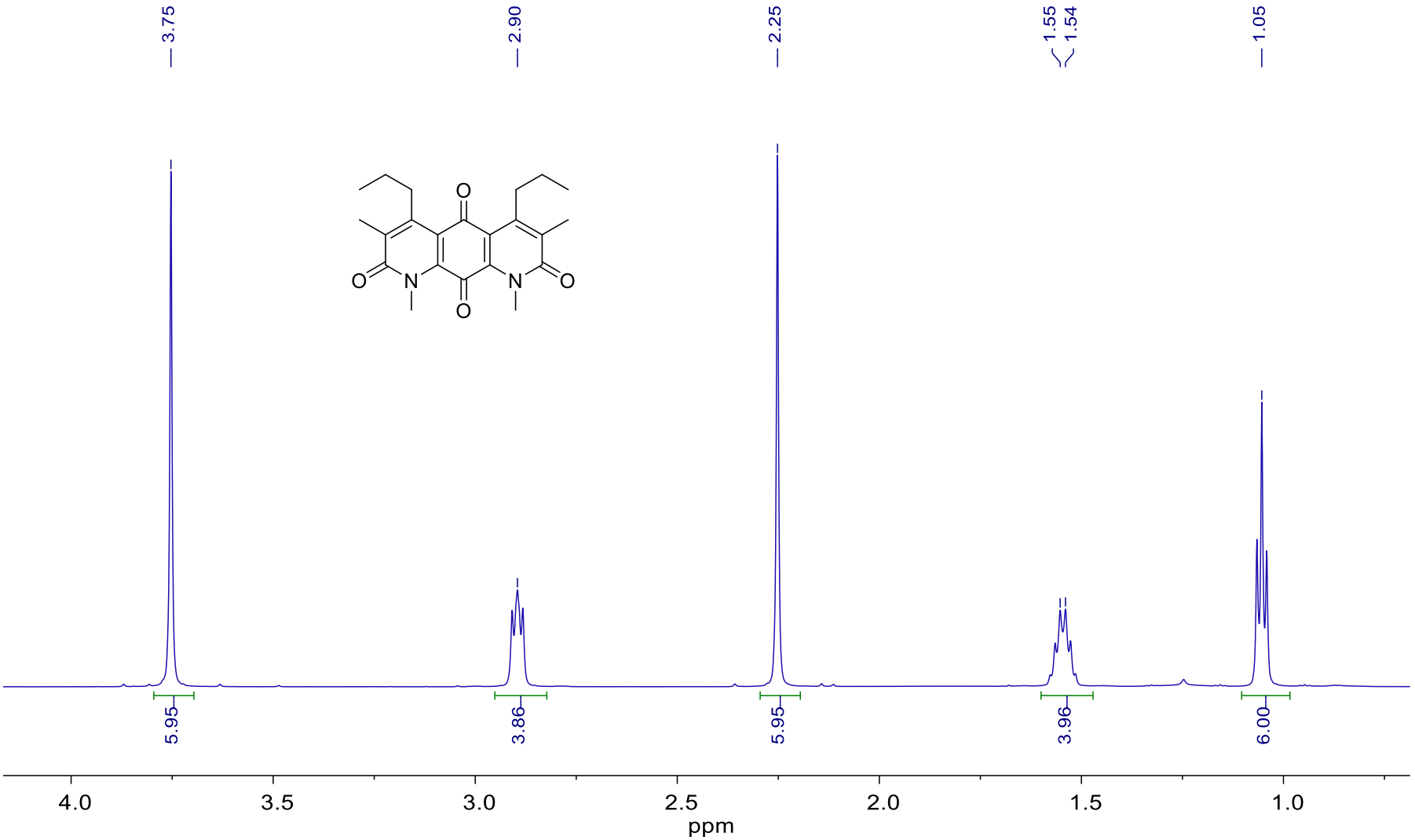

Figure A40. Expansion of ^{1}H NMR spectrum (600 MHz) of **8** in $CDCl_3$.

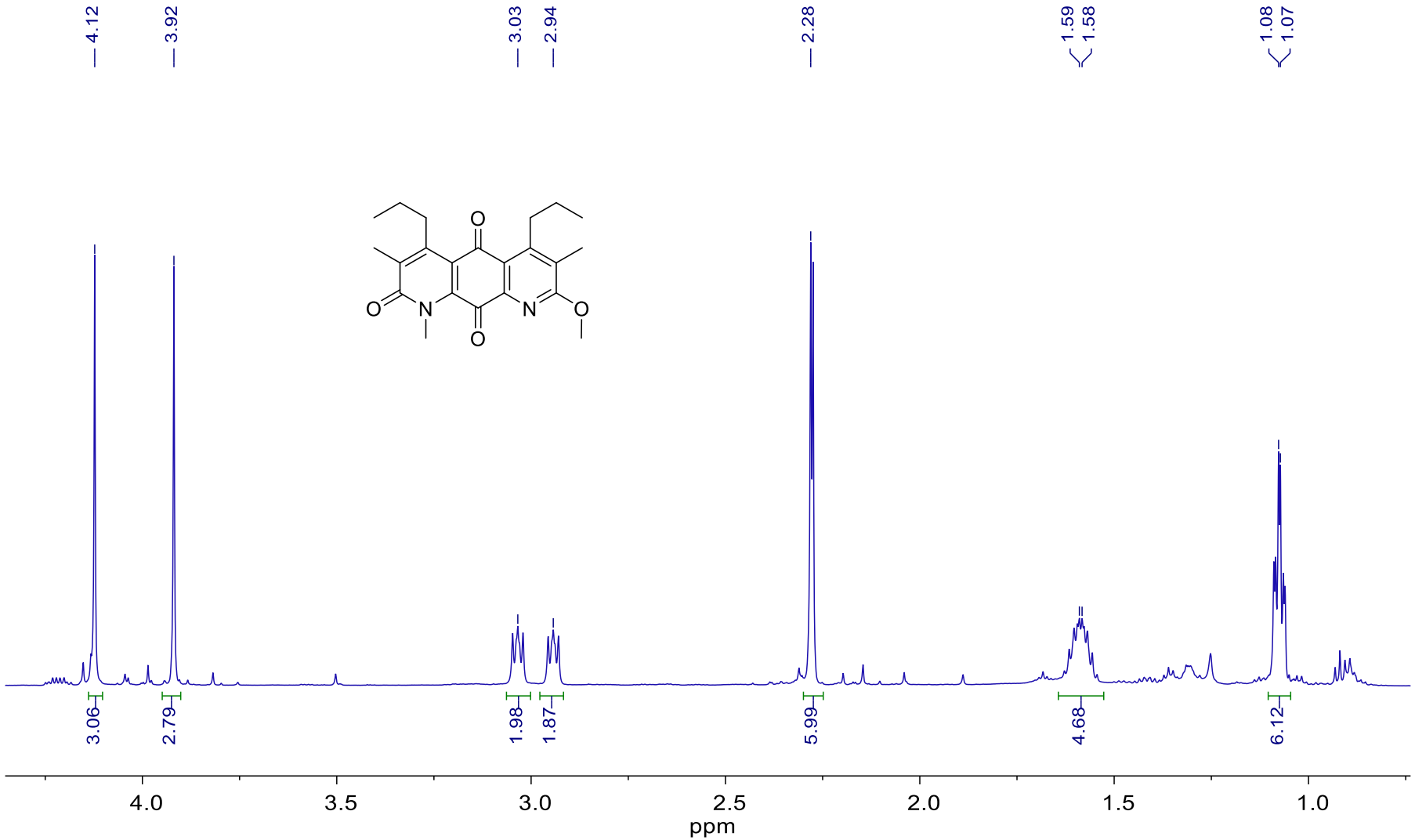

Figure A41. Plasmid maps for pCom8-PFR1500, pCom8-PFR1500L, and pBTL10.

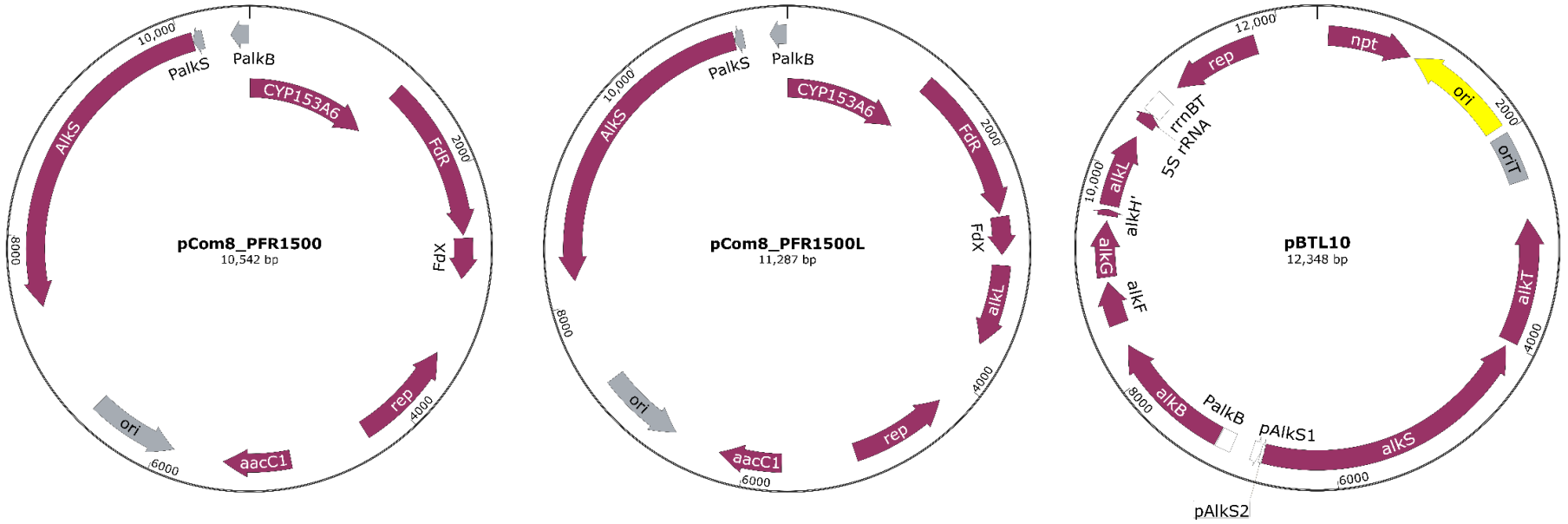

Figure A42. pCOM8 PFR1500 transformant extract ion chromatograms.

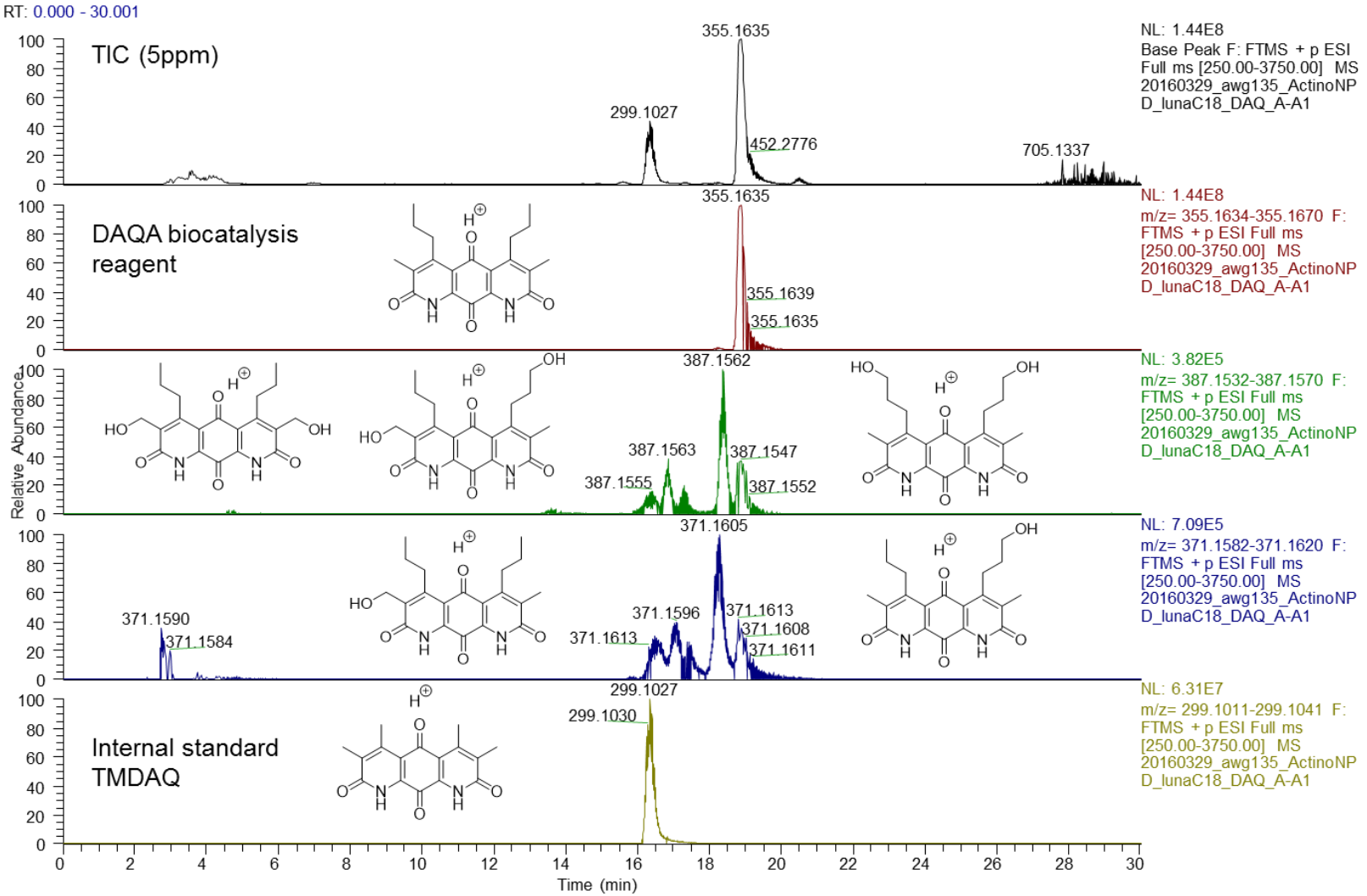

Figure A43. Unreacted synthetic DAQA negative control ion chromatograms.

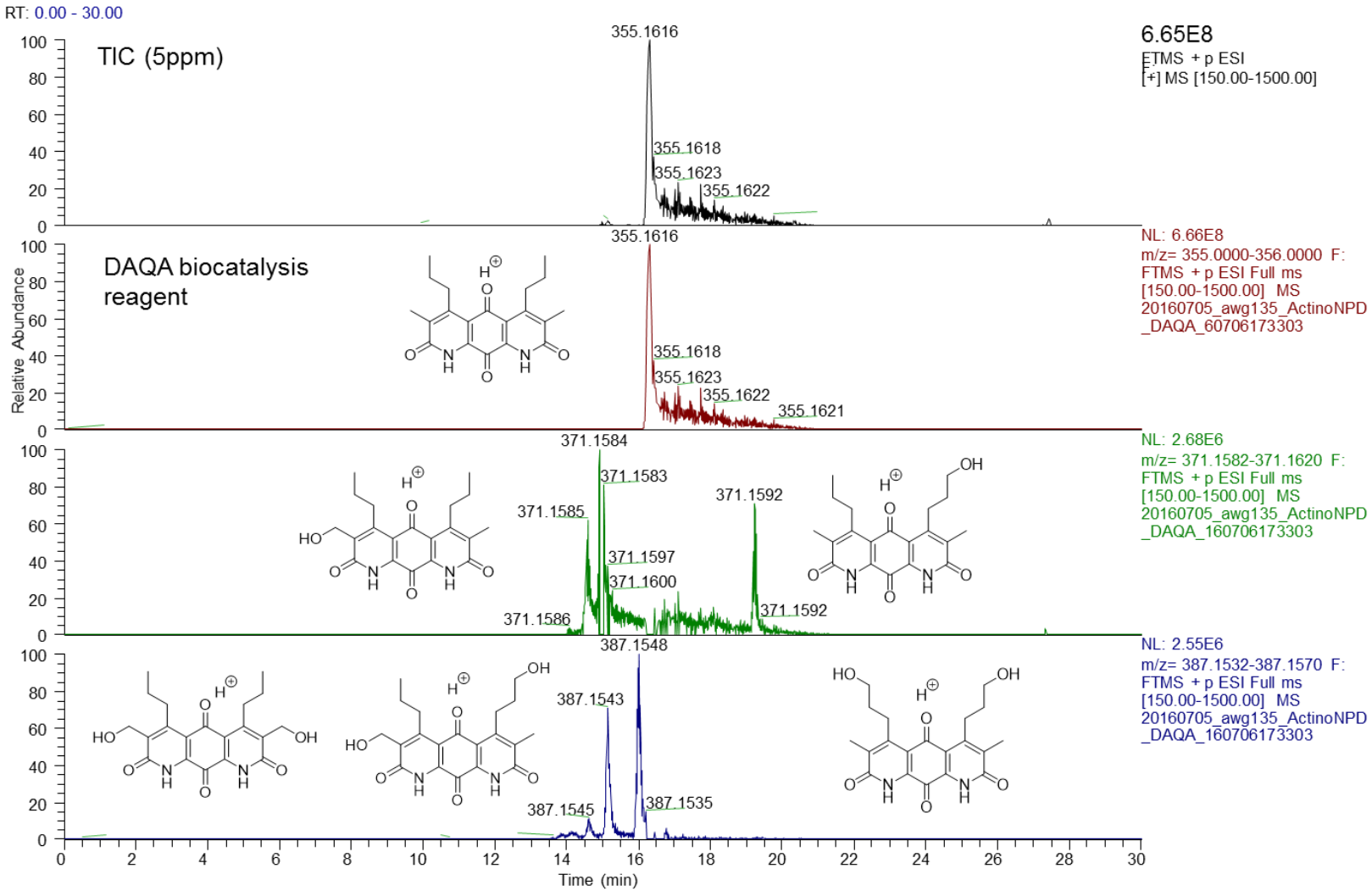

A2.2 Reference spectra and figures for: DIAZAQUINOMYCINS E–G, NOVEL DIAZA-ANTHRACENE ANALOGS FROM A MARINE-DERIVED *STREPTOMYCES* SP.

Figure A44. ^{1}H NMR spectrum (900 MHz) of **12** in $CDCl_3$ - 1% CF_3CO_2D.

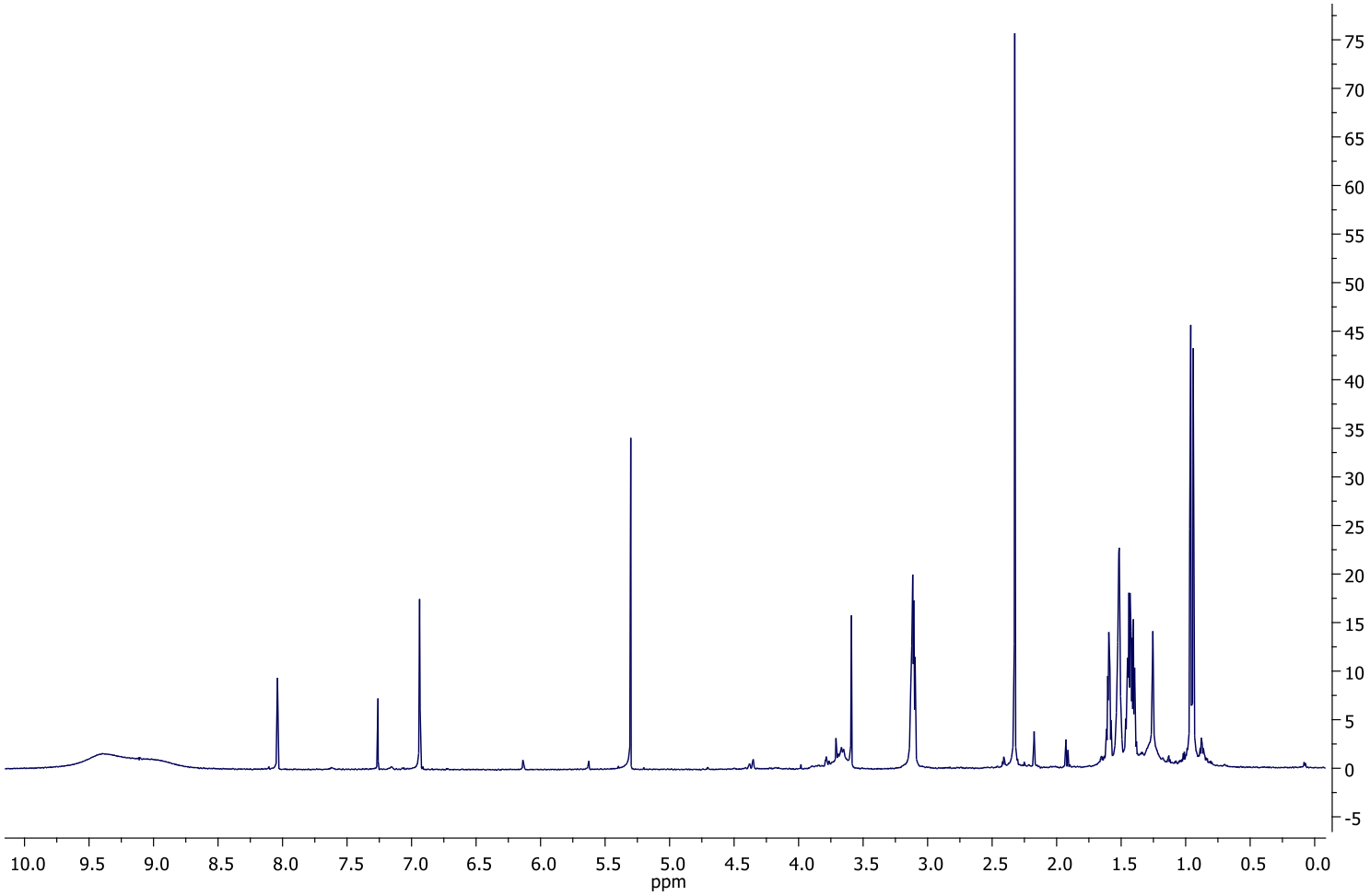

Figure A45. ^{13}C DEPTQ spectrum (226.2 MHz) of **12** in $CDCl_3$ - 1% CF_3CO_2D.

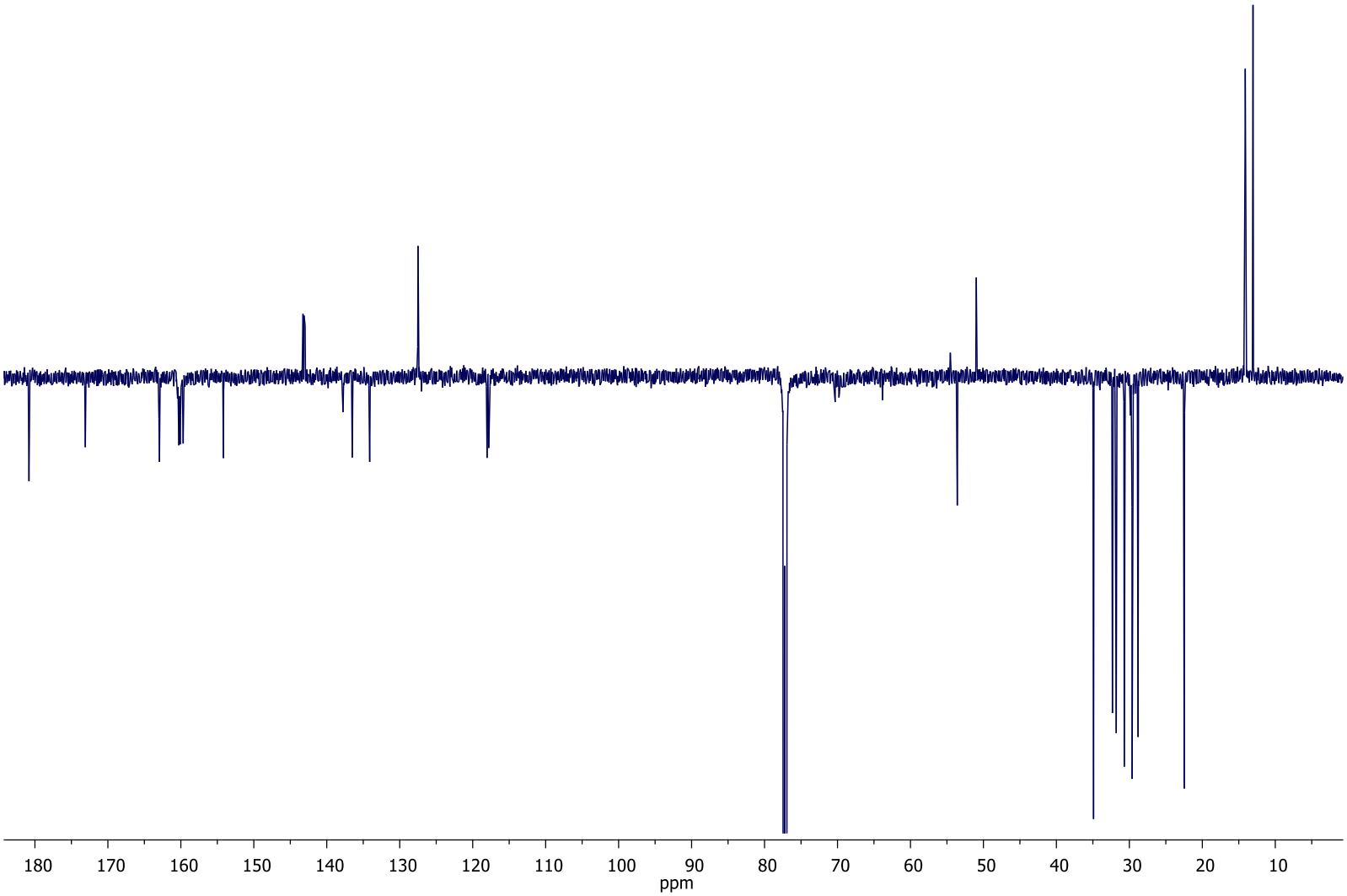

Figure A46. COSY spectrum (600 MHz) of **12** in $CDCl_3$ - 1% CF_3CO_2D.

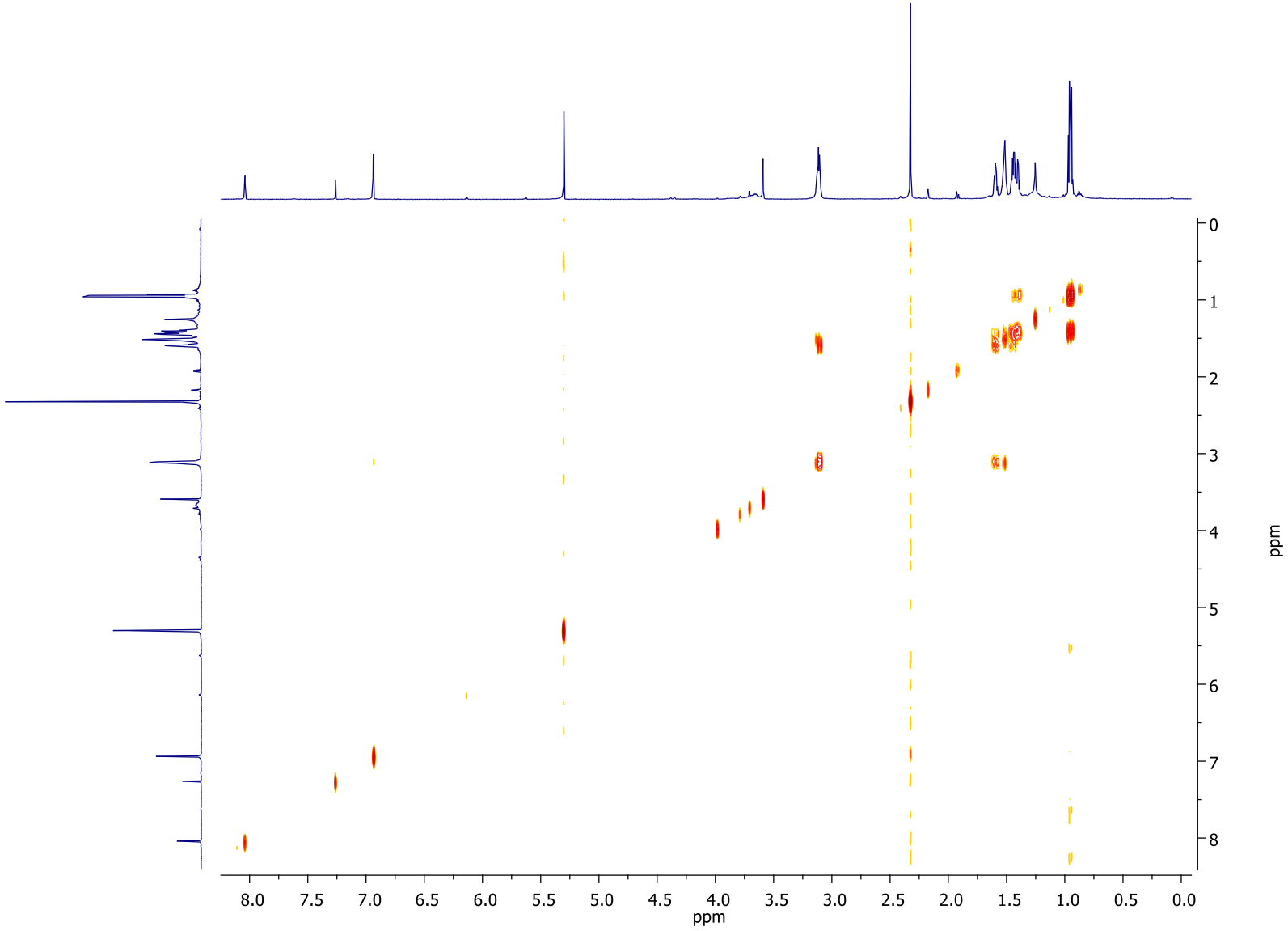

Figure A47. HMBC spectrum (600 MHz) of **12** in $CDCl_3$ - 1% CF_3CO_2D.

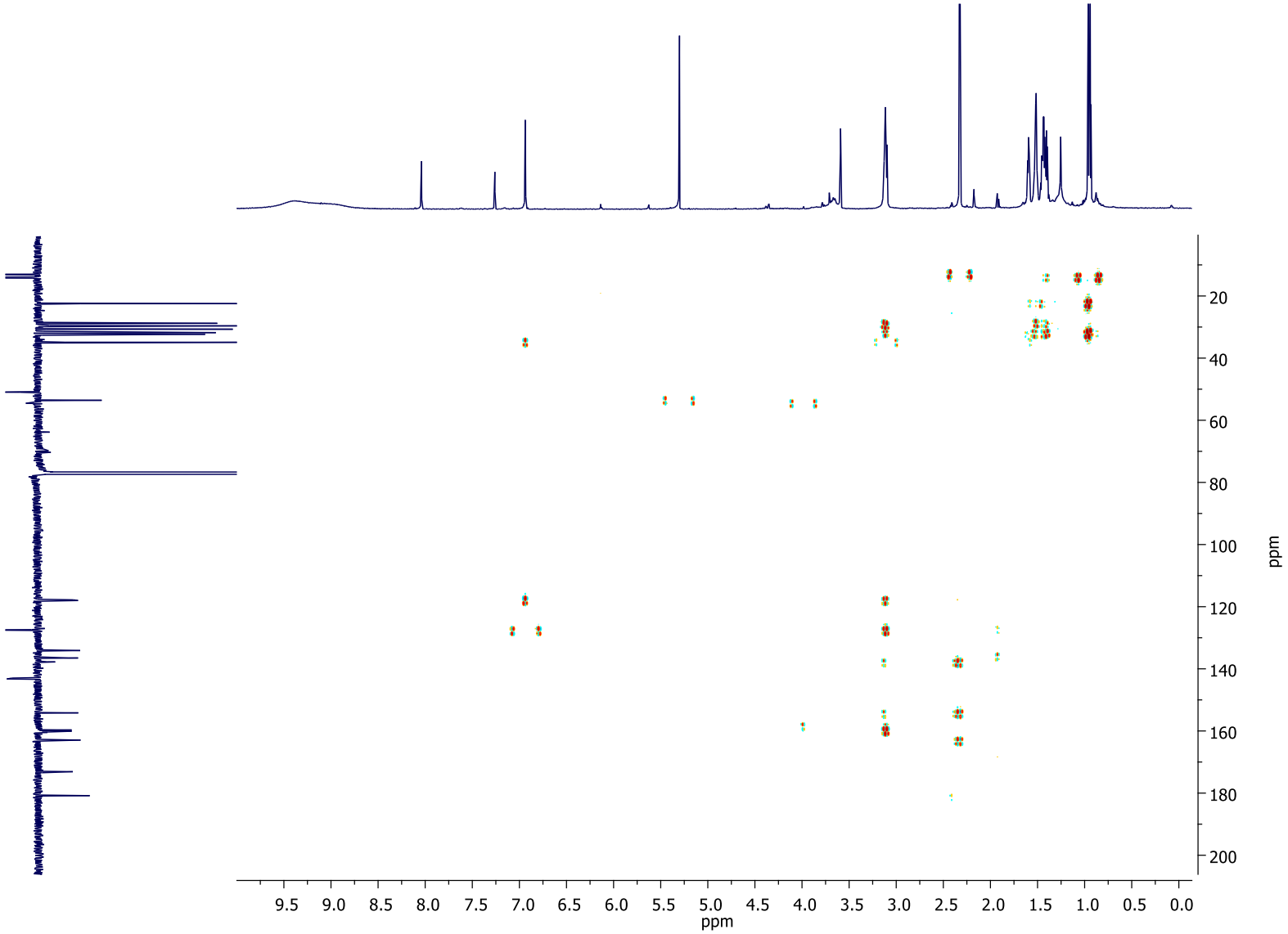

Figure A48. Selective 1D-TOCSY spectrum (600 MHz) of H_2-18 in **12** in $CDCl_3$ - 1% CF_3CO_2D.

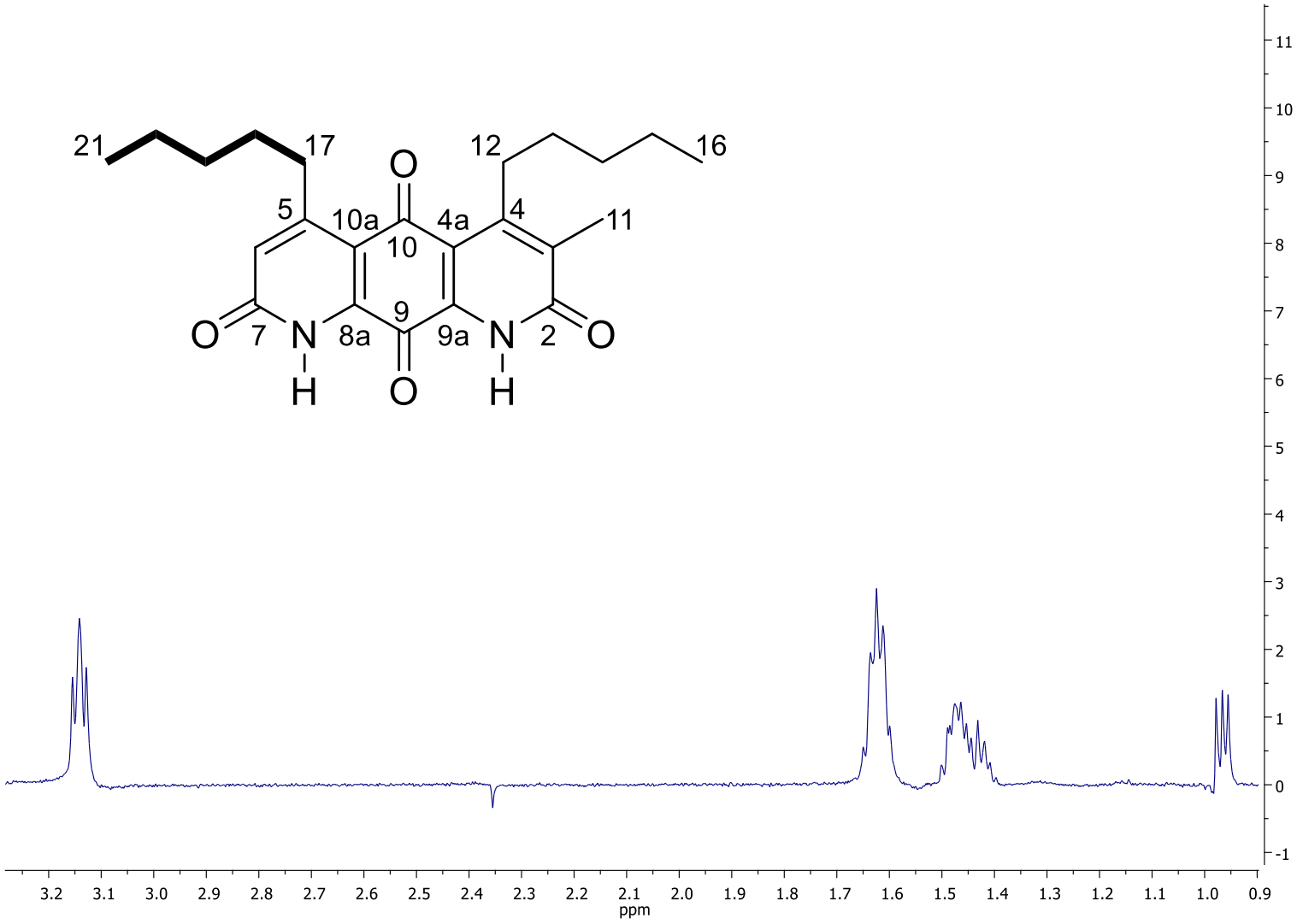

Figure A49. Selective 1D-TOCSY spectrum (600 MHz) of H_2-13 and H_2-14 in **12** in $CDCl_3$ - 1% CF_3CO_2D.

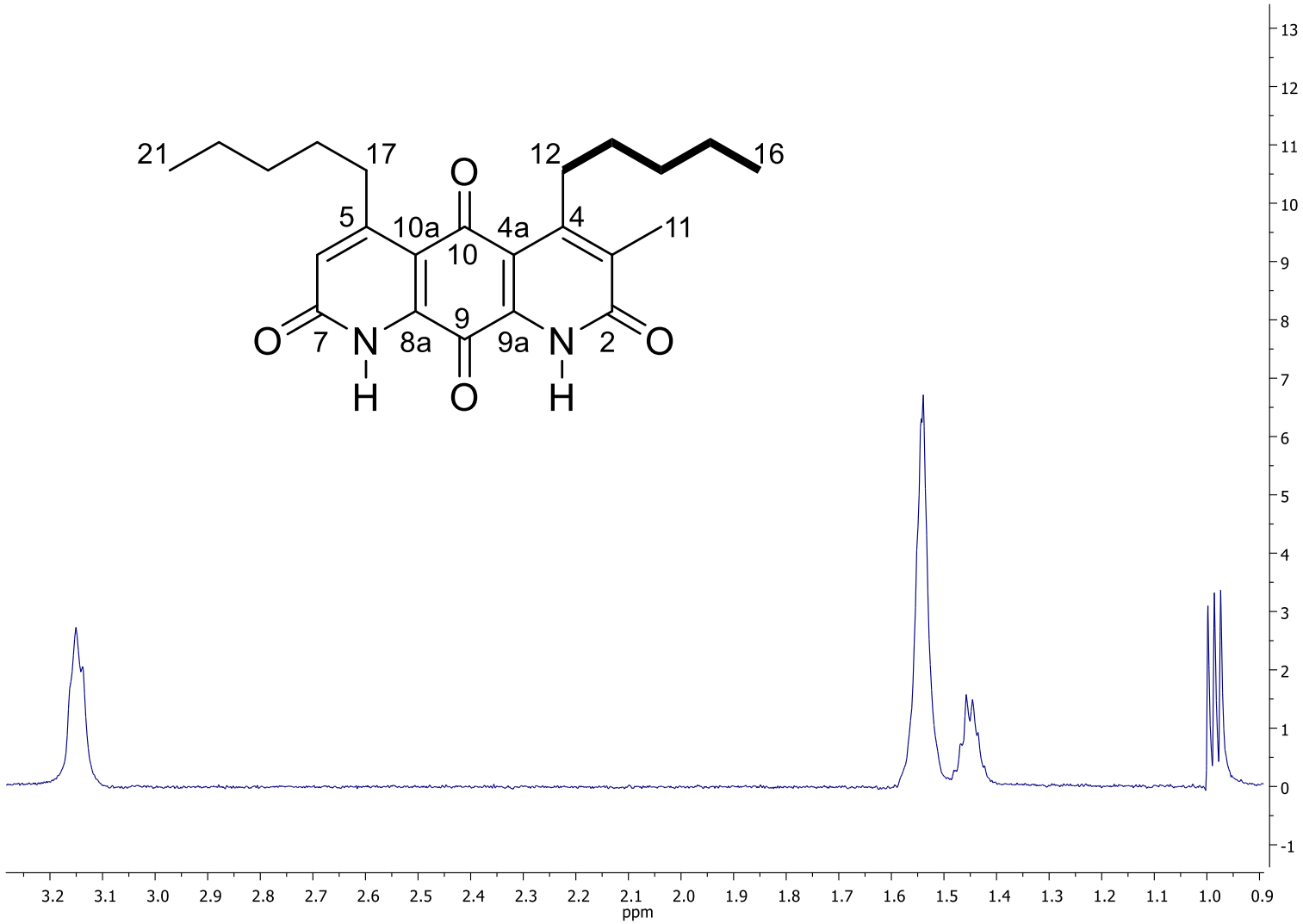

Figure A50. Selective 1D-TOCSY spectrum (600 MHz) of H_2-20 in **12** in $CDCl_3$ - 1% CF_3CO_2D.

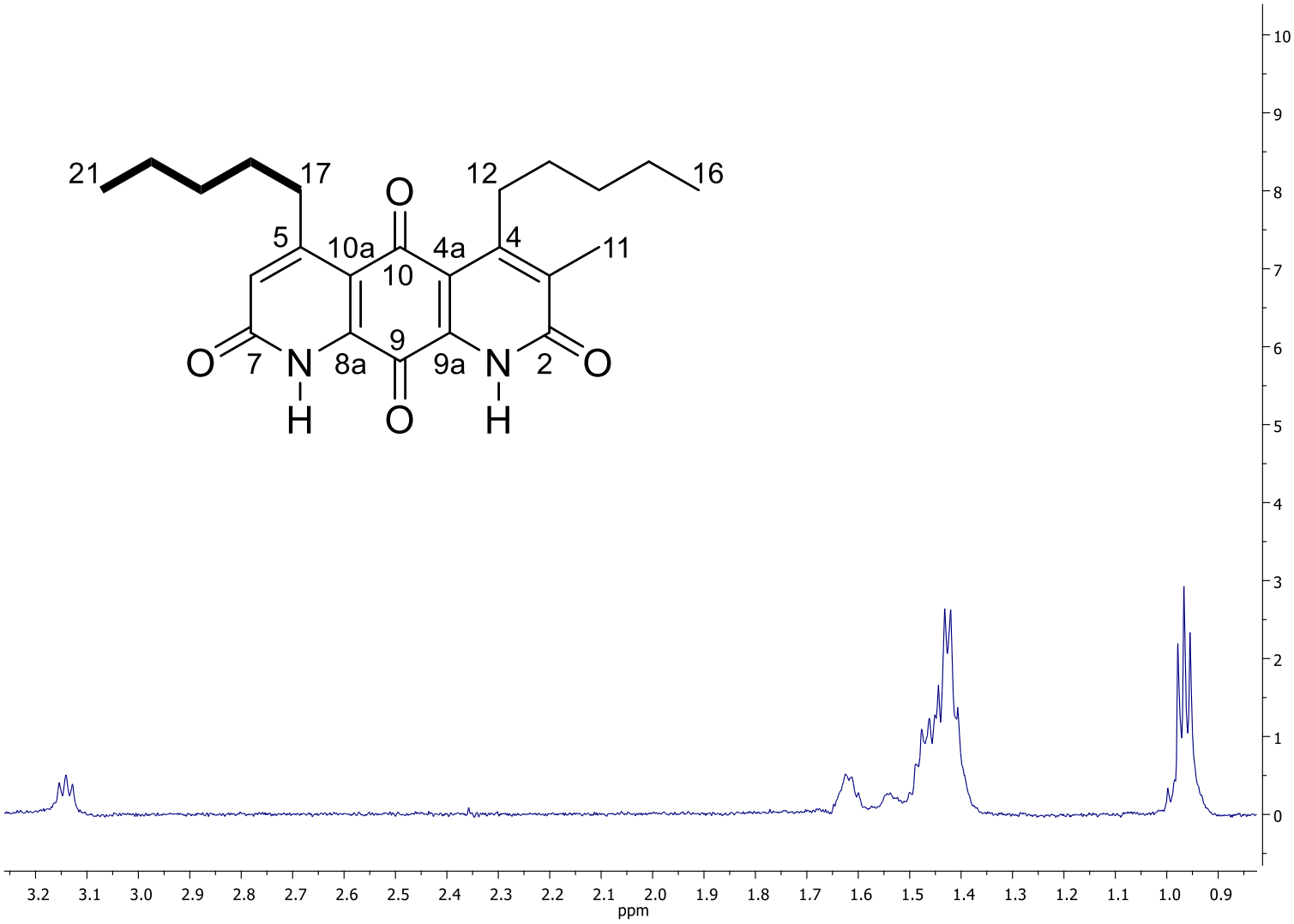

Figure A51. Expanded HR-ESI-IT-TOF mass spectra of **12**.

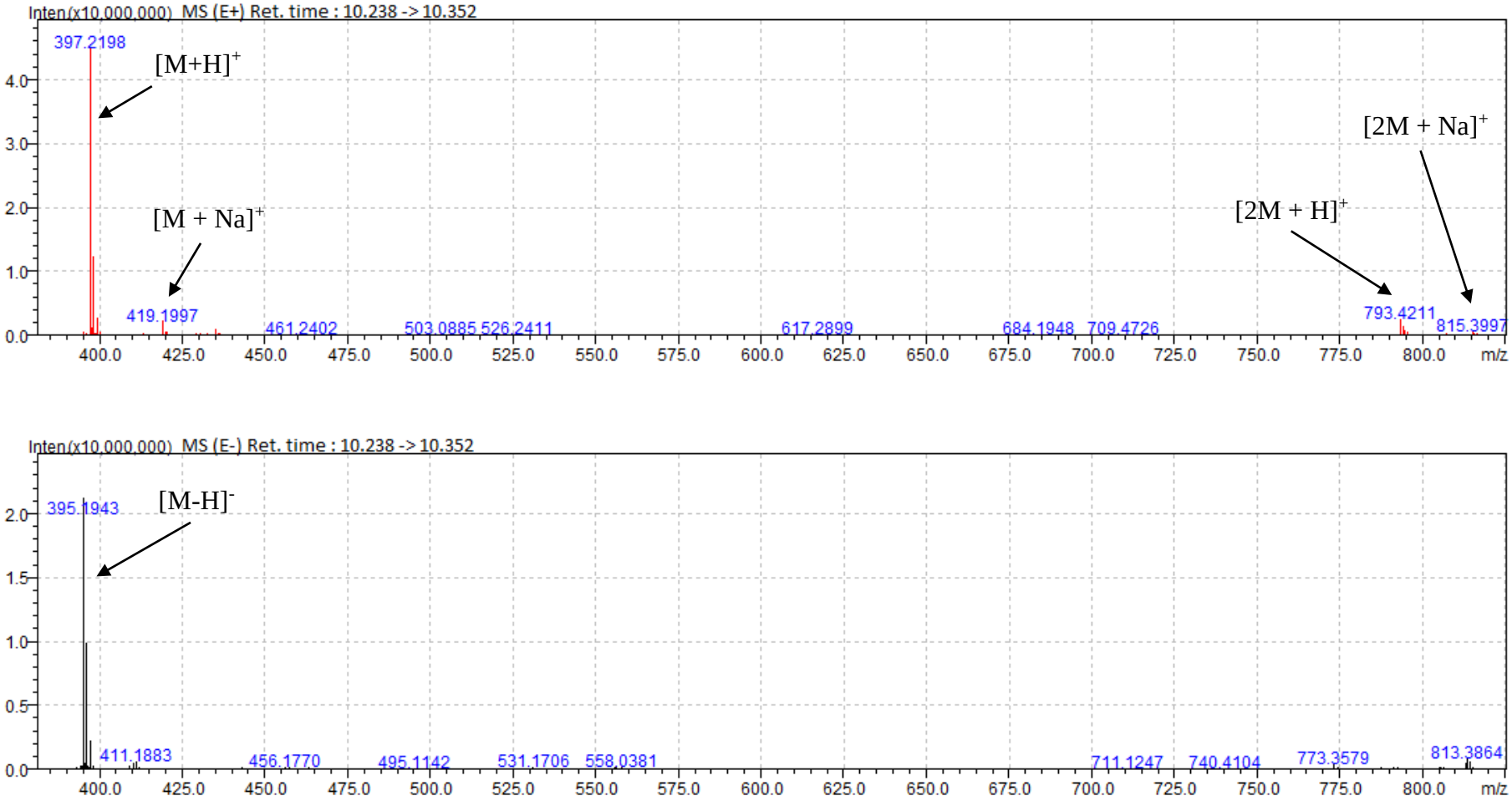

Figure A52. UV spectrum of **12** in ACN.

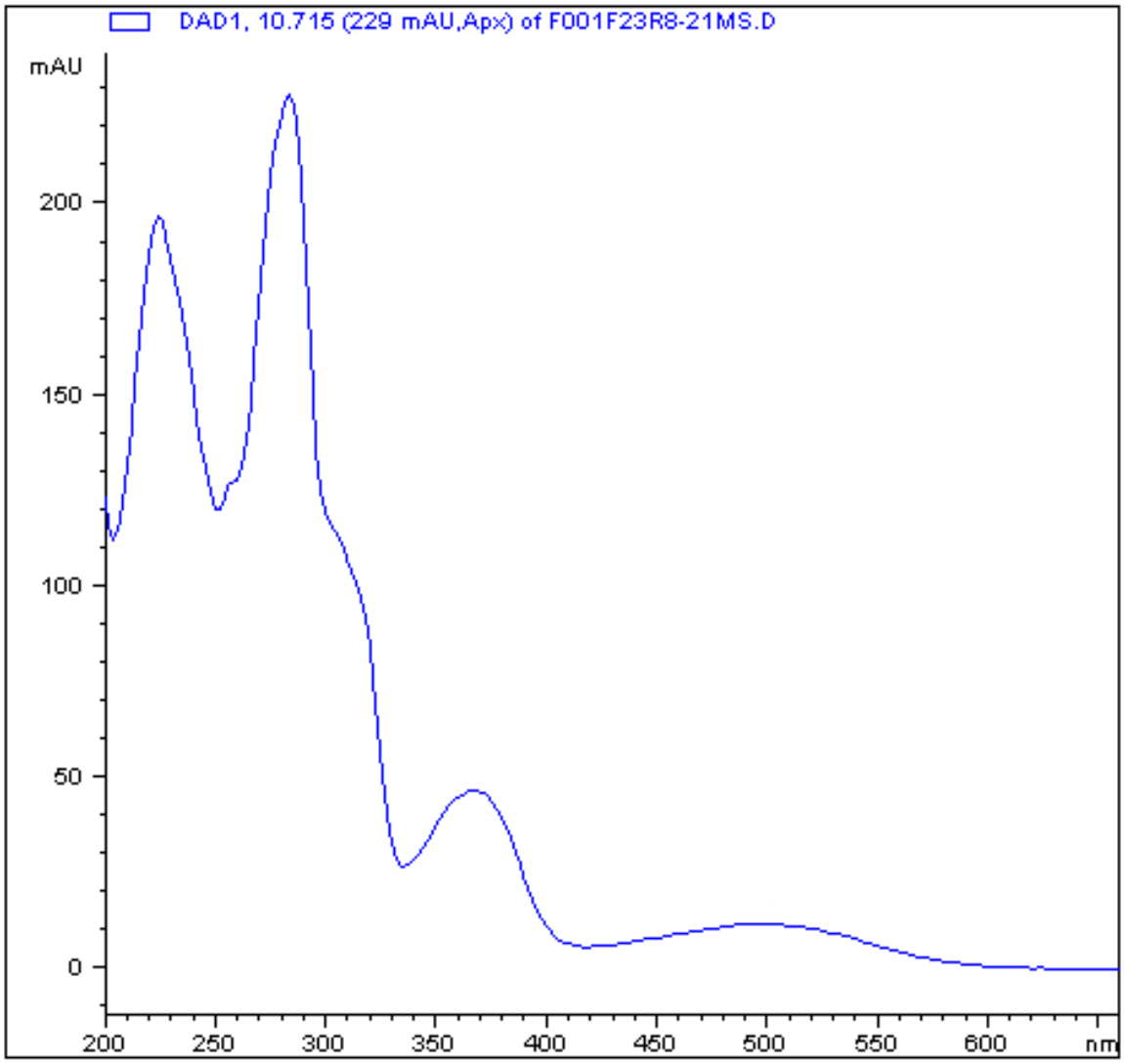

Table A5. ^{1}H and partial ^{13}C NMR data of **13** and **14** in $CDCl_3$ - 1% CF_3CO_2D.

Position	^{13}C [a]	^{1}H mult. (*J*, Hz) [b]
2		
3		
4		
4a		
5		
6	127.19	6.95 s and 6.98 s [c]
7		
8a		
9		
9a		
10		
10a		
11	12.77	2.34 s
12	32.65	3.12 t (7.9)
13	22.28	1.57 m
14	14.37	1.14 t (7.3)
15	34.50	3.13 t (7.5)
16	29.28	1.59 m
17	31.41	1.44 m
18	22.16	1.39 m
19	13.70	0.94 t (7.0)
20		
21		

[a] Resonances extracted from HSQC data; [b] 600 MHz;
[c] Chemically inequivalent α-methine hydrogens of DAQF and DAQG

Figure A53. ^{1}H NMR spectrum (600 MHz) of **13** and **14** in $CDCl_3$ - 1% CF_3CO_2D.

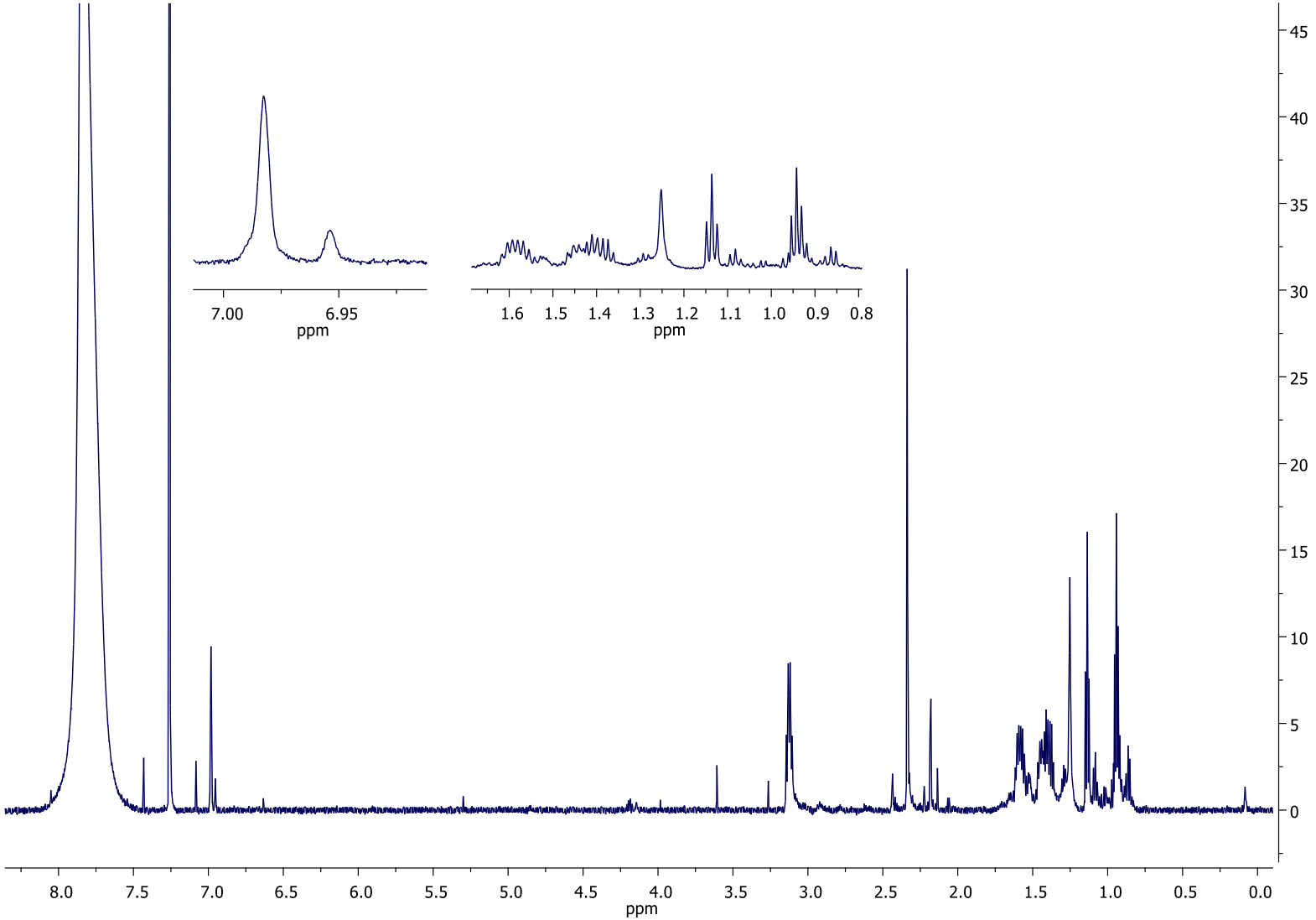

Figure A54. COSY spectrum (600 MHz) of **13** and **14** in $CDCl_3$ - 1% CF_3CO_2D.

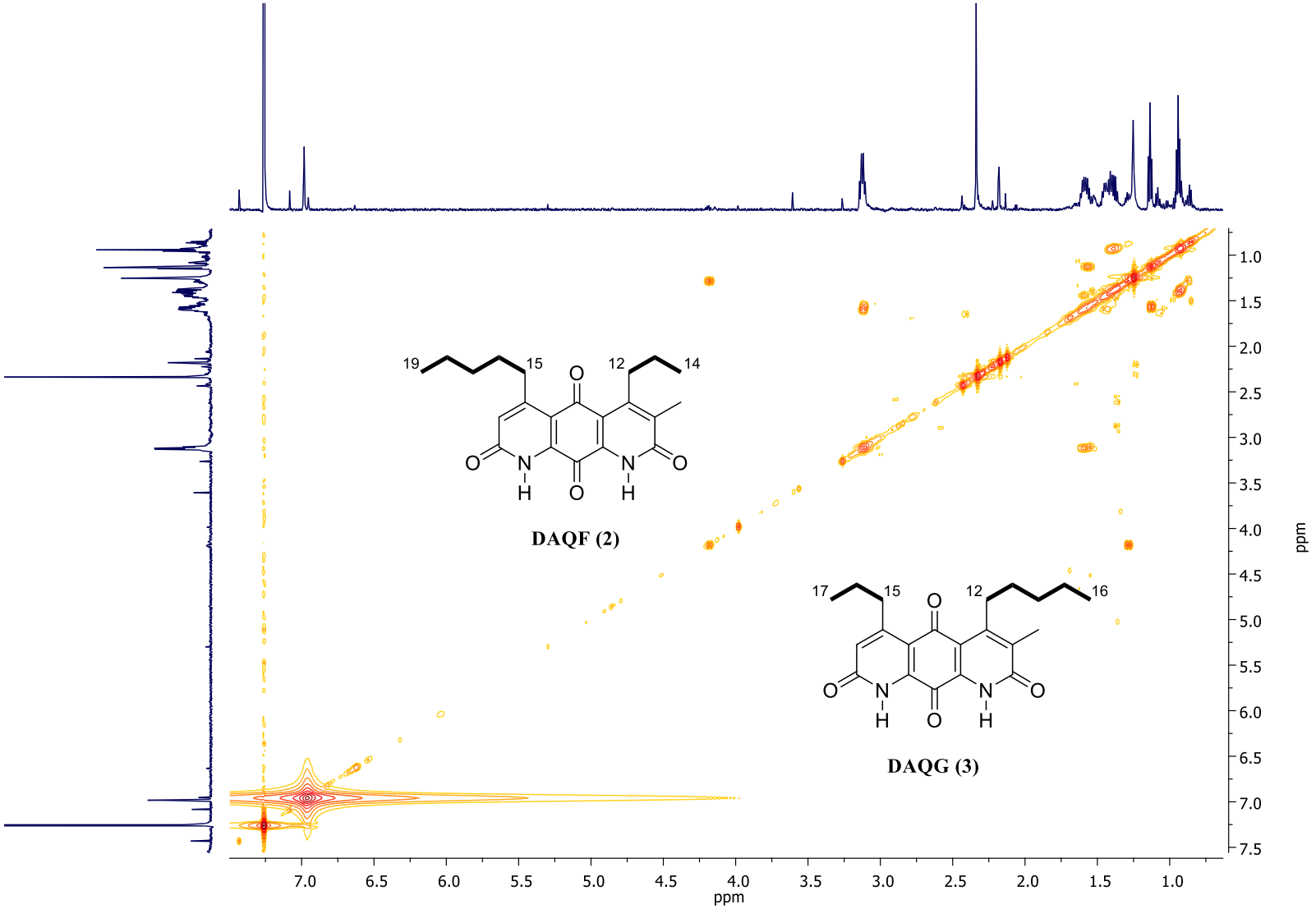

Figure A55. HSQC spectrum (600 MHz) of **13** and **14** in $CDCl_3$ - 1% CF_3CO_2D.

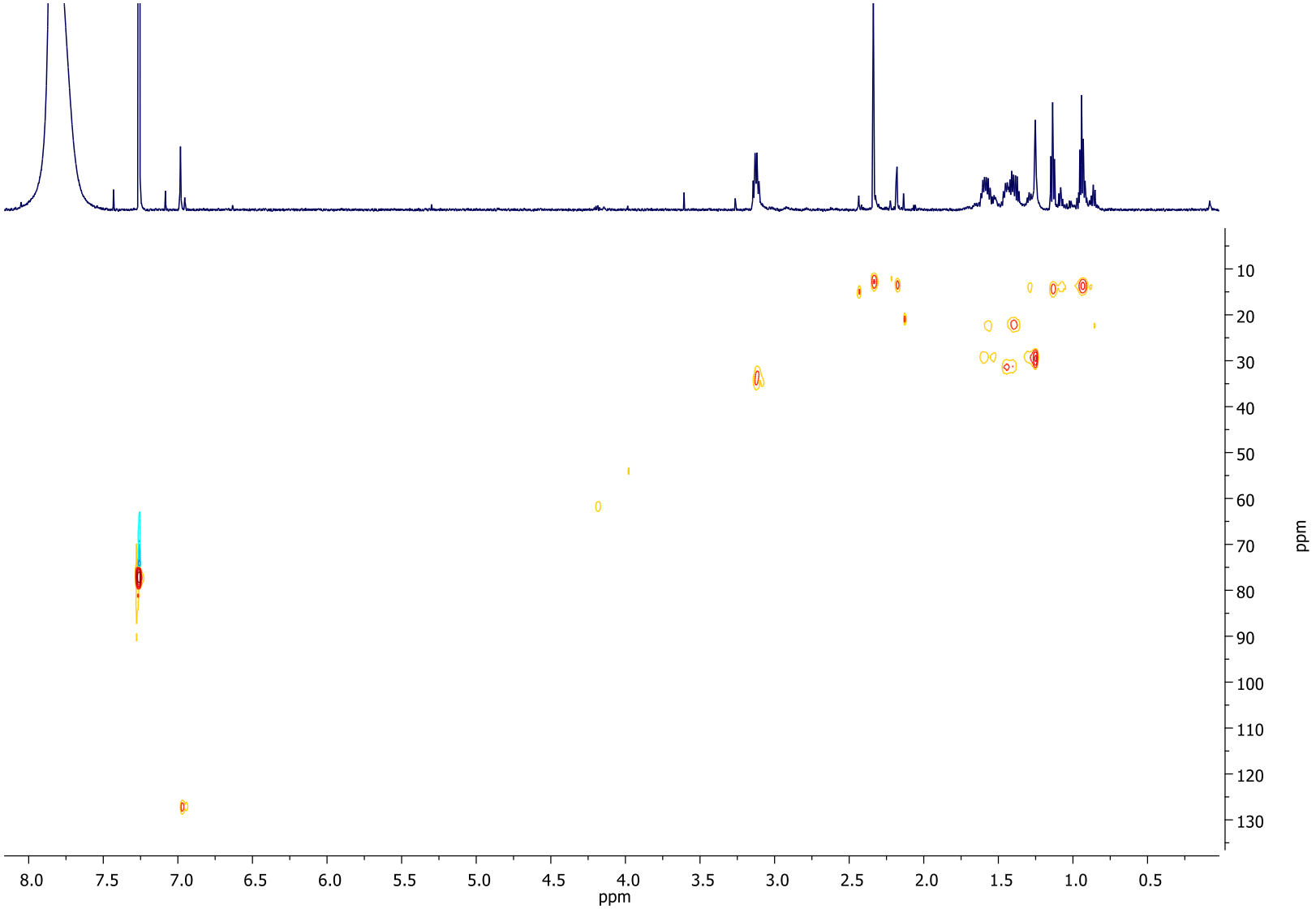

Figure A56. HMBC spectrum (600 MHz) of **13** and **14** in $CDCl_3$ - 1% CF_3CO_2D.

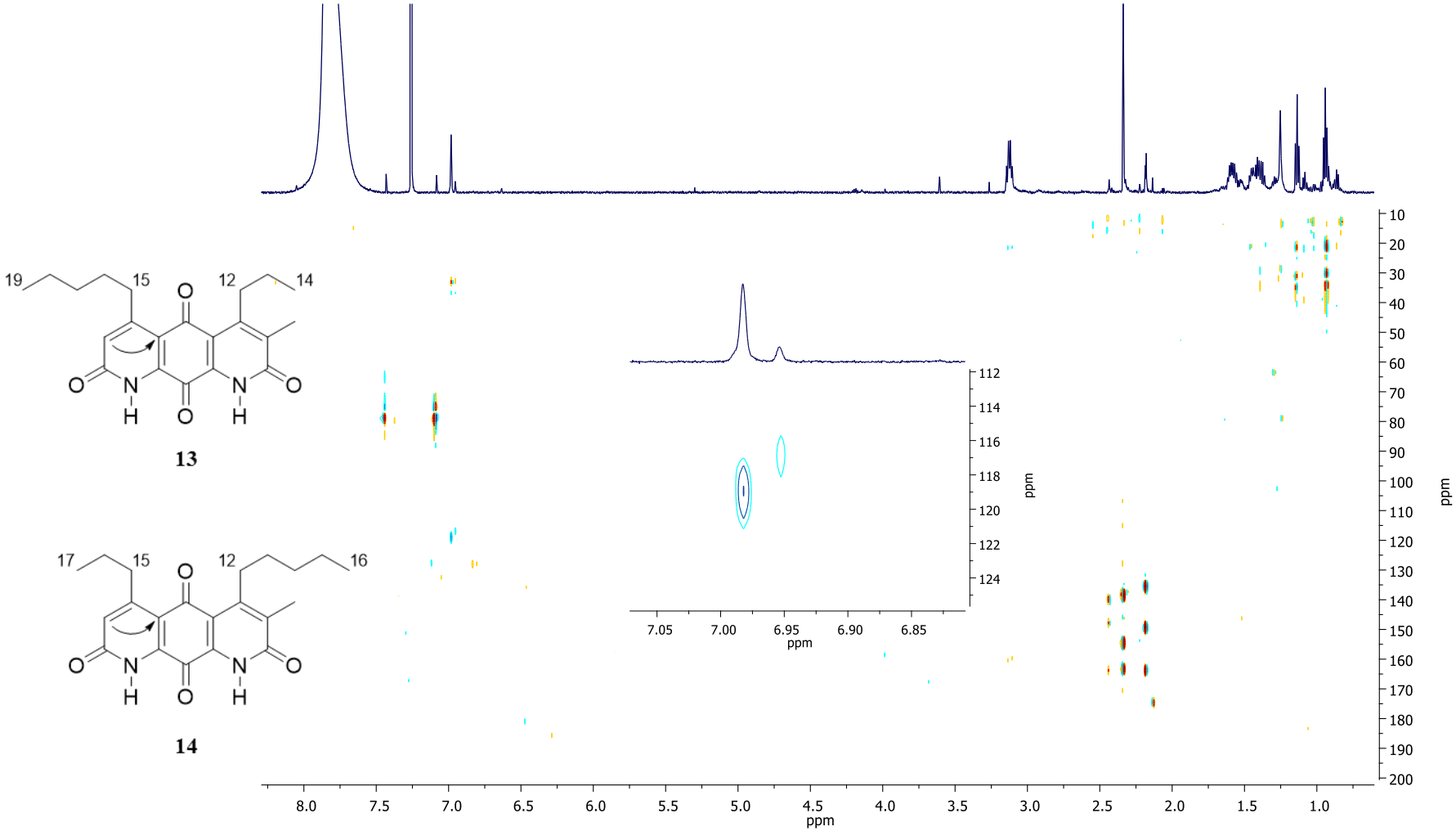

Inequivalency gives rise to two separate HMBC cross peaks (H6 to C10a in DAQF and DAQG).

Figure A57. Expanded HR-ESI-IT-TOF mass spectra of **13** and **14**.

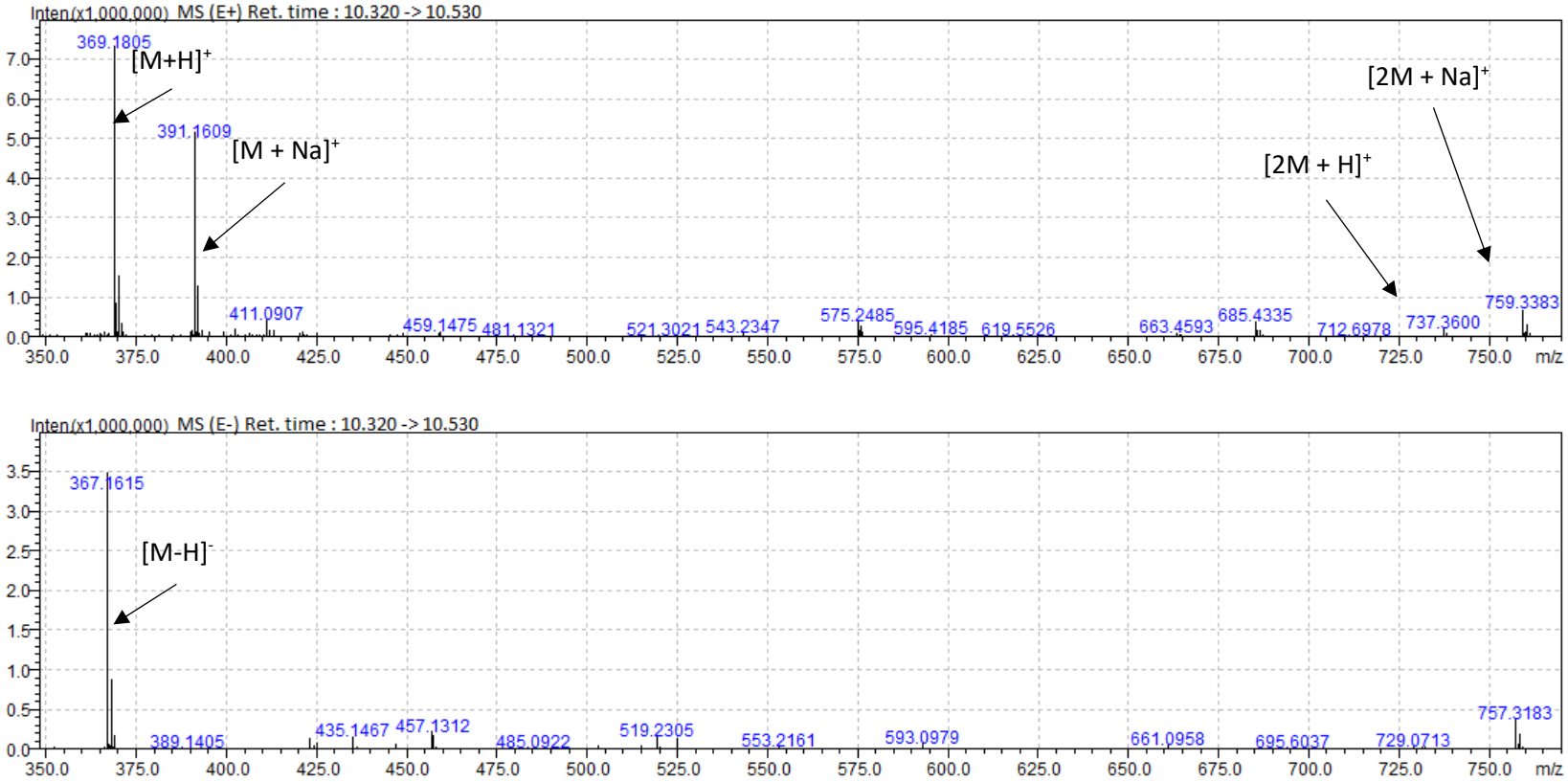

HR-ESI-IT-TOF MS *m/z* 369.1805 $[M + H]^+$ (calcd. for $C_{21}H_{25}N_2O_4$: 369.1814), *m/z* 367.1615 $[M - H]^-$ (calcd. for $C_{21}H_{23}N_2O_4$: 367.1663), *m/z* 391.1609 $[M + Na]^+$ (calcd. for $C_{21}H_{24}N_2O_4Na$: 391.1634), *m/z* 737.3600 $[2M + H]^+$ (calcd. for $C_{42}H_{49}N_4O_8$: 737.3550), and *m/z* 759.3383 $[2M + Na]^+$ (calcd. for $C_{42}H_{48}N_4O_8Na$: 759.3370).

Figure A58. UV spectrum of **13** and **14** mixture in ACN.

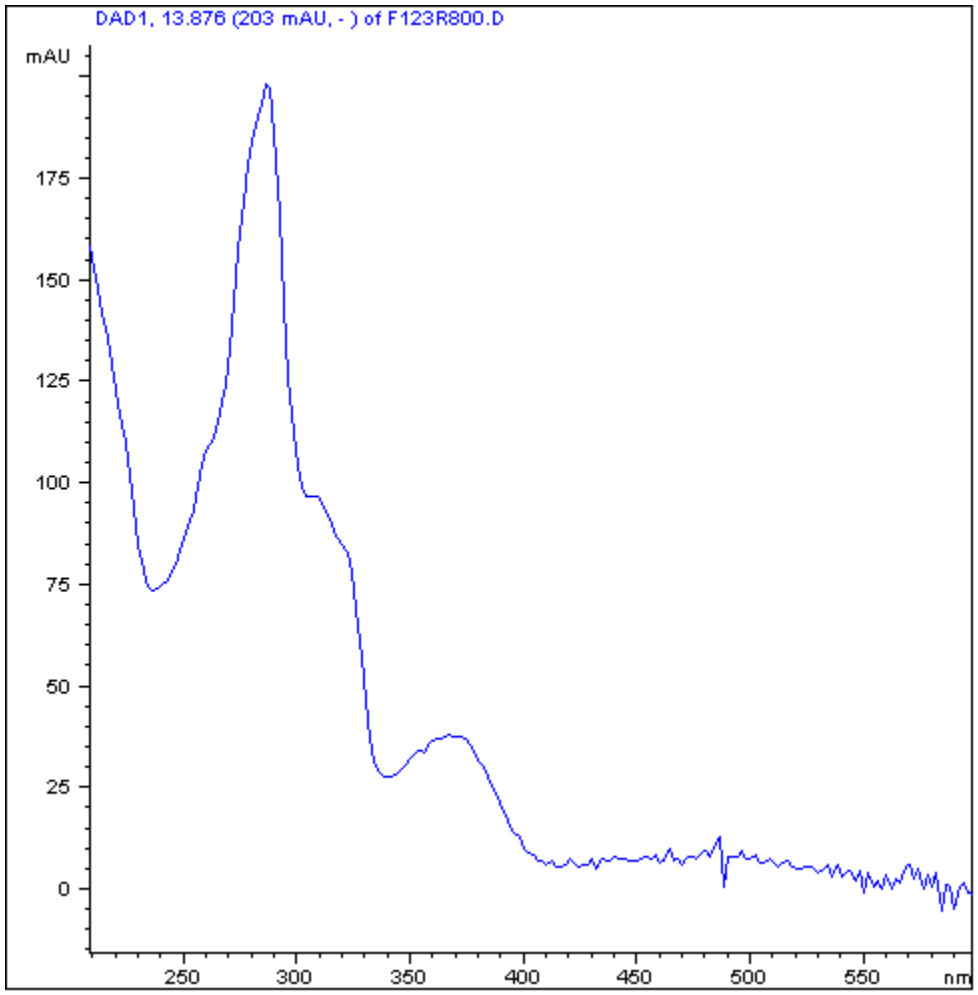

UV (MeOH) λ_{max} (log ε) = 280.5 (4.01), 359.0 (3.40), and a broad peak with maximum at 437.0 (2.66) nm.

Figure A59. Co-crystal structure of **13** and **14**.

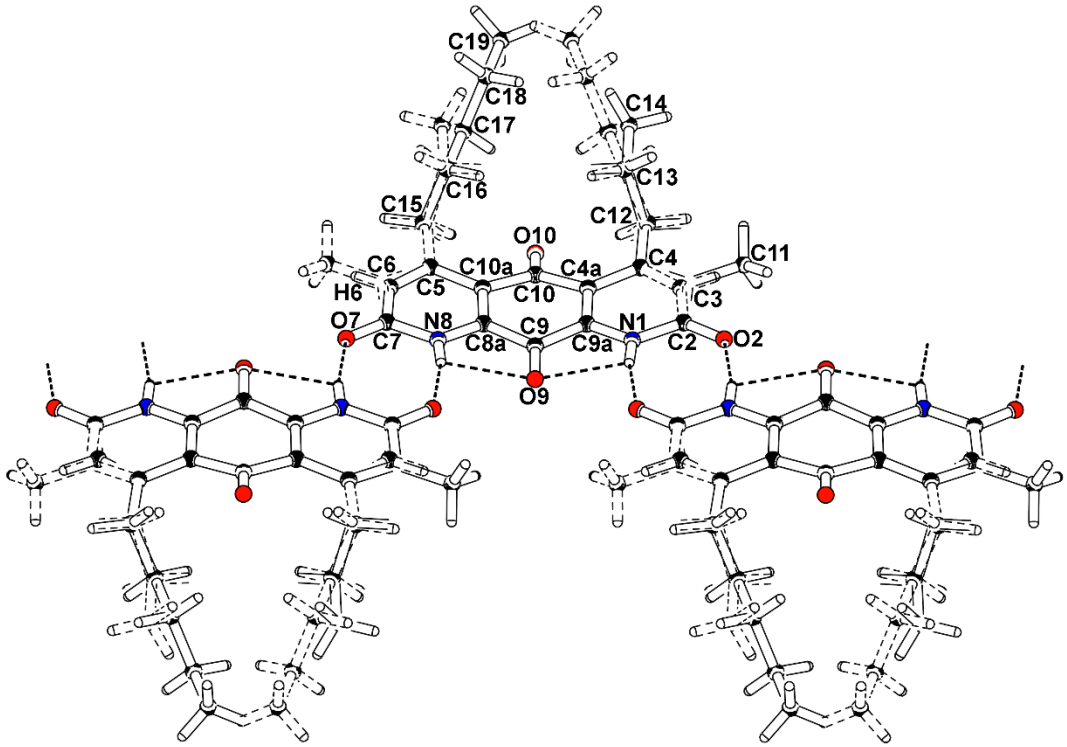

Structure numbered to emphasize DAQF occupancy in the co-crystal.

Figure A60. Deconvolution of co-crystal structure of **13** and **14**.

A: 39.8% = (0.704 x 0.566) x 100

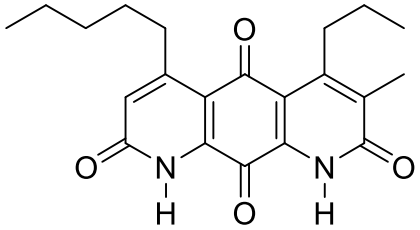

B: 30.6% = (0.704 x 0.434) x 100

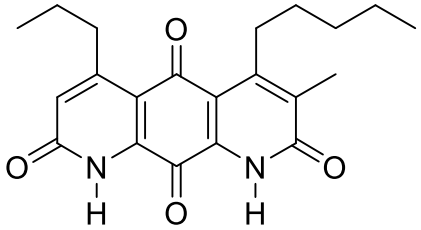

C: 16.8% = (0.296 x 0.566) x 100; same as **B**

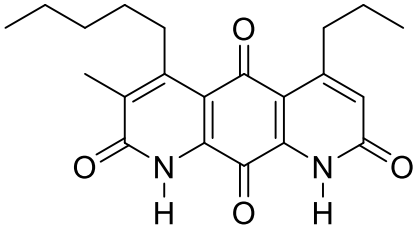

D: 12.8% = (0.296 x 0.434) x 100; same as **A**

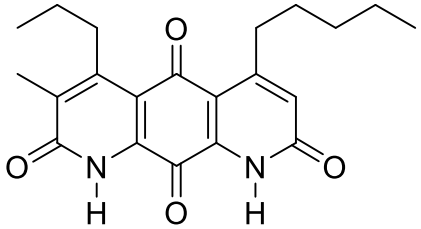

A + D = 39.8% + 12.8% = 52.6% DAQF

B + C = 30.6% + 16.8% = 47.4% DAQG

The methyl group at C3 is favored [0.704(8) to 0.296(8)], with the estimated standard deviation cited in parentheses; the propyl group at C4 is favored [0.566(9) to 0.434(9)]. Taken together, DAQF resides at the crystallographic site 52.6% to DAQG (47.4%).

As noted in the discussion, disordered water molecules are evident from the electron density maps. They occupy sites near the methine hydrogen atom, or near the end of the propyl group.

If both disordered groups were equal, then they would each refine to 0.5.

A2.3 Reference spectra and figures for: A PIMARANE DITERPENE AND CYTOTOXIC ANGUCYCLINES FROM A MARINE-DERIVED MICROMONOSPORA SP. IN VIETNAM'S EAST SEA.

Figure A61. ^{1}H NMR spectrum (600 MHz) of **15** in $CDCl_3$.

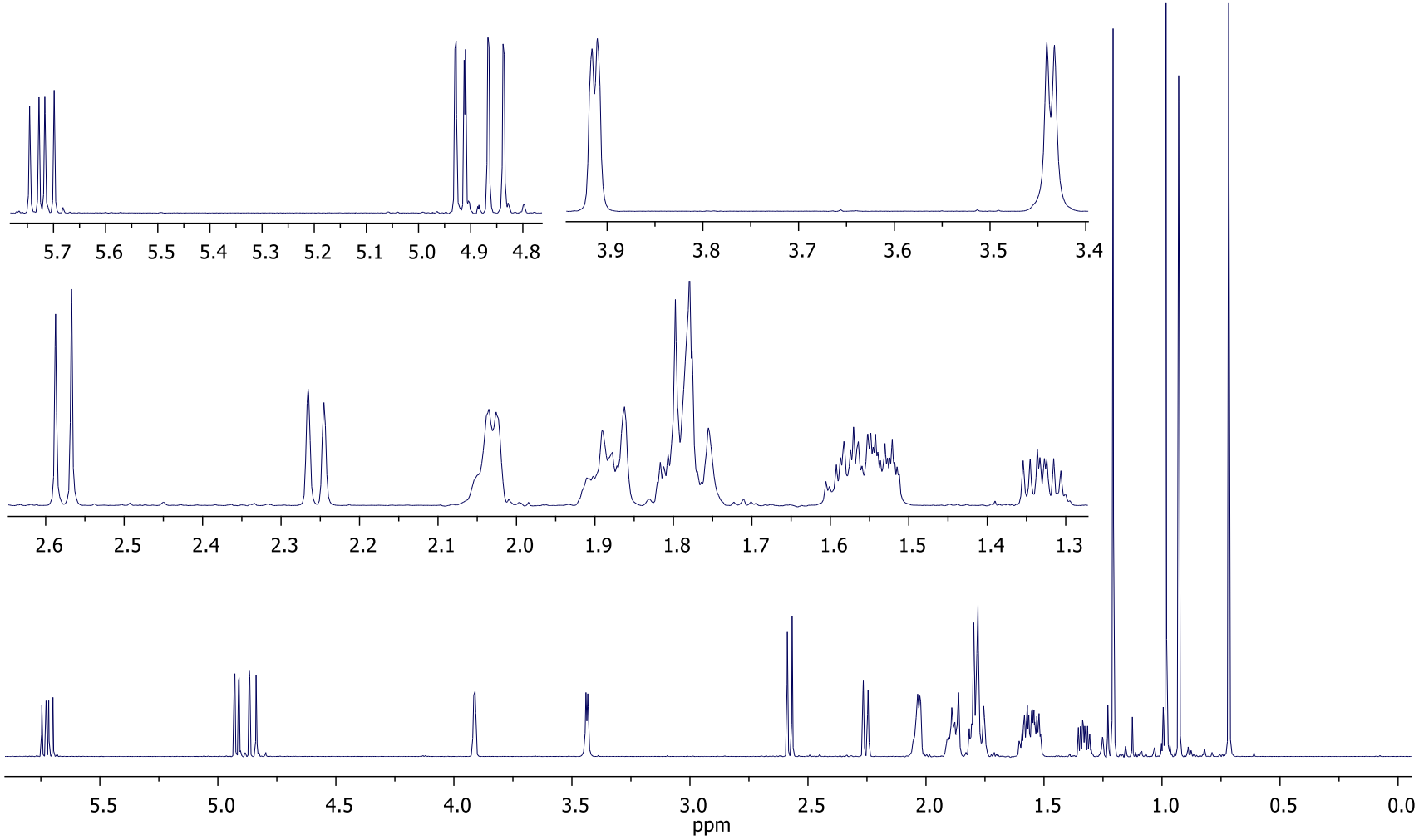

Figure A62. ^{13}C DEPTQ spectrum (226.2 MHz) of **15** in $CDCl_3$.

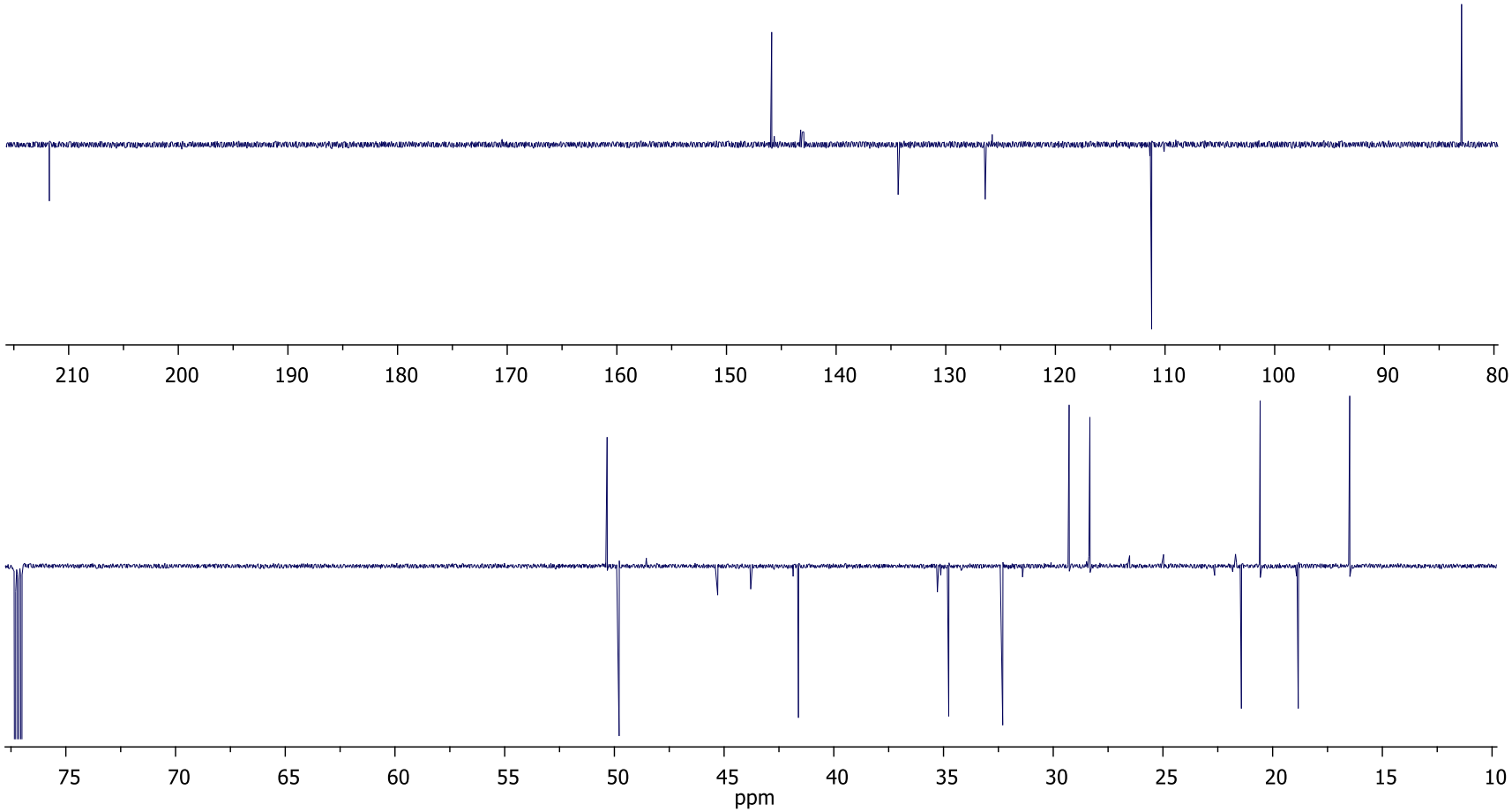

Figure A63. COSY spectrum (600 MHz) of **15** in $CDCl_3$.

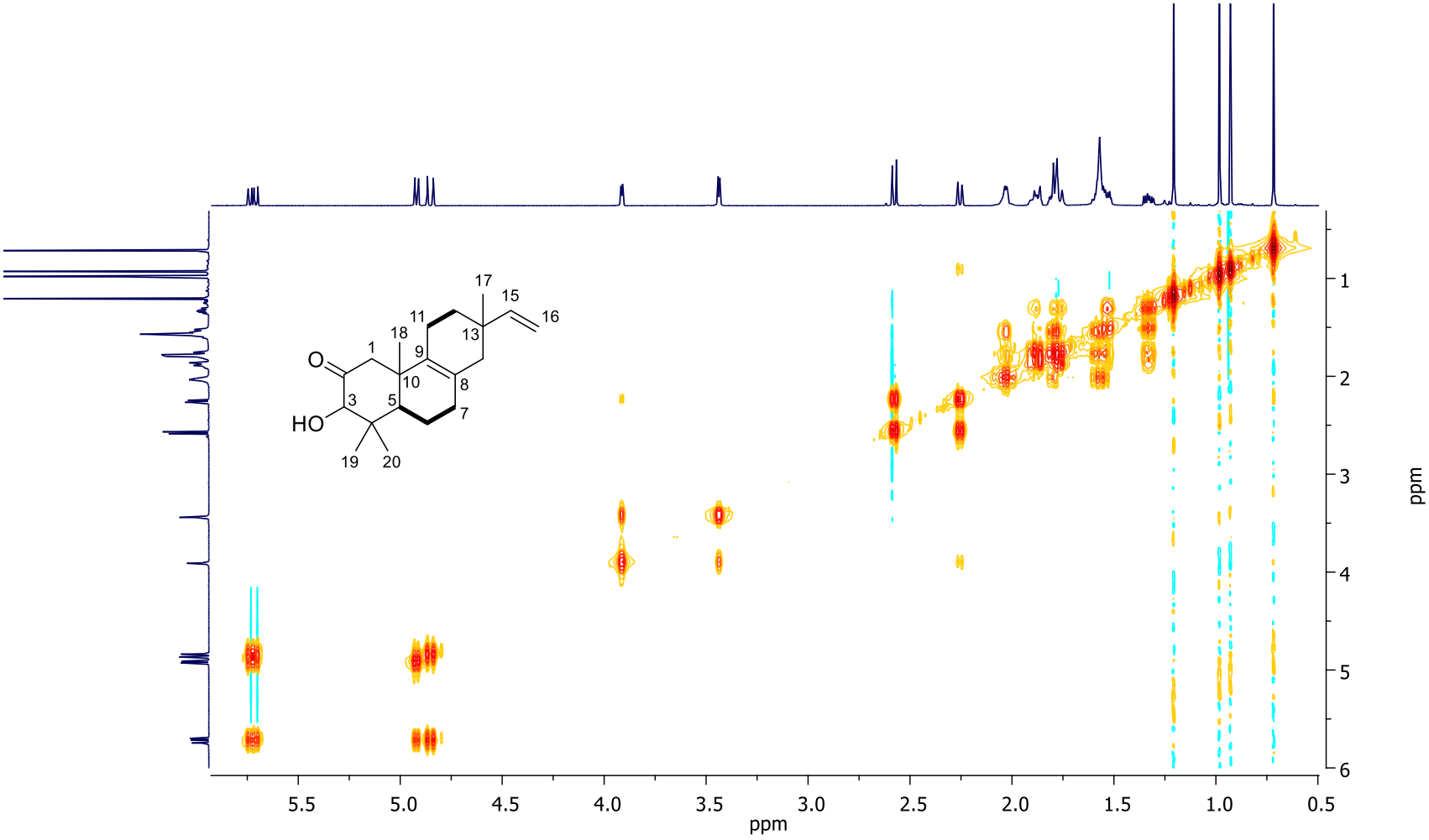

Figure A64. HSQC spectrum (600 MHz) of **15** in $CDCl_3$.

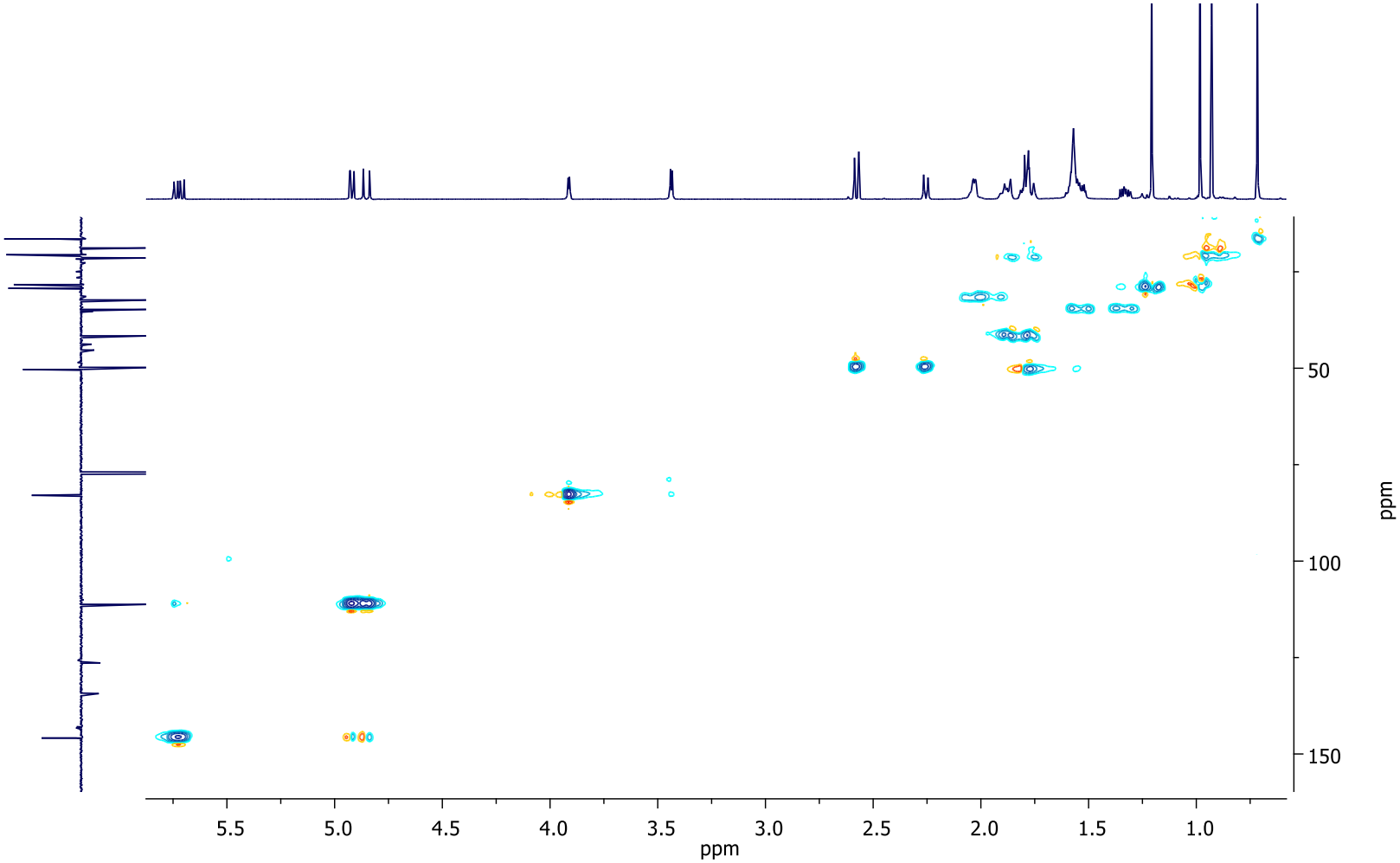

Figure A65. HMBC spectrum (600 MHz) of **15** in $CDCl_3$.

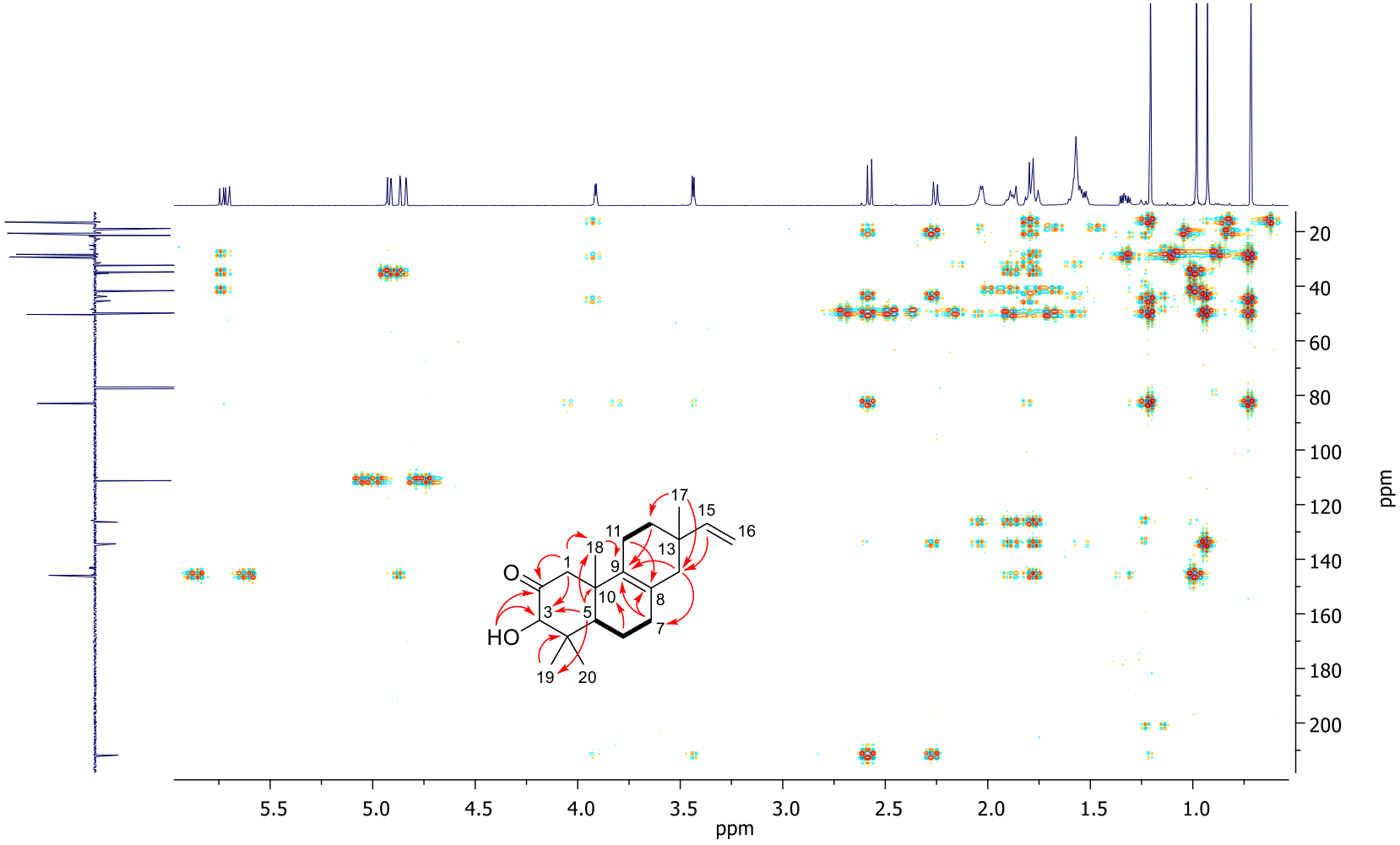

Table A6. ^{1}H NMR data (600 MHz) of **15** in $CDCl_3$ and C_6D_6.

Position	^{1}H, mult. (*J*, Hz) in $CDCl_3$ [a]	^{1}H, mult. (*J*, Hz) in C_6D_6 [a]
1 ax	2.25, d (12.3)	1.76, d (12.3)
eq	2.58, d (12.3)	2.40, d (12.3)
2		
3	3.91, d (4.0)	3.59, d (3.7)
3-OH	3.44, d (4.0)	3.66, d (3.7)
4		
5	1.78, m	1.45, dd (2.0, 12.5)
6	1.58, m	1.31, m
	1.80, m	1.50, m
7	2.03, m	1.76, m
8		
9		
10		
11 ax	1.76, m	1.58, m
eq	1.88, m	1.77, m
12 eq	1.33, m	1.15, m
ax	1.53, m	1.38, m
13		
14	1.76, m	1.60, m
	1.88, m	1.77, m
15	5.72, dd (17.5, 10.7)	5.73, dd (17.5, 10.7)
16	4.85, dd (17.5, 1.4)	4.91, dd (17.5, 1.4)
	4.92, dd (10.7, 1.4)	4.99, dd (10.7, 1.4)
17	0.98, s	0.98, s
18	0.93, s	0.81, s
19	1.21, s	1.13, s
20	0.72, s	0.72, s

[a] s = singlet; d = doublet; dd = doublet of doublets; m = multiplet.

Figure A66. ^{1}H NMR spectrum (600 MHz) of **15** in C_6D_6.

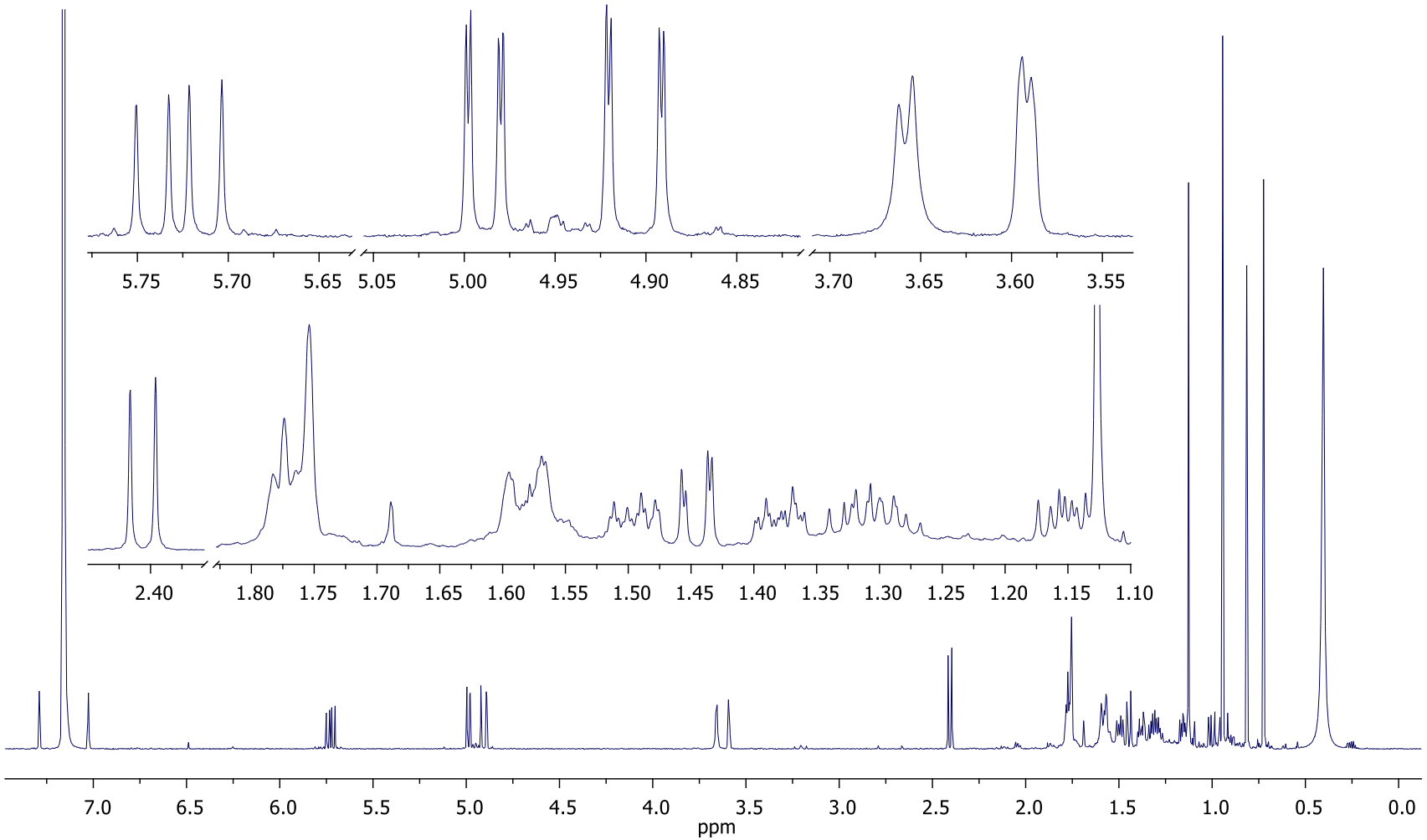

Figure A67. COSY spectrum (600 MHz) of **15** in C_6D_6.

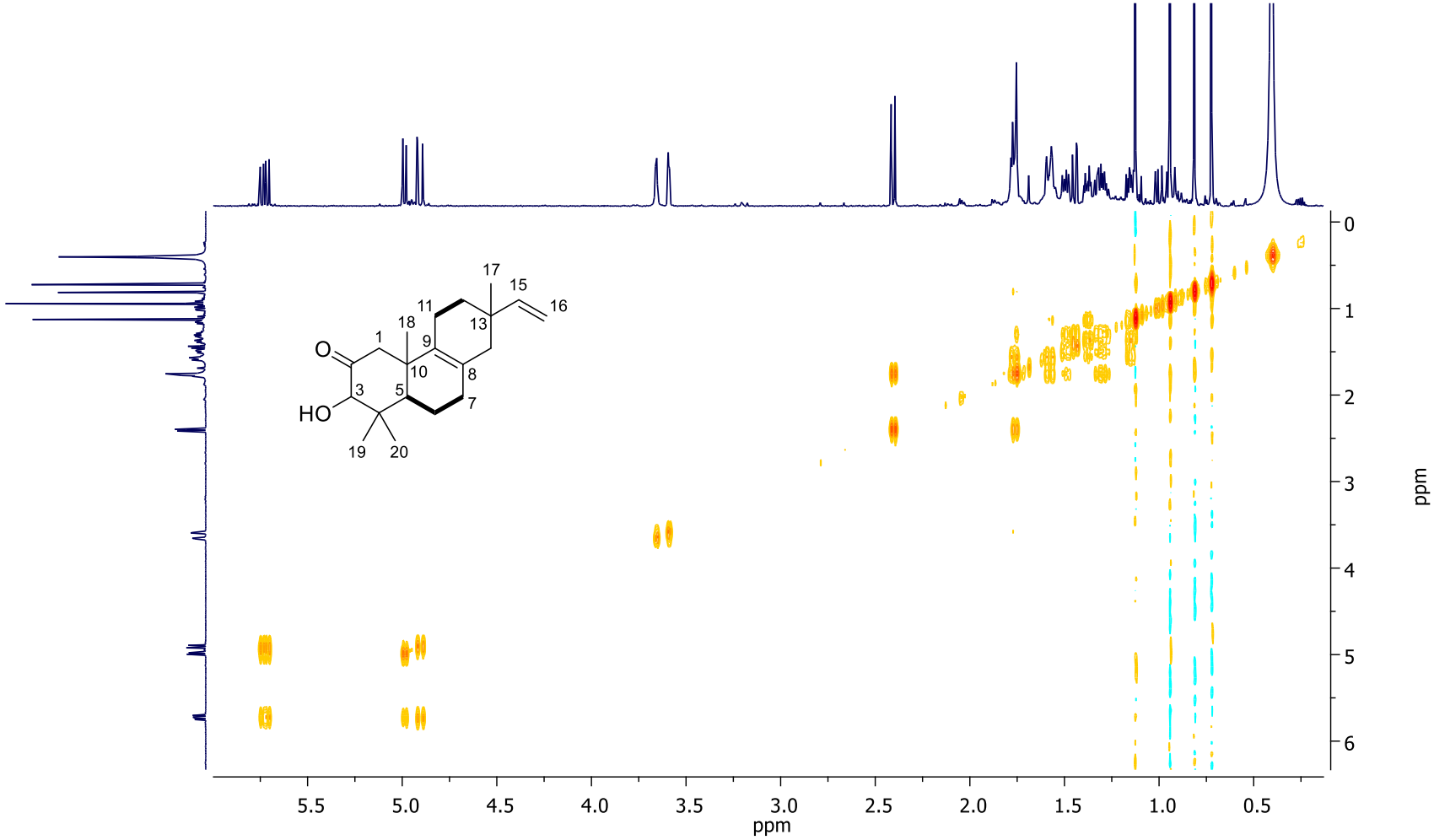

Figure A68. HSQC spectrum (600 MHz) of **15** in C_6D_6.

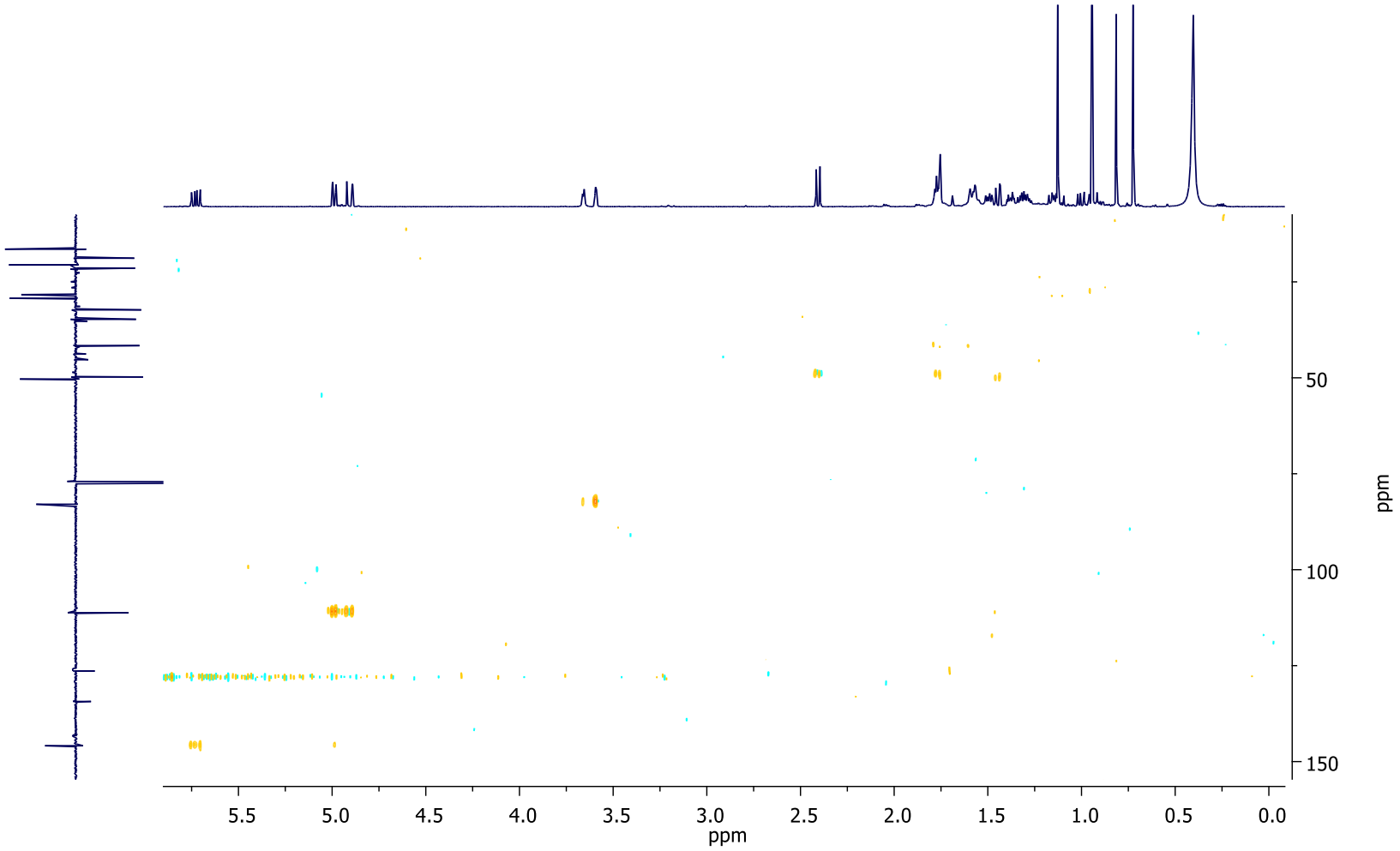

Figure A69. HMBC spectrum (600 MHz) of **15** in C_6D_6.

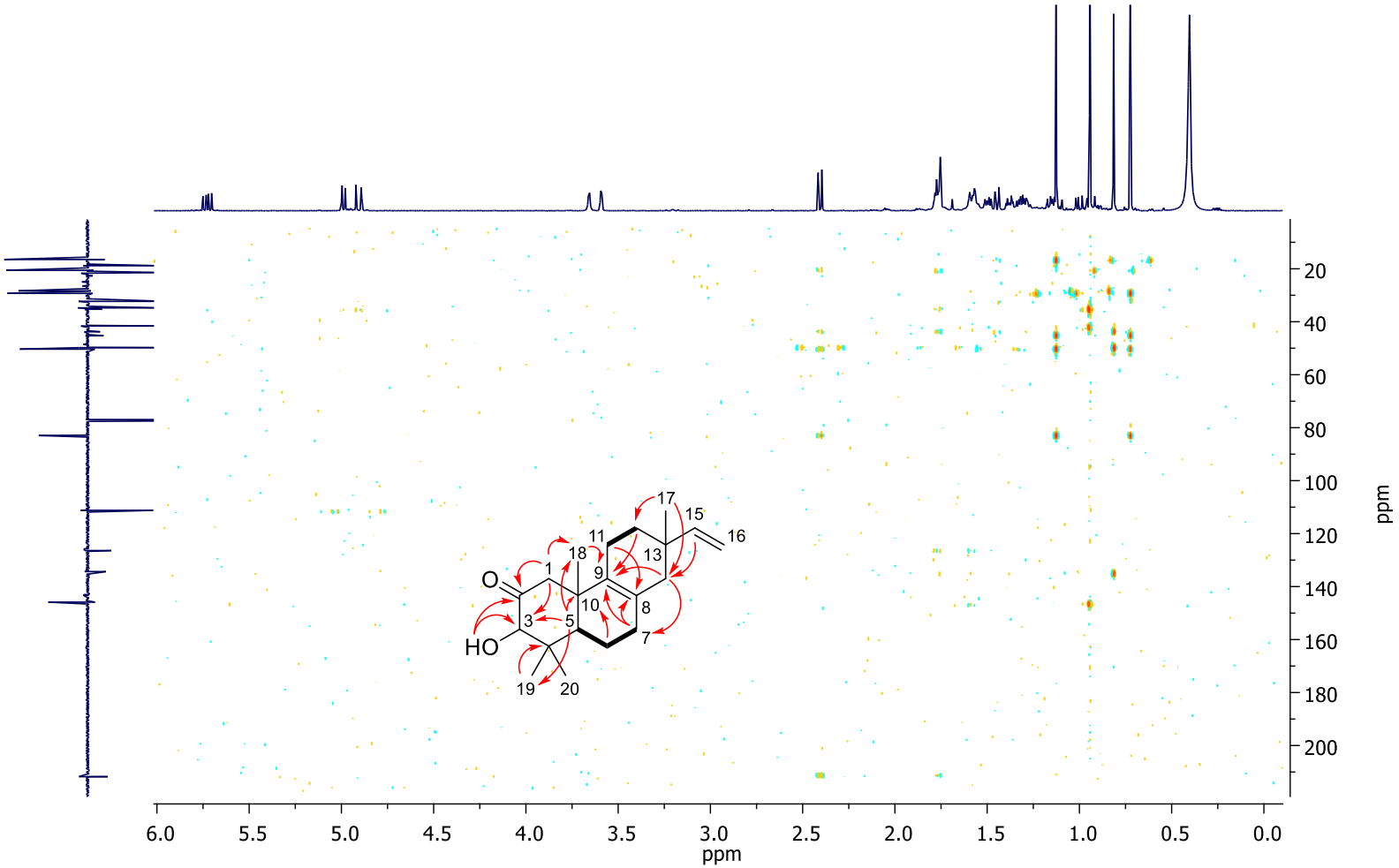

Figure A70. 1D-TOCSY spectra (600 MHz) of **15** in C_6D_6.

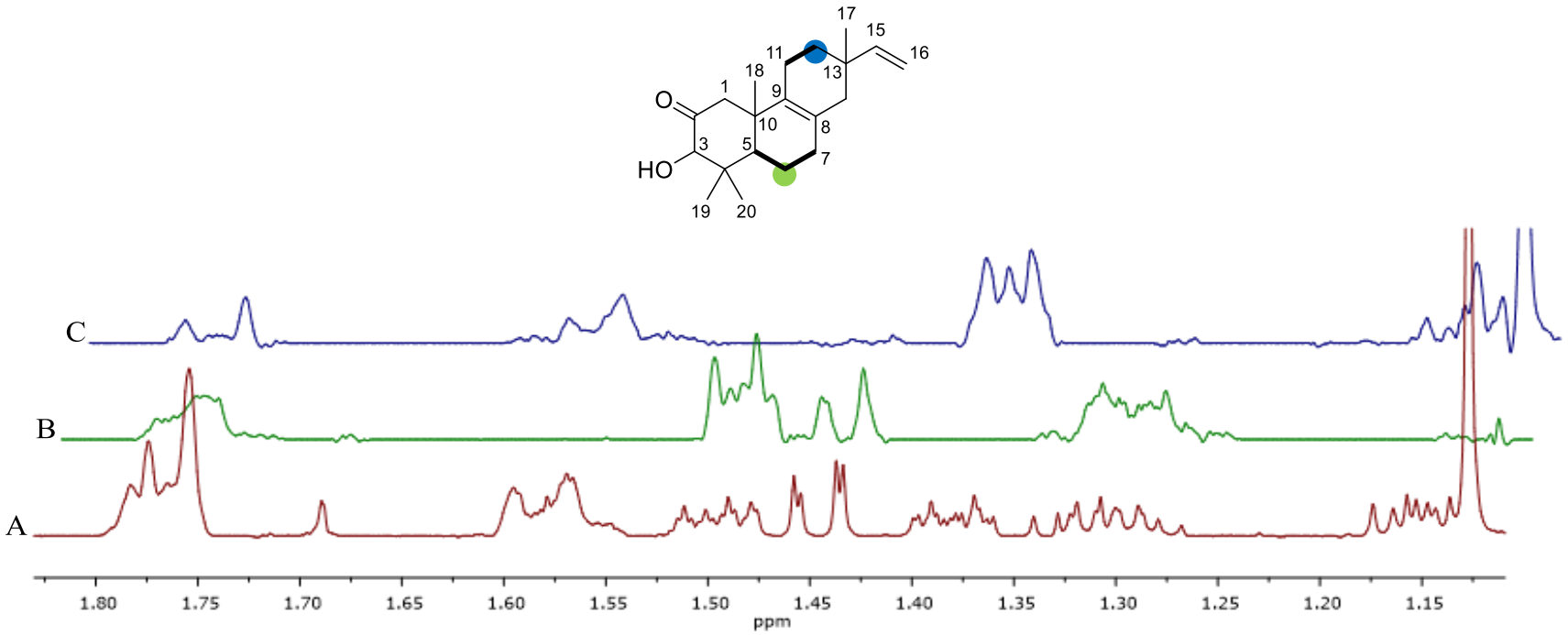

(A) Expansion of ^{1}H NMR spectrum (600 MHz) of **15**; (B) Expansion of 1D-TOCSY spectrum of **15** (irradiation of δ_H 1.30); (C) Expansion of 1D-TOCSY spectrum of **15** (irradiation of δ_H 1.15).

Figure A71. Expanded HR-ESI-Q-TOF mass spectrum of **15**.

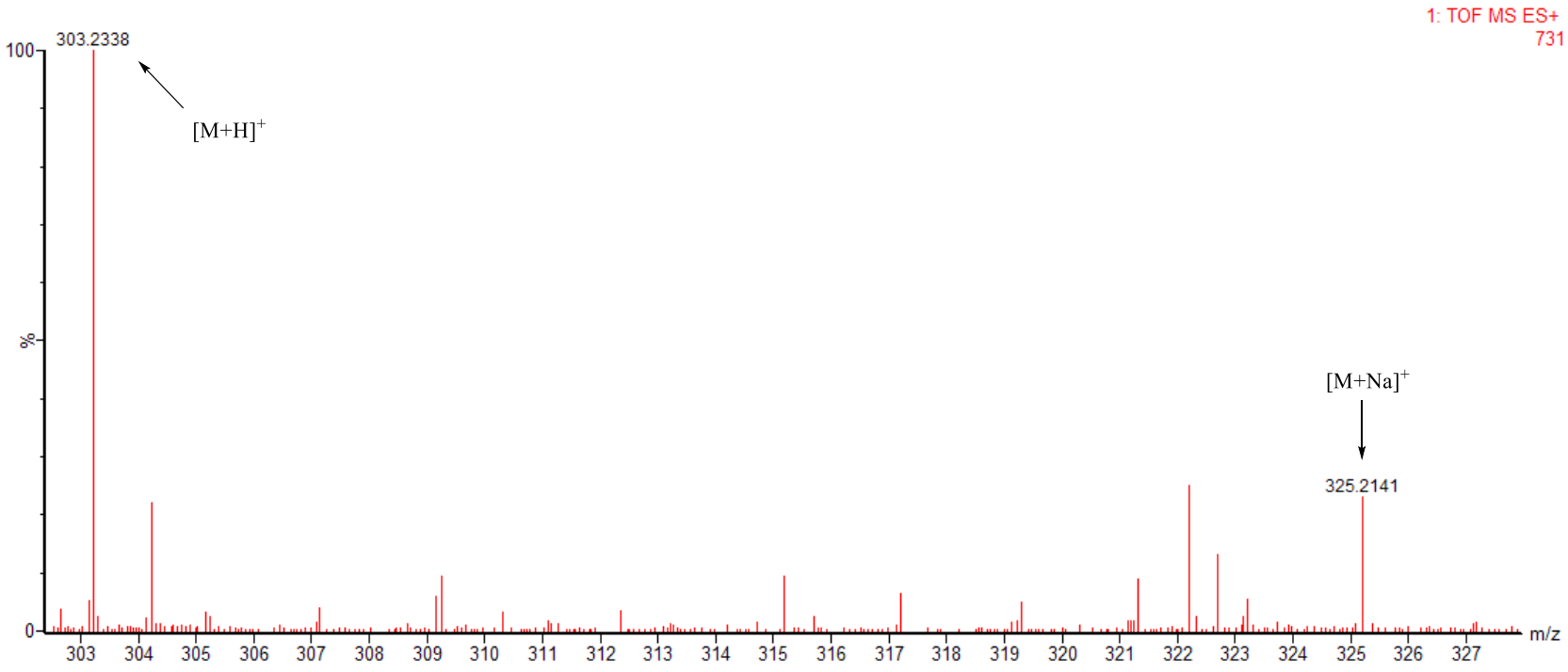

HR-ESI-Q-TOF MS *m/z* 303.2338 $[M + H]^+$ (calcd. for $C_{20}H_{31}O_2$: 303.2319), and *m/z* 325.2141 $[M + Na]^+$ (calcd. for $C_{20}H_{30}O_2Na$: 325.2138).

Figure A72. UV spectrum of **15** in methanol.

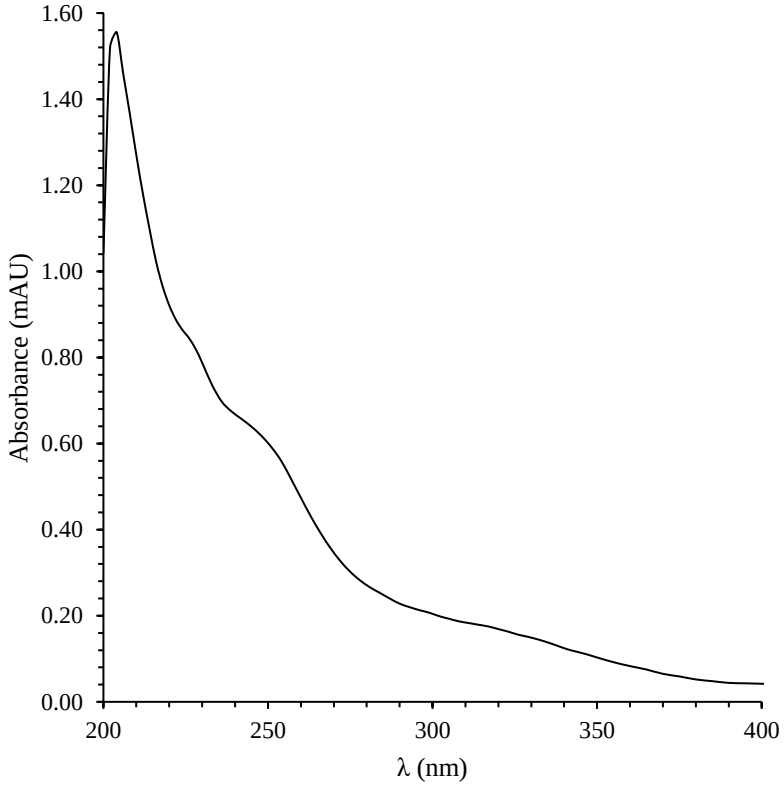

UV (MeOH) λ_{max} (log ε) = 204 (3.67) and shoulders at 228 (3.39) and 242 (3.30) nm.

Figure A73. CD spectrum of **15** in methanol.

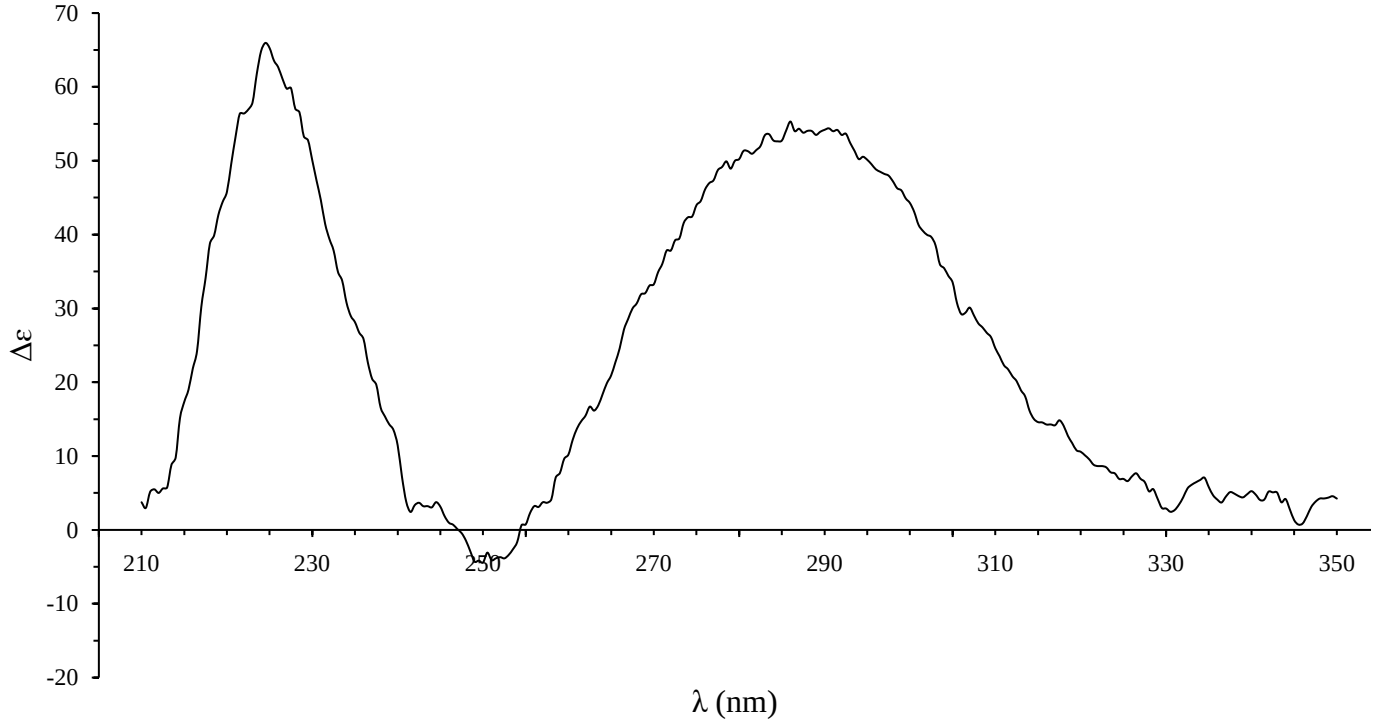

CD (c = 0.0031, MeOH): λ_{max} (Δε) = 225 (+65.2), 250 (-4.4), 290 (+54.4) nm.

Figure A74. ^{1}H NMR spectrum (600 MHz) of **16** in $CDCl_3$.

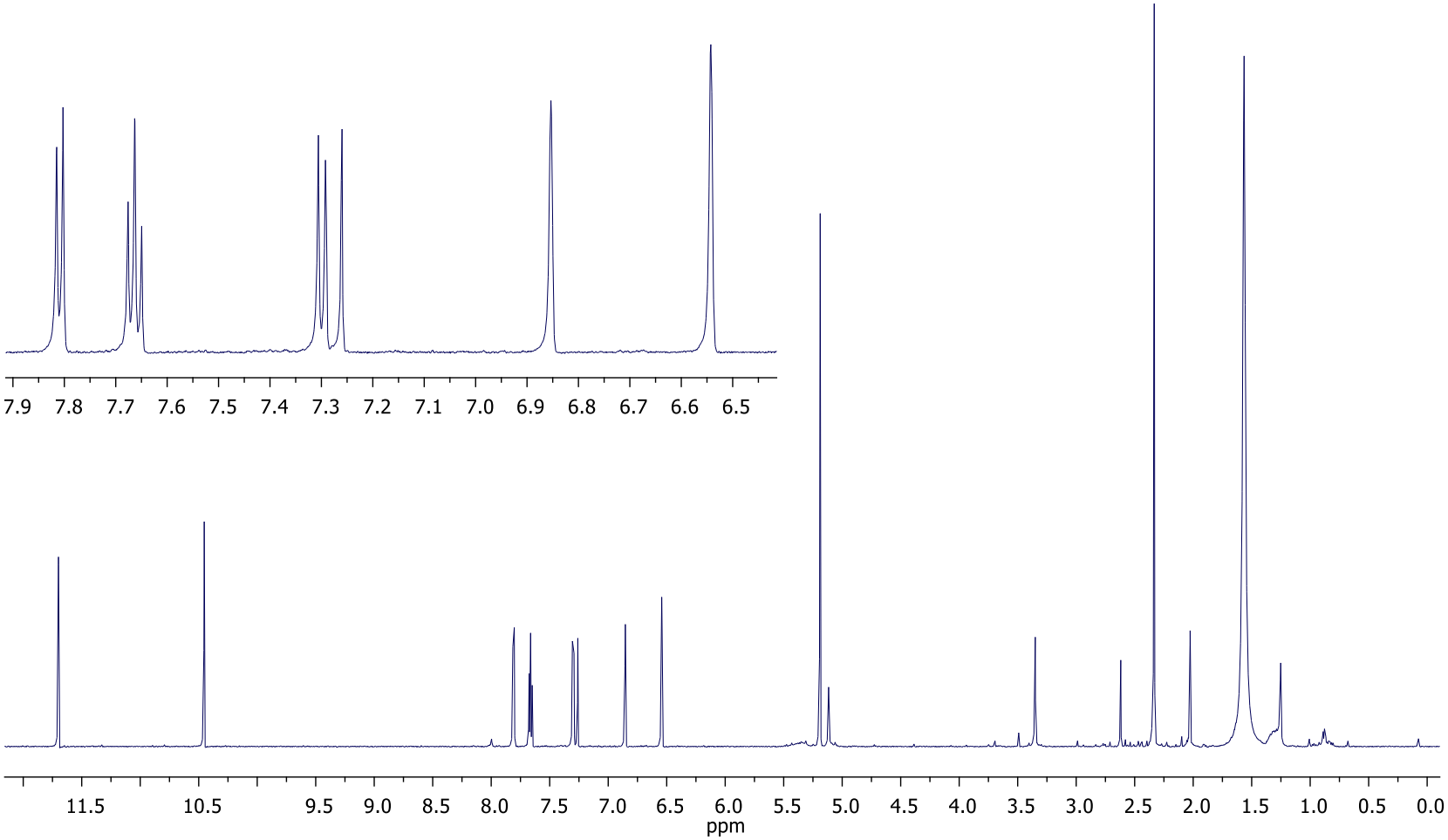

Figure A75. ^{13}C DEPTQ spectrum (226.2 MHz) of **16** in $CDCl_3$.

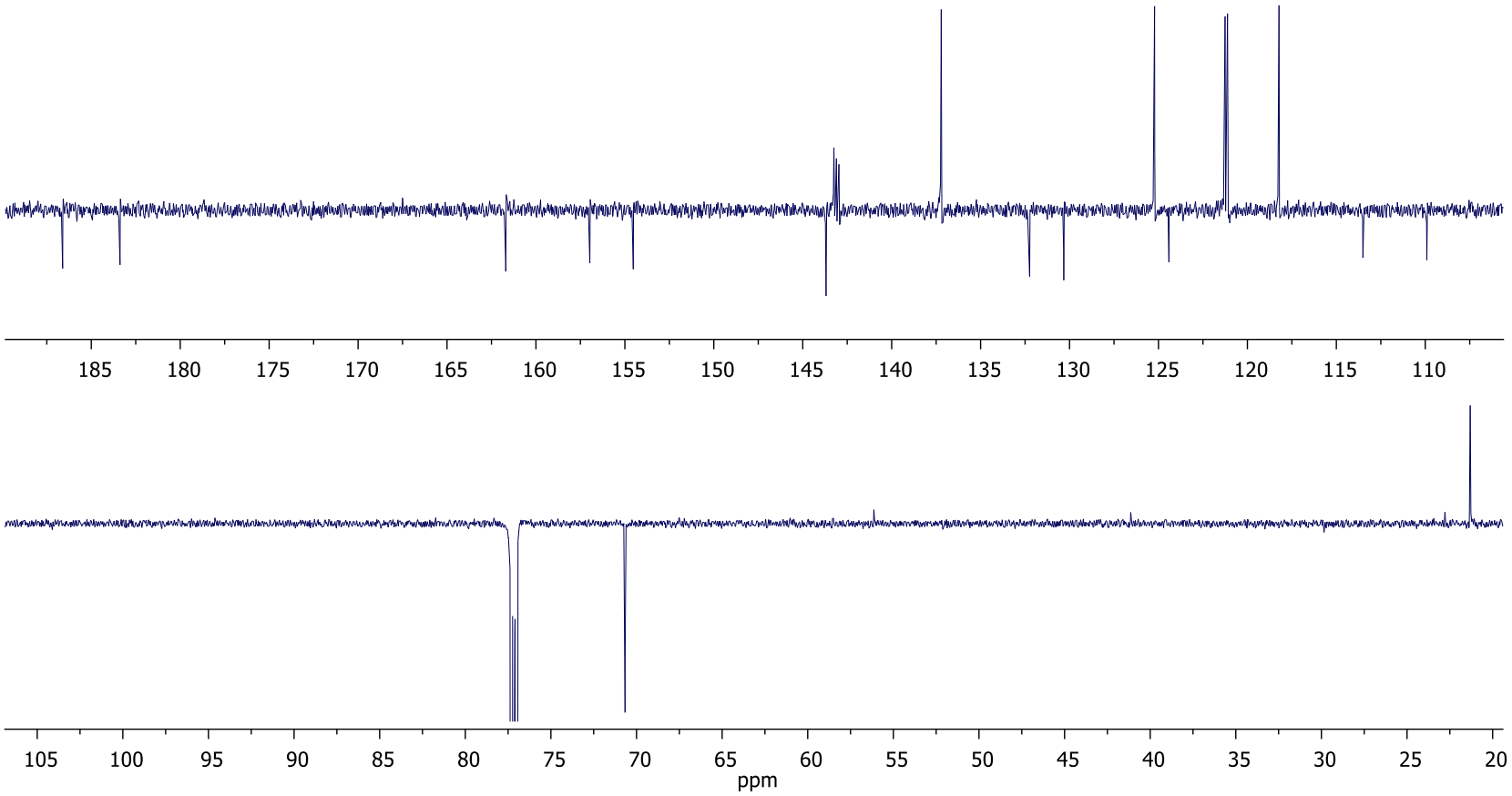

Figure A76. COSY spectrum (600 MHz) of **16** in $CDCl_3$.

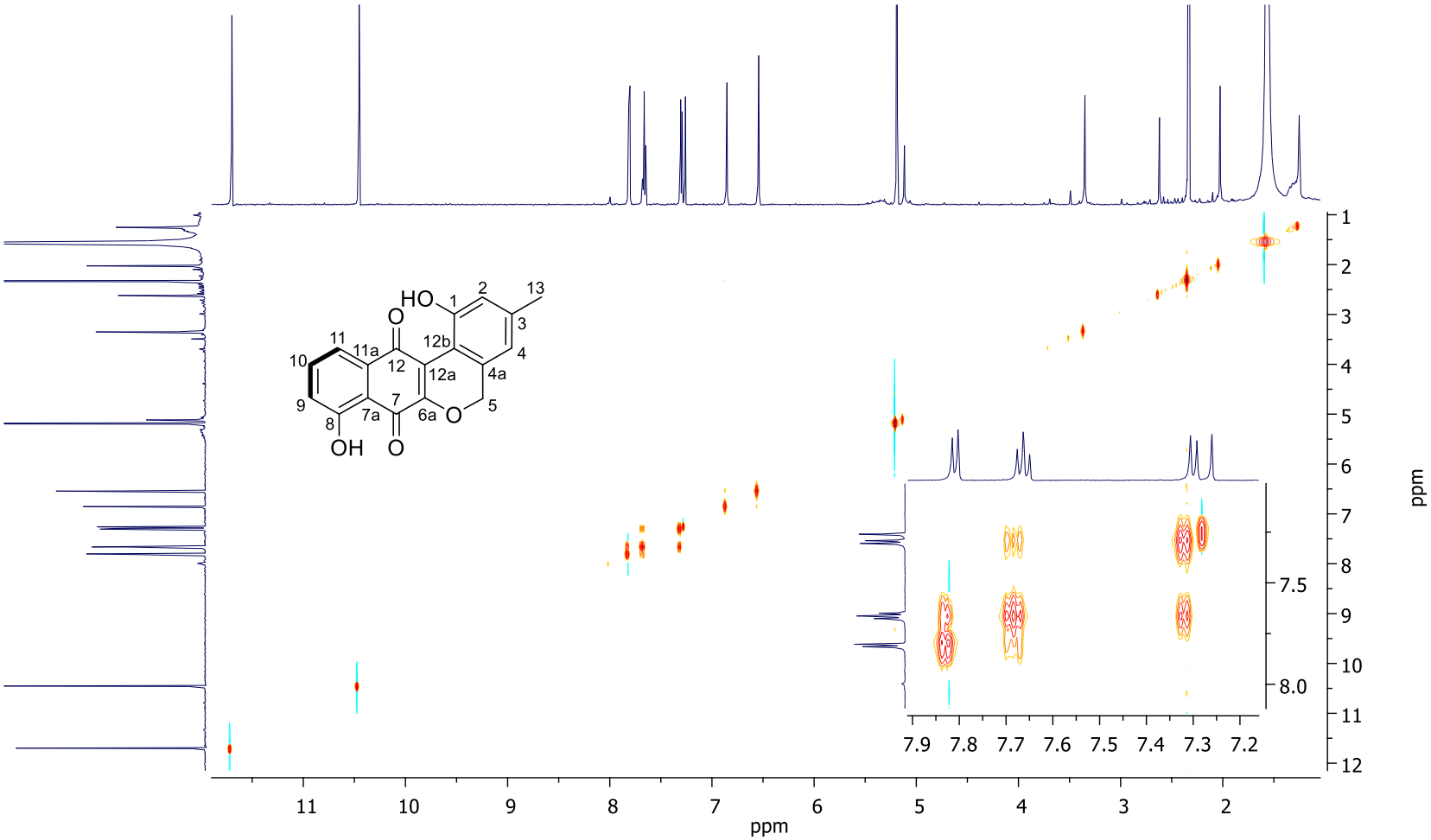

Figure A77. HSQC spectrum (600 MHz) of **16** in $CDCl_3$.

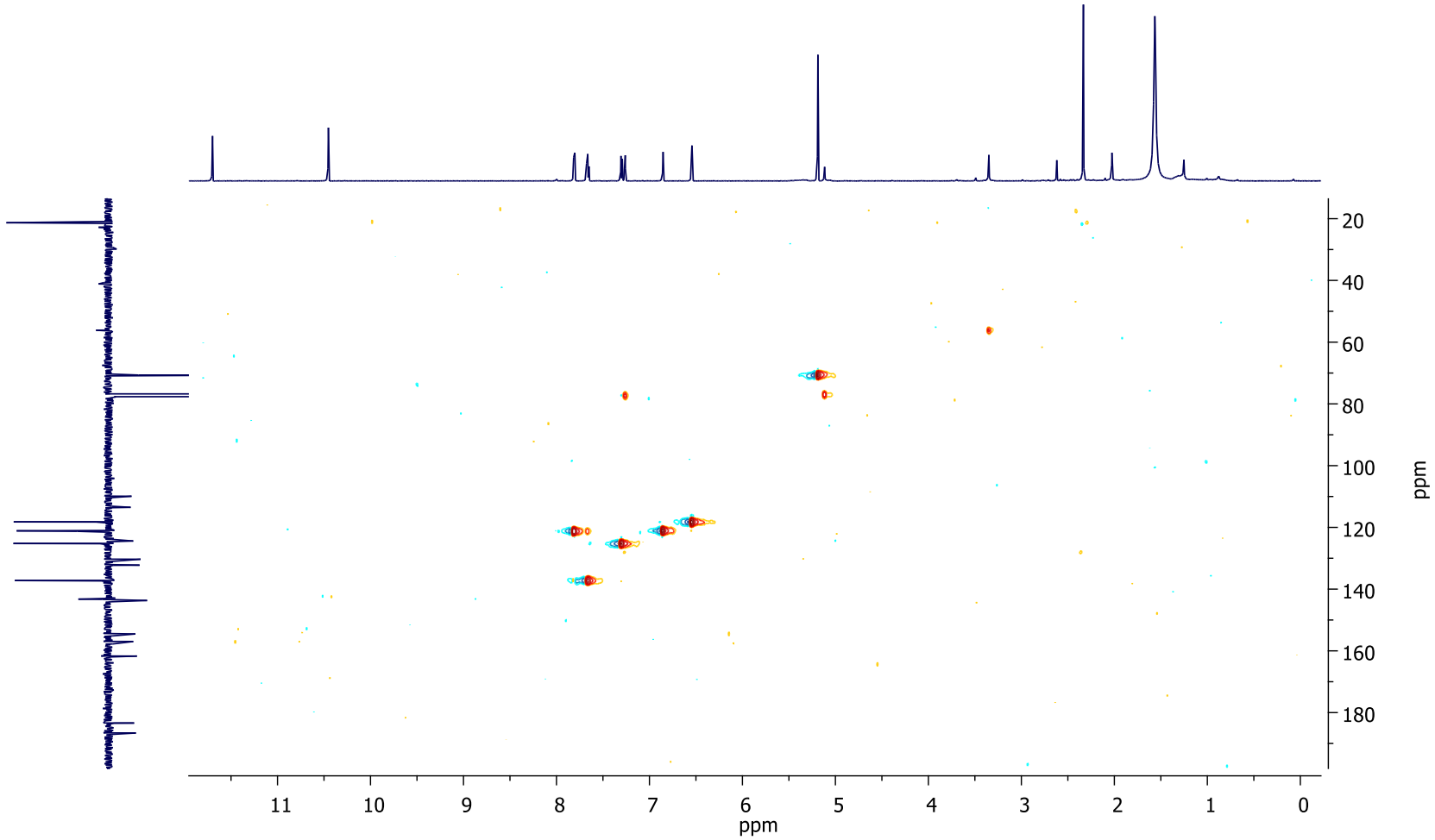

Figure A78. HMBC spectrum (600 MHz) of **16** in $CDCl_3$.

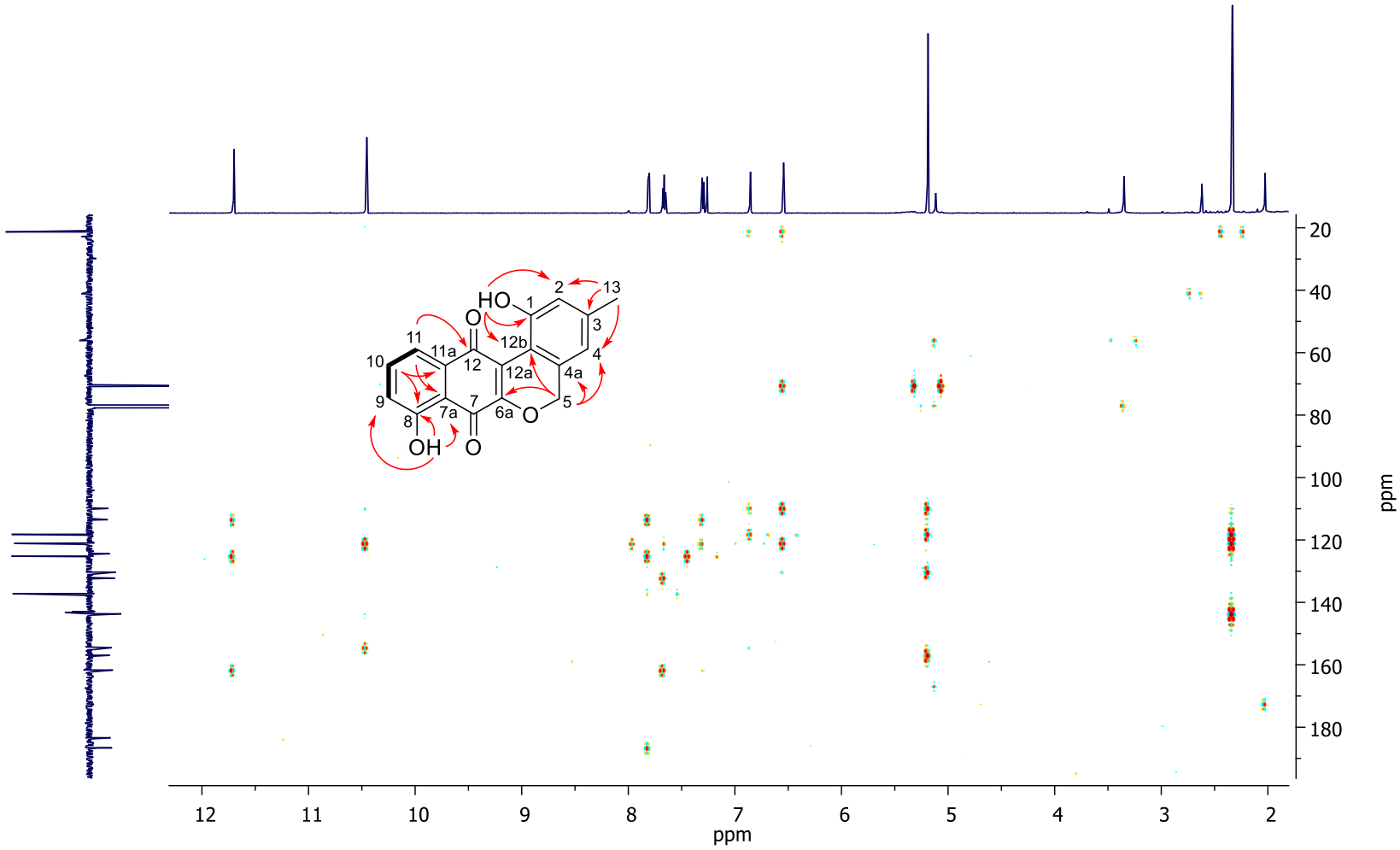

Figure A79. Expanded HR-ESI-Q-TOF mass spectrum of **16**.

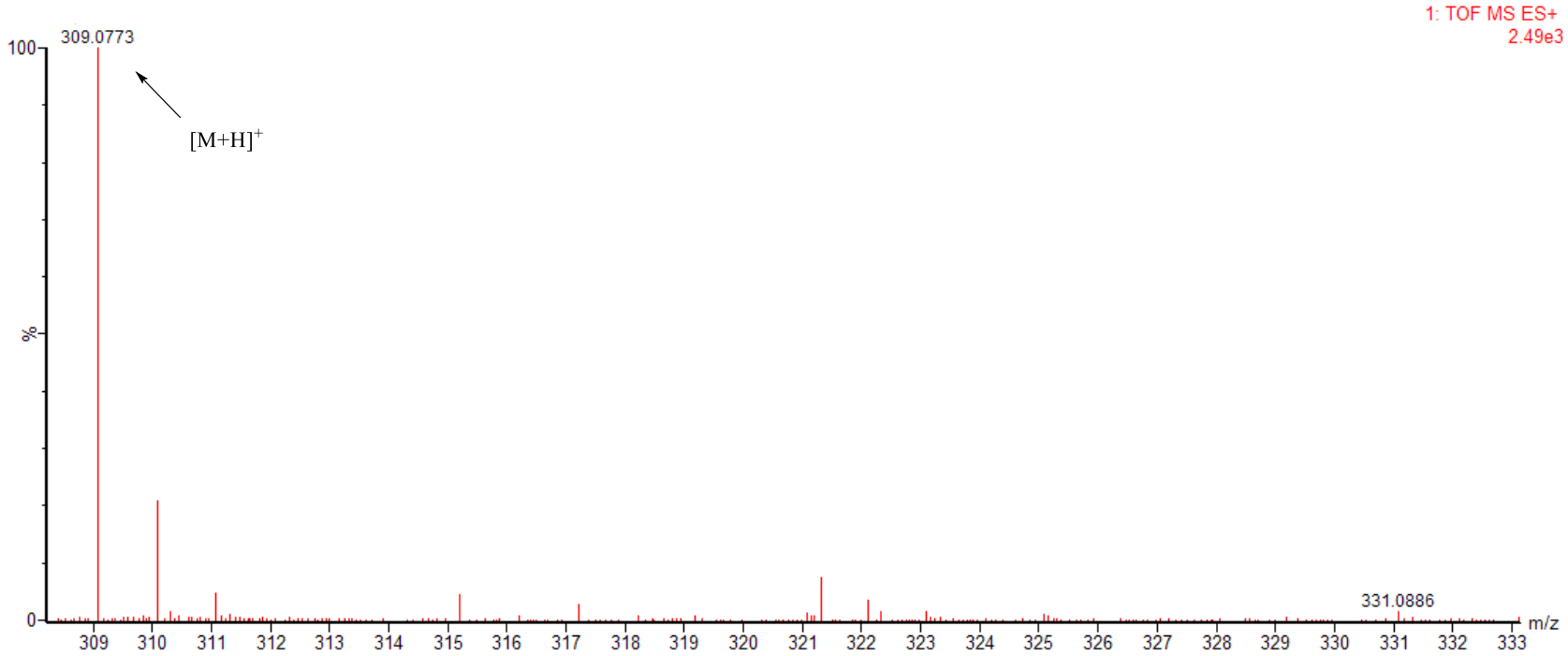

HR-ESI-Q-TOF MS *m/z* 309.0773 $[M + H]^+$ (calcd. for $C_{18}H_{13}O_5$: 309.0757).

Figure A80. UV spectrum of **16** in methanol.

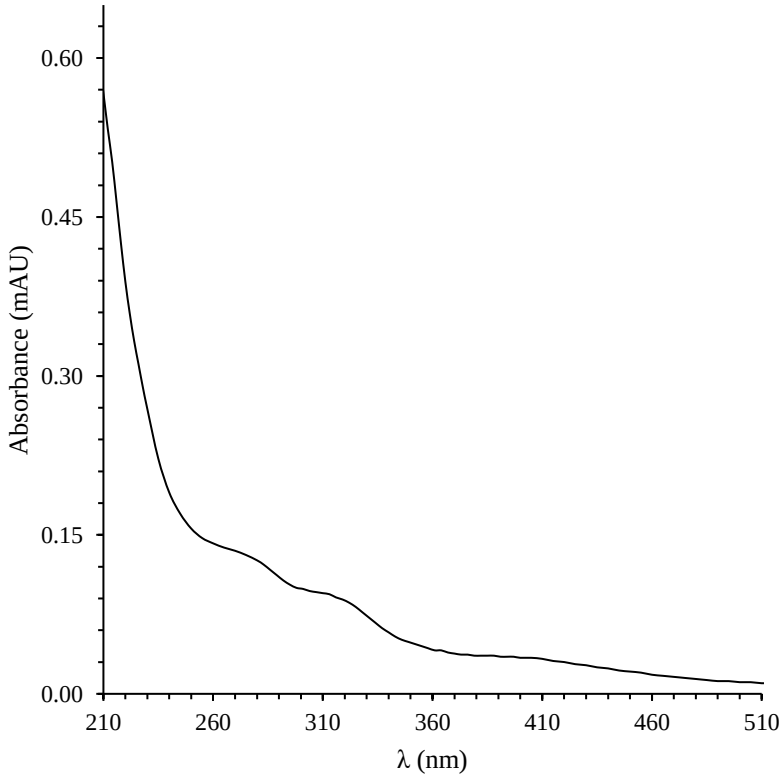

UV (MeOH) λ_{max} (log ε) = broad absorptions with maxima at 204 (3.57), 280 (2.86), 310 (2.73) and 410 (2.27) nm.

Figure A81. ^{1}H NMR spectrum (600 MHz) of dehydrorabelomycin (6-hydroxytetrangulol, **17)**[1-3] in $CDCl_3$.

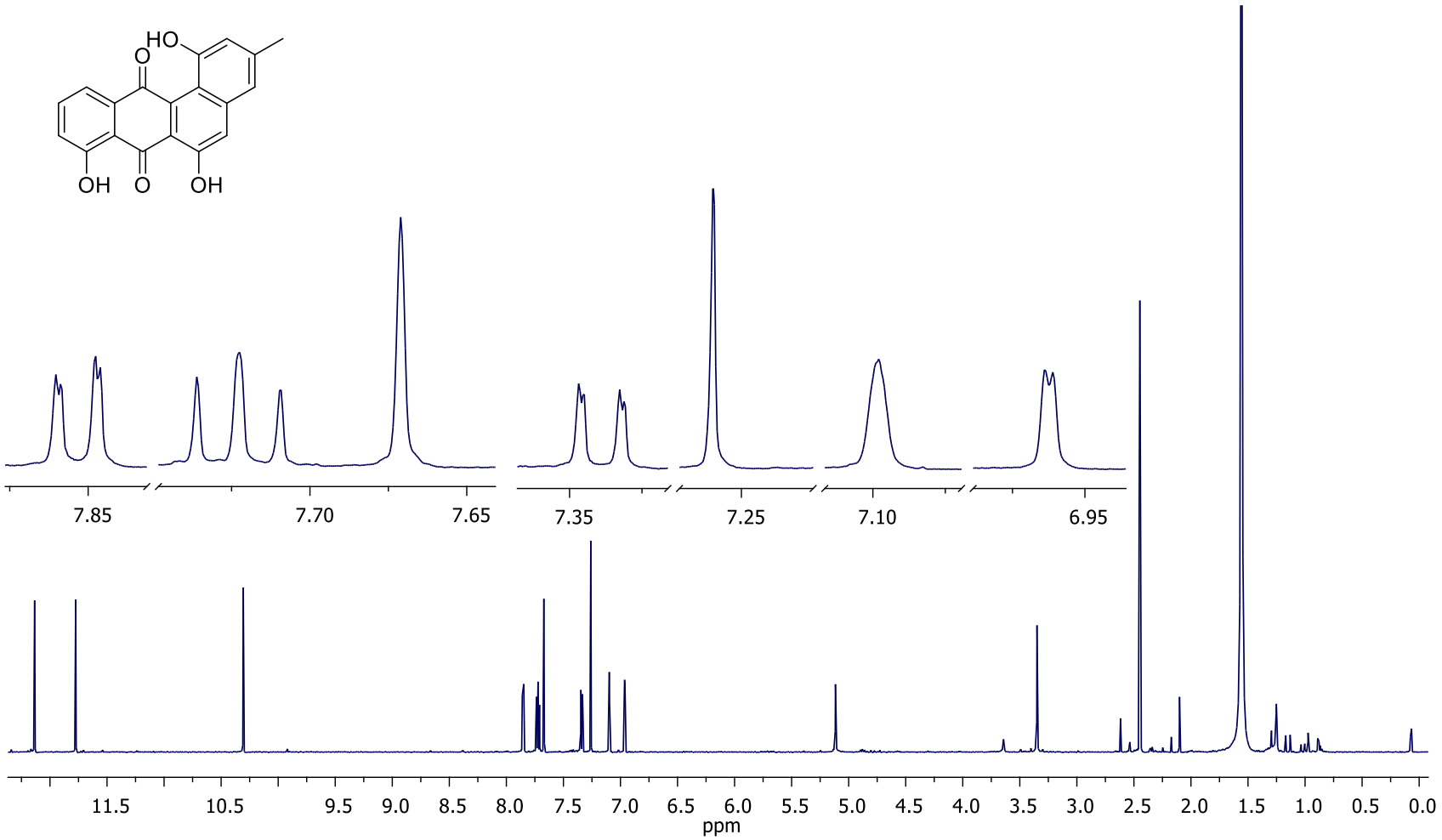

Figure A82. Expanded HR-ESI-Q-TOF mass spectrum of **17**.

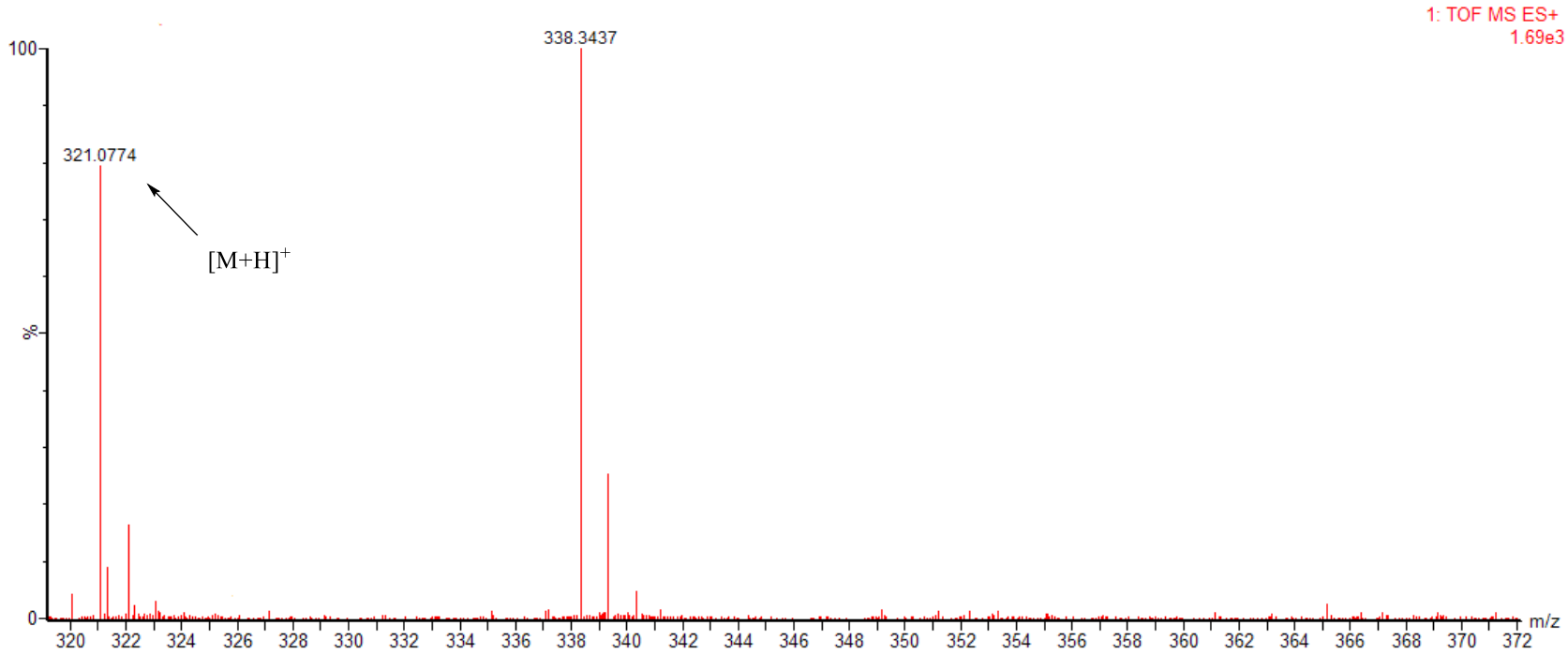

HR-ESI-Q-TOF MS *m/z* 321.0763 $[M + H]^+$ (calcd. for $C_{19}H_{13}O_5$: 321.0757).

Figure A83. ^{1}H NMR spectrum (600 MHz) of phenanthroviridone (phenanthroviridin aglycone, **18**)[4, 5] in $CDCl_3$.

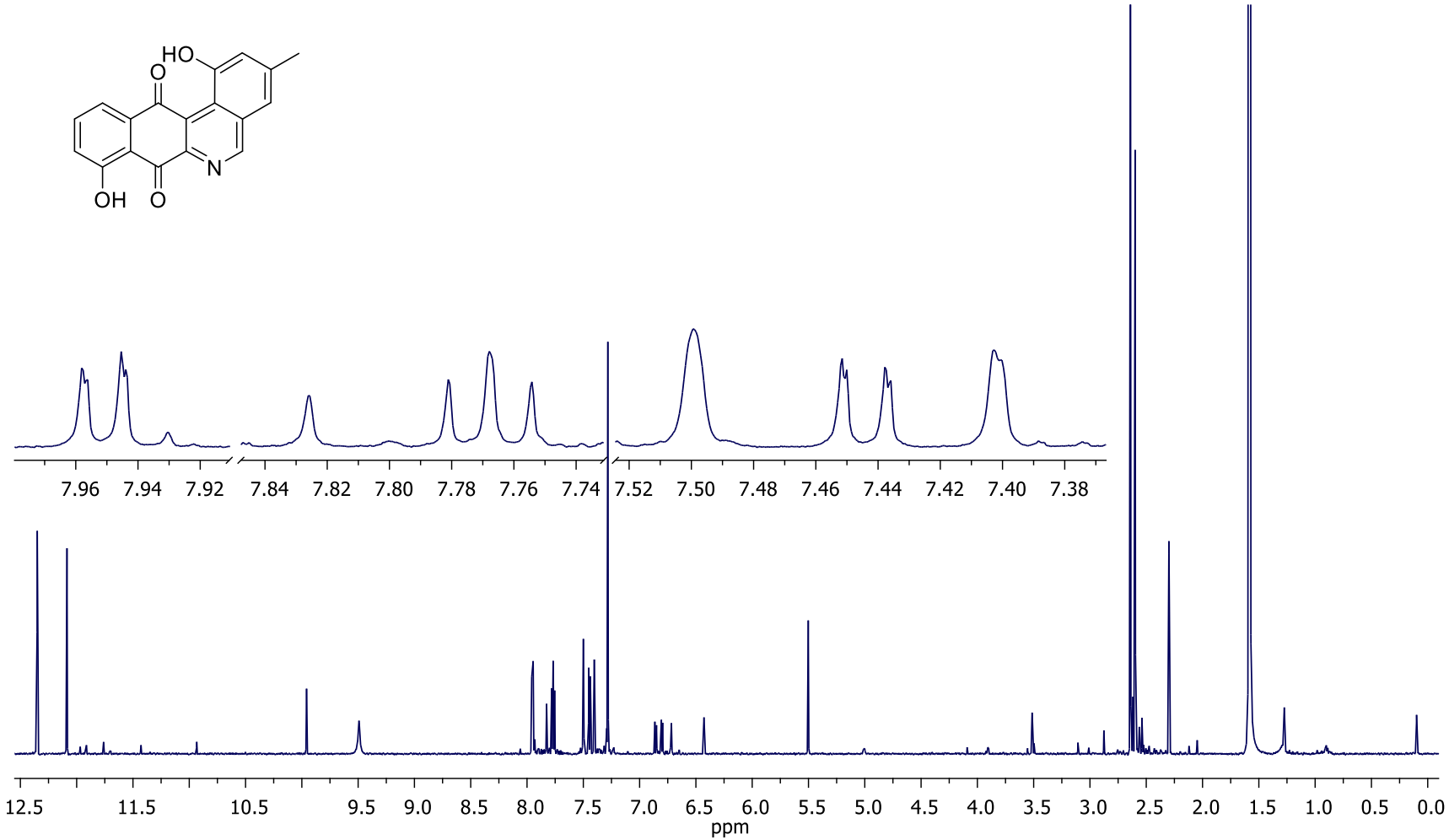

Figure A84. Expanded HR-ESI-Q-TOF mass spectrum of **18**.

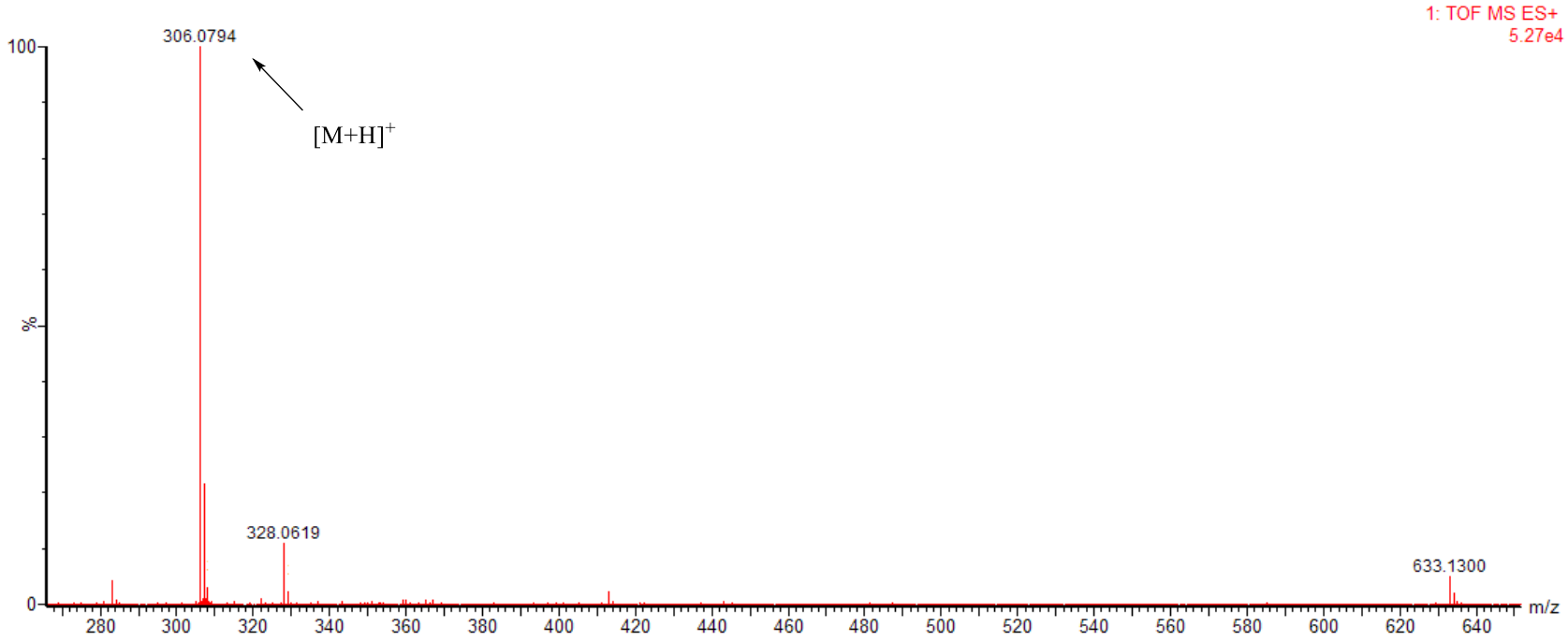

HR-ESI-Q-TOF MS *m/z* 306.0794 $[M + H]^+$ (calcd. for $C_{18}H_{12}NO_4$: 306.0761).

Figure A85. ^{1}H NMR spectrum (600 MHz) of WS-5995 A (**19**)[6, 7] in $CDCl_3$.

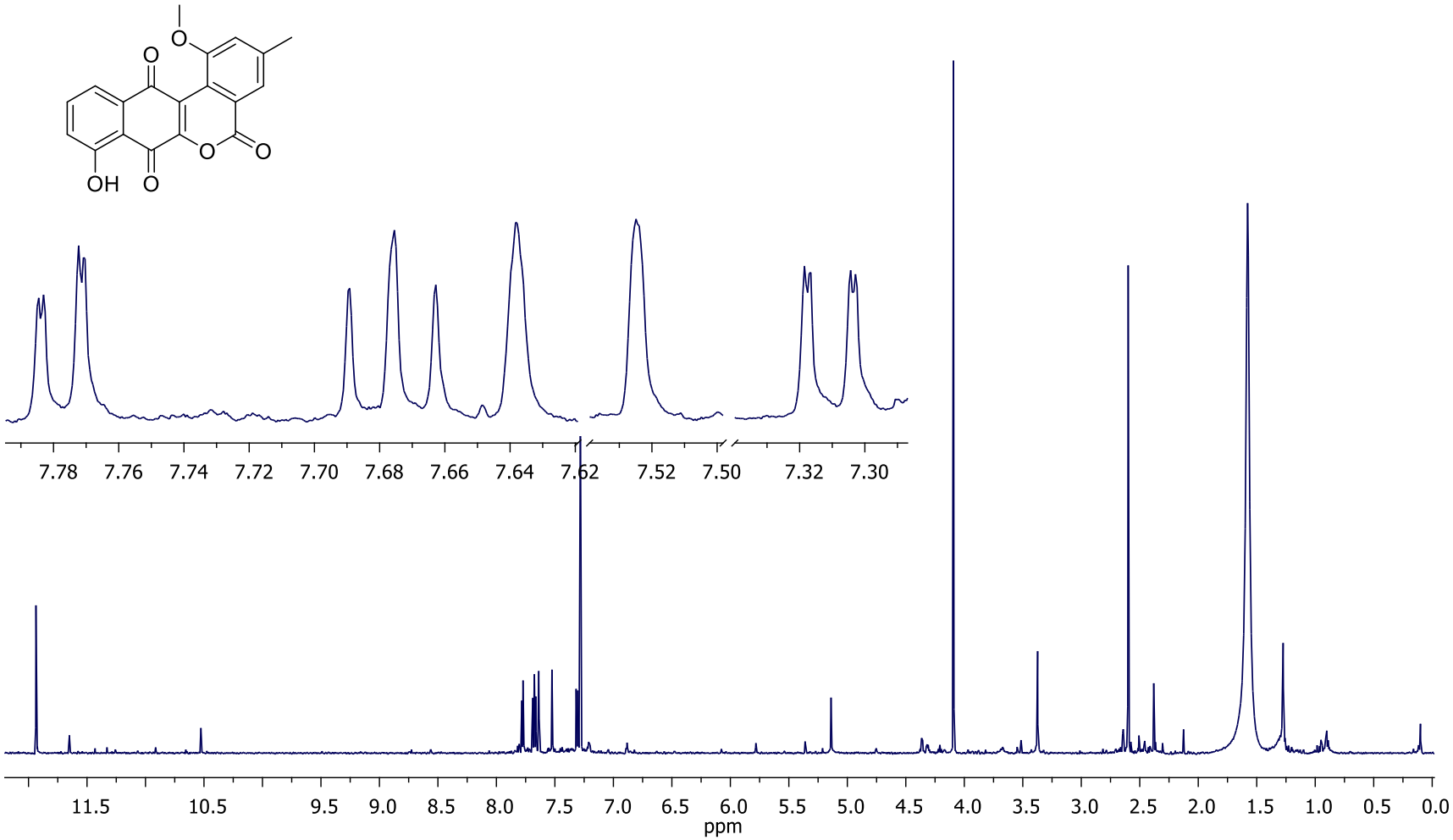

Figure A86. Expanded HR-ESI-Q-TOF mass spectrum of **19**.

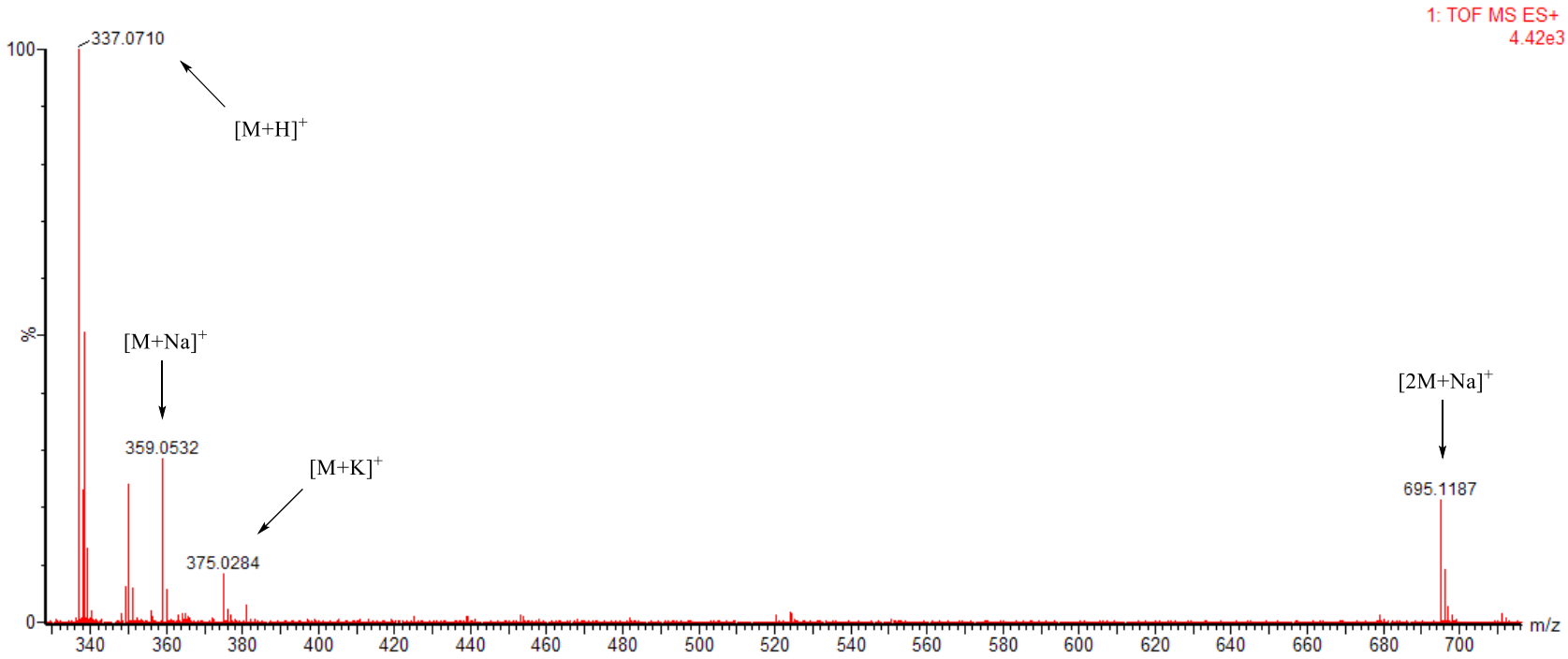

HR-ESI-Q-TOF MS *m/z* 337.0710 $[M + H]^+$ (calcd. for $C_{19}H_{13}O_6$: 337.0707), *m/z* 359.0532 $[M + Na]^+$ (calcd. for $C_{19}H_{12}O_6Na$: 359.0526), *m/z* 375.0284 $[M + K]^+$ (calcd. for $C_{19}H_{12}O_6K$: 375.0265), and *m/z* 695.1187 $[2M + Na]^+$ (calcd. for $C_{38}H_{24}O_{12}Na$: 695.1160).

A2.4 CITED LITERATURE

1. Yamashita, N.; Takashi, H.; Kazuo, S.; Haruo, S. 6-hydroxytetrangulol, a new CPP32 protease inducer produced by *Streptomyces* sp. *J. Antibiot.* **1998**, *1*, 79-81.
2. Liu, W. C.; Parker, L.; Slusarchyk, S.; Greenwood, G. L.; Grahm, S. F.; Meyers, E. Isolation, characterization, and structure of rabelomycin, a new antibiotic. *J. Antibiot.* **1970**, *23*, 437-441.
3. Yamashita, N. Manufacture of dehydrorabelomycin with *Streptomyces* species and use of the antibiotic agent as antitumor agent. JP 10201494 A, Aug 4, 1998.
4. Fendrich, G.; Zimmermann, W.; Gruner, J.; Auden, J. A. L. Phenanthridine derivatives, process for the preparation thereof, and compositions containing them. 1990.
5. Gore, M. P.; Gould, S. J.; Weller, D. D. Synthesis of putative intermediates in the biosynthesis of the kinamycin antibiotics: Total synthesis of phenanthroviridin aglycon and related compounds. *J. Org. Chem.* **1992**, *57*, 2774-2783.
6. Ikushima, H.; Iguchi, E.; Kohsaka, M.; Aoki, H.; Imanaka, H. *Streptomyces auranticolor* sp. nov., a new anticoccidial antibiotics producer. *J. Antibiot.* **1980**, *33*, 1103-1106.
7. Ikushima, H.; Okamoto, M.; Tanaka, H.; Ohe, O.; Kohsaka, M.; Aoki, H.; Imanaka, H. New anticoccidial antibiotics, WS-5995 A and B: I. Isolation and characterization. *J. Antibiot.* **1980**, *33*, 1107-1113.

LICENSE TO USE PUBLISHED WORKS

Chapter 2:

Title: Diaza-anthracene Antibiotics from a Freshwater-Derived Actinomycete with Selective Antibacterial Activity toward Mycobacterium tuberculosis

Author: Michael W. Mullowney, Chang Hwa Hwang, Andrew G. Newsome, et al

Publication: ACS Infectious Diseases

Publisher: American Chemical Society

Date: Apr 1, 2015

Copyright © 2015, American Chemical Society

Logged in as:
Michael Mullowney
LOGOUT

PERMISSION/LICENSE IS GRANTED FOR YOUR ORDER AT NO CHARGE

This type of permission/license, instead of the standard Terms & Conditions, is sent to you because no fee is being charged for your order. Please note the following:

- Permission is granted for your request in both print and electronic formats, and translations.
- If figures and/or tables were requested, they may be adapted or used in part.
- Please print this page for your records and send a copy of it to your publisher/graduate school.
- Appropriate credit for the requested material should be given as follows: "Reprinted (adapted) with permission from (COMPLETE REFERENCE CITATION). Copyright (YEAR) American Chemical Society." Insert appropriate information in place of the capitalized words.
- One-time permission is granted only for the use specified in your request. No additional uses are granted (such as derivative works or other editions). For any other uses, please submit a new request.

Chapters 3 and 4:

creative commons

Attribution 4.0 International (CC BY 4.0)

This is a human-readable summary of (and not a substitute for) the **license**.

Disclaimer

Free Cultural APPROVED FOR Works

You are free to:

Share — copy and redistribute the material in any medium or format

Adapt — remix, transform, and build upon the material

for any purpose, even commercially.

The licensor cannot revoke these freedoms as long as you follow the license terms.

Under the following terms:

Attribution — You must give **appropriate credit**, provide a link to the license, and **indicate if changes were made**. You may do so in any reasonable manner, but not in any way that suggests the licensor endorses you or your use.

No additional restrictions — You may not apply legal terms or **technological measures** that legally restrict others from doing anything the license permits.

Notices:

You do not have to comply with the license for elements of the material in the public domain or where your use is permitted by an applicable **exception or limitation**.

No warranties are given. The license may not give you all of the permissions necessary for your intended use. For example, other rights such as **publicity, privacy, or moral rights** may limit how you use the material.

VITAE

Michael W. Mullowney

Education

2012 – 2016	University of Illinois at Chicago, Chicago, IL
	NIH/NCCIH T32 and AFPE Predoctoral Training Fellow and PhD Candidate in Pharmacognosy, Department of Medicinal Chemistry and Pharmacognosy, College of Pharmacy.
2009 – 2012	DePaul University, Chicago, IL
	Post-baccalaureate studies in chemistry, biology, and calculus.
1998 – 2002	School of Art, Arizona State University, Tempe, AZ
	BFA with honors in Intermedia, May, 2002.
1996 – 1998	Rio Salado Community College, Tempe, AZ
	Studies in physics, Spanish, and pre-algebra.
1997	Universidad de Salamanca, Salamanca, Spain
	Study abroad in Spanish language and culture.

Employment

2013 – 2016	Department of Medicinal Chemistry and Pharmacognosy, College of Pharmacy, University of Illinois at Chicago, Chicago, IL NIH and AFPE Graduate Research Fellow to Dr. Brian T. Murphy
2012	College of Pharmacy, University of Illinois at Chicago
	Graduate Teaching Assistant
2011 – 2012	Freelance Organic and Biochemistry Chemistry Tutor
2011 – 2012	Kendall Hunt Publishing & Department of Chemistry, DePaul University
	Graphic Artist / Online Textbook Developer
2011 – 2012	Department of Chemistry, DePaul University
	Undergraduate Organic Chemistry Lab Teacher's Assistant
2010 – 2012	Department of Chemistry, DePaul University
	Research Assistant to Dr. Justin Maresh

Field Research Experience

2015	Two-week field collection trip to Iceland:

Collected and processed sediment and invertebrate samples in the East fjords marine environment and inland freshwater systems by free diving and SCUBA.

Collected marine sediment samples using PONAR from Icelandic Coast Guard vessel Thor.

2015 One-day field collection trip in Whitehall, MI:

Organized and directed preparations.

Collected sediment by PONAR and free diving in White Lake and Lake Michigan.

2014 Two-week field collection trip to Iceland:

Collected sediment and invertebrate samples in the Westfjords marine environment and inland freshwater systems by SCUBA.

Collected marine sediment samples using PONAR from Icelandic Coast Guard vessel Ægir.

2014 PADI Open Water Diver and Dry Suit Diver certified.

Awards and Honors

2015 International Association for Great Lakes Research (IAGLR) Scholarship

2015-2016 American Foundation for Pharmaceutical Research (AFPE) Predoctoral Fellowship in Pharmaceutical Sciences

2014 W. E. van Doren Scholar, Department of Medicinal Chemistry and Pharmacognosy, College of Pharmacy, University of Illinois at Chicago.

2013-2016 NIH NCCIH T32 Predoctoral Training Fellowship

Professional Societies

2015 – American Association for the Advancement of Science (AAAS)

2015 – International Association of Great Lakes Research (IAGLR)

2014 – American Society of Microbiology (ASM)

2013 – American Society of Pharmacognosy (ASP)

2010 – American Chemical Society (ACS)

Journalistic Publications

2015 Mullowney, M.W. Andersen Receives Farnsworth Award. *The American Society of Pharmacognosy Newsletter*, 2015, *51* (3) 8-9.

2013 Mullowney, M.W. Õmura Honored: 2013 ASP Research Achievement Award. *The American Society of Pharmacognosy Newsletter*, 2013, *49* (3) 5-6.

Peer-Reviewed Publications

2015 Mullowney, M.W.; Ó hAinmhire, E.; Tanouye, U.; Burdette, J.E.; Pham, V.C.; Murphy, B.T. A Pimarane Diterpene and Cytotoxic Angucyclines from a Marine-Derived *Micromonospora* sp. in Vietnam's East Sea. *Mar. Drugs.* **2015**, *13*, 5815-5827.

2015 Mullowney, M.W.; Newsome, A.; Wan, B.; Wei, X.; Tanouye, U.; Cho, S. H.; Franzblau S.G.; Murphy, B.T. Diaza-anthracene antibiotics from a freshwater-derived actinomycete that selectively inhibit *M. tuberculosis*. *ACS Infect. Dis.* **2015**, *1*, 168–174. (NOTE: This article was featured on the cover of the journal.)

2014 Mullowney, M.W.; Ó hAinmhire, E.; Shaikh, A.; Wei, X.; Tanouye, U.; Santarsiero, B.D.; Burdette, J.E.; Murphy, B.T. Diazaquinomycins E–G, novel diaza-anthracene analogs from a marine-derived *Streptomyces* sp. *Mar. Drugs.* **2014**, *12*, 3574-3586.

2014 Maresh, J. J.; Crowe, S.O.; Ralko, A.; Aparece, M.D.; Murphy, C.M.; Krzeszowiec, M.; Mullowney, M.W. Facile one-pot synthesis of tetrahydroisoquinolines from amino acids via hypochlorite-mediated decarboxylation and Pictet–Spengler condensation. *Tetrahedron Lett.* **2014**, *55*, 5047-5051.

Invited Presentations

2015 Mullowney, M.W.; Hwang, C.H.; Newsome, A.; Klein, L.; Shaikh, A.; Tanouye, U.; Cho, S.; Franzblau, S.G.; Murphy, B.T. *Natural Products Drug Discovery: Inhibitors of drug-resistant* M. tuberculosis *from aquatic actinomycetes*. Invited research talk presented at the "Careers in Scientific Research" event at DePaul University, Chicago, IL, May 15, 2015.

2014 Mullowney, M.W.; Hwang, C.H.; Newsome, A.; Klein, L.; Shaikh, A.; Tanouye, U.; Cho, S.; Franzblau, S.G.; Murphy, B.T. *Diaza-anthracene antibiotics that inhibit drug-resistant Mycobacterium tuberculosis*. Invited research talk presented at the Baxter-UIC NMR Exchange Meeting, Baxter Healthcare, Deerfield, IL, May 21, 2014.

Conference Presentations

2015 Mullowney, M.W.; Ó hAinmhire, E.; Tanouye, U.; Burdette, J.E.; Pham, V.C.; Murphy, B.T. A novel pimarane diterpene and cytotoxic angucyclines from a marine-derived *Micromonospora* sp. in Vietnam's East Sea. Poster presented at: The 47th annual conference of the American Society of Pharmacognosy, Copper Mountain, CO, July 27, 2015.

2015 Mullowney, M.W., Ó hAinmhire, E.; Tanouye, U.; Wan B.; Cho S.; Franzblau, S.G.; Burdette, J.E.; Pham, V.C.; Murphy, B.T. A novel diterpene and cytotoxic molecules from a marine-derived actinomycete in Vietnam. Poster presented at: The 53rd Annual MIKI Medicinal Chemistry Meeting in Miniature, The University of Kansas, Lawrence, KS, April 11, 2015.

2014 Mullowney, M.W.; Hwang, C.H.; Newsome, A.; Krishnamoorthy, K.; Roberts, D.; Klein, L.; Shaikh, A.; Tanouye, U.; Rathod, P.; Parish, T.; Cho, S.; Franzblau, S.G.; and Murphy, B.T. *Diaza-anthracene antibiotics from marine and freshwater-derived actinomycete bacteria that inhibit drug-resistant M. tuberculosis.* Poster presented at: The 2014 David J. Slatkin Symposium, Chicago State University, Chicago, IL, November 14, 2014.

2014 Mullowney, M.W.; Hwang, C.H.; Newsome, A.; Krishnamoorthy, K.; Roberts, D.; Klein, L.; Shaikh, A.; Tanouye, U.; Rathod, P.; Parish, T.; Cho, S.; Franzblau, S.G.; and Murphy, B.T. *Diaza-anthracene antibiotics from marine and freshwater-derived actinomycete bacteria that inhibit drug-resistant M. tuberculosis.* Poster presented at: The CMIDD 19th Annual Drug Discovery Symposium, Northwestern University, Chicago, IL, October 9, 2014.

2014 Mullowney, M.W.; Hwang, C.H.; Newsome, A.; Krishnamoorthy, K.; Roberts, D.; Klein, L.; Shaikh, A.; Tanouye, U.; Rathod, P.; Parish, T.; Cho, S.; Franzblau, S.G.; and Murphy, B.T. *Diaza-anthracene antibiotics from marine and freshwater-derived actinomycete bacteria that inhibit drug-resistant M. tuberculosis.* Poster presented at: The 52nd Annual MIKI Medicinal Chemistry Meeting in Miniature, University of Illinois at Chicago, Chicago, IL, April 12, 2014.

2014 Mullowney, M.W.; Hwang, C.H.; Newsome, A.; Krishnamoorthy, K.; Roberts, D.; Klein, L.; Shaikh, A.; Tanouye, U.; Rathod, P.; Parish, T.; Cho, S.; Franzblau, S.; and Murphy, B.T. *Diaza-anthracene antibiotics from marine and freshwater-derived actinomycete bacteria that inhibit drug-resistant M. tuberculosis.* Poster presented at: Marine Natural Products Gordon Research Conference: From Discovery to Human Health; Ventura, CA, March 5-6, 2014.

2014 Mullowney, M.W.; Hwang, C.H.; Newsome, A.; Krishnamoorthy, K.; Roberts, D.; Klein, L.; Shaikh, A.; Tanouye, U.; Rathod, P.; Parish, T.; Cho, S.; Franzblau, S.; and Murphy, B.T. *Diaza-anthracene antibiotics from marine and freshwater-derived actinomycete bacteria that inhibit drug-resistant M. tuberculosis.* Poster presented at: Marine Natural Products Gordon-Merck Research Seminar: Making Waves in Medicine, Ventura, CA, March 2, 2014.

2013 Shaikh, A.; Mullowney, M.W.; Ó hAinmhire, E.; Colunga-Hernandez, D.; Burdette, J.; and Murphy. B.T. *A new antimycin analog from a marine-derived Streptomyces sp.* Poster presented at: The 46th annual conference of the American Society of Pharmacognosy, St. Louis, MO, July 14, 2013.

Scholarly Presentations

2016 Mullowney, M.W.; Boshoff, H.; Singh, V.; Barry, C.; Mizrahi, V.; Cho, S.; Franzablau, S.G.; and Murphy, B.T. *Progress toward identification of the diazaquinomycin mechanism of action*. Research talk presented at the Specialized Metabolite Community, College of Pharmacy, University of Illinois at Chicago, Chicago, IL, September 1, 2016.

2014 Mullowney, M.W.; Newsome, A.; Klein, L.; Wei, X.; Cho, S.; Franzablau, S.G.; and Murphy, B.T. *Antibiotics from aquatic-derived actinomycetes that inhibit drug-resistant M. tuberculosis*. Research talk presented at the Center for Pharmaceutical Biotechnology, College of Pharmacy, University of Illinois at Chicago, Chicago, IL, October 30, 2014.

2013 Mullowney, M.W.; Newsome, A.; Klein, L.; Santarsiero, B.; Wei, X.; Cho, S.; and Murphy, B.T. *Diaza-anthracene antibiotics that inhibit drug-resistant Mycobacterium tuberculosis*. Research talk presented at the Center for Pharmaceutical Biotechnology, College of Pharmacy, University of Illinois at Chicago, Chicago, IL, November 7, 2013.

2011 Mullowney, M.W.; and Maresh, J. *Progress toward Cell-Assisted Synthesis of Novel Alkaloids.* Poster presented at: Chicago Area Undergraduate Research Symposium (CAURS), Chicago, IL, April, 2011.

2010 Krzeszowiec, M.W.; Speltz, T.; Lumbreras, E.; Terranova, E.; Aparece, M.; Mullowney, M.; and Maresh, J. *Progress toward Cell-Assisted Synthesis of Novel Alkaloids.* Poster presented at: Mathematics and Technology Showcase, DePaul University, Chicago, IL, November, 2010.

Editing and Review

2014 Linington, R.G.; Williams, P.G.; MacMillan, J.B. *Problems in Organic Structure Determination: A Practical Approach to NMR Spectroscopy*; Taylor & Francis, CRC Press: Boca Raton, FL, USA, 2015.

Technical Skills

Scientific Trained and proficient in NMR, HPLC, ELSD, GC, LC-MS, GC-MS, small molecule molecular networking, synthetic chemistry, plant cell culture, and microbiology.

Field PADI Open Water Diver and Dry Suit Diver certified; trained in sediment and marine invertebrate collection.